The Rosensweig instability
in isotropic magnetic gels

Von der Universität Bayreuth
zur Erlangung des Grades eines
„Doktors der Naturwissenschaften" (Dr. rer. nat.)
genehmigte Abhandlung

vorgelegt von

Stefan Bohlius

geboren in Lichtenfels/Bayern

Contents

List of Figures

Zusammenfassung

Die vorliegende Arbeit befasst sich mit der nichtlinearen theoretischen Analyse der Rosensweig Instabilität in isotropen magnetischen Gelen. Die Rosensweig Instabilität wurde erstmals im Jahr 1967 entdeckt und bezeichnet den Übergang einer zunächst flachen Grenzfläche zwischen einer magnetischen Flüssigkeit und einem nicht-magnetischen Medium zu einer hexagonal geordneten Stacheloberfläche, sobald ein senkrecht zur flachen Oberfläche angelegtes homogenes Magnetfeld einen bestimmten kritischen Wert überschreitet. Magnetische Flüssigkeiten, auch Ferrofluide genannt, sind kolloidale Suspensionen ferromagnetischer Nanoteilchen in einer gewöhnlichen, dem Anwendungszweck entsprechenden Trägerflüssigkeit, wie Wasser oder Benzol. Einem angelegten Magnetfeld ausgesetzt, verhalten sich Ferrofluide wie gewöhnliche paramagnetische Stoffe, jedoch ist ihre Permeabilität bis zu einer Größenordnung höher als in üblichen paramagnetischen Stoffen, weshalb man sie auch als superparamagnetisch bezeichnet.

Mit der Entdeckung der Rosensweig Instabilität wurde auch eine erste theoretische Beschreibung des Phänomens vorgestellt. An der freien Grenzfläche zwischen der Ferroflüssigkeit und dem darüber liegenden Vakuum überwiegen für niedrige Magnetfelder die stabilisierenden Kräfte der Gravitation und der Oberflächenspannung die destabilisierende Kraft des Magnetfeldes. Zwar besitzt ein homogenes Magnetfeld keine Kraftwirkung auf die Oberfläche, jedoch unterliegt die Grenzfläche den immer vorhandenen thermischen Fluktuationen, die das Magnetfeld lokal stören und so eine resultierende Kraft erzeugen. Bei genügend hohen Magnetfeldstärken übertrifft diese Kraft die Gravitation und die Oberflächenspannung und das Rosensweigmuster bildet sich aus.

Startet man den Vernetzungsprozess in einer Mischung aus Polymeren, Vernetzungsreagenzien und einem Ferrofluid, so erhält man ein isotropes Ferrogel, ein elastisches Medium, welches zusätzlich superparamagnetisches Verhalten aufweist. Ferrogele bilden eine neue Materialklasse, von der man sich Anwendungen in vielen technischen und medizinischen Bereichen erhofft. So gelten sie zum Beispiel als vielversprechende Kandidaten zur Herstellung künstlicher Muskeln oder von außen regelbarer Medien zur gezielten Wirkstofffreisetzung im Körper. Theoretisch lässt sich zeigen, dass auch die Oberfläche dieser Medien in einem angelegten Magnetfeld instabil wird, wobei die typische Wellenlänge im Vergleich zu gewöhnlichen Ferrofluiden unverändert bleibt, während die kritische Magnetfeldstärke mit wachsendem elastischen Schermodul steigt. Experimentell konnte dies bereits qualitativ bestätigt werden. Allerdings ist man in Experimenten auf sehr schwach vernetzte Gele angewiesen, da die kritische Magnetisierung anderenfalls größer als die Sätigungsmagnetisierung des elastischen Mediums ist.

Nach dem einführenden Kapitel und der Diskussion der grundlegenden hydrodynamischen Gleichungen zur Beschreibung isotroper magnetischer Gele in Kapitel 2, werden im dritten Kapitel die linearen Eigenschaften der Rosensweig Instabilität in isotropen Fer-

rogelen beleuchtet. Im Vergleich zu früheren Arbeiten beschränkt sich die Analyse nicht mehr allein auf rein elastische Medien, sondern schließt rein viskose Medien und die Kombination aus beiden mit ein. Besondere Aufmerksamkeit kommt in der Diskussion dem stationären Charakter der Rosensweig Instabilität zu. Dieser ist, wie sich herausstellt, als ein Grenzprozess zu interpretieren, bei welchem die Dynamik der charakteristischen Mode, die unterhalb der Schwelle zur Instabilität durch thermische Fluktuationen angeregt wird, mit Annäherung an die Schwelle immer stärker verlangsamt wird und schließlich zu einem statischen Oberflächenmuster führt. Als Konsequenz zeigt sich, dass man zur Berechnung der linearen Eigenvektoren ebenfalls gezwungen ist, diese zunächst für den dynamischen Fall zu berechnen und erst am Ende die entsprechenden stationären Grenzfälle zu bilden. Der Grund für dieses Grenzverhalten ist in der deformierbaren Oberfläche und im Besonderen in der daraus resultierenden kinematischen Randbedingung zu sehen. Letztere verknüpft die zeitliche Änderung der Position der Oberfläche mit der lokalen Geschwindigkeit normal zur Oberfläche. Würde man die Eigenschaft der stationären Instabilität von Beginn an verwenden, so bliebe die Oberfläche immer flach.

Kapitel 4 befasst sich schließlich mit der nichtlinearen Analyse der Rosensweig Instabilität in Ferrogelen mit Hilfe der Energiemethode. Im Jahr 1977 von Gailitis erstmals für Ferroflüssigkeiten vorgestellt, beruht die Energiemethode auf der Minimierung eines Oberflächenenergiefunktionals für verschiedene reguläre Oberflächenmuster. Die von Gailitis vorgestellte Oberflächenenergiedichte für Ferrofluide wird um die entsprechenden elastischen Energiebeiträge erweitert zu deren Berechnung die statischen Grenzwerte der linearen Eigenvektoren aus dem vorangegangenen Kapitel verwendet werden. Die resultierende Oberflächenenergiedichte wird bezüglich regulärer Streifen, Quadrate und Hexagone minimiert. Es zeigt sich, dass am Einsatz der Instabilität Hexagone das energetisch favorisierte Oberflächenmuster sind. Für hohe Magnetfeldstärken hingegen bilden Quadrate die bevorzugte Anordnung der Oberflächenstacheln. Beide Übergänge, von der flachen Oberfläche zu Hexagonen und von den Hexagonen zu Quadraten, werden von hysteretischen Regionen begleitet. Als ein wichtiger Kritikpunkt an dieser Methode wird aufgeführt, dass sie rigoros nur im Limes verschwindender magnetischer Suszeptibilitäten gültig ist, eine Voraussetzung, die für superparamagnetische Medien nicht erfüllt ist. Friedrichs und Engel erweiterten die Energiemethode für Geometrien mit endlicher Schichtdicke und diskutierten eine Abschätzung bis zu welchen magnetischen Suszeptibilitäten sinnvolle Resultate zu erwarten sind. Eine ähnliche Abschätzung wird in Kapitel 4 für magnetische Gele diskutiert. Es stellt sich heraus, dass der Gültigkeitsbereich der Energiemethode mit wachsendem Schermodul zu höheren magnetischen Suszeptibilitäten erweitert wird. Des weiteren bietet diese Methode lediglich einen energetischen Vergleich statischer Oberflächenmuster, wobei die Dynamik der Oberfläche zur Ausbildung dieser Muster und die darin involvierten dissipativen Prozesse völlig außer Acht gelassen werden. Die angesprochenen Nachteile der Energiemethode dienen schließlich als Motivation für eine schwach nichtlineare Analyse der fundamentalen hydrodynamischen Gleichungen und der Herleitung einer Amplitudengleichung.

Diesem Vorhaben ist Kapitel 5 gewidmet. Ganz besondere Beachtung verdient dabei die Bestimmung des adjungierten Systems für die Rosensweig Instabilität. Dieses ist zur Befriedigung der Fredholmschen Alternative, die wiederum die Amplitudengleichungen liefert, von zentraler Bedeutung. Frühere nichtlineare Diskussionen der Rosensweig Instabilität beschränkten sich entweder auf rein statische Gleichungen, die selbstadjungiert sind, oder auf reine Potentialströmungen, für die die Lösbarkeitsbedingung leicht

zu erfüllen ist, die aber keine spannungsfreie Oberfläche garantieren. Zur Herleitung der adjungierten Gleichungen und der dazugehörigen Randbedingungen wird zum einen die Erkenntnis aus der Diskussion der linearen Instabilität, dass das System als dynamisch zu betrachten und der statische Grenzfall erst am Ende zu vollziehen ist, benutzt. Des weiteren stellt es sich als wichtig heraus, die Gleichungen zunächst für ein kompressibles Medium zu adjungieren und ebenfalls erst am Ende die Näherung für inkompressible Medien zu bestimmen. Letztere Annahme garantiert während des Adjungierens einen symmetrischen Spannungstensor. Die physikalischen Lösungen der adjungierten Gleichungen und ihrer Randbedingungen besitzen die Eigenschaft, dass sich rechtslaufende Wellen im Originalsystem zu linkslaufenden Wellen im adjungierten System transformieren und umgekehrt.

Mit Hilfe der Lösungen des adjungierten Systems lassen sich nun die Lösbarkeitsbedingungen in der zweiten und dritten Störungsordnung erfüllen. Allerdings führen diese Bedingungen allein nicht zu den Amplitudengleichungen. Eine weitere besondere Eigenschaft der Rosensweig Instabilität ist, dass die treibende Kraft, das Magnetfeld, allein durch die Oberfläche vermittelt wird. In den hydrodynamischen Volumengleichungen äußert sich dies dadurch, dass die Magnetfeldgrößen nicht mehr auftreten und die Volumengleichungen somit von den Bestimmungsgleichungen der Magnetfeldgrößen entkoppeln. Dies ist eine direkte Konsequenz sowohl der Näherung, dass keine magnetostriktiven Effekte eine Rolle spielen, als auch der Annahme, dass das Magnetfeld auf der Zeitskala des Wachstums der Oberflächenstacheln bereits auf seinen Gleichgewichtswert relaxiert ist. Demnach enthält weder die Fredholmsche Alternative für die Volumengleichung noch die aus ihr abgeleiteten Beiträge zur Amplitudengleichung den Kontrollparameter, im vorliegenden Fall das angelegte Magnetfeld. Die Randbedingungen nehmen für die Rosensweig Instabilität eine wichtige Rolle ein. Für die Bestimmung des Kontrollparameters im Besonderen liefert die normale Randbedingung den gesuchten Zusammenhang zwischen dem Wachstum der Oberflächenstacheln und dem Kontrollparameter. Ein besonderes Merkmal der Rosensweig Instabilität besteht darin, dass nach der Ausbildung des Musters das Medium wieder vollständig zur Ruhe kommt und keine Strömungen mehr vorhanden sind. Das dynamische Verhalten wird demnach vollständig von der kinematischen Randbedingung bestimmt, die zeitliche Änderungen der Position der Oberfläche mit dem Geschwindigkeitsfeld verknüpft. Dies führt, wie gezeigt wird, zu einem unterschiedlichen zeitlichen Skalenverhalten der Lösbarkeitsbedingungen im Volumen und an der Oberfläche, welchem bei der Vereinigung der beiden Lösbarkeitsbedingungen zu einer Amplitudengleichung Rechnung getragen werden muss.

Zwei Punkte der abgeleiteten Amplitudengleichung sind besonders hervor zu heben: Zum einen ist es zum ersten Mal möglich den quadratischen Koeffizienten, dessen Existenz aus der gegebenen Symmetrie folgt, aus den fundamentalen hydrodynamischen Gleichungen abzuleiten. Dieser garantiert am Einsatz der Instabilität zum einen die Existenz von Hexagonen, zum anderen das Auftreten einer transkritischen Bifurkation. Beides sind experimentell bestätigte Eigenschaften der Rosensweig Instabilität. Zum anderen enthält die Amplitudengleichung für Ferrogele eine zweifache Zeitableitung. Diese ist proportional zum elastischen Schermodul und trägt somit der Volumenelastizität im Medium Rechnung. Die linearisierte Amplitudengleichung nimmt im Fall der Ferrogele die Gestalt eines gedämpften harmonischen Oszillators an und Störungen des ausgebildeten Oberflächenmusters zerfallen in Form einer gedämpften Schwingung. Im Fall der Rosensweig Instabilität in Ferroflüssigkeiten, deren zugehörige Amplitudengleichung ebenfalls bestimmt

wird, tritt diese zweifache Zeitableitung nicht auf.

Kapitel 6 befasst sich mit der Frage, inwieweit magnetische Membranen oder dünne Filme in einem äußeren Magnetfeld instabil werden können. Motiviert wird diese Fragestellung durch die vorangegangen Diskussionen, in denen gezeigt werden konnte, dass die treibende Kraft der Rosensweig Instabilität im Rahmen der in dieser Arbeit benutzten Näherungen allein durch die Grenzfläche vermittelt wird. Im Gegensatz zu früheren Diskussionen, in denen Filme mit variabler Dicke, insbesondere peristaltische Moden, analysiert wurden, werden hier unendlich dünne Schichten, deren beide Grenzflächen nur in Phase ausgelenkt werden können, betrachtet. Für die Behandlung unendlich dünner Schichten erweist es sich als sinnvoll so genannte Oberflächeneigenschaften der entsprechenden Medien zu definieren, wie der Oberflächenviskosität oder der Filmkompressibilität. Diese sind auf die Fläche bezogene Materialeigenschaften, die man aus den Volumeneigenschaften des entsprechenden Mediums im Grenzfall unendlich dünner Schichten berechnet. Ähnlich der Methode zur Bestimmung der viskosen und elastischen Flächenmodule wird die magnetische Flächenpermeabilität bestimmt. Dies ermöglicht es, die bereits bekannte Dispersionsrelation von Wellen in dünnen Filmen und Membranen um die entsprechenden magnetischen Beiträge zu erweitern.

Beschränkt man sich in einer linearen Stabilitätsanalyse auf den symmetrischen Fall, das heißt der isotrope Ferrogelfilm ist auf beiden Seiten vom gleichen Medium umgeben, so findet man, dass der Film linear nicht instabil werden kann. Eine intuitive Erklärung für dieses Verhalten erhält man, wenn man die Geometrie der magnetischen Feldlinien betrachtet. Diese werden an beiden Grenzflächen entgegengesetzt gebrochen. Im Grenzfall unendlich dünner Schichten verschwinden die Störfelder und mit ihnen die treibenden Feldgradienten. Eine Instabilität zeigt sich nur im Fall von anisotropen magnetischen Gelen oder im Fall eines magnetischen Kontrastes zwischen den beiden umgebenden Medien. Anisotrope Ferrogele besitzen eine interne Magnetisierung, die erzeugt wird, indem man den Vernetzungsprozess zu einem Gel in einem äußeren Magnetfeld vollzieht.

Neben der Rosensweig Instabilität besitzt auch die Marangoni Instabilität die Eigenschaft rein durch die Oberfläche getrieben zu sein. Temperaturfluktuationen auf der Oberfläche führen dort zu Fluktuationen der Oberflächenspannung, die dann wiederum Konvektion bedingen. Für die Marangoni Instabilität war ebenfalls kein adjungiertes System bekannt, das eine deformierbare Oberfläche berücksichtigt. Mit dem für das Adjungieren der Bestimmungsgleichungen der Rosensweig Instabilität entwickelten Formalismus werden im Kapitel 7 die entsprechenden adjungierten Gleichungen für die Marangoni Instabilität abgeleitet. Besondere Beachtung verdient die Marangoni Instabilität deswegen, weil die treibende Kraft tangential zur Oberfläche wirkt und somit das Komplement zur Rosensweig Instabilität bildet. Erschwert wird das Lösen der adjungierten Gleichungen jedoch durch eine Kopplung zwischen der Temperatur und dem Geschwindigkeitsfeld in den Volumengleichungen. Diese Kopplung stellt zwar nicht die treibende Kraft für die Konvektion dar, führt aber zu einer Abhängigkeit der adjungierten Eigenvektoren von den ursprünglichen Eigenvektoren. Ein ähnlich einfacher Zusammenhang zwischen den Oberflächenwellen im originalen und adjungierten System, wie im Fall der Rosensweig Instabilität, ist demnach nicht gegeben.

Chapter 1

Introduction

In this thesis we address the nonlinear description of the Rosensweig instability in isotropic magnetic gels. This introductory chapter provides the reader with the basic knowledge of the physical system under consideration and the phenomenology of the Rosensweig instability. To embed the present theoretical work in the context of nonlinear theory for the Rosensweig instability, an overview of previous investigations is presented.

1.1 Ferrofluids

One of the main constituents of magnetic gels are magnetic fluids, also referred to as ferrofluids. Ferrofluids do not exist in nature and were first produced in the 1930's as a tool to achieve a better understanding of ferromagnetism. Bitter [1] and Elmore [2] experimented with dispersed magnetic particles in a carrier liquid to visualize the magnetic field in the vicinity of the domain walls. The particle size was about $1\,\mu m$ and the method was based on the enhanced sedimentation process of the magnetic particles in regions with high field gradients. The development of modern ferrofluids for industrial and medical application was pioneered in the 1960's by Rosensweig [3].

These modern ferrofluids are colloidal suspensions of nanometer sized (the diameter is about $10\,nm$) ferromagnetic monodomain particles in a suitable carrier liquid. Due to the magnetic dipole-dipole interaction the particles tend to coagulate to form large aggregates that in turn are subject to sedimentation. To prevent them from coagulation the particles are either coated by polymers or they are charged. In the former case the steric hindrance due to the polymer tails prevents them from approaching each other close enough so that thermal fluctuations are still stronger than the attractive dipole-dipole interaction. In the latter case the repulsive Coulomb interaction overcomes the attractive dipole-dipole interaction. A schematic cartoon of a ferrofluid stabilized by a polymer coating can be viewed on the left hand side of fig. 1.1.

If a magnetic field is applied, the initially randomly oriented magnetic dipoles align parallel to the magnetic field on average and give a paramagnetic response analogous to usual paramagnetic materials. The measured permeability is of the order of 1 to 10 and therefore much higher than for usual substances showing paramagnetism. The behavior in external fields is therefore also referred to as superparamagnetism. On a microscopic level, the magnetic particles are thought to form structured aggregates such as columns (cf. the right hand side of fig. 1.1) or drops [4, 5, 6]. If the applied magnetic field is switched off again, the magnetization can relax in two different ways [3]. Either the relaxation is
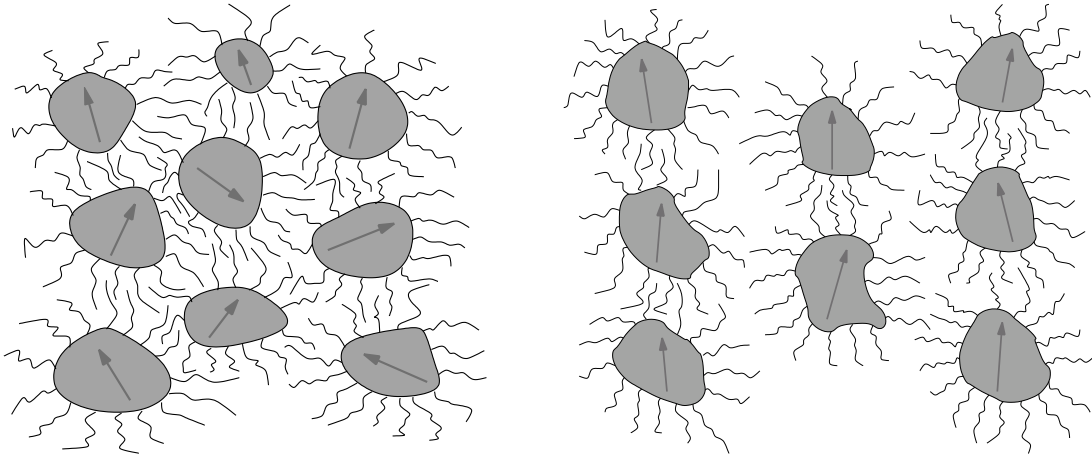
Figure 1.1: On the left: A sketch of a ferrofluid. The magnetic particles of nanometer size are coated by polymers to prevent coagulation. Without an external magnetic field, the direction of the intrinsic magnetic moments is distributed randomly. On the right: If a magnetic field is applied, the magnetic moments align preferentially to the field direction and columns are likely formed.

due to the reorientation of the magnetic particle itself with fixed particle magnetization, or the reorientation is achieved without a rotation of the particle but is solely due to an intrinsic reorientation of the dipole moment. The former case is referred to as the Brown relaxation and the latter case as Néel relaxation [3], but in real ferrofluids typically a combination of both relaxation modes is realized.

Modern ferrofluids find applications in technical as well as in medical areas. In computer hard drives, for example, ferrofluids are used as lubricants that are kept in place by magnetic forces which compensate for the gravitational field. In dampers they act as a damping agent, tunable in strength by varying an applied magnetic field. In medical applications they are good candidates for cancer therapy in the context of hyperthermia [7] or in the context of controlled drug release [8], as contrast agents for magnetic resonance spectroscopy or as tracers for relaxational measurements [9].

1.2 Ferrogels

Starting a cross-linking process in a mixture of a ferrofluid and a polymer solution with cross-linking agents, a superparamagnetic elastic medium, called ferrogel, is obtained. Magnetic gels combine the properties of usual ferrofluids with those of gels, known for example from [10, 11]. It is important to stress, that typically the surfactant polymers that stabilize the colloidal suspension do not contribute to the elastic network. The development of magnetic gels was pioneered by Zrínyi starting in 1996 [12] and they are now known as promising candidates for artificial muscles in technical and biomedical applications. As in standard ferrofluids, the magnetic moments of the nanoparticles are oriented randomly if no external field is applied. This situation is depicted on the right hand side of fig. 1.2. Exposed to an external magnetic field, a similar superparamagnetic response is measured as known from ferrofluids. In both cases, the magnetization in the medium can be described by a Langevin function in terms of the applied magnetic field.
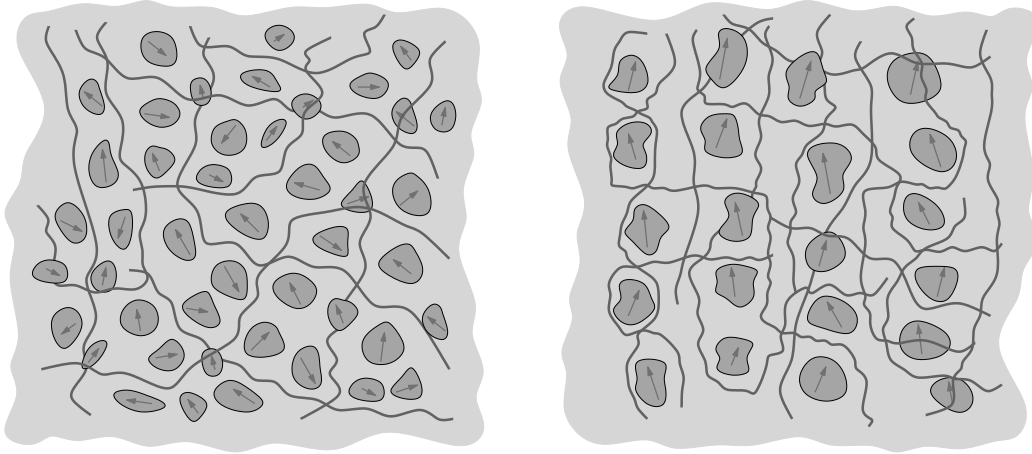
Figure 1.2: On the left: A sketch of an isotropic magnetic gel (the polymer coating is not drawn here). The magnetic nanoparticles are embedded in a polymer network. The directions of the magnetic moments are distributed randomly. On the right: If a magnetic field is applied during the crosslinking process, the aligned magnetic particles remain fixed in the polymer network and a permanent magnetization results.

Recently, magnetic gels have been produced, where the elastic network was not obtained by covalently cross-linked polymers but rather by physically linked ones. The resulting thermoreversible magnetic gel [13] shows a similar superparamagnetic response but has a temperature dependent shear modulus.

Instead of crosslinking the ferrogel in the absence of an externally given magnetic field, one could also start the cross-linking process with a magnetic field applied. The result is an elastic medium that stores a net magnetization even if the magnetic field is switched off again. Schematically the situation can be interpreted as depicted on the right hand side of fig. 1.2, where the addressed columns of magnetic particles are fixed within the elastic network. The detailed mechanism of how the average direction of the magnetic moments can be maintained is, however, not yet fully understood. The first anisotropic magnetic gels based on ferrofluids were synthesized independently by the Zrínyi group in Budapest [14] and by Collin et al. in Strasbourg [15][1]. The former group used a ferrofluid with a very high content of magnetic particles and were thus able to observe qualitatively an anisotropic magnetic, an anisotropic mechanical as well as an anisotropic swelling behavior. The Strasbourg group used a commercial ferrofluid with a smaller content of magnetic particles but was able to analyze carefully the quantitative anisotropic properties of the magnetic gel using piezo-rheometry (the experimental setup is described in [17, 18]). In their case anisotropic magnetic as well as anisotropic optical properties were observed, but no mechanical anisotropy could be measured. The described anisotropic ferrogels will be of particular interest in chapter 6, where we will discuss the stability of thin films and membranes.

---

[1]Actually, a first attempt to obtain elastic media showing a frozen-in magnetization has been undertaken earlier by Mitsumata et al. in 2002 [16]. However, the magnetic particle size in their case was in the order of $1\,mm$ and therefore in the range of typical magnetorheological fluids rather than of ferrofluids. As a consequence the resulting medium was extremely inhomogeneous and sometimes showed a preferred direction even without applying a magnetic field during the preparation process.

Figure 1.3: The experimental realization of the Rosensweig instability. On the left hand side the applied magnetic field (applied normal to the surface) is below the critical value whereas the picture on the right hand side is taken beyond the critical value. The containers diameter is of the order of 20 cm and the height as well as the diameter of the spikes is in the order of 1 cm.

1.3 The Rosensweig instability

The Rosensweig or normal field instability describes the phenomenon of a flat ferrofluid surface becoming unstable in an external magnetic field. The experimental setup consists of a Petri-dish filled with a ferrofluid which develops a flat surface in earth's gravitational field (as given in the photograph on the left of fig. 1.3). If one applies a homogeneous magnetic field oriented parallel to the surface normal, this flat surface becomes unstable beyond a certain critical magnetic field strength and a regular pattern of surface spikes arises (as seen on the right of fig. 1.3). Experimentally one observes a hexagonal arrangement of these surface spikes at the linear threshold [19].

With its discovery in 1967 [19] a first theoretical description for the normal field instability was given which allowed the determination of the critical magnetic field and the most unstable mode at onset in terms of the fluid properties. The model considered the force balance at the free surface between the stabilizing forces of surface tension and gravitation and the destabilizing magnetic force. Although the homogeneous magnetic field does not generate a force in the first place, the occurrence of surface perturbations render the local magnetic field inhomogeneous resulting in a local Kelvin force that drives the instability.

For a magnetic gel rather than a ferrofluid, the surface was also predicted to become unstable [20]. Additionally, however, the stabilizing elastic force has to be overcome by the magnetic field, which is why its critical value is shifted towards higher field strengths. The characteristic mode at onset, however, remains the same compared to usual ferrofluids and is given by the capillary mode. Recently the threshold shift has qualitatively been shown experimentally for a thermoreversible magnetic gel at the University of Bayreuth [21]. Since, however, the threshold magnetic field increases with increasing shear modulus, one is restricted to very weak gels, otherwise the threshold magnetization is higher than the saturation magnetization of the medium. To maintain a finite and constant shear modulus of the thermoreversible gel and to avoid creep flow, a time dependent magnetic field was applied which complicates the comparison between the experiments and theory.

At the moment more accurate experimental results can be obtained using inverse ferrofluids [22, 23, 24]. One calls a ferrofluid inverse, if non-magnetic particles are also dispersed in the ferrofluid. Usually the particles' diameter is of the order of micrometers and they are typically made of polystyrene. The onset of the Rosensweig instability in these fluids is shifted to higher magnetical field strengths, which cannot be solely explained

by dilution effects [25], but probably requires the assumption of a finite effective shear modulus, which may be responsible for the threshold shift.

Fig. 1.3 shows that a ferrofluid is a darkish brown, non-transparent medium and for this reason quantitative experimental results of nonlinear patterns are difficult to obtain optically. For supercritical magnetic field strengths the properties of the most unstable mode and its growth rate have been discussed theoretically as well as experimentally in [26, 27]. In 1984 Bacri and Salin [28] discovered the hysteretic nature of the transition between the flat surface and surface spikes. They used a very thin container ($\approx 200\,\mu m$) where the arising pattern was quasi one dimensional. This allowed the observation of the instability from the side exploiting the optical contrast between the magnetic fluid and the medium above. Using radioscopic methods [29], the hysteretic region between the flat surface and hexagons was accurately measured [30]. If the magnetic field is increased further, the hexagonal pattern is found to be unstable with respect to regular squares. Also this transition is accompanied by a hysteretic region and is experimentally discussed in [31, 32].

Experiments on the nonlinear regime for the Rosensweig instability in ferrogels have recently been started, but up to now no publications are available.

1.4 Nonlinear theoretical descriptions for the Rosensweig instability

Since its discovery, the Rosensweig instability has attracted the attention of experimentalists and theoreticians, alike. The work of the experimental scientists together with an intuitive linear description has been introduced in the previous section. A linear analysis, however, gives us no information about the amplitude and the spatial structure of the arising pattern nor on the nonlinear dynamic behavior. This is why nonlinear discussions of the governing basic equations are needed which will be the aim of this thesis. In the following the reader will find an introduction to previous nonlinear discussion of the normal field instability in ferrofluids.

1.4.1 The energy method

The energy method was the first attempt to theoretically access the nonlinear regime of the Rosensweig instability and was published in 1977 by Gailitis [33]. Gailitis discussed laterally unbounded ferrofluid layers of infinite depth. The application of this method to systems with a finite depth was later done by Friedrichs and Engel in [34]. The general idea of this energy-based approach is to find the dependence of the surface energy density of the fluid as a function of the surface deflection, the applied magnetic field, and the material parameters of the ferrofluid except for the viscosity, which has to be neglected completely in this approach. This energy density functional can then be minimized with respect to prescribed surface patterns. The patterns considered by Gailitis were regular stripes, squares and hexagons. The relative stability of which can then be given as a function of the applied magnetic field.

Gailitis found, that stripe patterns are always unstable with respect to one of the other two patterns. Below the linear threshold the flat surface is always a stable configuration whereas at the linear onset hexagons turn out to be energetically favored. Upon further

increase of the magnetic field, however, the hexagons become unstable with respect to squares and the previous hexagonal pattern transforms into a square pattern. Both transitions are found to be accompanied by hysteretic regions. In that respect the theoretical results qualitatively match the experimental findings. For finite fluid layer depths, the critical values for the magnetic field are shifted to higher strengths and the hysteretic behavior of both transitions becomes more pronounced [34].

In chapter 4 we will apply the energy method to the Rosensweig instability in isotropic magnetic gels to obtain a first estimate of the nonlinear patterns arising in ferrogels. However, there are severe drawbacks to this method. Therefore one has to use more fundamental methods to discuss the nonlinear regime.

1.4.2   Functional analysis approaches

The first approaches considering the basic hydrodynamic equations have been discussed by Twombly and Thomas [35, 36] and later on by Silber and Knobloch [37]. Both groups considered only static hydrodynamic equations under the condition that the velocity vanishes, reducing the Navier-Stokes equation to the hydrostatic pressure contribution. In this approximation the stress free surface is governed by the normal stress boundary condition whereas the tangential boundary conditions are trivially satisfied. Additionally, the static Maxwell equations were considered with the corresponding boundary conditions. This set of fundamental equations and boundary conditions is then expanded in terms of ϵ (the normalized difference between the applied magnetic field and the critical one) following the ideas of [38]. Since no time derivative is involved in the set of equations, it turns out to be self-adjoint and the solvability conditions in the higher orders of the expansion can be fulfilled. As stated by Silber and Knobloch [37], no stable pattern was found at the linear onset for realistic magnetic permeabilities. Another drawback of this method is, since it rests on the static assumption, that it cannot give predictions for the nonlinear dynamics in terms of an amplitude equation and that it neglects the possibility of oscillatory instabilities.

A different approach, using again the static approximation for the macroscopic set of equations, was presented by Friedrichs and Engel in 2003 [39]. In their discussion they focused on the normal stress boundary condition only. Inspired by [40], where it is shown that for a strong enough tangential component of the magnetic field two dimensional patterns can be suppressed and only stripes are the stable solution, they focused on the nonlinear discussion of stripes only.

Malik and Singh [41, 42, 43] were the first to discuss an $\epsilon-$expansion of the fundamental hydrodynamic equations allowing for dynamic processes. To circumvent the general solvability condition for the higher orders of the expansion, where one needs to know the adjoint system of equations, they restricted their discussion to potential flow only. This is an unphysical approximation, as we will see later on in our discussion, since only the vorticity contributions to the flow can guarantee that the tangential boundary conditions at the free surface are satisfied.

1.4.3   The Swift-Hohenberg approach

To compensate for the lack of dynamic descriptions, Kubstrup, Herrero and Pérez-García discussed the normal field instability in terms of a phenomenological Swift-Hohenberg

equation [44, 45]. In particular, they discussed the dynamics of stable fronts between hexagons and squares. A general ansatz for the surface deflection, which is not so different from the one used in the energy method approach, is substituted into a generalized Swift-Hohenberg equation and a set of amplitude equations is obtained. These amplitude equations are then solved numerically. This approach nicely reveals the stability dynamics between hexagons and squares in the nonlinear regime, but only on a phenomenological basis. The main disadvantage of this study is, that the coefficients in the amplitude equation have no relation whatsoever to real material properties. Nevertheless, a good qualitative agreement can be obtained fitting the phenomenological coefficients to the experimental results [31].

1.4.4 Numerical results

The methods discussed so far describe the dynamics of the Rosensweig instability in the weakly nonlinear regime. These methods allow one to discuss the dynamics and the arising pattern close to the threshold as long as the amplitudes stay small. A prediction of the final shape of a single surface spike cannot be obtained by these methods. Using a finite element method, Lavrova et al. determined the shape of one of the surface spikes [46] by integration of the basic hydrodynamic equations. In [30] the experimental and numerical results were compared and a very good agreement was observed.

1.5 The adjoint system and deformable surfaces

At a closer inspection of section 1.4.2 and the nonlinear approaches discussed therein, it is clear that there is still a crucial piece missing in the description of the nonlinear regime of the Rosensweig instability in the spirit of [38, 47, 48], namely the knowledge of the adjoint system of equations together with its boundary conditions. A first attempt to derive this was made by Lange in [49] who used a particular form of a scalar product known from discussions of the Marangoni instability. The attempt failed since this scalar product rests on the assumption of an undeformable surface; an assumption not appropriate for the case of the Rosensweig instability. In the presence of a deformable surface and for a dynamic system, the adjoint system with its boundary conditions was unknown. A detailed discussion and the derivation is given in this thesis in section 5.2.

As indicated already in the previous paragraph, the Rosensweig problem is not the only instability that involves a deformable surface. Another very prominent phenomenon, the Marangoni convection, sensitively depends on the deformability of the surface [50, 51]. In the Marangoni convection, small temperature fluctuations at the interface between the underlying fluid and the medium above induce fluctuations of the local surface tension that in turn cause the surface to deform. An analytical weakly nonlinear description for the Marangoni convection accounting for the deformability of the surface is still missing. Many authors [52, 53, 54, 55, 56] treated the nonlinear system assuming a flat undeformed boundary between two fluids. The reason is mainly due to the missing solution of the adjoint system in the presence of a deformable surface. The case of the Marangoni instability is of particular interest to us, since in contrast to the Rosensweig instability, the driving force of the instability acts purely tangentially to the surface. The method we used to derive the adjoint system for the Rosensweig instability can therefore be used for
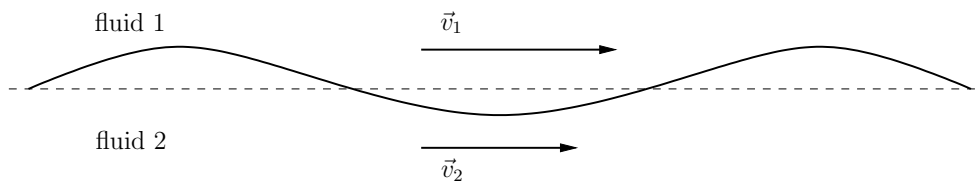
Figure 1.4: A qualitative sketch of the geometry appropriate for the Kelvin-Helmholtz instability. Two fluids move at different velocities with respect to each other. The initially flat interface becomes unstable against deformation beyond a critical velocity difference.

any arbitrary direction of the driving force.

A further situation where a deformed boundary becomes important for the nonlinear regime and more precisely, where the actual position of the boundary depends on the dynamics of the system as a whole, is the Faraday instability. Certain modes become unstable upon periodic normal vibrations of the medium. The weakly nonlinear analysis of this problem also crucially depends on the knowledge of the adjoint system. We will not deal with this phenomenon since a comprehensive nonlinear study of this problem has been given recently by Skeldon and Guidoboni in [57].

Two further examples where the deformability of the boundary is essential in the nonlinear regime are given by the Rayleigh-Taylor instability and the Kelvin-Helmholtz instability. In the Rayleigh-Taylor problem the stability of a denser liquid on top of a lighter liquid, both subject to a gravitational field, is analyzed. In the Kelvin-Helmholtz problem the stability of the interface between two fluids that move with different velocities with respect to each other is discussed (cf. fig. 1.4). The latter problem is of particular interest for the creation of low pressure systems in the global weather system as it occurs in the atmosphere at the boundary between the air at the cold polar caps and the west wind zone. The method we applied in finding the adjoint system for the Rosensweig and the Marangoni case can also be applied to these systems.

1.6   The scope of this thesis

The nonlinear behavior of the Rosensweig instability either in ferrofluids or in magnetic gels still contains many unsolved questions. In this thesis I will focus on the nonlinear analytic description of these phenomena in ferrogels putting particular attention on the derivation of the amplitude equation. A crucial step for this derivation will be the determination of the adjoint system with its boundary conditions. To set the stage for the special properties of the Rosensweig instability, we will extensively discuss the linear behavior and the possible patterns arising in the nonlinear regime using the energy method. In addition we will discuss the obtained amplitude equation for the special case of ferrofluids, because also in this case the amplitude equation derived from the basic hydrodynamic equations is still unknown. Since the boundary conditions play an important role in the discussion, we will also deal with thin films and membranes and discuss their linear stability properties in external magnetic fields. To conclude, our considerations are applied to derive the adjoint system of equations for the Marangoni instability.

Chapter 2

Macroscopic mathematical framework

In order to give a comprehensive theoretical description of the Rosensweig instability in isotropic ferrogels, we first have to define the physical and mathematical framework. We know, from experimental results, that the typical length scale of the instability is of the order of centimeters and the typical growth of the surface spikes takes place on a rather long time scale, say seconds (the growth can be followed by the naked eye). This suggests a viewpoint where we consider the medium continuous and macroscopic. The most suitable theory we can use is thus the generalized hydrodynamic theory [58, 59]. In this chapter the hydrodynamic approach will be introduced and we discuss the basic set of hydrodynamic equations one obtains for isotropic magnetic gels. This part is mainly based on, and summarizes, the results of the work of Jarkova et al. [60] and will be the basis for the nonlinear discussion. Additionally we specify the simplifications and extensions of this general set of equations that are appropriate for the Rosensweig instability.

2.1 The basic hydrodynamic equations

The generalized hydrodynamic approach utilizes simple symmetry and thermodynamic arguments to derive a general set of dynamic equations for certain macroscopic variables. These variables have to be identified for the particular system under consideration and this particular choice dramatically reduces the number of degrees of freedom one takes into account. In a microscopic description, for instance, one might model atoms of a certain species as point masses interacting with each other via specified potentials. To consider systems of macroscopic size like a glass of water, however, the number of point masses needed to model this system is of the order of Avogadro's constant. In fact, too many degrees of freedom to be handled. In a macroscopic theory one considers the mass density field instead, which reduces the number of free variables drastically. Calculating macroscopic properties of the system becomes feasible.

One big advantage of the hydrodynamic method is given by its generality, which allows its application to a vast number of systems as long as we are able to treat these systems macroscopically. However, since we average over very many degrees of freedom, phenomenological coefficients have to be introduced that are specific for the particular system. One of these phenomenological coefficients is, for example, the well known heat

conductivity. These coefficients contain the information of all the microscopic processes taking place in the medium, and they could theoretically be determined via Green-Kubo relations if all microscopic processes were known, but practically this is only possible in some limiting cases, as, for example, small densities. Therefore these coefficients are usually taken from experimental measurements.

2.1.1 Different classes of macroscopic variables

One can distinguish three different classes of macroscopic variables. The first class includes variables associated with global conservation laws. Assume a system with a conserved quantity, which by definition cannot decay or grow locally but which is allowed to be transported. The equilibration of this conserved quantity at different positions in space takes the longer, the farther these two positions are separated from one another. In reciprocal space this statement can be expressed as: the frequency of a process tends to vanish ($\omega \to 0$) if its wavenumber vanishes ($k \to 0$). This is exactly the mathematical formulation of the hydrodynamic limit which rests on the fact, that historically hydrodynamics dealt with conserved quantities.

The second class of variables, as a first generalization of hydrodynamics, includes variables that are connected to spontaneously broken continuous symmetries. What we refer to as a broken symmetry is the possibility that the Hamiltonian of a system is of higher symmetry than its eigenstates. One of the best known examples for this phenomenon is ferromagnetism, where the Hamiltonian is indeed invariant under rotation although there is an easy axis assigned to the system which is reflected in the eigenstates. In general there is no conserved quantity connected to this kind of variables (ferromagnetism is an exceptional case where the magnetization is a conserved quantity) [59], but they allow for excitations with infinite lifetime in the long wavelength limit, the so called Goldstone modes [59]. Therefore it seems reasonable to additionally include these variables into a macroscopic description.

The third and final class accounts for variables connected to microscopic degrees of freedom whose dynamics takes place on a timescale large enough that it enters the macroscopic regime. Consequently one can include these specific microscopic degrees of freedom into the macroscopic description. Otherwise the validity of the description would be restricted to time scales even larger to guarantee that this specific variable has relaxed to its equilibrium value. But it is worth mentioning, that these variables do not show the hydrodynamic limit, $\omega \not\to 0$ if $k \to 0$, and long wavelength excitations with a finite frequency may be retained. While the identification of the variables of the first two classes is completely systematic, the identification of variables of this last class is not straightforward and involves a deeper knowledge of the system.

2.1.2 Continuity and balance equations

If the macroscopic variables of a particular system are specified, one can turn to the derivation of equations that describe the dynamics of these variables. Assume first a macroscopic system in global thermodynamic equilibrium. The state of the system is then completely given by the numerical values of the macroscopic variables and one can define a thermodynamic potential that is a function of these macroscopic variables. Changes of the potential as a function of the macroscopic variables are related by the first law of

thermodynamics. In the following formulation E represents the internal energy, T the temperature, S the entropy, p the pressure, V the volume, μ the chemical potential and N the number of particles

$$dE \;=\; TdS - pdV + \mu dN \tag{2.1}$$

The conjugated fields T, p and μ can be obtained by partial differentiation of the energy density with respect to the associated variable while the other variables are kept constant. With the help of Euler's relation we can take the thermodynamic limit $V \to \infty$ and eliminate the volume from (2.1) which gives the local manifestation of the first law of thermodynamics [58]

$$d\varepsilon \;=\; Td\sigma + \mu d\rho \tag{2.2}$$

where ε and σ denote the energy density and the entropy density, respectively.

In the scope of a generalized hydrodynamic approach where we additionally account for variables associated with broken continuous symmetries and slowly relaxing variables, the Gibbs relation (2.2) also has to be generalized. This can be done by exploiting the fact that (2.2) is a total differential which allows one to introduce conjugated fields associated to the additional macroscopic variables. However, we then need the functional dependence of the energy density on the additional macroscopic variables. In our discussion we will always assume, that the system is close to thermodynamic equilibrium. This allows us to expand the energy density in terms of the macroscopic variables and their gradients. In order to do so, we have to consider the characteristics of the energy density. The equilibrium state is a stable state so that we have to provide a convex functional dependence. Furthermore the energy density should be invariant under inversion of space and time, under rigid translation and rigid rotation and it should be covariant upon Galilean transformation.

If the system is close to thermal equilibrium, it will try to achieve the equilibrated state by dynamical processes. For the first class of variables the corresponding expressions can be derived easily exploiting the fact, that they represent conserved quantities in the system. Let us assume a scalar field α which is the volume density of a conserved quantity with its corresponding flux density $\mathbf{j}^\alpha$. Since the amount of this particular quantity in an arbitrary volume V is conserved, temporal changes of this amount have to be balanced by a flux through the closed bounding surface of that volume. Mathematically speaking one observes

$$\frac{d}{dt} \int_V \alpha dV \;=\; -\oint_{\partial V} \mathbf{j}^\alpha \cdot d\mathbf{f} \tag{2.3}$$

where $d\mathbf{f}$ represents the surface area element of the closed surface[1]. Using Gauss' theorem one can transform the last expression into its local form and obtain the continuity equation for the macroscopic variable α

$$\frac{\partial}{\partial t}\alpha + \nabla \cdot \mathbf{j}^\alpha \;=\; 0 \tag{2.4}$$

---

[1]Throughout this thesis vectors are displayed in bold and their components using latin letters as indices, ∇ denotes the vector $\nabla = (\partial_x, \partial_y, \partial_z)$ and we will imply summation over repeated indices except otherwise stated. In the latter context δ_{ij} is the Kronecker symbol and ϵ_{ijk} the Levi-Cevità tensor.

What we are left with is to find an explicit expression for the flux density $\mathbf{j}^\alpha$ which can be constructed as a power series in terms of the thermodynamic forces (usually the gradients of the conjugated fields), where the same symmetry arguments have to be applied as in the case of the energy density. Usually one can distinguish two different types of contributions to the currents: One contribution that accounts for reversible processes preserving the entropy density and one contribution due to the irreversible processes that lead to an increase of entropy. For a set of macroscopic variables usually cross-coupling contributions are allowed, for example in a binary fluid mixture an applied temperature gradient not only causes a heat flux but also a concentration flux. Onsager stated [61, 62, 63], that in these cases the corresponding symmetric contributions have to be present as well. Picking up the last example, this corresponds to a heat flux caused by an applied concentration gradient.

For the other two kind of variables a straightforward derivation of the dynamic equations is not possible. However one can assume a similar dynamical behavior balancing the temporal change of the variable with a so called quasi current

$$\partial_t \beta + X^\beta \;\; = \;\; 0 \tag{2.5}$$

The quasi current itself can be constructed in the same way as the currents for the conserved macroscopic variables.

2.1.3   The case of isotropic ferrogels

We can now apply the hydrodynamic method discussed in the previous section to the special case of isotropic magnetic gels. The first derivation of the generalized hydrodynamic equations was given by Jarkova et al. [60]. We will follow their work and give their results needed for the discussion of the Rosensweig instability.

The energy functional and the Gibbs relation

We start with the identification of the macroscopic variables. In the case of isotropic magnetic gels, the first class of variables consists of the mass density ρ, the momentum density $\mathbf{g}$, the energy density ε and the concentration of the magnetic particles c. To account for the elastic degrees of freedom we introduce the elastic strain field ϵ_{ij} which belongs to the second class of variables. The strain field in amorphous solids is derived from crystals, where the long ranged positional order gives rise to the displacement vector field $\mathbf{u}$ as a hydrodynamic symmetry variable. In our description we will restrict ourselves to linear elasticity $\epsilon_{ij} = \frac{1}{2}(\partial_i u_j + \partial_j u_i)$. In usual ferrofluids the magnetization relaxes to the equilibrium value set by the external magnetic field. The appropriate relaxation time is much larger than all the other microscopic time scales. The same is true in magnetic gels. Therefore the magnetization $\mathbf{M}$ is taken as an additional macroscopic variable belonging to the third class of macroscopic variables[2]. The transformation behavior under time ϵ^T and spatial ϵ^P inversion is summarized in table 2.1.

In thermodynamic equilibrium all macroscopic variables are relaxed to their equilibrium values and one finds the Gibbs relation that relates infinitesimal changes of the

---

[2]The dynamics of the Rosensweig instability takes place on a time scale larger than the time scale of the dynamics of the magnetization. In that special case it is sufficient to exclude the magnetization again from the macroscopic dynamics as will be done in section 2.2.1.

macroscopic variable	time inversion ϵ^T	spatial inversion ϵ^P
ρ	$+1$	$+1$
ε	$+1$	$+1$
c	$+1$	$+1$
g_i	-1	-1
ϵ_{ij}	$+1$	$+1$
M_i	-1	$+1$

Table 2.1: *Table of the macroscopic variables important for the description of isotropic magnetic gels with their transformation behavior under time and spatial inversion*

macroscopic variables to infinitesimal changes of the entropy density σ

$$d\varepsilon = Td\sigma + \mu d\rho + \mu_c dc + v_i dg_i + H_i dB_i + h_i^M dM_i + \Psi_{ij} d\epsilon_{ij} \tag{2.6}$$

The corresponding thermodynamic conjugated fields are the temperature T, the chemical potential μ, the relative chemical potential μ_c, the velocity $\mathbf{v}$, the magnetic molecular field h_i^M and the elastic stress Ψ_{ij} and are defined as partial derivatives of the energy density with respect to the appropriate variable whilst the others are kept constant. The magnetic flux density $\mathbf{B}$ together with the magnetic field $\mathbf{H}$ have been introduced to account for the static Maxwell equations in our discussion.

In order to give explicit expressions for the thermodynamic conjugated variables introduced above and to determine the thermodynamic forces we have to give an explicit expression for the energy density. Assuming an expansion around the equilibrium value one finds

$$\begin{aligned}
\varepsilon = \ & \varepsilon_0 + \frac{1}{2}B^2 - \mathbf{B} \cdot \mathbf{M} + \frac{1}{2}\mu_{ijkl}\epsilon_{ij}\epsilon_{kl} - \frac{1}{2}\gamma_{ijkl}M_iM_j\epsilon_{kl} + \frac{1}{2}\alpha M_i^2 \\
& + \epsilon_{ii}(\chi^\rho\delta\rho + \chi^\sigma\delta\sigma + \chi^c\delta c)
\end{aligned} \tag{2.7}$$

where ε_0 represents the energy density of a binary fluid mixture. The coefficient α accounts for the dependence of the induced magnetization on the state of the medium, for example its temperature. Additionally α is a function of the applied magnetic field modeling the nonlinear magnetization behavior. In eq. (2.7) one can clearly distinguish the contributions due to the magnetic energy, the elastic energy, the cross coupling of the latter and the coupling between compression and the scalar field variables. Truncated at the quadratic order, this expansion is only valid for small elastic deformations of the medium. For large deformations one should extend the expansion to higher orders of ϵ_{ij} accounting for nonlinear elastic deformations. The elasticity tensor μ_{ijkl} and the magnetostrictive tensor γ_{ijkl} take the isotropic form where we give, as an example, the elasticity tensor

$$\mu_{ijkl} = \mu_1\delta_{ij}\delta_{kl} + \mu_2\left(\delta_{ik}\delta_{kl} + \delta_{il}\delta_{jk} - \frac{2}{3}\delta_{ij}\delta_{kl}\right) \tag{2.8}$$

with its two invariants given by the elastic compressibility μ_1 and the elastic shear modulus μ_2.

With the help of equations (2.6) and (2.7) one can give explicit expressions for the thermodynamic conjugated variables. The determination of the magnetic field **H** then provides the usual relation

$$H_i \;=\; \left(\frac{\partial \varepsilon}{\partial B_i}\right)_{\mathbf{M},\epsilon_{ij},\dots} = B_i - M_i \tag{2.9}$$

whereas one finds for the magnetic molecular field $\mathbf{h}^M$

$$h_i^M \;=\; \left(\frac{\partial \varepsilon}{\partial M_i}\right)_{\mathbf{B},\epsilon_{ij},\dots} = -B_i - \gamma_{ijkl}M_j\epsilon_{kl} + \alpha M_i \tag{2.10}$$

In the same manner one can give the elastic stress tensor Ψ_{ij} as

$$\Psi_{ij} \;=\; \left(\frac{\partial \varepsilon}{\partial \epsilon_{ij}}\right)_{\mathbf{M},\mathbf{B},\dots} = \mu_{ijkl}\epsilon_{kl} - \frac{1}{2}\gamma_{ijkl}M_kM_l + \delta_{ij}(\chi^\rho\delta\rho + \chi^\sigma\delta\sigma + \chi^c\delta c) \tag{2.11}$$

As already discussed in the previous section, the dynamic equations for the macroscopic variables of the first class can be derived in a straightforward manner from the fact that they are related to conserved quantities of the system. The dynamic equations for the macroscopic variables of the other two classes are chosen such that they resemble the structure of the previous ones. For the system of isotropic magnetic gels one deduces a set of dynamic equations

$$\partial_t\rho \,+\, \partial_i g_i = 0 \tag{2.12}$$

$$\partial_t\sigma \,+\, \partial_i(\sigma v_i) + \partial_i j_i^\sigma = \frac{R}{T} \tag{2.13}$$

$$\rho\partial_t c \,+\, (\rho v_i\partial_i)c + \partial_i j_i^c = 0 \tag{2.14}$$

$$\partial_t g_i \,+\, \partial_j\{v_j g_i + \delta_{ij}[p + \mathbf{B}\cdot\mathbf{H}] + \sigma_{ij}^{th} + \sigma_{ij}\} = 0 \tag{2.15}$$

$$\partial_t M_i \,+\, (v_j\partial_j)M_i + (\mathbf{M}\times\omega)_i + X_i = 0 \tag{2.16}$$

$$\partial_t\epsilon_{ij} \,+\, (v_k\partial_k)\epsilon_{ij} + Y_{ij} = 0 \tag{2.17}$$

where $\mathbf{j}^\sigma$ denotes the entropy current, $\mathbf{j}^c$ the concentration current of magnetic particles, σ_{ij} is the stress tensor and $\mathbf{X}$ and Y_{ij} denote the quasicurrents for the magnetization and the strain field, respectively. The vorticity $\vec{\omega}$ is given by $\omega_i = \frac{1}{2}\epsilon_{ijk}\partial_j v_k$ while σ_{ij}^{th} is given by

$$\sigma_{ij}^{th} \;=\; -\frac{1}{2}(B_iH_j + B_jH_i) + \frac{1}{2}(\Psi_{jk}\epsilon_{ki} + \Psi_{ik}\epsilon_{kj}) \tag{2.18}$$

In eq. (2.17) the assumption of a linear elastic medium has already been made. For a comprehensive description on nonlinear elastic properties of soft matter systems, the reader is referred to [64, 65, 66, 67, 68].

The Gibbs-Duhem relation, relating the thermodynamic pressure to the conserved quantities is given as

$$p \;=\; -\varepsilon + T\sigma + \mu\rho + \mathbf{g}\cdot\mathbf{v} \tag{2.19}$$

Equation (2.13) contains a source term R/T accounting for the entropy production needed for the dissipative processes. The second law of thermodynamics requires the dissipation functional R (a Lyapunov functional) either to vanish for reversible processes or to be positive for irreversible processes. The explicit expression for R can be obtained as a series expansion in terms of the thermodynamic forces applying the same symmetry arguments as for the energy density.

One is left with the determination of explicit expressions for the currents and quasi-currents which is done in the subsequent sections.

Irreversible dynamics

In the case of isotropic magnetic gels the Lyapunov functional R is given, up to second order, by

$$
\begin{aligned}
R &= \frac{1}{2}\kappa(\partial_i T)^2 + \frac{1}{2}\nu_{ijkl}A_{ij}A_{kl} + \frac{1}{2}D(\partial_i \mu_c)^2 + \frac{1}{2}b(h_i^M)^2 \\
&\quad + \frac{1}{2}\xi(\Psi_i)^2 + D^T(\partial_j T)(\partial_j \mu_c) + \Psi_i\left(\xi^T \partial_i T + \xi^c \partial_i \mu_c\right)
\end{aligned}
\tag{2.20}
$$

where the coefficients κ, D and D^T denote the heat conduction, diffusion and thermodiffusion, respectively. The tensor ν_{ijkl} represents the viscosity tensor which again takes the isotropic form

$$
\nu_{ijkl} = \nu_1 \delta_{ij}\delta_{kl} + \nu_2\left(\delta_{ik}\delta_{kl} + \delta_{il}\delta_{jk} - \frac{2}{3}\delta_{ij}\delta_{kl}\right)
\tag{2.21}
$$

with ν_1 being the compressional viscosity and ν_2 the shear viscosity. The dissipative contributions to the currents and quasicurrents are derived by taking the partial derivative of the dissipation function R with respect to the appropriate thermodynamic force. Finally one obtains

$$
j_i^{\sigma D} = -\kappa \partial_i T - D^T \partial_i \mu_c - \frac{1}{2}\xi^T \Psi_i
\tag{2.22}
$$

$$
j_i^{cD} = -D\partial_i \mu_c - D^T \partial_i T - \frac{1}{2}\xi^c \Psi_i
\tag{2.23}
$$

$$
\sigma_{ij}^D = -\nu_{ijkl}A_{kl}
\tag{2.24}
$$

$$
Y_{ij}^D = -\frac{1}{2}\left(\partial_i(\xi\Psi_j + \xi^T \partial_j T + \xi^c \partial_j \mu_c) + (i \longleftrightarrow j)\right)
\tag{2.25}
$$

$$
X_i^D = bh_i^M
\tag{2.26}
$$

where the abbreviations $A_{ij} = \frac{1}{2}(\partial_i v_j + \partial_j v_i)$ and $\Psi_i = \partial_j \Psi_{ij} = \partial_j \Psi_{ji}$ have been used.

Reversible dynamics

The reversible contributions to the currents and quasicurrents cannot be derived from a functional as the irreversible contributions. Instead one directly expands the currents and quasicurrents in terms of the thermodynamic forces using the general symmetry and invariance arguments. From all these possible contributions one only retains those, that

conserve energy or entropy upon substitution into the Gibbs relation (2.6). One finally obtains

$$j_i^{\sigma R} = -\kappa_{ij}^R(M)\partial_j T - D_{ij}^{TR}(M)\partial_j \mu_c + \xi_{ij}^{TR}(M)\partial_l \Psi_{jl} \tag{2.27}$$

$$j_i^{cR} = -D_{ij}^R(M)\partial_j \mu_c + D_{ij}^{TR}(M)\partial_j T + \xi_{ij}^{cR}(M)\partial_l \Psi_{lj} \tag{2.28}$$

$$\sigma_{ij}^R = -\Psi_{ij} - c_{kij}^R(M)h_k^M - \nu_{ijkl}^R(M)A_{kl} \tag{2.29}$$

$$Y_{ij}^R = -A_{ij} + \frac{1}{2}\lambda^M \left[\partial_i(\nabla \times \mathbf{h}^M)_j + \partial_j(\nabla \times \mathbf{h}^M)_i\right]$$

$$\qquad -\frac{1}{2}\left[\partial_i\left\{\xi_{jk}^R(M)\partial_l \Psi_{kl} + \xi_{jk}^{TR}(M)\partial_k T + \xi_{jk}^{cR}(M)\partial_k \mu_c\right\} + (i \longleftrightarrow j)\right] \tag{2.30}$$

$$X_i^R = b_{ij}^R(M)h_j^M + \lambda^M(\nabla \times \mathbf{\Psi})_i - c_{ijk}^R(M)A_{jk}. \tag{2.31}$$

where the transport coefficients are all odd functions of the magnetization $\mathbf{M}$ and are given up to linear order in $\mathbf{M}$ in [60]. The transport coefficient λ^M is new for isotropic ferrogels and describes the reversible dynamic coupling between the magnetization and the stress tensor. One realizes, that the reversible contributions to the currents and quasicurrents show the opposite behavior under time inversion as their irreversible counterparts.

2.2 Assumptions for the Rosensweig instability

In order to give a nonlinear description of the Rosensweig instability in isotropic magnetic gels it is worth simplifying the complete set of hydrodynamic equations as discussed in the previous section to focus on the basic mechanism driving the instability. Additionally, since we are about to discuss a surface phenomenon, we have to specify the boundary conditions that have to be fulfilled at the free boundary between the magnetic gel and the vacuum above.

2.2.1 The simplified bulk equations

To start, we can safely assume a constant temperature and a constant concentration of magnetic particles. This discards all contributions to the hydrodynamic currents and quasicurrents proportional to the temperature and concentration gradients. The corresponding symmetric contributions proportional to the gradient of the elastic stress in the currents associated with the concentration and the entropy density are assumed to be small enough so that we can neglect them ($\xi^T, \xi^{TR} \ll 1$ and $\xi^c, \xi^{cR} \ll 1$). Furthermore we assume no elastic stress diffusion in the medium ($\xi, \xi^R \ll 1$).

Another very important assumption for our discussion is, that even though the magnetic field is considered a slowly relaxing variable in the general hydrodynamic theory for isotropic magnetic gels, we assume that it relaxes fast enough on the time scale considered in our discussion of the Rosensweig instability. In that respect the magnetization is no longer a slowly relaxing variable and the corresponding dynamic equation (2.16) is adiabatically eliminated together with all crosscouplings in the hydrodynamic currents and quasicurrents that are proportional to the thermodynamic force associated to the magnetization. This assumption is justified by the fact that the growth of surface spikes takes place on a time scale long compared to the temporal variations of the magnetic field. The magnetic field is then defined by the static Maxwell equations and the corresponding boundary conditions at the surface. We also assume that the macroscopic

material parameters like the shear modulus and the shear viscosity are independent of the magnetization in the medium. This also implies that we will neglect magnetostriction in our discussions. Furthermore we assume a very small "reversible viscosity" ($\nu_{ijkl}^R \ll 1$) and will neglect the corresponding contributions in our analysis.

The gravitational force plays an important role in the phenomenon of the Rosensweig instability since it stabilizes the surface in the long wavelength limit, thus we have to account for this externally given force in our discussion. This can be easily done by adding the appropriate term to the generalized Navier-Stokes equation, where we will denote the acceleration due to gravity by $\mathbf{G}$. Eventually we end up with the following set of nonlinear dynamic equations

$$\partial_t \rho + \partial_k (\rho v_k) = 0 \tag{2.32}$$

$$\partial_t g_i + \partial_j T_{ij} = \rho G_i \tag{2.33}$$

$$\left(\partial_t + v_k \partial_k\right)\epsilon_{ij} - \frac{1}{2}\left(\partial_i v_j + \partial_j v_i\right) = 0 \tag{2.34}$$

with the stress tensor T_{ij} given by

$$
\begin{aligned}
T_{ij} = {} & g_i v_j + p\delta_{ij} - \left(B_i H_j - \frac{1}{2} B_k H_k\,\delta_{ij}\right) - \mu_2(\epsilon_{jk}\epsilon_{ki} + \epsilon_{ik}\epsilon_{kj}) - \hat{\mu}\epsilon_{kk}\epsilon_{ij} \\
& -2\mu_2\epsilon_{ij} - \hat{\mu}\delta_{ij}\epsilon_{kk} - \nu_2(\partial_j v_i + \partial_i v_j) - \hat{\nu}\delta_{ij}\partial_k v_k
\end{aligned}
\tag{2.35}
$$

In the simplified set of hydrodynamic equations (2.32) to (2.34) we still account for a compressible medium. The reason for that becomes clear in section 5.2 where the corresponding adjoint system is derived. Except for the derivation of the adjoint system, however, we can safely assume an incompressible medium. The coefficients $\hat{\mu} = \mu_1 - 2/3\,\mu_2$ and $\hat{\nu} = \nu_1 - 2/3\,\nu_2$ abbreviate the contributions vanishing for this incompressible limit.

Since we have assumed that the magnetic field and the magnetization in the medium relax fast, the bulk equations governing the magnetic field are given by the static Maxwell equations

$$\nabla \cdot \mathbf{B} = 0 \quad \text{and} \quad \nabla \cdot \mathbf{B}^{\text{vac}} = 0 \tag{2.36}$$

$$\nabla \times \mathbf{H} = 0 \quad \text{and} \quad \nabla \times \mathbf{H}^{\text{vac}} = 0 \tag{2.37}$$

where the superscript vac denotes the corresponding observables in vacuum.

The simplifications we have discussed so far have an important consequence on the character of the instability. Since the magnetic field can be expressed as the gradient of a scalar magnetic potential, the magnetic contributions to the bulk equations for the elastic medium cancel. One obtains a completely decoupled set of bulk equations for the elastic medium and the magnetic field. The derivation is straightforward but due to its importance, the detailed derivation is added as appendix A. The boundary conditions at the free surface are now the only link between the magnetic field and the magnetic medium as we will see in the following section.

2.2.2   The boundary conditions

As seen in the discussion so far, the boundary conditions play an important role in the Rosensweig problem. We therefore have to spend some time specifying and discussing them.

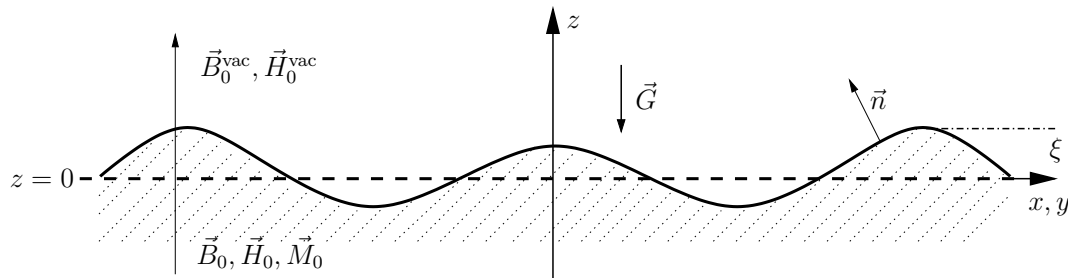
Figure 2.1: Qualitative sketch of the geometry under consideration for the description of the Rosensweig instability. The magnetic medium is occupying the negative half-space. The deflection of the deformable surface with respect to the flat surface at $z = 0$ is denoted by ξ with its unit normal vector $\mathbf{n}$ pointing upwards. The applied magnetic field is always parallel to the z axis, while the acceleration due to gravity $\mathbf{G}$ is acting in the opposite direction.

The geometry we have in mind for the theoretical discussion is inspired by the experimental setup [19]. However, we assume a horizontally infinitely extended boundary between the magnetic medium (below) and vacuum (above). We choose the coordinate system such that the initially flat boundary is located in the $z = 0$ plane. The deflection of the deformable surface from this initial state will be denoted as $\xi(x, y)$ in the following. Furthermore we assume both subsystems to be infinitely extended in positive and negative $z-$direction. Figure 2.1 sketches the geometry discussed so far. The externally given forces are additionally depicted. The gravitational force always acts along the negative $z-$axis whereas the applied magnetic field is directed in the opposite direction.

The assumptions mentioned above allow us to focus our attention on the boundary between vacuum and the magnetic medium situated at $z = \xi$. For the boundaries at $z = \infty$ and $z = -\infty$ we only require that the perturbations of the observables caused by the deformed surface are relaxed.

The boundary conditions at the free surface for the magnetic field and the magnetic flux density are straightforwardly given by Maxwell's theory [69], but are repeated here for completeness. One requires the normal component of the magnetic flux density and the tangential component of the magnetic field to be continuous at the boundary

$$\mathbf{n} \times \mathbf{H} = \mathbf{n} \times \mathbf{H}^{\mathrm{vac}} \tag{2.38}$$

$$\mathbf{n} \cdot \mathbf{B} = \mathbf{n} \cdot \mathbf{B}^{\mathrm{vac}} \tag{2.39}$$

where the normal vector $\mathbf{n}$ is given by

$$\mathbf{n} = \frac{\nabla(z - \xi)}{|\nabla(z - \xi)|} \tag{2.40}$$

Another important ingredient for the Rosensweig instability is the deformability of the boundary between the magnetic medium and the vacuum. It is reasonable to assume a stress free boundary condition at the surface. Since as long as there is a remaining stress acting on the surface, the surface will deform until all stresses are compensated. For the tangential stress boundary condition, these conditions result in a continuous internal tangential stress of the medium at the boundary. For the normal stress boundary

condition, however, we additionally have to consider the surface tension (denoted as σ_T in our discussion) and gravity which have to be compensated by the normal stress difference. Finally we end up with

$$\mathbf{n} \times \mathrm{T} \cdot \mathbf{n} = \mathbf{n} \times \mathrm{T}^{\mathrm{vac}} \cdot \mathbf{n} \tag{2.41}$$

$$\mathbf{n} \cdot \mathrm{T} \cdot \mathbf{n} - \mathbf{n} \cdot \mathrm{T}^{\mathrm{vac}} \cdot \mathbf{n} = \sigma_T \nabla \cdot \mathbf{n} - \rho G \xi \tag{2.42}$$

In eq. (2.42) the contribution due to gravity has been written explicitly. In general, the corresponding force in the Navier-Stokes equation (2.33) can be incorporated into the stress tensor T_{ij} by considering the gravitation potential according to

$$\rho G_i = -\rho G \delta_{iz} = -\partial_j (\rho G z \delta_{ij}) \tag{2.43}$$

The potential is isotropic in space and can therefore be assigned as an additional pressure contribution. As a consequence, the gravitation will only enter the normal stress boundary condition.

The deformability of the surface is not yet completely implemented in our description. We can do this by giving a dynamic equation for the actual position of the surface. This condition is inherently valid only at the surface itself and can therefore be considered as an additional boundary condition. Since any temporal change of the interface is related to the movement of matter, we have

$$\frac{d}{dt} \xi = v_z \tag{2.44}$$

which can be viewed as a macroscopic definition of the interface in a continuum description. This boundary condition is often referred to as the kinematic boundary condition. As we will discuss next, this condition leads to an eigenvalue problem and to the dispersion relation between the frequency and the wavelength of a surface mode.

Chapter 3

Recalling the linear problem

In this chapter we will focus on the linear aspects of the Rosensweig instability in isotropic magnetic gels. Parts of this chapter can be understood as a summary of previous works [70, 20], however it will also provide an easy introduction to the rather special nature of the kinematic boundary condition and the possible mathematical problems in the presence of dynamical deformable surfaces. This will help us in understanding the nonlinear regime and especially the way we treat it mathematically.

3.1 The ground state

The system of equations and boundary conditions (2.32-2.34) and (2.41-2.42) always has the trivial ground state solution, where the surface is flat ($\xi(x, y, t) \equiv 0, \mathbf{n}_0 = \mathbf{e}_z$), flow and deformations are absent ($\mathbf{v} = 0$, $\epsilon_{ij} = 0$), and the fields are constant ($\mathbf{M}_0 = M_0 \mathbf{e}_z$ with $M_0 = (1 - 1/\mu)B_0$). The continuity equation (2.32) and the dynamic equation for the strain field (2.34) are then satisfied identically whereas the Navier-Stokes equation reads

$$\partial_j \left(p_0 \delta_{ij} - B_{0i} H_{0j} + \frac{1}{2} B_{0k} H_{0k} \delta_{ij} \right) \;=\; -\rho G \delta_{iz} \tag{3.1}$$

For the lateral dimensions in $x-$ and $y-$direction these equations are easily satisfied by any pressure $p_0 = p_0(z)$, which is obtained by using $i = z$ as

$$p_0(z) \;=\; -\rho G z + p_0(z = 0) \tag{3.2}$$

Furthermore we have to guarantee a stress free surface. The tangential stress boundary conditions are identically satisfied for this ground state solution, whereas the normal boundary condition reads

$$p_0(z = 0) \;=\; -\frac{1}{2} \left(1 - \frac{1}{\mu} \right) B_0^2 \tag{3.3}$$

which results upon substituting into (3.2) the final ground state pressure

$$p_0(z) \;=\; -\rho G z - \frac{1}{2} \left(1 - \frac{1}{\mu} \right) B_0^2 \tag{3.4}$$

The system of equations therefore requires a non-zero, constant stress contribution due to the magnetic field, $-(1/2)(1 - 1/\mu)B_0^2$, to the hydrostatic pressure, which is of minor relevance, since in an incompressible[1] system the pressure has no physical meaning anymore and merely serves as an auxiliary quantity that guarantees $\nabla \cdot \mathbf{v} = 0$ for all times, if flow is present.

It is worth mentioning here, that the ground state is the only state where the gravitational force contributes via the bulk equations. For the perturbed states, the gravitation only enters the analysis via the boundary conditions.

3.2   Linear deviations from the ground state

For finite temperatures the system will be subject to thermal fluctuations which cause the surface to undulate randomly. These fluctuations can be viewed as a spectrum of propagating and damped surface waves (cf. fig. 2.1, p. 18) with a wave vector $\mathbf{k} = (k_x, k_y, 0)$ and with the frequency consisting of a real ω and an imaginary part $-\sigma$

$$\xi(x, y, t) = \hat{\xi}e^{-ik_x x - ik_y y + i\omega t + \sigma t} \tag{3.5}$$

and where $\hat{\xi}$ denotes the amplitude which is undetermined in the linear theory. In case of $\omega = 0$, a stationary spatially periodic pattern is obtained. Generally ω is a complex function of $\mathbf{k}$. Fourier modes of the type (3.5) can be superimposed as appropriate, and deviations from the ground state of all the other variables have to be proportional to $\xi(x, y, t)$. Linear deviations of the surface normal from the ground state due to undulations are given by[2] $\mathbf{n}^{(1)} \equiv \mathbf{n} - \mathbf{n}_0 = (-\partial_x\xi, -\partial_y\xi, 0)$.

The fact that the systems of hydrodynamic bulk equations decouples from the magnetic bulk equations enables us to solve the two bulk systems separately. A detailed derivation of the magnetic fields can be found in appendix B whereas here we just repeat the final results. The linear deviations of the magnetic field and induction from the ground state value, $\mathbf{b}^{(1)} \equiv \mathbf{B}^{(1)} - \mathbf{B}_0$ and $\mathbf{h}^{(1)} = \mathbf{H}^{(1)} - \mathbf{H}_0$, both for the ferrogel and the vacuum, still obey the linear electrostatic equations, $\mathbf{b}^{(1)} = \mu\mathbf{h}^{(1)}$, $\mathrm{div}\mathbf{b}^{(1)} = 0 = \mathrm{curl}\mathbf{h}^{(1)}$. This allows for the introduction of a magnetic scalar potential [69] $\mathbf{h}^{(1)} = -\nabla\Phi^{(1)}$ that is determined by the Laplace equation with the appropriate solutions

$$\Phi^{(1)} = -\frac{M_0}{1 + \mu}\xi(x, y, t)e^{kz} \tag{3.6}$$

$$\Phi^{(1)\mathrm{vac}} = \frac{\mu M_0}{1 + \mu}\xi(x, y, t)e^{-kz}\,. \tag{3.7}$$

for the lower (ferrogel) and upper (vacuum) half plane, respectively and $k^2 = k_x^2 + k_y^2$.

---

[1]In section 2.2.1 we still allowed for a compressible superparamagnetic medium. This assumption is necessary to derive the set of adjoint linear equations with its corresponding boundary conditions as we will see in section 5.2. For the discussion of the Rosensweig instability, however, we can safely assume an incompressible medium.

[2]The superscript (1) is just added for a consistent notation with chapter 5 and describes the deviations from the ground state in linear order.

The system of hydrodynamic bulk equations reads in linearized form

$$\rho \partial_t v_i^{(1)} + \partial_i p^{(1)} - \nu_2 \partial_j (\partial_i v_j^{(1)} + \partial_j v_i^{(1)}) - 2\mu_2 \partial_j \epsilon_{ij}^{(1)} = 0 \qquad (3.8)$$

$$\partial_t \epsilon_{ij}^{(1)} - \frac{1}{2}(\partial_i v_j^{(1)} + \partial_j v_i^{(1)}) = 0 \qquad (3.9)$$

$$\partial_i v_i^{(1)} = 0 \qquad (3.10)$$

The usual way to solve this system is to distinguish the irrotational flow contributions from the rotational ones, $\mathbf{v}^{(1)} = \mathbf{v}^{(1)pot} + \mathbf{v}^{(1)rot}$, where both parts can be deduced from a scalar potential $\varphi^{(1)}$ and a vector potential $\mathbf{\Psi}^{(1)}$, respectively

$$\mathbf{v}^{(1)pot} = \nabla \varphi^{(1)} \quad \text{and} \quad \mathbf{v}^{(1)rot} = \nabla \times \mathbf{\Psi}^{(1)}. \qquad (3.11)$$

The incompressibility of the medium requires $\Delta \varphi^{(1)} = 0$ and leads to the ansatz

$$\varphi^{(1)} = \hat{\varphi}^{(1)} \, \xi(x, y, t) e^{kz} \qquad (3.12)$$

for the scalar velocity potential. The vector velocity potential can be written as

$$\mathbf{\Psi}^{(1)} = \hat{\mathbf{\Psi}}^{(1)} \, \xi(x, y, t) e^{qz} \qquad (3.13)$$

where the amplitudes $\hat{\varphi}^{(1)}$ and $\hat{\mathbf{\Psi}}^{(1)}$ and the decay length q^{-1} are still undetermined. Since only two of the three amplitudes $\hat{\mathbf{\Psi}}^{(1)}$ can be independent, we set $\hat{\Psi}_z^{(1)} = 0$ without loss of generality resulting in $\mathbf{v}^{(1)rot} = (-q\Psi_y^{(1)}, q\Psi_x^{(1)}, -ik_x\Psi_y^{(1)} + ik_y\Psi_x^{(1)})$.

The strain $\epsilon_{ij}^{(1)}$ can be expressed by the velocity via eq. (3.9) and the linear pressure deviation, $p^{(1)} \equiv p - p_0$ is determined by eq. (3.8). With the help of eq. (3.9), $i\omega\partial_j\epsilon_{ij}^{(1)} = (1/2)\Delta v_i^{(1)}$, eq. (3.8) takes the linear form

$$i\omega\rho v_i^{(1)} + \partial_i p^{(1)} - \left(\nu_2 + \frac{\mu_2}{i\omega}\right)\Delta v_i^{(1)} = 0 \qquad (3.14)$$

Taking div and curl of eq. (3.14) we get [71]

$$p^{(1)} = -i\omega\rho\varphi^{(1)} + \text{const.} \qquad (3.15)$$

$$\text{and} \quad q^2 = k^2 - \frac{\rho\omega^2}{\mu_2 + i\omega\nu_2} \qquad (3.16)$$

respectively, where the unimportant constant in the pressure can be ignored.

3.3 Surface wave dispersion relation

We are left with three amplitudes, $\hat{\varphi}^{(1)}, \hat{\Psi}_x^{(1)}, \hat{\Psi}_y^{(1)}$, that have to be related to the undulation amplitude, $\hat{\xi}$, by the stress boundary conditions (2.41) and (2.42) and the kinematic boundary condition (2.44). For the linear analysis we could, without loss of generality, choose the in-plane wave vector $\mathbf{k}$ to be parallel to the $x-$axis, as done in [20]. With the nonlinear analysis in mind, it is worth considering an arbitrary direction of the wave vector. For linear deviations from the ground state and with the solutions obtained for
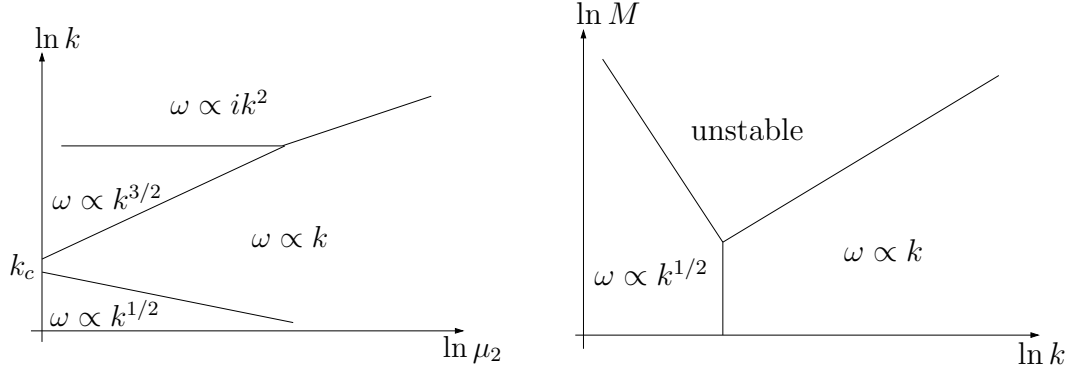
Figure 3.1: Schematic plots of the different surface wave regimes described by eq. (3.20) as in [71]. One encounters gravitational waves with $\omega \propto k^{1/2}$, Rayleigh elastic waves with $\omega \propto k$ and capillary waves with $\omega \propto k^{3/2}$ as depicted on the left. On the right an unstable region develops for strong magnetic fields.

the magnetic fields, the stress boundary conditions can be written in terms of the flow potentials as (cf. appendix C)

$$\tilde{\mu}_2(\partial_z^2 - \partial_y^2)\Psi_x^{(1)} + \tilde{\mu}_2(\partial_y\partial_x)\Psi_y^{(1)} + 2\tilde{\mu}_2\partial_y\partial_z\varphi^{(1)} = 0 \qquad (3.17)$$

$$\tilde{\mu}_2(\partial_x\partial_y)\Psi_x^{(1)} + \tilde{\mu}_2(\partial_z^2 - \partial_x^2)\Psi_y^{(1)} - 2\tilde{\mu}_2\partial_x\partial_z\varphi^{(1)} = 0 \qquad (3.18)$$

$$-(2\tilde{\mu}_2\partial_z\partial_y + G\rho\partial_y + \sigma_T k^2\partial_y - \frac{\mu}{1+\mu}M_0^2\partial_z\partial_y)\Psi_x^{(1)}$$

$$+(2\tilde{\mu}_2\partial_z\partial_x + G\rho\partial_x + \sigma_T k^2\partial_x - \frac{\mu}{1+\mu}M_0^2\partial_z\partial_x)\Psi_y^{(1)}$$

$$+(2\tilde{\mu}_2\partial_z^2 + G\rho\partial_z + \sigma_T k^2\partial_z - \rho\omega^2 - \frac{\mu}{1+\mu}M_0^2\partial_z^2)\varphi^{(1)} = 0 \qquad (3.19)$$

all taken at $z = 0$ and with the frequency dependent $\tilde{\mu}_2(\omega) \equiv \mu_2 + i\omega\nu_2$ describing (kinematic) elasticity and viscosity.

To have a nontrivial solution for equations (3.17-3.19) the determinant of coefficients must vanish. This leads to the dispersion relation of surface waves for ferrogels

$$\rho\omega^2\left(2\tilde{\mu}_2(\omega)k^2 - \rho\omega^2\right) + \rho\omega^2\left(\sigma_T k^3 + \rho Gk + 2\tilde{\mu}_2(\omega)k^2 - \frac{\mu}{1+\mu}M_0^2 k^2\right)$$

$$-4\tilde{\mu}_2^2(\omega)\,k^4\left[1 - \left(1 - \frac{\rho\omega^2}{\tilde{\mu}_2(\omega)k^2}\right)^{1/2}\right] = 0 \quad (3.20)$$

In the absence of an external magnetic field ($M_0 = 0$) eq. (3.20) reduces to the dispersion relation for non-magnetic gels [71]. It also contains, as a special case, the surface wave dispersion relation for ferrofluids (in an external field) by choosing $\tilde{\mu}_2 = i\omega\nu_2$. It can be generalized to viscoelastic ferrofluids, whose elasticity relaxes on a time scale τ^{-1}, by replacing μ_2 with $i\omega\tau\mu_2/(1+i\omega\tau)$ [71].

The dispersion relation (3.20) is very complicated and it is impossible to solve it analytically for $\omega(k)$. For non-magnetic gels it is known that there are basically three wave regimes (neglecting dissipation or damping) (cf. fig. 3.1): $\rho\omega^2 = \sigma_T k^3$ (capillary waves), $\rho\omega^2 = \tilde{\alpha}\mu_2 k^2$ (Rayleigh elastic waves), and $\omega^2 = Gk$ (gravity water waves) for

small wavelengths ($k \gg \mu_2/\sigma_T$, $\sqrt{\rho G/\sigma_T}$), intermediate ones ($\rho G/\mu_2 \ll k \ll \mu_2/\sigma_T$), and large ones ($k \ll \rho G/\mu_2$, $\sqrt{\rho G/\sigma_T}$), respectively, where $\tilde{\alpha}$ is a number of order unity. For typical material values ($\mu_2 \approx 1$ kPa, $\sigma_T \approx 0.02$ kg/sec^2) waves at wavelengths of 10^{-4} m and below (with frequencies of 50 kHz and above) are of purely capillary type, while for wavelengths above 1 m (and frequencies below 10 Hz) the gravity character dominates; this regime is, thus, irrelevant for usual ferrogel samples. In between, for typical wavelengths of 10^{-2} m and frequencies of 100 - 1000 Hz the elastic nature of the wave is prevailing. This scenario also applies to isotropic ferrogels in the absence of a field. The effect of a normal external magnetic field on the surface is a destabilizing one [3]. From eq. (3.20) it is evident that an external field leads to an effective reduction of the surface stiffness (provided by surface tension, gravity or elasticity) and decreases the frequency (squared) of the propagating waves in all regimes by $\sim M_0^2 k^2$. If the field is large enough, this reduction is the dominating effect and can lead to $\omega = 0$ and thus, to the breakdown of propagating waves. In the next section it is shown that this is indeed related to the Rosensweig instability.

3.4 Rosensweig instability

As mentioned already, eq. (3.20) is a complicated relation between the frequency of a surface wave implicitly given as a function of its wave vector. For a better understanding of the Rosensweig instability it is worth considering the simplification of eq. (3.20) to the case of an inviscid ($\nu_2 = 0$) magnetic fluid

$$\rho \omega^2 = \rho G k - \frac{\mu}{1+\mu} M_0^2 k^2 + \sigma_T k^3 \tag{3.21}$$

as has been done in [3, 19]. This is not a physical assumptions which we will have to correct later on, but it already reveals the static nature of the Rosensweig instability and the resulting dispersion relation (3.21) can be treated analytically. Upon minimizing (3.21) with respect to the frequency ω and the wave vector k one straightforwardly obtains the linear threshold of a static instability ($\omega \equiv 0$)

$$M_c^2 = 2 \frac{1+\mu}{\mu} \sqrt{\rho G \sigma_T} \tag{3.22}$$

beyond which the flat surface is unstable with respect to periodic patterns with a characteristic wave vector (cf. fig. 3.1)

$$k_c = \sqrt{\frac{\rho G}{\sigma_T}} \tag{3.23}$$

The fact that the instability is static is, however, rather singular. This can be observed by plotting (3.21) as is shown in fig. 3.2 (with the material properties taken from the commercial ferrofluid EMG 901 as given for example in [72]). Without a magnetic field one obtains the behavior of an ideal fluid where the gravitational wave regime can be distinguished very clearly as well as the transition to the capillary regime. Upon increasing the magnetic field, the contribution due to the magnetization becomes more and more dominant and at a magnetization of about $6600 A/m$ a branch of anomalous dispersion arises. More interesting for the Rosensweig instability is the necessary minimum that
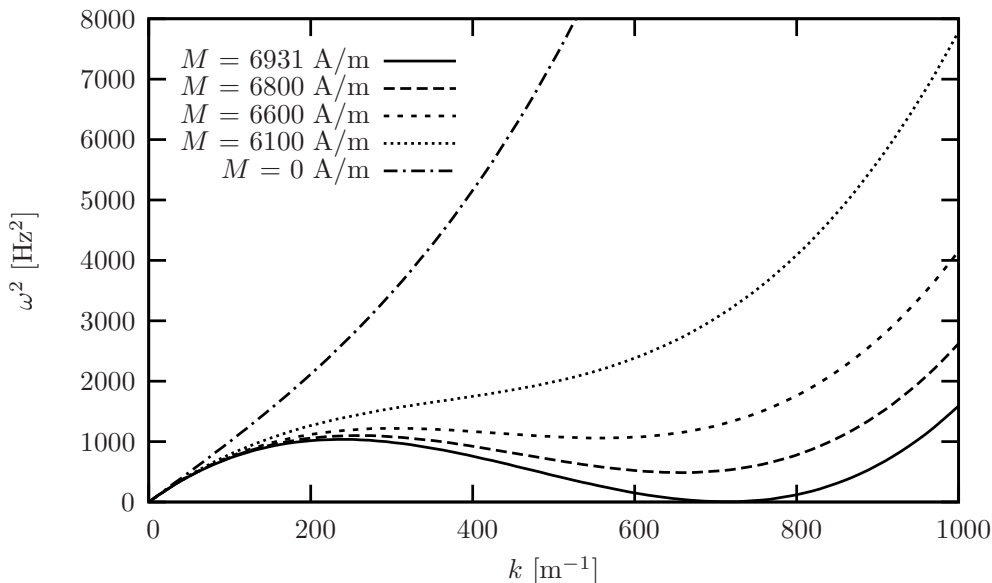
Figure 3.2: The dispersion relation of surface waves in a usual magnetic fluid for different values of the externally applied magnetic field. The numerical parameter values are taken from the ferrofluid EMG 901 ($\rho = 1.53 \cdot 10^3 \frac{kg}{m^3}$, $\sigma_T = 29.5 \cdot 10^{-3} \frac{N}{m}$ and $\mu = 28.0 \cdot 10^{-7} \frac{T}{m}$).

comes along with it. This relative minimum is shifted to lower ω values as the external magnetic field is increased and eventually it becomes the absolute one touching the abscissa at the characteristic wave vector for the critical magnetic field. In physical terms we can interpret this in a slightly different way. Below the critical magnetic field all modes show a finite oscillation in time. As soon as we approach the critical magnetic field the oscillation of the characteristic mode dies out resulting in the growth of a static pattern. The interpretation of the Rosensweig instability as the limiting case of surface waves with a vanishing frequency will be of importance for the nonlinear regime as we will see later.

With the same procedure we can discuss the dispersion relation for magnetic gels (3.20). The characteristic mode turns out to be the same as for the case of ferrofluids, given by the capillary mode (3.23). This can be understood recalling the fact that the elastic contributions enter the dispersion relation with the same $k-$order as the magnetic contributions. The critical magnetic field is instead shifted towards higher magnetic fields [20] according to

$$M_c^2 \;\; = \;\; 2\frac{1+\mu}{\mu}\left(\sqrt{\rho G \sigma_T} + \mu_2\right) \tag{3.24}$$

which is less surprising, since elasticity increases the surface stiffness. In the special cases of realistic ferrofluids with a finite viscosity ($\mu_2 = 0$ and $\nu_2 \neq 0$) and of ferrorubbers ($\nu_2 = 0$ and $\mu_2 \neq 0$) it can be shown analytically that only a static instability $\omega = 0$ is possible at the linear onset [70, 20]. For the general case (3.20) of realistic magnetic gels with a finite viscosity and a finite shear modulus numerical calculations show the absence of an oscillatory instability at onset.

Also in the general case of ferrogels, the static character of the instability is the limiting case of dynamical processes at the surface. To illustrate this, we can plot the dispersion
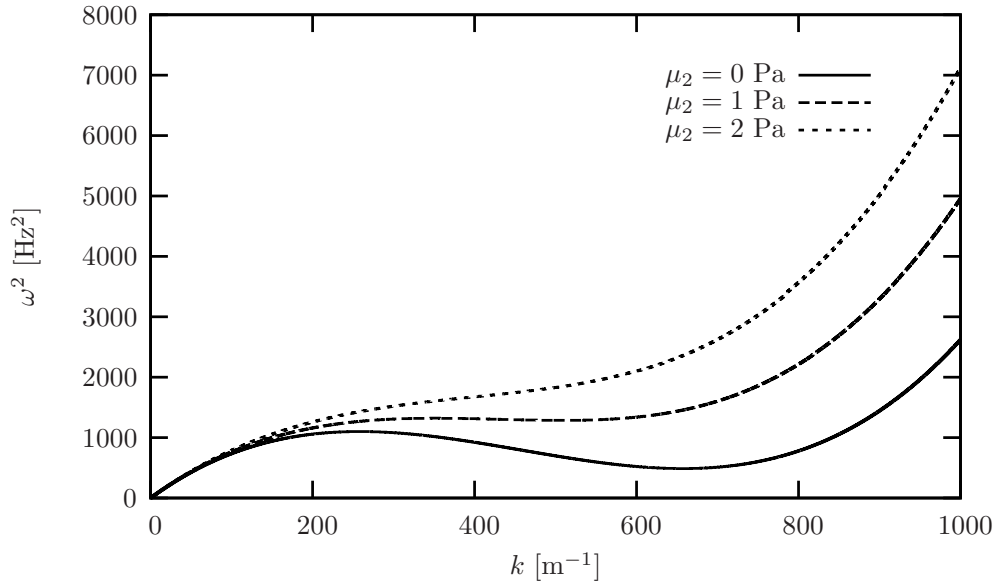
Figure 3.3: The dispersion relation of surface waves on an isotropic magnetic gel at a fixed external magnetic field of $0.98M^{\mathrm{crit.}}$ and for different values of the elastic shear modulus. The numerical parameters for the other material properties are taken from the ferrofluid EMG 901 ($\rho = 1.53 \cdot 10^3 \frac{kg}{m^3}$, $\sigma_T = 29.5 \cdot 10^{-3} \frac{N}{m}$, $\mu = 28.0 \cdot 10^{-7} \frac{T}{m}$ and $\nu_2 = 6.5 \cdot 10^{-6} \frac{m^2}{s}$).

relation in the general viscoelastic case (fig. 3.3). The different graphs have been obtained as numerical solutions of (3.20) where the material parameters are again taken from the ferrofluid EMG 901 with a varying value for the elastic shear modulus μ_2 and where the magnetic field is kept constant at about 98% of the critical magnetic field. Due to the numerical resolution we only had access to elastic moduli up to 2 Pa. However, it remains illustrative that the elastic contributions act opposite to the magnetic field and that the limiting case of a static instability is approached either for increasing magnetic fields or for decreasing shear moduli. An elastic shear modulus of 2 Pa is extremely weak, but fig. 3.3 additionally illustrates that already a low shear modulus influences the dynamic behavior of the surface drastically close to the linear threshold.

3.5 The linear eigenvectors

The condition to find a solution of the linearized set of hydrodynamic equations has been discussed in the previous two sections. A solution can be found by first considering the two tangential stress boundary conditions (3.17,3.18) which allow one to express the amplitudes for the vector potential $\boldsymbol{\Psi}^{(1)}$ in terms of the amplitude of the scalar potential

$$\hat{\Psi}_x^{(1)} = -\frac{2k(-ik_y)}{q^2 + k^2}\hat{\varphi}^{(1)} \qquad \text{and} \qquad \hat{\Psi}_y^{(1)} = +\frac{2k(-ik_x)}{q^2 + k^2}\hat{\varphi}^{(1)} \qquad (3.25)$$

The kinematic boundary condition can then be used to find the explicit expression for the amplitude of the scalar potential

$$\hat{\varphi}^{(1)} \;=\; i\omega \frac{q^2 + k^2}{k(q^2 - k^2)}. \qquad (3.26)$$

In the limiting case of $\omega \to 0$, which corresponds to the approach of the onset of the Rosensweig instability if $k = k_c$, the amplitudes of the potentials diverge with $1/\omega$. Since, however, the potentials are a mathematical tool to solve the system of equations, we need not worry about that, yet.

Substituting the expression for the potentials into eq. (3.11), we eventually obtain the three components of the velocity field

$$v_x^{(1)} = \sum_i (-ik_{ix}) \left(e^{k_i z} - 2\frac{q_i k_i}{q_i^2 + k_i^2} e^{q_i z} \right) \frac{i\omega(q_i^2 + k_i^2)}{k_i(q_i^2 - k_i^2)} \xi_i \tag{3.27}$$

$$v_y^{(1)} = \sum_i (-ik_{iy}) \left(e^{k_i z} - 2\frac{q_i k_i}{q_i^2 + k_i^2} e^{q_i z} \right) \frac{i\omega(q_i^2 + k_i^2)}{k_i(q_i^2 - k_i^2)} \xi_i \tag{3.28}$$

$$v_z^{(1)} = \sum_i k_i \left(e^{k_i z} - 2\frac{k_i^2}{q_i^2 + k_i^2} e^{q_i z} \right) \frac{i\omega(q_i^2 + k_i^2)}{k_i(q_i^2 - k_i^2)} \xi_i , \tag{3.29}$$

where the index i accounts for the fact that in a linear analysis of the instability the direction of the unstable mode remains degenerate and a whole set of characteristic modes with different directions may grow.

We can exploit eq. (3.9) and eventually find the expressions for the components of the strain tensor, where again the index i accounts for the different possible modes of the same modulus

$$\epsilon_{zz}^{(1)} = \sum_i \frac{(q_i^2 + k_i^2)e^{k_i z} - 2q_i k_i e^{q_i z}}{q_i^2 - k_i^2} k_i \xi_i \tag{3.30}$$

$$\epsilon_{xz}^{(1)} = \sum_i (-ik_{ix}) \left(e^{k_i z} - e^{q_i z} \right) \frac{q_i^2 + k_i^2}{q_i^2 - k_i^2} \xi_i \tag{3.31}$$

$$\epsilon_{yz}^{(1)} = \sum_i (-ik_{iy}) \left(e^{k_i z} - e^{q_i z} \right) \frac{q_i^2 + k_i^2}{q_i^2 - k_i^2} \xi_i \tag{3.32}$$

$$\epsilon_{xy}^{(1)} = -\sum_i k_{ix} k_{iy} \frac{q_i^2 + k_i^2}{k_i(q_i^2 - k_i^2)} \left(e^{k_i z} - 2\frac{q_i k_i}{q_i^2 + k_i^2} e^{q_i z} \right) \xi_i \tag{3.33}$$

$$\epsilon_{xx}^{(1)} = -\sum_i k_{ix}^2 \frac{q_i^2 + k_i^2}{k_i(q_i^2 - k_i^2)} \left(e^{k_i z} - 2\frac{q_i k_i}{q_i^2 + k_i^2} e^{q_i z} \right) \xi_i \tag{3.34}$$

$$\epsilon_{yy}^{(1)} = -\sum_i k_{iy}^2 \frac{q_i^2 + k_i^2}{k_i(q_i^2 - k_i^2)} \left(e^{k_i z} - 2\frac{q_i k_i}{q_i^2 + k_i^2} e^{q_i z} \right) \xi_i . \tag{3.35}$$

We realized previously, that the introduced potentials diverge when approaching the linear onset. The velocity and strain field, as the observables of the system, should instead acquire a physical solution in the limit of a stationary instability. Taking the limit $\omega \to 0$,
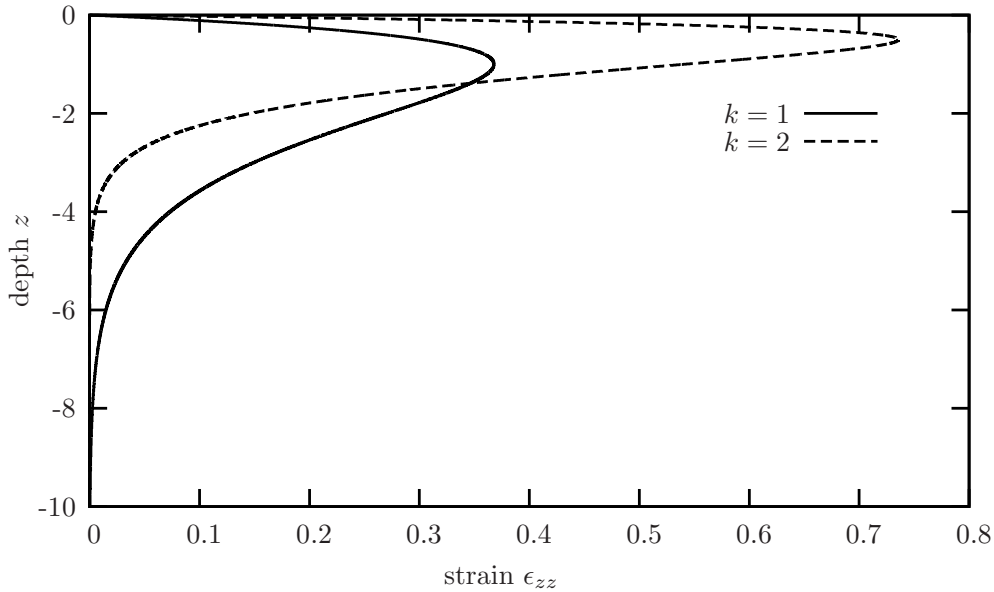
Figure 3.4: The absolute value of the zz−component of the strain field for two particular modes, $k = 1$ and $k = 2$ respectively, according to (3.37) as a function of depth and for an arbitrary infinitesimal deflection of the surface at a given point (x, y). The surface modes are measured in units of the characteristic wave vector k_c, lengths in units of its inverse, k_c^{-1}.

we obtain the following eigenvectors at the linear onset

$$v_i^{(1)} = 0 \tag{3.36}$$

$$\epsilon_{zz}^{(1)} = -\sum_i k_i^2 z e^{k_i z} \xi_i(\omega = 0) \tag{3.37}$$

$$\epsilon_{xz}^{(1)} = -\sum_i (-ik_{ix}) k_i z e^{k_i z} \xi_i(\omega = 0) \tag{3.38}$$

$$\epsilon_{yz}^{(1)} = -\sum_i (-ik_{iy}) k_i z e^{k_i z} \xi_i(\omega = 0) \tag{3.39}$$

$$\epsilon_{xy}^{(1)} = \sum_i k_{ix} k_{iy} z e^{k_i z} \xi_i(\omega = 0) \tag{3.40}$$

$$\epsilon_{xx}^{(1)} = \sum_i k_{ix}^2 z e^{k_i z} \xi_i(\omega = 0) \tag{3.41}$$

$$\epsilon_{yy}^{(1)} = \sum_i k_{iy}^2 z e^{k_i z} \xi_i(\omega = 0) \tag{3.42}$$

The velocity field vanishes identically whereas the strain field acquires a finite stationary value. Fig. 3.4 gives the strain (and correspondingly the stress) distribution in the medium for two different surface modes as a function of the depth starting from the surface. The wave vectors are measured in units of the characteristic wave vector k_c (3.23) and the depth is measured in units of the inverse characteristic wave vector k_c^{-1}.

At this point, the crucial difference between the Rosensweig instability and other commonly discussed instabilities becomes obvious. Mediated by the kinematic boundary condition, the velocity field vanishes. What one observes is not a stationary finite flow field

as, for example, in the case of the Rayleigh-Bénard convection, but the static deformation of the surface with no flow in the medium. As we will see in our nonlinear discussion, this vanishing of the flow field will force us to treat the system dynamically.

3.6   On the normal stress boundary condition

In the previous discussion we showed, that the character of the Rosensweig instability and the dynamical behavior of the bulk solutions of the hydrodynamic equations are crucially dependent on the kinematic boundary condition. In finding the eigenvectors, we did not use the normal stress boundary condition, which rather must be satisfied additionally. To check whether it is fulfilled one can substitute the obtained eigenvectors into eq. (3.19). One realizes then that the dispersion relation (3.20) is regained which is typical for eigenvalue problems. In the linear discussion, the system of equations is therefore solved completely. As we will see in chapter 5, the normal stress boundary condition in higher orders is not satisfied automatically but provides an additional solvability condition.

Chapter 4

Nonlinear discussion using the energy method

A very first nonlinear description of the Rosensweig instability was given by Gailitis in 1977. The general idea is to express the surface energy density of the free deformable surface in terms of the deformation $\xi(x, y, t)$ and minimize this energy density with respect to different regular surface patterns. Although this method does not provide us with any dynamic properties of the instability, we will take this method as a starting point to get an impression on how the elasticity influences the energetically static patterns[1].

4.1 Surface energy density

Describing usual ferrofluids within the framework of the energy minimization method, the expression for the energy density at the surface was first given by Gailitis [33]. Assuming an incompressible ferrofluid occupying the negative half-space, the surface energy density has three contributions. A gravitational term accounting for the hydrostatic energy, a contribution due to surface tension and the energetic contribution of the magnetic field that is applied perpendicular to the initially flat surface. Averaging the entire surface one obtains [33] as the difference in energy density with respect to the flat configuration

$$\mathcal{U}(\xi) = \frac{1}{2}\rho G \left\langle \xi^2(x,y) \right\rangle + \sigma_T \left\langle \sqrt{1 + (\nabla\xi(x,y))^2} \right\rangle + \frac{1}{2} \left\langle \int\limits_{-\infty}^{+\infty} \frac{B^2(x,y,z)}{\mu} dz \right\rangle$$

(4.1)

In our notation the surface deflection from its unperturbed flat state is described by $\xi(x, y)$ and the magnetic induction by $\mathbf{B}$. The surface energy density depends on the mass density ρ, the gravitational acceleration G, the surface tension σ_T and the magnetic permeability of the medium μ. Averaging with respect to the surface S is understood in the following usual way

$$\langle F(x,y) \rangle = \lim_{S \to \infty} \frac{1}{S} \iint_S F(x,y)\, dxdy$$

(4.2)

---

[1]The results of this chapter have been published in [73].

For the surface deflection itself we take a superposition of different wave vectors that can be divided into two groups. The first group will contain all those vectors whose wavelength corresponds to the critical one. The second group accounts for all the possible higher harmonic wave vectors, constructed from the main modes via superposition with Fourier modes in space ($\mathbf{k}$) and time (ω)

$$\xi(x, y, t) = \sum_{i=1}^{M} A_{\mathbf{k}_i} \cos(\mathbf{k}_i \cdot \mathbf{r}) e^{i\omega t} + \sum_{\substack{i,j=1 \\ \mathbf{k}_i \pm \mathbf{k}_j \neq 0}}^{N} A_{\mathbf{k}_i \pm \mathbf{k}_j} \cos((\mathbf{k}_i \pm \mathbf{k}_j) \cdot \mathbf{r}) e^{i\omega t}. \qquad (4.3)$$

In that ansatz we already assume regular 2−dimensional patterns.

Starting to describe elastic media with this method, we have to account for the elastic degrees of freedom. This may be done by just adding an additional energetic contribution due to elastic deformations (described by the strain field ϵ_{ij}) to the surface energy density (4.1) as given in chapter 2 by eq. (2.7)

$$\left\langle \int_{-\infty}^{\xi} \frac{1}{2} \mu_{ijkl} \epsilon_{ij} \epsilon_{kl} \, dz \right\rangle \qquad (4.4)$$

It is sufficient to take the integral with respect to z just from the bottom ($-\infty$) to the top (ξ) of the ferrogel, since we assume vacuum in the positive half-space (cf. chapter 2). The explicit form of the elastic tensor μ_{ijkl} is given by eq. (2.8) and takes the following form in an incompressible medium with μ_2 being the elastic shear modulus

$$\mu_{ijkl} = \mu_2 \left(\delta_{ik}\delta_{jl} + \delta_{il}\delta_{jk} \right) \qquad (4.5)$$

In total we therefore get the following expression for the surface energy density in an incompressible, isotropic ferrofluid that is now left for minimization with respect to different regular patterns arising at the gel-vacuum interface beyond the linear threshold

$$\mathcal{U}(\xi) = \left\langle \frac{\rho G}{2} \xi^2 + \sigma_T \sqrt{1 + (\partial_x \xi)^2 + (\partial_y \xi)^2} + \frac{1}{2\mu_0 \mu} \int_{-\infty}^{+\infty} B^2(x,y,z) dz \right.$$
$$\left. + 2\mu_2 \int_{-\infty}^{\xi} (\epsilon_{xy}^2 + \epsilon_{yz}^2 + \epsilon_{xz}^2) \, dz + \mu_2 \int_{-\infty}^{\xi} (\epsilon_{xx}^2 + \epsilon_{yy}^2 + \epsilon_{zz}^2) \, dz \right\rangle \qquad (4.6)$$

For the rest of our discussions in this chapter we will introduce dimensionless units. These are chosen such, that lengths are measured in units of the inverse characteristic wave vector $k_c^{-1} = \sqrt{\sigma_T/\rho G}$, energy densities in terms of σ_T, the magnetic field in units of the critical magnetic field, and the elastic shear modulus μ_2 in terms of $\sqrt{\sigma_T \rho G}$.

Substituting the solutions of the strain field that we obtained in the linear order (3.37-3.42) we can formulate the final expression for the surface energy density in terms of the surface deflection $\xi(x, y, t)$. The non-elastic parts – represented by the first three terms in eq. (4.6) – are taken from the discussions of Gailitis [33], because they do not change in the presence of elasticity. The fourth and fifth contribution in eq. (4.6) are integrated

and lead to the expression for the energy density up to fourth order of the amplitude A of the surface deflection $\xi(x, y)$

$$
\begin{aligned}
\mathcal{U} &= -\frac{1}{2}\mathcal{E}(B_0, 1)\sum_{i=1}^{N} A_{\mathbf{k}_i}^2 + \frac{\mu_2}{2}\sum_{i=1}^{N}\mathcal{C}(\mathbf{k}_i)A_{\mathbf{k}_i}^2 - \mathcal{Q}(2\pi/3)\sum_{\substack{i,j,l\leq N \\ \mathbf{k}_i \pm \mathbf{k}_j \pm \mathbf{k}_l}} A_{\mathbf{k}_i}A_{\mathbf{k}_j}A_{\mathbf{k}_l} \\
&\quad + \frac{1}{4}\mathcal{K}(0)\sum_{i=1}^{N}A_{\mathbf{k}_i}^4 + \sum_{i,j\leq N}\mathcal{K}(\theta_{ij})A_{\mathbf{k}_i}^2 A_{\mathbf{k}_j}^2 \\
&\quad - \frac{1}{2}\sum_{i=1}^{N}\left(\mathcal{Q}(0)A_{\mathbf{k}_i}^2 A_{2\mathbf{k}_i} + (\mathcal{E}(B_0, 2) - \mu_2\mathcal{C}(2\mathbf{k}_i))A_{2\mathbf{k}_i}^2\right) \\
&\quad - \sum_{\pm}\sum_{\substack{i<j\leq N \\ |\mathbf{k}_i \pm \mathbf{k}_j|\neq 1}}\left(\mathcal{Q}(\pi/4 \pm \theta_{ij} \mp \pi/4)A_{\mathbf{k}_i}A_{\mathbf{k}_j}A_{\mathbf{k}_i\pm\mathbf{k}_j}\right. \\
&\qquad\qquad\qquad \left. + \frac{1}{2}\left(\mathcal{E}(B_0, |\mathbf{k}_i \pm \mathbf{k}_j|) - \mu_2\mathcal{C}(\mathbf{k}_i \pm \mathbf{k}_j)\right)A_{\mathbf{k}_i\pm\mathbf{k}_j}^2\right) + \mathcal{O}(A^5)
\end{aligned}
\tag{4.7}
$$

where θ_{ij} denotes the angle between the i-th and the j-th mode under consideration. The analytical coefficients of the non-elastic contributions in eq. (4.7) have been given already by Gailitis [33]. For completeness they are repeated here. The elastic coefficients follow from averaging eq. (4.6) and are given here as functions of the components of the different wave vectors

$$
\mathcal{E}(B_0, k) = \tilde{\epsilon}k - \frac{1}{2}(1 - k)^2
\tag{4.8}
$$

$$
\begin{aligned}
\mathcal{K}(\theta_{ij}) &= \sin^3(\theta_{ij}/2) + \cos^3(\theta_{ij}/2) - \frac{9}{16} - \frac{1}{8}\cos(\theta_{ij}) \\
&\quad + \eta^2\left(2 - \sin(\theta_{ij}/2) - \cos(\theta_{ij}/2) - \sin^3(\theta_{ij}/2) - \cos^3(\theta_{ij}/2)\right)
\end{aligned}
\tag{4.9}
$$

$$
\mathcal{Q}(\theta_{ij}) = \eta\left(2\cos(\theta_{ij}/2) - \cos^2(\theta_{ij}/2)\right)
\tag{4.10}
$$

$$
\mathcal{C}(\mathbf{k}_i) = \frac{k_{ix}^2 k_{iy}^2}{2k_i^3} + \frac{k_{ix}^2}{2k_i} + \frac{k_{iy}^2}{2k_i} + \frac{k_{ix}^4}{4k_i^3} + \frac{k_{iy}^4}{4k_i^3} + \frac{\mathbf{k}_i^4}{4k_i^3}
\tag{4.11}
$$

where $\tilde{\epsilon} = B_0^2/B_c^2 - 1$ is the control parameter with respect to the threshold B_c of usual ferrofluids and with $\eta = \chi/(2 + \chi)$ where χ denotes the magnetic susceptibility.

As a first step to minimize expression (4.7) we note, that all contributions with higher harmonics are – similar to the case of usual ferrofluids – of the form

$$
\mathcal{Q}(\pi/4 \pm \theta_{ij} \mp \pi/4)A_{\mathbf{k}_i\pm\mathbf{k}_j} - \frac{1}{2}\left(\mathcal{E}(B_0, |\mathbf{k}_i \pm \mathbf{k}_j|) - \mu_2\mathcal{C}(\mathbf{k}_i \pm \mathbf{k}_j)\right)A_{\mathbf{k}_i\pm\mathbf{k}_j}^2
\tag{4.12}
$$

Minimizing separately with respect to these higher harmonic amplitudes, we find

$$
A_{\mathbf{k}_i\pm\mathbf{k}_j} = \frac{\mathcal{Q}(\pi/4 \pm \theta_{ij} \mp \pi/4)}{\mathcal{E}(B_0, |\mathbf{k}_i \pm \mathbf{k}_j|) - \mu_2\mathcal{C}(\mathbf{k}_i \pm \mathbf{k}_j)}
\tag{4.13}
$$

Substitution into eq. (4.7) leads to the final form of the surface energy density as a function

of the basic mode amplitudes

$$
\begin{aligned}
\mathcal{U} \;=\; & -\frac{1}{2}\sum_{i=1}^{N}\left(\mathcal{E}(B_0,|\mathbf{k}_i|)-\mu_2\mathcal{C}(\mathbf{k}_i)\right)A_{\mathbf{k}_i}^2 - \mathcal{Q}(2\pi/3)\sum_{\substack{i,j,l\le N\\ \mathbf{k}_i\pm\mathbf{k}_j\pm\mathbf{k}_l=0}}A_{\mathbf{k}_i}A_{\mathbf{k}_j}A_{\mathbf{k}_l} \\
& +\frac{1}{4}\sum_{i=1}^{N}\left(\mathcal{K}(0)+\frac{1}{2}\frac{\mathcal{Q}^2(0)}{\mathcal{E}(B_0,|2\mathbf{k}_i|)-\mu_2\mathcal{C}(2\mathbf{k}_i)}\right)A_{\mathbf{k}_i}^4 \\
& +\sum_{i<j\le N}\left(\mathcal{K}(\theta_{ij})+\frac{1}{2}\frac{\mathcal{Q}^2(\theta_{ij})}{\mathcal{E}(B_0,|\mathbf{k}_i+\mathbf{k}_j|)-\mu_2\mathcal{C}(\mathbf{k}_i+\mathbf{k}_j)}\right. \\
& \left.+\frac{1}{2}\frac{\mathcal{Q}^2(\pi-\theta_{ij})}{\mathcal{E}(B_0,|\mathbf{k}_i-\mathbf{k}_j|)-\mu_2\mathcal{C}(\mathbf{k}_i-\mathbf{k}_j)}\right)A_{\mathbf{k}_i}^2 A_{\mathbf{k}_j}^2 \qquad (4.14)
\end{aligned}
$$

4.2   Linear stability

Being an expansion up to fourth order in the amplitudes, eq. (4.14) contains the results we know already from the linear stability analysis of chapter 3. Discussing the linear order in the dynamic equations corresponds to a discussion of the second order in an energy functional description. We therefore have to minimize

$$
\mathcal{E}(B_0,k)-\mu_2\mathcal{C}(\mathbf{k}_i) \;=\; \tilde{\epsilon}k-\frac{1}{2}(1-k)^2-\mu_2 k \qquad (4.15)
$$

Determining the minimum of this expression with respect to k leads to

$$
\frac{\partial}{\partial k}\left(\tilde{\epsilon}k-\frac{1}{2}(1-k)^2-\mu_2 k\right) \;=\; \tilde{\epsilon}-\mu_2+(1-k)=0 \qquad (4.16)
$$

$$
\tilde{\epsilon}k-\frac{1}{2}(1-k)^2-\mu_2 k \;=\; 0 \qquad (4.17)
$$

The first equation represents the definition of a minimum itself, while the second condition represents the exchange of stability at onset. Below threshold the flat surface is stable with respect to a deformed one, and the energy density difference (4.14) is therefore negative. If the deformed surface is stable, its energy density is positive. As the solution of eqs. (4.16,4.17) we find in dimensionless units

$$
k=1 \qquad \text{and} \qquad \tilde{\epsilon}=\mu_2 \qquad (4.18)
$$

These solutions agree with the findings of chapter 3 and [20], where we could show that the characteristic wavelength at onset is not changed compared to usual ferrofluids while the threshold itself is enhanced by the shear modulus of the medium.

4.3   Stability of different Geometries

We discuss the stability of one of the regular patterns against the other ones. The specific geometries used to calculate $\mathcal{C}(\mathbf{k}_i)$ in eq. (4.11) are illustrated in fig. 4.1. We also assume the magnetic field close to the critical one permitting us to take the wave vector identical to the characteristic wave vector at onset, $k=1$.
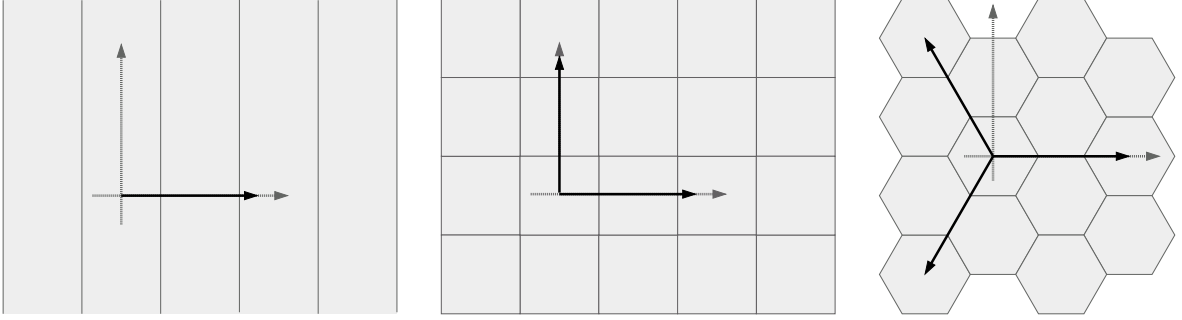
Figure 4.1: The sketch depicts the orientation of the main modes with respect to an arbitrarily chosen coordinate system (light grey) on the surface. In the discussion we consider stripes, squares and hexagons.

4.3.1 Stripe solutions

Starting with the simplest case, we discuss the stability of stripe patterns on the surface. For convenience we take the only wave vector appearing parallel to the $x-$axis, $k_i = \delta_{ix}$ and obtain

$$\mathcal{U} = -\frac{1}{2}(\tilde{\epsilon} - \mu_2)A^2 + \frac{1}{4}\left(\frac{5}{16} + \frac{\eta^2}{4(\tilde{\epsilon} - \mu_2) - 1}\right)A^4 \qquad (4.19)$$

For simplicity we follow [33, 34] and neglect $\tilde{\epsilon}$ in the denominator of the fourth order term without any noticeable change of the results. Minimizing (4.19) with respect to the amplitude we get

$$A_R = \sqrt{\frac{\tilde{\epsilon} - \mu_2}{\frac{5}{16} - \frac{\eta^2}{1+4\mu_2}}} \qquad (4.20)$$

and

$$\left.\frac{\partial^2 \mathcal{U}}{\partial A^2}\right|_{A=A_R} = 2(\tilde{\epsilon} - \mu_2) = 0 \qquad (4.21)$$

Thus, from this discussion we cannot draw any conclusion for the stability of stripes (as was the case for $\mu_2 = 0$ [33]).

4.3.2 Squares

We now start to discuss two main modes perpendicular to each other yielding a square lattice (cf. fig. 4.1). To calculate the coefficient $\mathcal{C}$, eq. (4.11), we take without loss of generality the two wave vectors to be $\mathbf{k}_1 = (1, 0)$ and $\mathbf{k}_2 = (0, 1)$ and obtain

$$\begin{aligned}\mathcal{U} = {} & -\frac{1}{2}(\tilde{\epsilon} - \mu_2)(A_1^2 + A_2^2) - \frac{1}{2}\frac{-5 + 16\eta^2 - 20\mu_2}{32(1 + 4\mu_2)}(A_1^4 + A_2^4) \\ & + \left(-\frac{9}{16} + \frac{1}{\sqrt{2}} + \eta^2 \frac{15 - 13\sqrt{2} + 4\left(-3 + 2\sqrt{2}\right)\mu_2}{6 - 4\sqrt{2} + 4\sqrt{2}\mu_2}\right)A_1^2 A_2^2 \qquad (4.22)\end{aligned}$$

Figure 4.2: Graphs separating regions in the $\chi - \tilde{\epsilon} - plane$ in which the amplitudes of squares are smaller or higher than 0.25 for different values of the elastic shear modulus μ_2. The critical magnetic susceptibility is enhanced with higher shear modulus.

where we have again neglected $\tilde{\epsilon}$ in the denominator of the fourth order terms. Minimizing eq. (4.22) leads to the amplitude $A_S = A_S(\tilde{\epsilon}, \mu_2, \eta)$

$$A_S = \sqrt{\frac{4(\tilde{\epsilon} - \mu_2)(1 + 4\mu_2)\big[3 - 2\sqrt{2}(1 - \mu_2)\big]}{N_S}} \tag{4.23}$$

with the denominator N_S given by

$$
\begin{aligned}
N_S = & (1 + 4\mu_2)\big[74\sqrt{2} - 103 + (26\sqrt{2} - 64)\mu_2\big] \\
& + 16\eta^2\big[12 - 11\sqrt{2} + (48 - 46\sqrt{2})\mu_2 + 16(2\sqrt{2} - 3)\mu_2^2\big]
\end{aligned}
\tag{4.24}
$$

Obviously $\tilde{\epsilon} - \mu_2 > 0$ is a necessary condition for the stability of square solutions.

In fig. 4.2 the value of the control parameter $\tilde{\epsilon}$ is plotted as a function of the magnetic susceptibility χ for $A_S = 0.25$ and different values of the shear modulus μ_2. The graphs separate configurations in the parameter space with amplitudes smaller (below the curve) and higher (above the curve) than $A_S = 0.25$ and the divergence for finite magnetic susceptibilities indicates that for a infinitesimal small control parameter $\tilde{\epsilon}$ the amplitudes are already infinitely large. In [34], for $\mu_2 = 0$, the plot has been used to estimate the maximum magnetic susceptibility at which the method diverges. As can be seen in fig. 4.2, for finite shear modulus the validity range of the method is increased to larger magnetic susceptibilities. For hexagons (cf. sec. 4.3.3) a similar result is obtained. The plot additionally illustrates the fact already stated by Gailitis himself that this energy method is rigorously valid only in the limit of a vanishing magnetic susceptibility.

Following the method of Gailitis [33] i.e. starting with a more general ansatz for the wave vectors that include stripes as a special case, we find that even for $\mu_2 > 0$ stripes are always unstable with respect to squares.
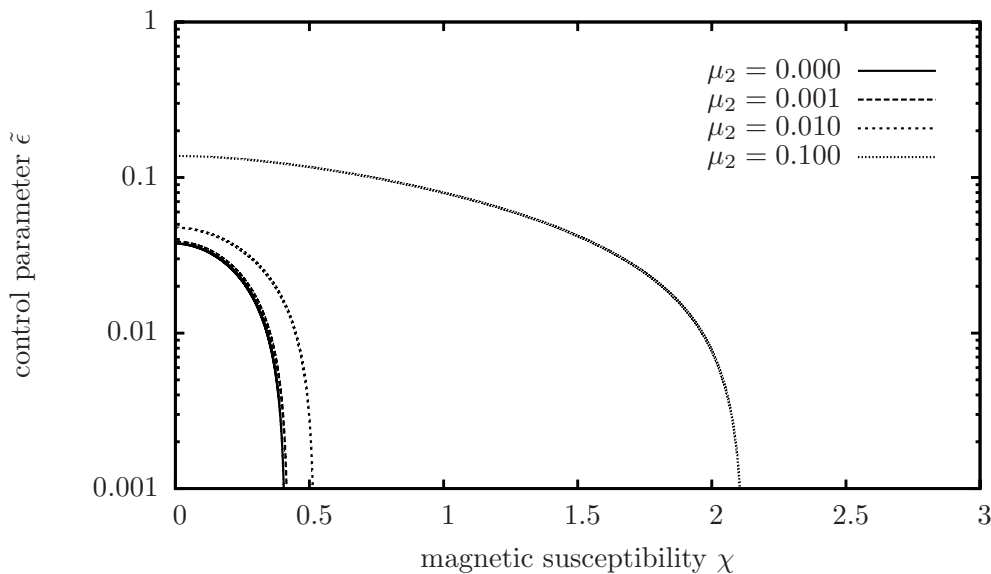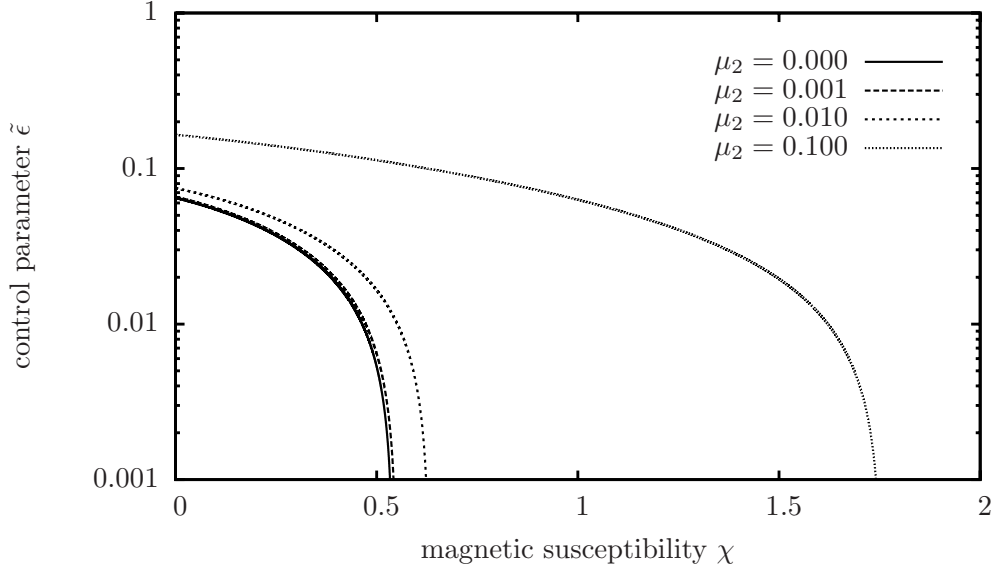
Figure 4.3: Graphs separating regions in the $\chi - \tilde{\epsilon}-$plane in which the amplitudes of hexagons are smaller or higher than 0.25 for different values of the elastic shear modulus μ_2. The critical magnetic susceptibility is enhanced with higher shear modulus.

4.3.3 Hexagons

We now discuss a regular hexagonal pattern generated by the three main wave vectors with angles of $2\pi/3$ (cf. fig. 4.1). The difference in surface energy density with respect to the flat surface, eq. (4.14), becomes

$$
\mathcal{U} = -\frac{1}{2}(\tilde{\epsilon} - \mu_2)(A_1^2 + A_2^2 + A_3^2) - \frac{3}{4}\eta A_1 A_2 A_3 + \frac{1}{4}\left[\frac{5}{16} - \frac{\eta^2}{1 + 4\mu_2}\right](A_1^4 + A_2^4 + A_3^4)
$$
$$
+ \left[-\frac{15}{32} + \frac{3}{8}\sqrt{3} + \left(\frac{11}{8} - \frac{7\sqrt{3}}{8}\right)\eta^2 - \frac{\left(\frac{3}{4} - \sqrt{3}\right)^2 \eta^2}{\left(1 - \sqrt{3}\right)^2 + 2\sqrt{3}\mu_2}\right](A_1^2 A_2^2 + A_2^2 A_3^2 + A_1^2 A_3^2)
$$
$$
\tag{4.25}
$$

In the following we will refer to the expressions written in the first and second square bracket as $\beta(0, \mu_2)$ and $\beta(2\pi/3, \mu_2)$, respectively, since in the limit of vanishing elasticity they are identical to the ones given by Gailitis [33]. For the same reason we will also refer to $3/4\eta$ as γ.

For the regular hexagonal pattern we obtain from (4.25) by minimization

$$
A_H = A_1 = A_2 = A_3 = \frac{\gamma \pm \sqrt{\gamma^2 + 4(\tilde{\epsilon} - \mu_2)[\beta(0, \mu_2) + 4\beta(2\pi/3, \mu_2)]}}{2[\beta(0, \mu_2) + 4\beta(2\pi/3, \mu_2)]} \tag{4.26}
$$

The hexagonal solutions exist only if the square root in eq. (4.26) is real, and they are stable, if the second derivative of eq. (4.25) with respect to the amplitudes is negative, leading to the conditions

$$
\frac{-1}{4[\beta(0, \mu_2) + 4\beta(2\pi/3, \mu_2)]} < \frac{\tilde{\epsilon} - \mu_2}{\gamma^2} < 2\frac{\beta(2\pi/3, \mu_2) + \beta(0, \mu_2)}{[2\beta(2\pi/3, \mu_2) - \beta(0, \mu_2)]^2} \tag{4.27}
$$
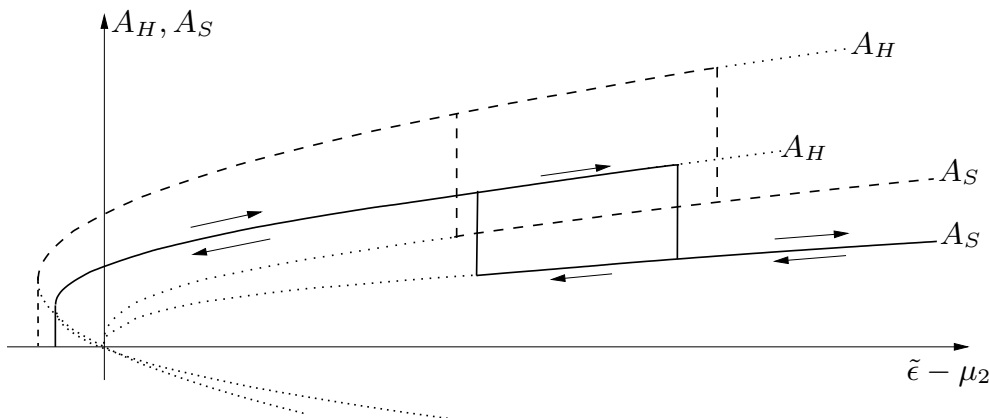
Figure 4.4: Qualitative sketch (not to scale) of the evolution of the amplitudes for squares (A_S) and hexagons (A_H). The dashed lines correspond to the case of a ferrofluid while the solid lines qualitatively describe the behavior for ferrogels with finite shear modulus μ_2. The dotted lines represent the energetically unstable branches.

Since the β-values are positive (at least for $\chi \leq 1$), hexagons can exist already below the linear threshold $\tilde{\epsilon} = \mu_2$. This existence range shrinks, however, for ferrogels compared to ferrofluids, since $\beta(\theta_{ij}, \mu_2) > \beta(\theta_{ij}, 0)$ for both $\theta_{ij} = 2\pi/3$ and 0. For the same reason the amplitude of the hexagonal pattern (4.26) decreases with increasing elastic modulus. Clearly, elasticity stabilizes a system against the Rosensweig instability, which is manifest not only in an increase of the (linear) threshold, but also in a decrease of the spike height. One can discuss the magnitude of the amplitudes as a function of the parameters $\tilde{\epsilon}$ and χ for the hexagonal solution in the same way as done for the square solution in section 4.3.2. Fig. 4.3 presents the corresponding plot for hexagons with the same qualitative result, that with increasing shear modulus the validity range of this method is extended towards higher magnetic susceptibilities.

Following the method of Gailitis superposing hexagons and squares, we investigate the relative stability of hexagons and squares. We find that squares are unstable with respect to hexagons under the condition

$$\frac{\tilde{\epsilon} - \mu_2}{\gamma^2} \quad < \quad \frac{\beta(0, \mu_2) + 2\beta(\pi/2, \mu_2)}{[2\beta(2\pi/3, \mu_2) + 2\beta(\pi/6, \mu_2) - 2\beta(\pi/2, \mu_2) - \beta(0, \mu_2)]^2}, \quad (4.28)$$

which is just Gailitis' expression, but with μ_2 dependent β-abbreviations

$$\beta(\pi/2, \mu_2) \quad = \quad -\frac{9}{16} + \frac{1}{\sqrt{2}} + \frac{15 - 13\sqrt{2} - 4(3 - 2\sqrt{2})\mu_2}{6 - 4\sqrt{2} + 4\sqrt{2}\mu_2}\eta^2 \quad (4.29)$$

$$\beta(\pi/6, \mu_2) \quad = \quad \frac{3}{32}(4\sqrt{6} - 7) + \frac{116 - 41\sqrt{6} - (64 - 28\sqrt{6})\mu_2}{16(2 - \sqrt{6} - 2\mu_2)}\eta^2 \quad (4.30)$$

Figure 4.4 shows the magnitude of the amplitudes as a function of the control parameter for a finite and a vanishing shear modulus, respectively. We note a decrease in size of the hysteretic region (for negative $\tilde{\epsilon} - \mu_2$) with increasing shear modulus. While in the case of no elasticity the lower boundary is at -0.25, it is shifted to -0.24 for a

shear modulus of $\mu_2 = 0.1$ (both values taken for a magnetic susceptibility of $\chi = 0.1$)[2]. The second hysteretic region for the transition between squares and hexagons also shrinks with increasing μ_2. For instance, the lower boundary of the hysteresis loop at 5.7 (for the right hand side of eq. (4.28)) for $\mu_2 = 0$ increases to 6.9 for $\mu_2 = 0.1$, while the upper boundary of the hysteresis loop at 540 for $\mu_2 = 0$ is reduced to 480 for $\mu_2 = 0.1$ ($\chi = 0.1$). This result should be experimentally detectable, at least qualitatively.

4.4 Some drawbacks of the energy method

One of the major drawbacks of this method is, that it is only valid in the asymptotic limit of a vanishing magnetic susceptibility χ. This can be easily realized by inspection of fig. 4.2. For high enough magnetic susceptibilities the amplitude diverges for arbitrarily small control parameters $\tilde{\epsilon}$. This is why we had to scale the stability boundaries given in eqs. (4.27,4.28) with γ in order to compensate the divergence. For a nonlinear theory for magnetic fluids this validity limit is not satisfying.

The method relies on the static energetic comparison of different surface deformations with respect to each other. It allows the determination of possible surface patterns but it does not tell us which pattern will be finally achieved. The selection process of a real pattern is additionally governed by dissipative processes. The Rosensweig instability, however, differs from other instabilities in that its final state is static and no dissipation occurs. But during the growth of the surface spikes energy is dissipated and this may play a role in the selection process. Additionally we realized in the discussions so far, that the occurrence of static surface spikes is the limit of a previously dynamic surface mode that freezes in its dynamics. Furthermore, as soon as the control parameter is beyond its critical value and as long as the final state is not achieved, the system is out of equilibrium and the definition of the potential (as is the energy) is not straightforward.

As mentioned already, the energy method gives us first hints to become familiar with the Rosensweig phenomenon. What we would like to have instead is a full weakly nonlinear analysis of the basic hydrodynamic equations that also captures the dynamical processes during growth and that additionally considers dissipation. The derivation of a dynamic amplitude equation that may solve the addressed problems will be the subject of the following chapter 5.

---

[2]Recall that we introduced dimensionless units on page 32.

Chapter 5

The amplitude equation

> *The physical, chemical, and biological systems [...] are often quite complicated and the equations and boundary conditions describing them are not always known precisely. Even when they are known, as is the case for many hydrodynamic instabilities, a linear analysis already requires numerical evaluation and a direct analytical approach is impossible beyond threshold. The perturbation methods described below are a partial response to this situation, though calculation of the appropriate coefficients can be difficult even if the starting equations are known precisely.*
>
> *M. C. Cross and P. C. Hohenberg [48]*

The discussion from the previous chapters provides us with a first understanding of the Rosensweig instability. Chapter 3 taught us, that we should interpret the stationarity of the normal field instability rather as a limiting process where the frequency of the characteristic mode vanishes. In chapter 4 we discussed the energetically favored surface patterns, but we realized some problems with the energy method. In this chapter we will discuss the nonlinear regime starting from the fundamental hydrodynamic equations and use an $\epsilon-$expansion to access the weakly nonlinear regime[1]. In this context ϵ denotes the normalized difference between the actually applied magnetic field and its critical value. The information we obtained so far will be of great importance on how we finally access this regime.

5.1 Introduction

We will perform a weakly nonlinear analysis of the basic set of hydrodynamic equations as pioneered by Schlüter, Lortz and Busse [38] and Newell and Whitehead [47] for the Rayleigh-Bénard system to obtain a set of amplitude equations in the case of the Rosensweig instability. The weakly nonlinear analysis is a perturbative approach and rests on the assumption that close to the linear threshold the nonlinear state can be expressed by a small perturbation from the ground state which is expanded in terms of the control parameter ϵ. The lowest order in ϵ determines the linear stability as already discussed in chapter 3. The amplitudes of these disturbances, which are still undetermined in the

---

[1]Parts of this chapter have been published in [74], others are prepared for publication [75].

linear perturbative order (cf. chapter 3), have to fulfill certain equations in the higher perturbative orders to guarantee the solvability of the nonlinear hydrodynamic equations. These amplitude equations in turn are nonlinear dynamic differential equations describing the cooperative dynamics of a set of critical modes subject to nonlinear interactions. In this introductory section we will introduce this method and will focus on key problems one encounters when applying this method to the Rosensweig instability. For a comprehensive introduction to the weakly nonlinear analysis and on amplitude equations, the reader is referred to [48, 76, 77].

5.1.1 Nonlinear expansion

Performing a weakly nonlinear analysis of the stationary state evolving slightly beyond the linear threshold M_c, we have to expand the macroscopic variables in terms of ϵ, the normalized difference between the actual applied magnetic field and the critical one

$$\{p, \mathbf{B}, \mathbf{H}, \mathbf{M}\} = \{p_0, \mathbf{B}_c, \mathbf{H}_c, \mathbf{M}_c\} + \epsilon\{p^{(1)}, \mathbf{B}^{(1)}, \mathbf{H}^{(1)}, \mathbf{M}^{(1)}\} + \ldots \quad (5.1)$$

$$\{\mathbf{v}, \epsilon_{ij}, \xi\} = 0 + \epsilon\{\mathbf{v}^{(1)}, \epsilon_{ij}^{(1)}, \xi^{(1)}\} + \ldots \quad (5.2)$$

The magnetic field, however, is an externally given parameter acting as the control parameter. The series expansion of $\mathbf{H}$ (5.1) can therefore be reinterpreted as the definition of ϵ. Note, that this definition of ϵ is not the same definition as used in chapter 4, which is supposed to be the appropriate definition in the case of the Rosensweig instability. We will see later that the definition of ϵ used here leads consistently to the control parameter as used in the previous sections.

In our linear discussion (chapter 3), we modeled the surface deflection $\xi(x, y, t)$ using plane waves $\xi(x, y, t) = \hat{\xi} e^{i\omega t - i\mathbf{k}\cdot\mathbf{r}}$, where the amplitude $\hat{\xi}$ is a common factor in all contributions of the linearized hydrodynamic equations and therefore remains undetermined. In a nonlinear discussion, we have to extend this ansatz to address the possibility of nonlinear interactions between a set of critical modes. The most general ansatz as a starting point for a nonlinear discussion is to assume N of these characteristic modes with different orientations. Each of these modes i consists of a right and a left traveling contribution denoted by the subscripts R and L, respectively. Since the surface deflection as an observable has to be real, we have to add the corresponding complex conjugate which is denoted by an asterisk

$$\xi^{(1)} = \sum_i^N \xi_{iR} + \xi_{iL} + \xi_{iR}^* + \xi_{iL}^*$$

$$= \sum_i^N \hat{\xi}_{iR} e^{i\omega_i t - i\mathbf{k}_i\cdot\mathbf{r}} + \hat{\xi}_{iL} e^{-i\omega_i t - i\mathbf{k}_i\cdot\mathbf{r}} + \hat{\xi}_{iR}^* e^{-i\omega_i t + i\mathbf{k}_i\cdot\mathbf{r}} + \hat{\xi}_{iL}^* e^{i\omega_i t + i\mathbf{k}_i\cdot\mathbf{r}} \quad (5.3)$$

Besides the expansion of the hydrodynamic variables, we can also consider to rescale time and space in order to further separate the dynamics to capture the long wavelength and the long time scale cooperative dynamics of the individual characteristic modes. One can interpret this rescaling in the sense that we permit the amplitude $\hat{\xi}$ to be slowly dependent on time[2] and space, respectively. In the present discussion we will discard the

---

[2]The time t as used in eq. (5.3) is then considered the "fast" time scale of the surface waves (or of

possible rescaling of space and focus on surface patterns that arise homogeneously and that do not show any long wavelength variation. As mentioned already, the rescaling of time can be interpreted in the sense that the dynamics of the amplitudes $\hat{\xi}$ itself takes place on the slow timescales

$$t^{(1)} = \epsilon t \quad \text{and} \quad t^{(2)} = \epsilon^2 t \tag{5.4}$$

so that $\hat{\xi}_{iR} \rightarrow \hat{\xi}_{iR}(t^{(1)}, t^{(2)}, \dots)$ and correspondingly for the left traveling contributions and their corresponding complex conjugates. This rescaling of time will lead to the substitution for the time derivative

$$\partial_t \longrightarrow \partial_t^{(0)} + \epsilon \partial_t^{(1)} + \epsilon^2 \partial_t^{(2)} + \dots \tag{5.5}$$

These are, as we will see later, the time scales of the growth of the surface spikes.

5.1.2 The solvability condition for higher orders

Fredholm's theorem and the adjoint system

With the rescaling of time and the expansion of the macroscopic variables in terms of ϵ, the whole system of differential equations can be expanded in terms of ϵ. Let $\mathcal{L}_0$ be the linear differential operator and $|\phi\rangle = |\phi^{(0)}\rangle + \epsilon |\phi^{(1)}\rangle + \dots$ the macroscopic state vector. The basic hydrodynamic equations as given by eqs. (2.32-2.34) then read in general form

$$\mathcal{L}_0 |\phi^{(1)}\rangle = 0 \tag{5.6}$$
$$\mathcal{L}_0 |\phi^{(2)}\rangle = |\mathcal{N}(\phi^{(1)}, \phi^{(1)})\rangle + |\mathcal{T}(\partial_t^{(1)} \phi^{(1)})\rangle \tag{5.7}$$
$$\vdots = \vdots$$

where every order in ϵ needs to be satisfied separately.

The first equation (5.6) represents the linearized set of equations as used in the linear stability analysis of chapter 3, where the explicit translation of equation (5.6) is given by eqs. (3.8-3.10). Furthermore, eq. (5.6) defines the kernel of the linear operator $\mathcal{L}_0$, given by the linear eigenvectors $|\phi^{(1)}\rangle$. In the second perturbative order the set of equations (5.7) becomes inhomogeneous due to the nonlinear nature of the basic set of equations (represented by $\mathcal{N}(\cdot, \cdot)$) and due to the rescaling of time (represented by $\mathcal{T}(\cdot)$). In the case that these inhomogeneities reproduce elements of the kernel of the linear operator $\mathcal{L}_0$, equation (5.7) cannot be solved. The necessary condition that the inhomogeneities need to be orthogonal to the subspace spanned by the linear eigenvectors $|\phi\rangle$ provides us with an additional solvability condition. This condition is named after Fredholm and reads for the second order

$$\langle \phi | \mathcal{N}(\phi^{(1)}, \phi^{(1)}) \rangle + \langle \phi | \mathcal{T}(\partial_t^{(1)} \phi^{(1)}) \rangle = 0 \tag{5.8}$$

where $\langle \cdot | \cdot \rangle$ denotes a suitable scalar product about which we will talk shortly.

---

general thermodynamic fluctuations in the case of other hydrodynamic instabilities) even though it is already a macroscopic time scale. The dynamics of the amplitudes $\hat{\xi}$ is in turn assumed to take place on an even slower time scale. The same arguments hold if we rescale spatial coordinates.
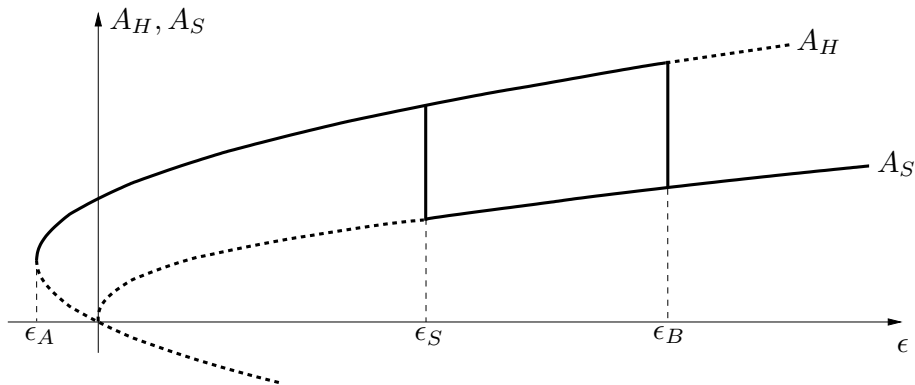
Figure 5.1: The general bifurcation scheme for amplitude equations of the form (5.9) according to [78, 48]. The analytical expressions for the limits of stability ϵ_A, ϵ_B and ϵ_S are given in the main text. The solid lines represent the stable branches whereas the dotted lines correspond to the unstable ones.

Amplitude equations in general

The solvability condition (5.8) provides an additional equation and the still under-determined system of equations is closed to fix the amplitude $\hat{\xi}$. If this condition, valid in the second order, is combined with the corresponding condition in the third order, one obtains the so called amplitude equations which define possible nonlinear solutions for the amplitudes of the critical modes that are necessary to satisfy the basic hydrodynamic equations. In the absence of the inversion symmetry $\hat{\xi}_i \longrightarrow -\hat{\xi}_i$ (which is the case for the Rosensweig instability), the usual structure of this amplitude equation is, written in appropriate units, given by [48]

$$\partial_t \hat{\xi}_1 = \epsilon \hat{\xi}_1 - \hat{\gamma} \hat{\xi}_2^* \hat{\xi}_3^* - \left[|\hat{\xi}_1|^2 + g_1(\theta_{ij}) \left(|\hat{\xi}_2|^2 + |\hat{\xi}_3|^2 \right) \right] \hat{\xi}_1 \qquad (5.9)$$

together with its cyclic permutations $1 \rightarrow 2 \rightarrow 3 \rightarrow 1$ and where θ_{ij} denotes the angle between two different critical modes that become unstable at the linear threshold. The quadratic coefficient $\hat{\gamma}$ in eq. (5.9) is nonzero only for the hexagonal pattern ($\theta_{ij} = 2\pi/3$). In this case this contribution dominates close to the threshold and renders the bifurcation transcritical.

In 1990 Ciliberto et al. [78] discussed the set of equations given by (5.9) using a linear stability analysis to determine the stability regimes of a hexagonal pattern with respect to a stripe pattern. Later, additionally the possibility of a square pattern was considered [79, 80]. For a nonzero quadratic coefficient $\hat{\gamma}$, the hexagon solution is the stable surface pattern at the linear threshold. The bifurcation from the flat surface state is transcritical and hexagons remain stable even below the linear threshold as long as

$$\epsilon > \epsilon_A = -\frac{\hat{\gamma}^2}{4(1 + 2g_1(\theta_{ij} = 2\pi/3))} \qquad (5.10)$$

The hexagon solution is stable for all control parameters $\epsilon > \epsilon_A$ if $g_1(\theta_{ij} = 2\pi/3) < 1$ and $1 + 2g_1(\theta_{ij} = 2\pi/3) < g_1(\theta_{ij} = \pi/2) + 2g_1(\theta_{ij} = \pi/6)$. For $g_1(\theta_{ij} = 2\pi/3) > 1$ they loose stability with respect to either stripes or squares at

$$\epsilon_B = \frac{\hat{\gamma}^2(2 + g_1(\theta_{ij} = 2\pi/3)}{(1 - g_1(\theta_{ij} = \pi/2))^2} \qquad (5.11)$$

whereas if $1 + 2g_1(\theta_{ij} = 2\pi/3) > g_1(\theta_{ij} = \pi/2) + 2g_1(\theta_{ij} = \pi/6)$ this happens at

$$\epsilon_B = \frac{\hat{\gamma}^2(g_1(\theta_{ij} = \pi/2) + 2g_1(\theta_{ij} = \pi/6))}{(1 + 2g_1(\theta_{ij} = 2\pi/3) - g_1(\theta_{ij} = \pi/2) - 2g_1(\theta_{ij} = \pi/6))^2} \qquad (5.12)$$

Stripes and squares turn out to be mutually exclusive patterns. In the case that $g_1(\theta_{ij} = \pi/2) < 1$, $g_1(\theta_{ij} = \pi/6) + g_1(\theta_{ij} = 2\pi/3) < 1 + g_1(\theta_{ij} = \pi/2)$ and for large enough control parameters

$$\epsilon > \epsilon_S = \frac{\hat{\gamma}^2(1 + g_1(\theta_{ij} = \pi/2))}{(1 + g_1(\theta_{ij} = \pi/2) - g_1(\theta_{ij} = 2\pi/3) - g_1(\theta_{ij} = \pi/6))^2} \qquad (5.13)$$

squares are the stable surface pattern. Otherwise the stripe pattern turns out to be stable for control parameters larger than

$$\epsilon_S = \frac{\hat{\gamma}^2}{(1 - g_1(\theta_{ij} = 2\pi/3))} \qquad (5.14)$$

A schematic bifurcation diagram according to these considerations is drawn in fig. 5.1, where A_H denotes the amplitude of hexagons and A_S the amplitude of either squares or stripes, depending on which of these patterns is the preferred one.

The scalar product

We have some freedom to choose a scalar product that is suitable for our discussion of the nonlinear regime. In chapter 2 we found, that the bulk magnetic equations completely decouple from the bulk hydrodynamic equations, leaving us with no control parameter in the bulk for the nonlinear regime. At a first glance, this circumstance impedes the derivation of an amplitude equation as known for instance for the Rayleigh-Bénard convection, if we used the usual scalar product given by

$$\langle \cdot | \cdot \rangle = \lim_{L \to \infty} \frac{1}{4L^2} \int\limits_{-L}^{L} dx \int\limits_{-L}^{L} dy \int\limits_{-\infty}^{\xi} dz \int\limits_{0}^{\tau} dt \; \overline{\cdot} \cdot \qquad (5.15)$$

To circumvent this problem, an extended scalar product can be introduced that, additionally to the bulk equations, is applied to certain boundary conditions, in particular to those containing a control parameter [54]. With a scalar product like that, Lange [49] tried to derive the adjoint system in the case of the Rosensweig instability. He failed in doing so, since he could not translate the surface contributions at the deformable surface into a set of adjoint boundary conditions.

The kind of scalar product used by Lange was previously introduced by Dauby et al. [54] to describe the nonlinear regime of purely surface tension driven convection, the Marangoni instability. The approach was successful, since the authors assumed a flat, undeformable surface. In the case of the Marangoni instability this assumption is comprehensible, since what one is after is the flow field that develops in the bulk and not the deformation of the surface. An assumption instead, that is not appropriate for the Rosensweig instability since the flow field for the static nonlinear regime vanishes identically and the only observable is the deformed surface.

In the present nonlinear analysis we hence return to the usual scalar product (5.15) but explicitly expand all boundary values in terms of the surface deflection ξ. Additionally we treat the system dynamically, to retain a non-trivial kinematic boundary condition. With these assumptions we are able to derive the adjoint system inevitably needed to satisfy (5.8). A detailed derivation of the necessary boundary conditions and the derivation of the adjoint system is given in appendix C and in section 5.2, respectively. The problem with the missing control parameter in the bulk equations is solved in section 5.3.4 by realizing, that the boundary conditions for the higher orders still contain contributions proportional to the main characteristic modes $\xi^{(1)}$. One of these contributions contains, because the system is still treated as dynamic, a time derivative of the amplitude, whereas the other contributions are proportional to the control parameter.

5.2 The adjoint system for the Rosensweig instability

5.2.1 Dynamic surfaces

The general idea of our approach is to treat the surface as dynamic with surface waves propagating on the free surface, as long as the magnetic field is below its critical value. As discussed in chapter 3 we can distinguish the limiting cases of capillary waves for very short wavelengths, gravitational waves for rather long wavelengths and Rayleigh elastic waves in the intermediate regime and only in the case of gels. Furthermore, below the critical point of the instability, all of these waves are damped, but get excited again by thermal agitation. When reaching the critical value of the control parameter, the damping of one characteristic mode becomes weak and finally vanishes exactly at the critical point. In the stationary case this coincides with the slowing down of this particular mode, so that the initially traveling waves transform into a static pattern. This process can be seen by inspection of the dispersion relation as plotted for example in fig. 3.2 (p. 26) for ferrofluids or in fig. 3.3 (p. 27) for magnetic gels.

As a consequence of this, we assume the entire linear problem to be time dependent from the beginning and in particular keep the time dependence for the derivation of the adjoint system. We will recognize later, that also for the higher perturbative orders the dynamic treatment is important. Only in the end of the discussion we will, based on the discussion of the dispersion relation, take the static limit of the system.

5.2.2 Basic equations and ground state

The macroscopic equations appropriate for the discussion of the nonlinear Rosensweig instability have already been discussed in chapter 2 and are given by (2.32-2.35). We do not make at this stage the incompressibility approximation in order to maintain the symmetric structure of the Navier-Stokes equation which turns out to be necessary for the adjoining process. Only at the end we will simplify the formulas by assuming incompressibility. As long as we consider the medium as compressible, we need an equation of state. Due to the assumption that no magnetostrictive effects are important in our discussion, this equation of state can be assumed to be the barotropic equation

$$\delta p \;=\; c^2 \delta \rho \tag{5.16}$$

with the speed of sound c. As Jarkova et al. stated in [60], the modification of the speed of sound and especially the anisotropy effect in the presence of an external magnetic field is proportional to the magnetostrictive constants and therefore of no importance in our discussion. The considered geometry is sketched in fig. 2.1 on page 18 and is briefly repeated here. The infinitely extended surface is initially situated at $z = 0$. For convenience the magnetic medium is filling the negative half-space whereas the vacuum is assumed to occupy the positive one. The gravitational force is assumed to point downwards and the applied magnetic field is oriented parallel to the $z-$axis.

To find the adjoint system of equations with its corresponding boundary conditions to the linear problem, we linearize eqs. (2.32) to (2.35) with respect to the initially flat surface according to the scaling behavior of the individual variables as described in (5.1,5.2). We finally obtain

$$\rho_0 \partial_t v_i^{(1)} + \partial_i p^{(1)} - \nu_2 \partial_j (\partial_i v_j^{(1)} + \partial_j v_i^{(1)}) - \hat{\nu} \partial_i \partial_k v_k^{(1)} - 2\mu_2 \partial_j \epsilon_{ij}^{(1)} - \hat{\mu} \partial_i \epsilon_{kk}^{(1)} = 0 \quad (5.17)$$

$$\partial_t \epsilon_{ij}^{(1)} - \frac{1}{2}(\partial_i v_j^{(1)} + \partial_j v_i^{(1)}) = 0 \quad (5.18)$$

$$\partial_t \rho^{(1)} + \partial_i (\rho_0 v_i^{(1)}) = 0 \quad (5.19)$$

5.2.3 The linear equations and the adjoint system

If we use the general notation of chapter 5.1.2, the system of dynamic bulk equations for the Rosensweig instability can be written in terms of an eleven dimensional state vector, that we will define in the following way

$$|\phi\rangle = \left(v_x, v_y, v_z, p, \epsilon_{xx}, \epsilon_{yy}, \epsilon_{zz}, \epsilon_{xy}, \epsilon_{xz}, \epsilon_{yz}, \rho \right) \quad (5.20)$$

We will skip the discussion of the magnetic part of the system of equations. This part completely decouples from the dynamic part of the medium as stated above and reduces within our assumptions to the Laplace equation for the magnetic potential. The Laplace equation is self-adjoint and a homogenous equation. Therefore Fredholm's theorem is satisfied automatically. The solutions for the magnetic field variables are discussed in detail in appendix B.

Using the definition given above we can write the system of linear equations (5.17-5.19) together with the equation of state of the medium (5.16) in the following form, which can be taken to be the definition for the linear operator $\mathcal{L}_0$.

$$\mathcal{L}_0 |\phi^{(1)}\rangle = 0 \quad (5.21)$$

To find the adjoint operator $\mathcal{L}_0^\dagger$, and especially the adjoint boundary conditions, we use the following identity with $\bar{\phi}$ denoting the adjoint state

$$\langle \bar{\phi} | \mathcal{L}_0 \phi^{(1)} \rangle = \langle \mathcal{L}_0^\dagger \bar{\phi} | \phi^{(1)} \rangle \quad (5.22)$$

The left hand side of this equation corresponds to the following integral using the standard

scalar product (5.15), which we have to integrate by parts,

$$\lim_{L\to\infty}\frac{1}{4L^2}\int\limits_{-L}^{L}dx\int\limits_{-L}^{L}dy\int\limits_{-\infty}^{\xi}dz\int\limits_{0}^{t}dt\left\{\right.$$

$$+\bar{v}_x\left\{\left(\rho_0\partial_t-\nu_2\partial_i^2-(\hat{\nu}+\nu_2)\partial_x^2\right)v_x^{(1)}-\hat{\nu}\partial_x\partial_y v_y^{(1)}-\nu_2\partial_y\partial_x v_y^{(1)}-\hat{\nu}\partial_x\partial_z v_z^{(1)}-\nu_2\partial_z\partial_x v_z^{(1)}\right.$$
$$\left.+\partial_x p^{(1)}-2\mu_2\partial_x\epsilon_{xx}^{(1)}-\hat{\mu}\partial_x\epsilon_{xx}^{(1)}-\hat{\mu}\partial_x\epsilon_{yy}^{(1)}-\hat{\mu}\partial_x\epsilon_{zz}^{(1)}-2\mu_2\partial_y\epsilon_{xy}^{(1)}-2\mu_2\partial_z\epsilon_{xz}^{(1)}\right\}$$

$$+\bar{v}_y\left\{-\hat{\nu}\partial_z\partial_x v_x^{(1)}-\nu_2\partial_x\partial_z v_x^{(1)}+\left(\rho_0\partial_t-\nu_2\partial_i^2-(\hat{\nu}+\nu_2)\partial_y^2\right)v_y^{(1)}-\hat{\nu}\partial_y\partial_z v_z^{(1)}-\nu_2\partial_z\partial_y v_z^{(1)}\right.$$
$$\left.+\partial_y p^{(1)}-\hat{\mu}\partial_y\epsilon_{xx}^{(1)}-2\mu_2\partial_y\epsilon_{yy}^{(1)}-\hat{\mu}\partial_y\epsilon_{yy}^{(1)}-\hat{\mu}\partial_y\epsilon_{zz}^{(1)}-2\mu_2\partial_x\epsilon_{xy}^{(1)}-2\mu_2\partial_z\epsilon_{yz}^{(1)}\right\}$$

$$+\bar{v}_z\left\{-\hat{\nu}\partial_z\partial_x v_x^{(1)}-\nu_2\partial_x\partial_z v_x^{(1)}-\hat{\nu}\partial_z\partial_y v_y^{(1)}-\nu_2\partial_y\partial_z v_y^{(1)}+\left(\rho_0\partial_t-\nu_2\partial_i^2-(\hat{\nu}+\nu_2)\partial_z^2\right)v_z^{(1)}\right.$$
$$\left.+\partial_z p^{(1)}-\hat{\mu}\partial_z\epsilon_{xx}^{(1)}-\hat{\mu}\partial_z\epsilon_{yy}^{(1)}-2\mu_2\partial_z\epsilon_{zz}^{(1)}-\hat{\mu}\partial_z\epsilon_{zz}^{(1)}-2\mu_2\partial_x\epsilon_{xz}^{(1)}-2\mu_2\partial_y\epsilon_{yz}^{(1)}\right\}$$

$$+\bar{p}\left\{\partial_x v_x^{(1)}+\partial_y v_y^{(1)}+\partial_z v_z^{(1)}+\frac{\partial_t\rho^{(1)}}{\rho_0}\right\}$$

$$+\bar{\epsilon}_{xx}\left\{-\partial_x v_x^{(1)}+\partial_t\epsilon_{xx}^{(1)}\right\}+\bar{\epsilon}_{yy}\left\{-\partial_y v_y^{(1)}+\partial_t\epsilon_{yy}^{(1)}\right\}+\bar{\epsilon}_{zz}\left\{-\partial_z v_z^{(1)}+\partial_t\epsilon_{zz}^{(1)}\right\}$$

$$+\bar{\epsilon}_{xy}\left\{-\frac{\partial_y}{2}v_x^{(1)}-\frac{\partial_x}{2}v_y^{(1)}+\partial_t\epsilon_{xy}^{(1)}\right\}+\bar{\epsilon}_{xz}\left\{-\frac{\partial_z}{2}v_x^{(1)}-\frac{\partial_x}{2}v_z^{(1)}+\partial_t\epsilon_{xz}^{(1)}\right\}$$

$$+\bar{\epsilon}_{yz}\left\{-\frac{\partial_z}{2}v_y^{(1)}-\frac{\partial_y}{2}v_z^{(1)}+\partial_t\epsilon_{yz}^{(1)}\right\}+\bar{\rho}\left\{\frac{\partial_t p^{(1)}}{\rho_0}-c^2\frac{\partial_t\rho^{(1)}}{\rho_0}\right\}\right\}\tag{5.23}$$

This leads to the adjoint linear operator

$$\mathcal{L}_0^\dagger\ =\ \begin{pmatrix} A & C \\ B & D \end{pmatrix}\tag{5.24}$$

with the abbreviations

$$A\ =\ \begin{pmatrix} -\rho\partial_t-\nu_2\partial_i^2-(\hat{\nu}+\nu_2)\partial_x^2 & -\hat{\nu}\partial_x\partial_y-\nu_2\partial_y\partial_x & -\hat{\nu}\partial_x\partial_z-\nu_2\partial_z\partial_x \\ -\hat{\nu}\partial_y\partial_x-\nu_2\partial_x\partial_y & -\rho\partial_t-\nu_2\partial_i^2-(\hat{\nu}+\nu_2)\partial_y^2 & -\hat{\nu}\partial_y\partial_z-\nu_2\partial_z\partial_y \\ -\hat{\nu}\partial_z\partial_x-\nu_2\partial_x\partial_z & -\hat{\nu}\partial_z\partial_y-\nu_2\partial_y\partial_z & -\rho\partial_t-\nu_2\partial_i^2-(\hat{\nu}+\nu_2)\partial_z^2 \\ -\partial_x & -\partial_y & -\partial_z \end{pmatrix}\tag{5.25}$$

$$B\ =\ \begin{pmatrix} 2\mu_2\partial_x+\hat{\mu}\partial_x & \hat{\mu}\partial_y & \hat{\mu}\partial_z \\ \hat{\mu}\partial_x & 2\mu_2\partial_y+\hat{\mu}\partial_y & \hat{\mu}\partial_z \\ \hat{\mu}\partial_x & \hat{\mu}\partial_y & 2\mu_2\partial_z+\hat{\mu}\partial_z \\ 2\mu_2\partial_y & 2\mu_2\partial_x & 0 \\ 2\mu_2\partial_z & 0 & 2\mu_2\partial_x \\ 0 & 2\mu_2\partial_z & 2\mu_2\partial_y \\ 0 & 0 & 0 \end{pmatrix}\tag{5.26}$$

$$C = \begin{pmatrix} -\partial_x + \frac{1}{\rho_0}(\partial_x \rho_0) & \partial_x & 0 & 0 & \frac{1}{2}\partial_y & \frac{1}{2}\partial_z & 0 & 0 \\ -\partial_y + \frac{1}{\rho_0}(\partial_y \rho_0) & 0 & \partial_y & 0 & \frac{1}{2}\partial_x & 0 & \frac{1}{2}\partial_y & 0 \\ -\partial_z + \frac{1}{\rho_0}(\partial_z \rho_0) & 0 & 0 & \partial_z & 0 & \frac{1}{2}\partial_x & \frac{1}{2}\partial_y & 0 \\ 0 & 0 & 0 & 0 & 0 & 0 & 0 & -\frac{1}{\rho_0}\partial_t \end{pmatrix} \tag{5.27}$$

$$D = \begin{pmatrix} 0 & -\partial_t & 0 & 0 & 0 & 0 & 0 & 0 \\ 0 & 0 & -\partial_t & 0 & 0 & 0 & 0 & 0 \\ 0 & 0 & 0 & -\partial_t & 0 & 0 & 0 & 0 \\ 0 & 0 & 0 & 0 & -\partial_t & 0 & 0 & 0 \\ 0 & 0 & 0 & 0 & 0 & -\partial_t & 0 & 0 \\ 0 & 0 & 0 & 0 & 0 & 0 & -\partial_t & 0 \\ -\frac{1}{\rho_0}\partial_t & 0 & 0 & 0 & 0 & 0 & 0 & -\frac{c^2}{\rho_0}\partial_t \end{pmatrix} \tag{5.28}$$

While integrating eq. (5.23) by parts, one also obtains surface contributions, which have to vanish to fulfill eq. (5.22). The most important parts are the contributions due to the $z-$integration. At the bottom ($z = -\infty$) they are always 0, since the eigenvectors of the linear system exponentially decay with increasing depth (3.27-3.35). The condition, that they should also vanish at the surface, defines the adjoint boundary conditions at the free surface. At this point we can just state that the following sum should vanish

$$0 \overset{!}{=} \bar{v}_x(-\nu_2\partial_z v_x^{(1)} - \nu_2\partial_x v_z^{(1)} - \mu_2\epsilon_{xz}^{(1)}) + v_x^{(1)}(\nu_2\partial_z\bar{v}_x + \nu_2\partial_x\bar{v}_z - \frac{1}{2}\bar{\epsilon}_{xz})$$

$$+ \bar{v}_y(-\nu_2\partial_z v_y^{(1)} - \nu_2\partial_y v_z^{(1)} - \mu_2\epsilon_{yz}^{(1)}) + v_y^{(1)}(\nu_2\partial_z\bar{v}_y + \nu_2\partial_y\bar{v}_z - \frac{1}{2}\bar{\epsilon}_{yz})$$

$$+ \bar{v}_z(-\hat{\nu}\partial_i v_i^{(1)} - 2\nu_2\partial_z v_z^{(1)} - \hat{\mu}\epsilon_{ii}^{(1)} - 2\mu_2\epsilon_{zz}^{(1)} + p^{(1)}) + v_z^{(1)}(\hat{\nu}\partial_i\bar{v}_i + 2\nu_2\partial_z\bar{v}_z + \bar{p} - \bar{\epsilon}_{zz}) \tag{5.29}$$

Using the two tangential boundary conditions of the original system (C.3,C.4) those contributions in (5.29) vanish that are proportional to $\bar{v}_x$ or $\bar{v}_y$. Using the normal stress boundary condition (C.5) in the second last term of (5.29), we implement the gravitational, the surface tension and the magnetic contributions into the adjoint boundary conditions. This also ensures the presence of the driving force in the boundary conditions of the adjoint system. With the help of the kinematic boundary condition (eq. (2.44)) in the original case, which reduces in the linear order to $v_z^{(1)} = i\omega\xi^{(1)}$, we can then substitute $v_z^{(1)}$ ending up with the necessary condition at the surface

$$0 = v_x^{(1)}\left(\nu_2\partial_z\bar{v}_x + \nu_2\partial_x\bar{v}_z - \frac{1}{2}\bar{\epsilon}_{xz}\right) + v_y^{(1)}\left(\nu_2\partial_z\bar{v}_y + \nu_2\partial_y\bar{v}_z - \frac{1}{2}\bar{\epsilon}_{yz}\right)$$

$$+ \xi^{(1)}\left(G\rho_0\bar{v}_z - \frac{\mu M_0^2}{1+\mu}k\bar{v}_z + \sigma_T k^2\bar{v}_z + i\omega\bar{p} + i\omega\hat{\nu}\partial_i\bar{v}_i + 2i\omega\nu_2\partial_z\bar{v}_z - i\omega\bar{\epsilon}_{zz}\right) \tag{5.30}$$

We can split this condition into three separate parts. This choice is suggested by the fact, that within the scalar product we used, the velocities $v_x^{(1)}$ and $v_y^{(1)}$ are independent

components. We therefore find as boundary conditions at the free surface in the adjoint case

$$\nu_2 \partial_z \bar{v}_x + \nu_2 \partial_x \bar{v}_z - 1/2\,\bar{\epsilon}_{xz} = 0 \quad (5.31)$$

$$\nu_2 \partial_z \bar{v}_y + \nu_2 \partial_y \bar{v}_z - 1/2\,\bar{\epsilon}_{yz} = 0 \quad (5.32)$$

$$G\rho_0 \bar{v}_z - \frac{\mu M_0^2}{1+\mu} k\bar{v}_z + \sigma_T k^2 \bar{v}_z + i\omega \bar{p} + i\omega \hat{\nu} \partial_k \bar{v}_k + 2i\omega \nu_2 \partial_z \bar{v}_z - i\omega \bar{\epsilon}_{zz} = 0 \quad (5.33)$$

The horizontal boundary conditions originating from the horizontal integrations are satisfied automatically, since we take the limit of an infinitely extended layer. The only additional condition we get is due to the time integration, but this is not important in the limit of a stationary instability we will discuss in the following, but it should be taken into account if one handles oscillatory instabilities, e.g. the Faraday instability.

At this point we restrict our calculations to an incompressible medium assuming $\partial_i \bar{v}_i = 0 = \bar{\epsilon}_{ii}$ ($\rho_0 \equiv \rho$). The adjoint system of equations, $\mathcal{L}_0^\dagger \bar{\phi} = 0$, then reads

$$-\rho \partial_t \bar{v}_i - \partial_i \bar{p} - \nu_2 \partial_j \partial_j \bar{v}_i + \frac{1}{2}(\partial_i \bar{\epsilon}_{\underline{ii}} + \partial_j \epsilon_{ij}) = 0 \quad (5.34)$$

$$-\partial_t \bar{\epsilon}_{ij} + 2\mu_2 (\partial_i \bar{v}_j + \partial_j \bar{v}_i)(1 - \frac{1}{2}\delta_{\underline{ij}}) = 0 \quad (5.35)$$

$$\partial_i \bar{v}_i = 0 \quad (5.36)$$

where underlined indices are not summed over. Their structure is similar to those of the original equations (3.8-3.10).

Following the same approach as for the original linear system, namely using the dynamic equations for the strain field in the momentum conservation equation, we get as a first step

$$\rho \bar{\omega}^2 \bar{v}_i - i\bar{\omega} \partial_i \bar{p} + \tilde{\mu}_2(\bar{\omega}) \partial_j (\partial_j \bar{v}_i + \partial_i \bar{v}_j) = 0 \quad (5.37)$$

$$\partial_i \bar{v}_i = 0 \quad (5.38)$$

where we used the abbreviation $\tilde{\mu}_2(\bar{\omega}) = \mu_2 - i\bar{\omega} \nu_2$. We will separate the velocity field into two parts. One due to potential flow and the second due to vorticity flow. Fulfilling the dynamic bulk equations, we obtain the inverse decay length $\bar{q}^2 = k^2 - \rho \bar{\omega}^2 / \tilde{\mu}_2(\bar{\omega})$ for the vorticity flow with respect to the $z-$axis. The solvability condition for the adjoint boundary conditions then leads to the dispersion relation for surface waves in the adjoint system.

$$\bar{\omega}^2 \rho \left(2k^2 \tilde{\mu}_2(\bar{\omega}) - \bar{\omega}^2 \rho\right) + \bar{\omega}^2 \rho \left[-\frac{\bar{\omega}}{\omega}\left(G\rho - \frac{\mu M_0^2}{1+\mu}k + \sigma_T k^2\right)k + 2\tilde{\mu}_2(\bar{\omega})k^2\right]$$
$$-(2k^2 \tilde{\mu}_2(\bar{\omega}))^2 \left(1 - \sqrt{1 - \frac{\bar{\omega}^2 \rho}{\tilde{\mu}_2(\bar{\omega})k^2}}\right) = 0$$
$$(5.39)$$

Eq. (5.39) reduces to the original dispersion relation (eq. (3.20)) if $\bar{\omega} = -\omega$. This is the physical solution, since the adjoint space acquires an easy and obvious physical interpretation: Considering the surface in its general form with left and right traveling

waves (eq. (5.3)) and the corresponding adjoint surface deflection using the solution given above

$$
\begin{aligned}
\xi_i^{(1)} &= \hat{\xi}_{iR} e^{i\omega_i t - i\mathbf{k}_i \cdot \mathbf{r}} + \hat{\xi}_{iL} e^{-i\omega_i t - i\mathbf{k}_i \cdot \mathbf{r}} + c.c. & (5.40) \\
\bar{\xi}_i &\equiv \bar{\hat{\xi}}_{iR} e^{i\bar{\omega}_i t - i\mathbf{k}_i \cdot \mathbf{r}} + \bar{\hat{\xi}}_{iL} e^{-i\bar{\omega}_i t - i\mathbf{k}_i \cdot \mathbf{r}} + c.c. \\
&= \bar{\hat{\xi}}_{iR} e^{-i\omega_i t - i\mathbf{k}_i \cdot \mathbf{r}} + \bar{\hat{\xi}}_{iL} e^{i\omega_i t - i\mathbf{k}_i \cdot \mathbf{r}} + c.c. & (5.41)
\end{aligned}
$$

(*c.c.* is the complex conjugate) we recognize by comparing equations (5.40) and (5.41), that a right traveling wave transforms into a left traveling wave in the adjoint system and vice versa, leading to the conditions:

$$
\bar{\hat{\xi}}_R = \hat{\xi}_L \qquad \bar{\hat{\xi}}_L = \hat{\xi}_R \qquad (5.42)
$$

5.2.4   Adjoint eigenvectors for the Rosensweig instability

Up to now all calculations have been performed without giving an explicit expression for the kinematic boundary condition at the surface in the adjoint system. To calculate the adjoint eigenvectors we have to specify that condition. However, it cannot be obtained by integrating by parts, since it is of a completely different type compared to the boundary conditions (C.3-C.5). While the former ones are derived using the stress balance at the surface, the kinematic boundary condition is phenomenological in nature. For surface waves in the adjoint space we therefore require a kinematic boundary condition of exactly the same structure as in the original case.

$$
\begin{aligned}
v_z^{(1)}(\omega) &= \partial_t \xi^{(1)}(\omega) = i\omega \xi^{(1)}(\omega) & (5.43) \\
\bar{v}_z(\bar{\omega}) &= \partial_t \bar{\xi}(\bar{\omega}) = i\bar{\omega} \bar{\xi}(\bar{\omega}) & (5.44)
\end{aligned}
$$

Following the same way to calculate the eigenvectors as in the case of the original system (cf. chapter 3), we get for the amplitudes of the vorticity flow potential (recall $\bar{q}^2 = k^2 - \rho\bar{\omega}^2/(\mu_2 - i\bar{\omega}\nu_2)$)

$$
\begin{aligned}
\bar{\hat{\Psi}}_x &= ik_y \frac{2k}{\bar{q}^2 + k^2} \bar{\hat{\varphi}} & (5.45) \\
\bar{\hat{\Psi}}_y &= -ik_x \frac{2k}{\bar{q}^2 + k^2} \bar{\hat{\varphi}} & (5.46)
\end{aligned}
$$

and of the scalar potential

$$
\bar{\hat{\varphi}} = i\bar{\omega} \frac{\bar{q}^2 + k^2}{k(\bar{q}^2 - k^2)} \qquad (5.47)
$$

where $\bar{\Psi}_i$ denote the components of the vector potential of the velocity defined by the rotational part of flow $\bar{\mathbf{v}}^{\text{rot}} = \nabla \times \bar{\mathbf{\Psi}}$. The scalar potential $\bar{\varphi}$ is connected to the potential flow $\bar{\mathbf{v}}^{\text{pot}} = \nabla\bar{\varphi}$.

The components of the adjoint velocities then become similar to the ones known from the original system (cf. section 3.5), and – as in the original system – they vanish in the

case of a stationary instability

$$\bar{v}_x = \bar{\omega}\frac{k_x}{k}\left(e^{kz} - \frac{2\bar{q}k}{\bar{q}^2 + k^2}e^{\bar{q}z}\right)\frac{\bar{q}^2 + k^2}{\bar{q}^2 - k^2}\bar{\xi} \tag{5.48}$$

$$\bar{v}_y = \bar{\omega}\frac{k_y}{k}\left(e^{kz} - \frac{2\bar{q}k}{\bar{q}^2 + k^2}e^{\bar{q}z}\right)\frac{\bar{q}^2 + k^2}{\bar{q}^2 - k^2}\bar{\xi} \tag{5.49}$$

$$\bar{v}_z = i\bar{\omega}\left(e^{kz} - \frac{2k^2}{\bar{q}^2 + k^2}e^{\bar{q}z}\right)\frac{\bar{q}^2 + k^2}{\bar{q}^2 - k^2}\bar{\xi} \tag{5.50}$$

For the adjoint strain field we get

$$\bar{\epsilon}_{zz} = 2\mu_2 k\left(e^{kz} - \frac{2\bar{q}k}{\bar{q}^2 + k^2}e^{\bar{q}z}\right)\frac{\bar{q}^2 + k^2}{\bar{q}^2 - k^2}\bar{\xi} \tag{5.51}$$

$$\bar{\epsilon}_{xx} = 2\mu_2\frac{k_x^2}{k}\left(e^{kz} - \frac{2\bar{q}k}{\bar{q}^2 + k^2}e^{\bar{q}z}\right)\frac{\bar{q}^2 + k^2}{\bar{q}^2 - k^2}\bar{\xi} \tag{5.52}$$

$$\bar{\epsilon}_{yy} = 2\mu_2\frac{k_y^2}{k}\left(e^{kz} - \frac{2\bar{q}k}{\bar{q}^2 + k^2}e^{\bar{q}z}\right)\frac{\bar{q}^2 + k^2}{\bar{q}^2 - k^2}\bar{\xi} \tag{5.53}$$

$$\bar{\epsilon}_{xy} = -4\mu_2\frac{k_x k_y}{k}\left(e^{kz} - \frac{2\bar{q}k}{\bar{q}^2 + k^2}e^{\bar{q}z}\right)\frac{\bar{q}^2 + k^2}{\bar{q}^2 - k^2}\bar{\xi} \tag{5.54}$$

$$\bar{\epsilon}_{xz} = -4i\mu_2 k_x\left(e^{kz} - e^{\bar{q}z}\right)\frac{\bar{q}^2 + k^2}{\bar{q}^2 - k^2}\bar{\xi} \tag{5.55}$$

$$\bar{\epsilon}_{yz} = -4i\mu_2 k_y\left(e^{kz} - e^{\bar{q}z}\right)\frac{\bar{q}^2 + k^2}{\bar{q}^2 - k^2}\bar{\xi} \tag{5.56}$$

Obviously the adjoint strain components have the same structure as the components in the original case and they also show a finite static limit. However, they do not have the same units. While the strain field in the original case is dimensionless, the adjoint strain field is proportional to the shear modulus μ_2. This is consistent with the scalar product (5.23), where all contributions need to have the same dimension. One could avoid the dimension of the adjoint strain field by defining a scalar product with a metric containing units in the fifth to the tenth component.

The reasons why previous attempts to solve the adjoint problem have failed are, at least, twofold. One crucial part in our discussion is to treat the medium as compressible. This ensures e.g. the presence of the contribution $\sim \partial_j\partial_i v_j^{(1)}$ in the Navier-Stokes equation. During the process of adjoining, commutativity of gradients in this term requires that the surface terms $\sim \bar{v}_i\partial_i v_j^{(1)}$ and $\sim \bar{v}_j\partial_i v_i^{(1)}$ are equivalent, which would be violated if incompressibility is applied before. The assumption of an incompressible fluid is therefore too strong a restriction. An even more important point is to treat the system as a dynamic one. The subtle reason for that is manifest in the dynamic boundary condition of the surface deflection. Assuming stationarity from the beginning would imply an always undeformed surface because the vertical velocity at the surface would vanish in any case. However, this velocity component needs to be finite to allow the surface to deform. The marginal point where the spikes are about to develop (or the final point where the spikes have fully developed) are then obtained as the static limit $\omega \to 0$ of the full dynamic behavior.

5.3 The second perturbative order

The fact that within our assumptions the magnetic bulk equations completely decouple from the hydrodynamic bulk equations, has two important consequences. On the one hand this allows us to discuss and solve these two systems subsequently, i.e. we first solve the magnetic part in a given perturbative order for a given surface deflection ξ, and feed back this solution into the respective order of the hydrodynamic system. The detailed discussion of the magnetic field is given in appendix B. On the other hand, however, we have to face the problem that the control parameter (the magnetization or the magnetic field in our case) does not occur in the hydrodynamic bulk equations and that the bulk equations for the magnetic system are homogeneous in all perturbative orders, which makes it impossible to obtain the control parameter in the next order by Fredholm's theorem, only. The coupling between these two systems is, however, mediated by the surface, and more precisely by the normal stress boundary condition. Satisfying the normal stress boundary condition provides us with an additional condition supplementing Fredholm's theorem as we will see in section 5.3.4.

According to the general expression (5.7) the set of hydrodynamic bulk equations is given in the second perturbative order by

$$\rho \partial_t^{(0)} v_i^{(2)} + \partial_i p^{(2)} - 2\mu_2 \partial_j \epsilon_{ij}^{(2)} - \nu_2 \big(\partial_j \partial_i v_j^{(2)} + \partial_j \partial_j v_i^{(2)} \big)$$
$$= -\rho \partial_t^{(1)} v_i^{(1)} - \partial_j \big(\rho v_i^{(1)} v_j^{(1)} - 2\mu_2 \epsilon_{jk}^{(1)} \epsilon_{ki}^{(1)} \big) \quad (5.57)$$

$$\partial_t^{(0)} \epsilon_{ij}^{(2)} - \frac{1}{2} \big(\partial_i v_j^{(2)} + \partial_j v_i^{(2)} \big) = -\partial_t^{(1)} \epsilon_{ij}^{(1)} - v_k^{(1)} \partial_k \epsilon_{ij}^{(1)} \quad (5.58)$$

$$\partial_i v_i^{(2)} = 0 \quad (5.59)$$

The structure of these equations suggests two kind of solutions. One contribution is proportional to the main characteristic modes $\xi^{(1)}$ and a second one proportional to the second harmonics $\xi^{(2)}$ given by

$$\xi^{(2)} = k_c \sum_{i,j} (\xi_i \xi_j + \xi_i \xi_j^* + c.c.) \quad (5.60)$$

The corresponding boundary conditions at the surface $z = \xi$ are expanded in the same manner as the bulk hydrodynamic equations (for a detailed discussion cf. app. C). Additionally, however, one has to consider that the linear eigenvectors are dependent on z with contributions either $\sim e^{k_c z}$ or $\sim e^{qz}$ (eqs. (3.27-3.35)). The boundary conditions have to be evaluated at $z = \xi$ and since ξ itself is expanded in terms of ϵ, one has to expand the exponential functions $e^{k_c z}$ and e^{qz} first with respect to z to substitute afterwards the series expansion of ξ (eq. (5.2)). As a result we obtain effective boundary conditions that have to be evaluated at $z = 0$. For the tangential contributions these effective boundary conditions read

$$2\mu_2 \epsilon_{yz}^{(2)} + \nu_2 \big(\partial_z v_y^{(2)} + \partial_y v_z^{(2)} \big) = \Omega_{yz}^{(2)} \quad (5.61)$$
$$2\mu_2 \epsilon_{xz}^{(2)} + \nu_2 \big(\partial_z v_x^{(2)} + \partial_x v_z^{(2)} \big) = \Omega_{xz}^{(2)} \quad (5.62)$$

where the inhomogeneities are abbreviated by $\Omega_{ij}^{(2)}$ and are listed in app. C, eqs. (C.11) and (C.10). The inhomogeneities for the tangential stress boundary conditions are solely

proportional to the second harmonics $\xi^{(2)}$ which is different for the normal stress boundary condition

$$
\begin{aligned}
2\mu_2\epsilon_{zz}^{(2)} &+ 2\nu_2\partial_z v_z^{(2)} - p^{(2)} + G\rho\xi^{(2)} - \mu H_c\partial_z\Phi^{(2)} + \mu_0 H_c^{\text{vac}}\partial_z\Phi^{(2)\text{vac}} \\
&= \Omega_{zz}^{(2)} - \sigma_T\Delta\xi^{(2)} + \frac{\mu}{1+\mu}M^{(1)}M_c k_c\xi^{(1)}
\end{aligned}
\tag{5.63}
$$

with $\Omega_{zz}^{(2)}$ given in eq. (C.12). Finally, the kinematic boundary condition describing explicitly the deformable surface reads in second order

$$
\partial_t^{(0)}\xi^{(2)} + \partial_t^{(1)}\xi^{(1)} + \left(v_i^{(1)}\partial_i\right)\xi^{(1)} = v_z^{(2)} + \xi^{(1)}\partial_z v_z^{(1)}
\tag{5.64}
$$

The last contribution in eq. (5.64) is due to the fact, that in second order the surface, at which the boundary conditions have to be evaluated, is already deflected.

5.3.1 The solvability condition in second order

The general solvability condition discussed in section 5.1.2 is applied to the set of second order equations (5.57-5.59) and explicitly reads

$$
\langle\bar{v}_i|-\partial_t^{(1)}(\rho v_i^{(1)}) - \partial_j(\rho v_i^{(1)}v_j^{(1)} - 2\mu_2\epsilon_{jk}^{(1)}\epsilon_{ki}^{(1)})\rangle + \langle\bar{\epsilon}_{ij}|-\partial_t^{(1)}\epsilon_{ij}^{(1)} - v_k^{(1)}\partial_k\epsilon_{ij}^{(1)}\rangle = 0
\tag{5.65}
$$

At this point one might be tempted to use the fact that the Rosensweig instability is a static one (in linear approximation) and substitute $\omega^{(0)} = \sigma^{(0)} = 0$ as well as the static limits of the adjoint and original eigenvectors into condition (5.65). The solvability condition would then reduce to

$$
\langle\bar{\epsilon}_{ij}|-\partial_t^{(1)}\epsilon_{ij}^{(1)}\rangle = (\pm i\omega^{(1)} + \sigma^{(1)})\langle\bar{\epsilon}_{ij}|\epsilon_{ij}\rangle = 0
\tag{5.66}
$$

corresponding to the solution $\omega^{(1)} = 0 = \sigma^{(1)}$. Here, we have replaced $\partial_t^{(1)}$ by $\pm i\omega^{(1)} + \sigma^{(1)}$ (for right- and left-traveling waves, respectively) implying a normal mode ansatz for the time dependence of the amplitudes. Of course, $\omega^{(0)} = 0$ is the correct solution in the stationary limit. However, in that limit the connection between bulk equations and boundary conditions is lost (cf. eqs. (2.34) and (2.44)) and an amplitude equation cannot be derived. Therefore, one must still treat the system as fully dynamic at least at those places related to the kinematic boundary condition and to the velocity/strain relation, and satisfy Fredholm's theorem with the time derivative $\partial_t^{(0)}$ being finite. One can, however, at non-crucial instances simplify the calculations by the fact that $\omega^{(0)}$ is small, but only at the very end one can take $\omega^{(0)} \equiv 0$.

The solvability condition (5.65) consists of two different parts. One containing spatial derivatives and the other the (scaled) time derivative $\partial_t^{(1)}$. We first discuss the latter part. The integration upon x and y is straightforwardly done and only retains contributions that are proportional to $\delta(\mathbf{k}_i - \mathbf{k}_j)$. After integration with respect to z we end up with

the following expression,

$$
\langle \bar{v}_i | \, \partial_t^{(1)}(\rho v_i^{(1)}) \rangle + \langle \bar{\epsilon}_{ij} | \, \partial_t^{(1)} \epsilon_{ij}^{(1)} \rangle
$$

$$
= \; i\omega^{(1)} \Big\{ 8\mu_2 \frac{k_c(k_c^2 + q^2)^2}{q(k_c + q)^3} - \rho([\omega^{(0)}]^2 - [\sigma^{(0)}]^2) \frac{4k_c^6 + 6k_c^5 q + 6k_c^4 q^2 + 6k_c^3 q^3 + 2k_c^2 q^4}{q k_c^3 (k_c + q)^3} \Big\}
$$

$$
\times \Big(\hat{\xi}_{iL}^* \hat{\xi}_{iR} e^{2i\omega t} - \hat{\xi}_{iL} \hat{\xi}_{iR}^* e^{-2i\omega t} \Big) e^{2\sigma t}
$$

$$
+ \; \sigma^{(1)} \Big\{ 8\mu_2 \frac{k_c(k_c^2 + q^2)^2}{q(k_c + q)^3} - \rho([\omega^{(0)}]^2 - [\sigma^{(0)}]^2) \frac{4k_c^6 + 6k_c^5 q + 6k_c^4 q^2 + 6k_c^3 q^3 + 2k_c^2 q^4}{q k_c^3 (k_c + q)^3} \Big\}
$$

$$
\times \Big(\hat{\xi}_{iL}^* \hat{\xi}_{iR} e^{2i\omega t} + \hat{\xi}_{iL} \hat{\xi}_{iR}^* e^{-2i\omega t} + \hat{\xi}_{iR} \hat{\xi}_{iR}^* + \hat{\xi}_{iL} \hat{\xi}_{iL}^* \Big) e^{2\sigma t} \tag{5.67}
$$

For the second order contributions we finally get

$$
\langle \bar{v}_i | \, \partial_t^{(1)}(\rho v_i^{(1)}) \rangle + \langle \bar{\epsilon}_{ij} | \, \partial_t^{(1)} \epsilon_{ij}^{(1)} \rangle
$$

$$
= \; i\omega^{(1)} 4\mu_2 k_c (\hat{\xi}_{iL}^* \hat{\xi}_{iR} - \hat{\xi}_{iL} \hat{\xi}_{iR}^*) + \sigma^{(1)} 4\mu_2 k_c (\hat{\xi}_{iL}^* \hat{\xi}_{iR} + \hat{\xi}_{iL} \hat{\xi}_{iR}^* + \hat{\xi}_{iR} \hat{\xi}_{iR}^* + \hat{\xi}_{iL} \hat{\xi}_{iL}^*) \tag{5.68}
$$

where the static limit has safely been performed.

Up to now it has been possible to do the calculations without specifying the actual number of modes contributing to the nonlinear pattern and the results are applicable for any value of N and in particular for any angle between these modes. This is changed when the second part of eq. (5.65), containing the spatial derivatives, is considered. Two of these terms turn out to be irrelevant for the second order solvability condition since they are at least proportional to $[\partial_t^{(0)}]^2$ and therefore vanish in the static limit. The only relevant term, $2\mu_2 \langle \bar{v}_i | \, \partial_j^{(0)}(\epsilon_{jk}^{(1)} \epsilon_{ki}^{(1)}) \rangle$, generally vanishes, except when three linear modes oriented at $2\pi/3$ relative to each other are interacting. This hexagonal order is enforced by the integration upon x and y. Integrating with respect to z yields in lowest order of $\omega^{(0)}$ and $\sigma^{(0)}$

$$
2\mu_2 \langle \bar{v}_i \partial_j^{(0)}(\epsilon_{jk}^{(1)} \epsilon_{ki}^{(1)}) \rangle = -3i\omega^{(0)} \mu_2 k_c^2 \big(\hat{\xi}_{1R} \hat{\xi}_{2R} \hat{\xi}_{3R} - \hat{\xi}_{1L} \hat{\xi}_{2L} \hat{\xi}_{3L} + \hat{\xi}_{1R} \hat{\xi}_{2R} \hat{\xi}_{3L} + \hat{\xi}_{1R} \hat{\xi}_{2L} \hat{\xi}_{3R}
$$

$$
- \hat{\xi}_{1L} \hat{\xi}_{2R} \hat{\xi}_{3R} - \hat{\xi}_{1L} \hat{\xi}_{2L} \hat{\xi}_{3R} - \hat{\xi}_{1L} \hat{\xi}_{2R} \hat{\xi}_{3L} + \hat{\xi}_{1R} \hat{\xi}_{2L} \hat{\xi}_{3L} - c.c. \big)
$$

$$
- 3\sigma^{(0)} \mu_2 k_c^2 \big(\hat{\xi}_{1R} \hat{\xi}_{2R} \hat{\xi}_{3R} + \hat{\xi}_{1L} \hat{\xi}_{2L} \hat{\xi}_{3L} + \hat{\xi}_{1R} \hat{\xi}_{2R} \hat{\xi}_{3L} + \hat{\xi}_{1R} \hat{\xi}_{2L} \hat{\xi}_{3R}
$$

$$
+ \hat{\xi}_{1L} \hat{\xi}_{2R} \hat{\xi}_{3R} + \hat{\xi}_{1L} \hat{\xi}_{2L} \hat{\xi}_{3R} + \hat{\xi}_{1L} \hat{\xi}_{2R} \hat{\xi}_{3L} + \hat{\xi}_{1R} \hat{\xi}_{2L} \hat{\xi}_{3L} + c.c. \big) \tag{5.69}
$$

Eqs. (5.68) and (5.69) are the two parts that enter the solvability condition eq. (5.65), which we are now going to solve. The imaginary part yields the condition

$$
4i\omega^{(1)}(\hat{\xi}_{iL}^* \hat{\xi}_{iR} - \hat{\xi}_{iL} \hat{\xi}_{iR}^*) = -3i\omega^{(0)} k_c(\hat{\xi}_{1R} \hat{\xi}_{2R} \hat{\xi}_{3R} - \hat{\xi}_{1L} \hat{\xi}_{2L} \hat{\xi}_{3L} + \hat{\xi}_{1R} \hat{\xi}_{2R} \hat{\xi}_{3L} + \hat{\xi}_{1R} \hat{\xi}_{2L} \hat{\xi}_{3R}
$$

$$
- \hat{\xi}_{1L} \hat{\xi}_{2R} \hat{\xi}_{3R} - \hat{\xi}_{1L} \hat{\xi}_{2L} \hat{\xi}_{3R} - \hat{\xi}_{1L} \hat{\xi}_{2R} \hat{\xi}_{3L} + \hat{\xi}_{1R} \hat{\xi}_{2L} \hat{\xi}_{3L} - c.c. \big) \tag{5.70}
$$

This condition is identically fulfilled by the ansatz

$$
\hat{\xi}_{iL} = \hat{\xi}_{iR} = \hat{\xi}_i \qquad \text{and} \qquad \hat{\xi}_{iL}^* = \hat{\xi}_{iR}^* = \hat{\xi}_i^* \tag{5.71}
$$

which is the solution one expects for the stationary case, since in that limit one cannot distinguish right from left traveling waves.

Using this result for evaluating the real part, we obtain

$$
2\sigma^{(1)} \sum_i \hat{\xi}_i \hat{\xi}_i^* = -3\sigma^{(0)} k_c(\hat{\xi}_1 \hat{\xi}_2 \hat{\xi}_3 + \hat{\xi}_1^* \hat{\xi}_2^* \hat{\xi}_3^*) \tag{5.72}
$$

which obviously is solved by

$$\sigma^{(1)}\hat{\xi}_1 = -\sigma^{(0)}k_c\hat{\xi}_2^*\hat{\xi}_3^* \qquad \text{and} \qquad |\hat{\xi}_1|^2 = |\hat{\xi}_2|^2 = |\hat{\xi}_3|^2 \tag{5.73}$$

and all its cyclic permutations $1 \to 2 \to 3 \to 1$ and their complex conjugates. Equation (5.73) tells us, that the slow variable $\sigma^{(1)}$ scales in the bulk with $\sigma^{(0)}$, indicating that $\sigma^{(1)}/\sigma^{(0)}$ stays finite in the static limit. This behavior is mediated by the the kinematic boundary condition $d_t\xi = v_z$ (2.44). As a consequence, the velocity field as well as the adjoint velocity field are proportional to the time derivative as we realized in eqs. (3.27-3.29) and (5.48-5.50). This is physically reasonable, since in the case of the Rosensweig instability the velocity field vanishes if the surface pattern has fully developed and the hydrodynamic bulk equations are trivially fulfilled by $\mathbf{v} \equiv 0$, the same solution as for the initially undeformed ground state. This singular behavior, unique for the Rosensweig instability, is scaled out by the choice of a dimensionless time derivative $\tilde{\partial}_T^{(1)} = \sigma^{(1)}/\sigma^{(0)}$ for the bulk hydrodynamic equations. Using this time derivative, eq. (5.73) can be rewritten as

$$\tilde{\partial}_T^{(1)}\hat{\xi}_1 = -k_c\hat{\xi}_2^*\hat{\xi}_3^* \tag{5.74}$$

Equation (5.74) gives the relation among the three amplitudes of the second order deflection, $\xi^{(1)}$, characteristic for hexagon patterns. For any other regular pattern the right hand side of eq. (5.69) is zero implying, that there is no nonlinear interaction between two different modes in the second order for those patterns.

What is missing in eq. (5.74), which in a sense can be viewed as a primitive form of an amplitude equation, is a contribution proportional to the control parameter $\mathbf{M}^{(1)}$. This is due to the fact, that the two bulk systems of magnetic and hydrodynamic equation decouple completely. The control parameter enters the amplitude equation via the normal stress boundary condition, the only way magnetic and hydrodynamic subsystems are interacting.

5.3.2 Solutions proportional to the characteristic modes $\xi^{(1)}$

Before we can exploit the normal stress boundary condition in section 5.3.4, we have to determine the solution of the hydrodynamic contributions, eqs. (5.57-5.62). From Fredholm's theorem we learned, under what conditions we can find a solution to the system of equations in the second perturbative order. We distinguish solutions of the system of equations that are either proportional to $\xi^{(1)}$ or proportional to $\xi^{(2)}$. In this subsection we concentrate on the part proportional to $\xi^{(1)}$. Inspired by the linear discussion, we use a scalar $\varphi^{(2,1)}$ and a vector potential $\mathbf{\Psi}^{(2,1)}$ for the potential and the vorticity flow, respectively. For the contributions proportional to the main characteristic modes $\xi^{(1)}$, the governing equations read

$$\Delta\varphi^{(2,1)} = 0 \tag{5.75}$$

$$\rho\Delta\partial_t^{(0)}\varphi^{(2,1)} + \Delta p^{(2,1)} = -\rho\Delta\partial_t^{(1)}\varphi^{(1)} \tag{5.76}$$

$$\rho(\partial_t^{(0)})^3\Psi_i^{(2,1)} - \tilde{\mu}_2\Delta\partial_t^{(0)}\Psi_i^{(2,1)} = -\mu_2\Delta\partial_t^{(1)}\Psi_i^{(1)} - \rho(\partial_t^{(0)})^2\partial_t^{(1)}\Psi_i^{(1)} \tag{5.77}$$

with the abbreviation $\tilde{\mu}_2 = \mu_2 + \nu_2\partial_t^{(0)}$. On the right hand side of these equations the first order (linear) potentials act as inhomogeneities.

The appropriate boundary conditions for the flow potentials are derived in appendix C.3 and read for tangential stress

$$\tilde{\mu}_2\big(\partial_z^2 - \partial_y^2\big)\Psi_x^{(2,1)} + \tilde{\mu}_2\partial_y\partial_x\Psi_y^{(2,1)} + 2\tilde{\mu}_2\partial_z\partial_y\varphi^{(2,1)} = 0 \tag{5.78}$$

$$\tilde{\mu}_2\big(\partial_z^2 - \partial_x^2\big)\Psi_y^{(2,1)} + \tilde{\mu}_2\partial_x\partial_y\Psi_x^{(2,1)} - 2\tilde{\mu}_2\partial_z\partial_x\varphi^{(2,1)} = 0 \tag{5.79}$$

The physical boundary conditions have to be taken at $z = \xi^{(1)}$ in the second order. This leads to additional contributions in $\xi^{(1)}$, which have already been taken into account in the effective boundary conditions eqs. (5.78) and (5.79). The latter therefore have to be taken at $z = 0$.

The kinematic boundary condition now involves the slow timescale $t^{(1)}$ and reads

$$v_z^{(2,1)} = \partial_t^{(1)}\xi^{(1)} \tag{5.80}$$

We start with the particular inhomogeneous solutions of eqs. (5.76) and (5.77) for the vector potential $\mathbf{\Psi}$ and the pressure p, respectively. It can be checked that the following fields satisfy the inhomogeneous bulk equations

$$\Psi_i^{(2,1)} = \hat{\Psi}_i^{(2,1)\mathrm{inhom}}\xi^{(1)}ze^{qz} \quad\text{and}\quad p^{(2,1)\mathrm{inhom}} = -\rho\partial_t^{(1)}\varphi^{(1)} \tag{5.81}$$

with the amplitudes for the vector potential given by

$$\hat{\Psi}_x^{(2,1)\mathrm{inhom}} = -\frac{\mu_2 + \tilde{\mu}_2}{\tilde{\mu}_2 q}\partial_t^{(1)}\partial_y \quad\text{and}\quad \hat{\Psi}_y^{(2,1)\mathrm{inhom}} = \frac{\mu_2 + \tilde{\mu}_2}{\tilde{\mu}_2 q}\partial_t^{(1)}\partial_x \tag{5.82}$$

The inhomogeneous solutions do not yet satisfy the boundary conditions (5.78) and (5.79). Substituting $\mathbf{\Psi}^{\mathrm{inhom}}$ into eq. (5.78) results in an additional source of tangential stress at the boundary due to the inhomogeneous solutions, which can be balanced by the homogeneous ones

$$\tilde{\mu}_2\big(\partial_z^2 - \partial_y^2\big)\Psi_x^{(2,1)\mathrm{hom}} + \tilde{\mu}_2\partial_y\partial_x\Psi_y^{(2,1)\mathrm{hom}} + 2\tilde{\mu}_2\partial_z\partial_y\varphi^{(2,1)} = \partial_y\left(\tilde{\mu}_2\frac{\mu_2 + \tilde{\mu}_2}{\tilde{\mu}_2}\partial_t^{(1)}\xi^{(1)}\right) \tag{5.83}$$

If we use the following ansatz for the homogeneous solutions of the flow potentials $\mathbf{\Psi}^{(2,1)\mathrm{hom}}$ and $\varphi^{(2,1)}$

$$\Psi_x^{(2,1)\mathrm{hom}} = -\partial_y\hat{\Psi}^{(2,1)}e^{qz}\xi^{(1)}, \quad \Psi_y^{(2,1)\mathrm{hom}} = \partial_x\hat{\Psi}^{(2,1)}e^{qz}\xi^{(1)} \quad\text{and}\quad \varphi^{(2,1)} = \hat{\varphi}^{(2,1)}e^{k_c z}\xi^{(1)} \tag{5.84}$$

the amplitudes $\hat{\Psi}^{(2,1)}$ are given by

$$\hat{\Psi}^{(2,1)} = \frac{2k_c}{q^2 + k_c^2}\hat{\varphi}^{(2,1)} - 2\frac{\mu_2 + \tilde{\mu}_2}{\tilde{\mu}_2(q^2 + k_c^2)}\partial_t^{(1)} \tag{5.85}$$

Note that q is the inverse decay length of the linear transverse modes with $q^2 = k_c^2 + \rho[\partial_t^{(0)}]^2/(\mu_2 + \nu_2\partial_t^{(0)})$ (chapter 3) and $\partial_t^{(1)}$ is a short hand notation for $\pm i\omega^{(1)} + \sigma^{(1)}$, as before.

The homogeneous solution of the pressure $p^{(2,1)\mathrm{hom}}$ is straightforwardly given by eq. (5.76)

$$p^{(2,1)\mathrm{hom}} = -\rho\partial_t^{(0)}\varphi^{(2,1)} \tag{5.86}$$

and if we exploit the kinematic boundary condition (5.80), the solution of the scalar flow potential $\varphi^{(2,1)}$ can be determined as

$$\hat{\varphi}^{(2,1)} = \frac{q^2 + k_c^2}{k_c(q^2 - k_c^2)} \left(\partial_t^{(1)} - 2k_c^2 \frac{\mu_2 + \tilde{\mu}_2}{\tilde{\mu}_2(q^2 + k_c^2)} \partial_t^{(1)} \right) \tag{5.87}$$

With the help of the flow potentials the velocity fields are determined

$$v_z^{(2,1)} = \frac{1}{q^2 - k_c^2} \left\{ \left[q^2 - \frac{2\mu_2 + \tilde{\mu}_2}{\tilde{\mu}_2} k_c^2 \right] e^{k_c z} + 2\frac{\mu_2}{\tilde{\mu}_2} k_c^2 e^{qz} - \frac{\mu_2 + \tilde{\mu}_2}{\tilde{\mu}_2} k_c^2 (q^2 - k_c^2) \frac{z e^{qz}}{q} \right\} \partial_t^{(1)} \xi_i^{(1)} \tag{5.88}$$

$$v_x^{(2,1)} = \frac{i k_{i,x}}{\tilde{\mu}_2(q^2 - k_c^2)} L(z) \partial_t^{(1)} \xi_i^{(1)} \qquad \text{and} \qquad v_y^{(2,1)} = \frac{i k_{i,y}}{\tilde{\mu}_2(q^2 - k_c^2)} L(z) \partial_t^{(1)} \xi_i^{(1)} \tag{5.89}$$

with the abbreviation

$$L(z) = \left[\tilde{\mu}_2(q^2 - k_c^2) - 2\mu_2 k_c^2 \right] \frac{e^{k_c z}}{k_c} + \left[2\mu_2 q^2 - (\mu_2 - \tilde{\mu}_2)(q^2 - k_c^2)(1 + qz) \right] \frac{e^{qz}}{q} \tag{5.90}$$

from which the strain fields follow

$$\epsilon_{zz}^{(2,1)} = -\frac{\mu_2 + \tilde{\mu}_2}{\tilde{\mu}_2} k_c^2 L_+(z) \frac{\partial_t^{(1)}}{\partial_t^{(0)}} \xi_i^{(1)} \tag{5.91}$$

$$\epsilon_{ab}^{(2,1)} = \frac{\mu_2 + \tilde{\mu}_2}{\tilde{\mu}_2} k_{i,a} k_{i,b} L_-(z) \frac{\partial_t^{(1)}}{\partial_t^{(0)}} \xi_i^{(1)} \tag{5.92}$$

$$\epsilon_{az}^{(2,1)} = i k_{i,a} \frac{\mu_2 + \tilde{\mu}_2}{2\tilde{\mu}_2} \left\{ \frac{2}{q^2 - k_c^2} \left[2k_c^2 e^{k_c z} - (q^2 + k_c^2) e^{qz} \right] + \left(1 + qz + \frac{k_c^2}{q} z \right) e^{qz} \right\} \frac{\partial_t^{(1)}}{\partial_t^{(0)}} \xi_i^{(1)} \tag{5.93}$$

for $\{a, b\} \in \{x, y\}$ with

$$L_\pm = \frac{2}{q^2 - k_c^2} \left(k_c e^{k_c z} - q e^{qz} \right) \pm \frac{1 + qz}{q} e^{qz} \tag{5.94}$$

This concludes the derivation of the second order eigenfunctions that are proportional to $\xi^{(1)}$. These solutions satisfy every condition except the normal stress boundary condition. The latter will be used to determine the still unknown first order correction to the control parameter, $M^{(1)}$, which finally enters the amplitude equation as the linear contribution. We postpone the actual derivation of these contributions to section 5.3.4.

5.3.3 Solutions proportional to the higher harmonics $\xi^{(2)}$

We are left with solving the system of hydrodynamic equations in the second perturbative order, eqs. (5.57-5.59), for the higher harmonic contributions proportional to $\xi^{(2)}$. The appropriate set of bulk equations reads, if we use again the representation with a scalar potential and a vector potential,

$$\Delta\left[\rho(\partial_t^{(0)})^2 \varphi^{(2,2)} + \partial_t^{(0)} p^{(2,2)} \right] = \partial_i \left[-2\mu_2 \partial_j(v_k^{(1)} \partial_k \epsilon_{ij}^{(1)}) - \partial_t^{(0)} \partial_j(\rho v_i^{(1)} v_j^{(1)} - 2\mu_2 \epsilon_{jk}^{(1)} \epsilon_{ki}^{(1)}) \right] \tag{5.95}$$

$$\left[\rho(\partial_t^{(0)})^2 - \tilde{\mu}_2 \Delta \right] \left[\partial_i \partial_m \Psi_m^{(2,2)} - \Delta \Psi_i^{(2,2)} \right] \tag{5.96}$$

$$= \epsilon_{ijk} \partial_j \left[-2\mu_2 \partial_m(v_l^{(1)} \partial_l \epsilon_{km}^{(1)}) - \partial_t^{(0)} \partial_l(\rho v_k^{(1)} v_l^{(1)} - 2\mu_2 \epsilon_{lm}^{(1)} \epsilon_{km}^{(1)}) \right]$$

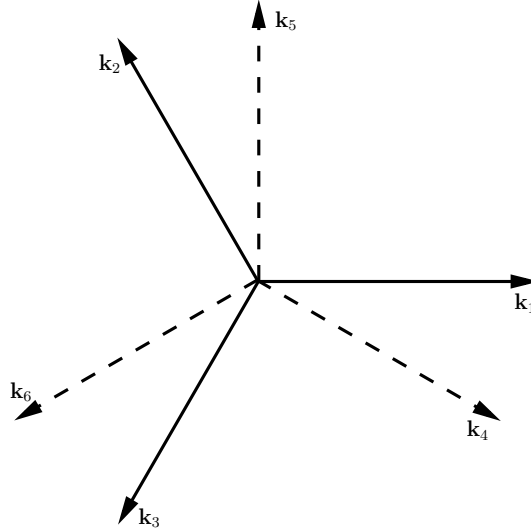$$\Delta \varphi^{(2,2)} = 0 \tag{5.97}$$

Figure 5.2: The sketch shows the relative orientation of the wave vectors under consideration in the amplitude equations (5.150,5.152). It allows to discuss the stability of hexagons and squares and their interaction.

The first equation determines the pressure contribution $p^{(2,2)}$. Since the pressure appears only in the normal stress boundary condition, this is dealt with in section 5.3.4. Next we construct a particular inhomogeneous solution of eq. (5.97) for the vector potential $\mathbf{\Psi}$. The most general ansatz necessary reads

$$\Psi_k^{(2,2)\text{inhom}} = -\epsilon_{zkl} \sum_{N,M} \sum_{i,j} \partial_l \left(\Psi_{NMij}^{\text{inhom}}(z)\, \xi_{iN}\xi_{jM} + \tilde{\Psi}_{NMij}^{\text{inhom}}(z)\, \xi_{iN}^*\xi_{jM} + c.c. \right) \quad (5.98)$$

Here, summation over all relevant modes i,j is implied (e.g. $\{i,j\} \in \{1,2,3\}$, $\{i,j\} \in \{1,5\}$, and $i = j = 1$ for hexagons, squares, and rolls, respectively, fig. 5.2) as well as over right and left traveling waves $\{N,M\} \in \{R,L\}$, cf. eq. (5.3). Substituting this ansatz into the dynamic equations and matching the coefficients with the inhomogeneous contributions of the vorticity equation (5.96) yields the functions $\Psi_{NMij}^{\text{inhom}}(z)$ and $\tilde{\Psi}_{NMij}^{\text{inhom}}(z)$. Since their general form is extremely bulky, in appendix D only the coefficients $\Psi_{NMij}^{\text{inhom}}(z)$ and $\tilde{\Psi}_{NMij}^{\text{inhom}}(z)$ for hexagonal ($ij = ji = 13 = 23 = 31$) and square patterns ($ij = ji = 15$) as well as for stripe solutions ($ij = 11$) are listed.

The general solution is the sum of the particular inhomogeneous and a general homogeneous solution, $\Psi_k^{(2,2)} = \Psi_k^{(2,2)\text{inhom}} + \Psi_k^{(2,2)\text{hom}}$. It has to satisfy the effective tangential boundary conditions (cf. appendix C.3)

$$\tilde{\mu}_2(\partial_z^2 - \partial_y^2)\Psi_x^{(2,2)} + \tilde{\mu}_2\partial_y\partial_x\Psi_y^{(2,2)} + 2\tilde{\mu}_2\partial_z\partial_y\varphi^{(2,2)} =$$
$$\partial_y \sum_{N,M} \sum_{i,j} (\hat{F}'_{NMij}\xi_{iN}\xi_{jM} + \hat{\tilde{F}}'_{NMij}\xi_{iN}\xi_{jm}^* + c.c.) \quad (5.99)$$

with suitably abbreviated amplitudes $\hat{F}'_{NMij}$. The special form of the right hand side is obtained, if in eq. (C.14) the first order expressions for the variables are explicitly put in. Substituting the inhomogeneous solutions $\Psi_i^{(2,2)\text{inhom}}$ into eq. (5.99) a modified boundary

condition for the homogeneous solution results

$$\tilde{\mu}_2(\partial_z^2 - \partial_y^2)\Psi_x^{(2,2)\text{hom}} + \tilde{\mu}_2\partial_y\partial_x\Psi_y^{(2,2)\text{hom}} + 2\tilde{\mu}_2\partial_z\partial_y\varphi^{(2,2)} =$$
$$\partial_y \sum_{N,M}\sum_{i,j}(\hat{F}_{NMij}\xi_{iN}\xi_{jM} + \tilde{\hat{F}}_{NMij}\xi_{iN}\xi_{jm}^* + c.c.) \quad (5.100)$$

since the inhomogeneous solution does not satisfy the boundary condition. In particular, on the right hand side the inhomogeneous part of the boundary conditions at $z = 0$ is modified

$$\hat{F}_{NMij} = \hat{F}'_{NMij} + \hat{F}_{NMij}^{\text{inhom}} \quad (5.101)$$
$$\text{with} \quad \hat{F}_{NMij}^{\text{inhom}}\xi_{iN}\xi_{jM} = -\tilde{\mu}_2(2\partial_x^2 - \partial_z^2)\Psi_{NMij}^{\text{inhom}}(z)\mid_{z=0}\xi_{iN}\xi_{jM} \quad (5.102)$$

Similarly one obtains the y component of the tangential boundary condition starting from eq. (C.15).

Now the general homogeneous solutions of $\Psi_k^{(2,2)\text{hom}}$ and $\varphi^{(2,2)}$ can be obtained by using the ansaetze

$$\varphi^{(2,2)} = \sum_{N,M}\sum_{i,j}(\hat{\varphi}_{NMij}\,e^{k_{1ij}z}k_c\xi_{iN}\xi_{jM} + \tilde{\hat{\varphi}}_{NMij}\,e^{k_{2ij}z}k_c\xi_{iN}^*\xi_{jM} + c.c.) \quad (5.103)$$

$$\Psi_k^{(2,2)\text{hom}} = -\epsilon_{zkl}\sum_{N,M}\sum_{i,j}\partial_l(\hat{\Psi}_{NMij}^{\text{hom}}\,e^{q_{1ij}z}k_c\xi_{iN}\xi_{jM} + \tilde{\hat{\Psi}}_{NMij}^{\text{hom}}\,e^{q_{2ij}z}k_c\xi_{iN}^*\xi_{jM} + c.c.) \quad (5.104)$$

where the characteristic wave vector k_c is just used to give the amplitudes $\hat{\varphi}_{NMij}$, $\tilde{\hat{\varphi}}_{NMij}$, $\hat{\Psi}_{NMij}^{\text{hom}}$ and $\tilde{\hat{\Psi}}_{NMij}^{\text{hom}}$ the same physical units as the corresponding amplitudes in the linear discussion and where, again, the first summation is over right and left traveling waves and the second one over the fundamental modes involved. In order to satisfy the Laplace equation (5.97), the inverse decay lengths k_{1ij} and k_{2ij} of the second order scalar potential are given by

$$k_{1ij} = k_c\sqrt{2 + 2\cos\theta_{ij}} \quad (5.105)$$
$$k_{2ij} = k_c\sqrt{2 - 2\cos\theta_{ij}} \quad (5.106)$$

and depend on the angle between the i-th and the j-th mode. The inverse decay length for the rotational flow contributions read correspondingly

$$q_{1ij}^2 = k_{1ij}^2 + \frac{\rho[D_t^{(0)}]^2}{\mu_2 + \nu_2\,D_t^{(0)}} \quad (5.107)$$

and accordingly q_{2ij} by substituting k_{2ij}^2 for k_{1ij}^2 in eq. (5.107). Here, $D_t^{(0)}$ is an abbreviation for the Fourier transformed time derivative and takes the values $i\omega^{(0)} + \sigma^{(0)}$, $\sigma^{(0)}$, and $-i\omega^{(0)} + \sigma^{(0)}$ when applied to RR, RL or LR, and LL modes, respectively. The bulk equations and boundary conditions are fulfilled for the amplitudes

$$\hat{\Psi}_{RRij}^{\text{hom}} = \frac{q_{1ij}^2}{\tilde{\mu}_2 k_c(q_{1ij}^4 + q_{1ij}^2 k_{1ij}^2)}\left(\hat{F}_{RRij} - 2\tilde{\mu}_2 k_{1ij}k_c\hat{\varphi}_{RRij}\right) \quad (5.108)$$

and

$$
\hat{\varphi}_{RRij}\xi_{iR}\xi_{jR} = \frac{q_{1ij}^2 + k_{1ij}^2}{k_c k_{1ij}(q_{1ij}^2 - k_{1ij}^2)}\Bigg\{ k_c D_t^{(0)}\xi_{iR}\xi_{jR} - k_{1ij}^2 \frac{\hat{F}_{RRij}}{\tilde{\mu}_2(q_{1ij}^2 + k_{1ij}^2)}\xi_{iR}\xi_{jR} - 2\xi^{(1)}\partial_z v_z^{(1)}
$$
$$
+ \frac{1}{q_{1ij}^2 + k_{1ij}^2}\Big[(k_{1ij}^2\partial_z^2 + q_{1ij}^2[\partial_x^2 + \partial_y^2])\hat{\Psi}_{RRij}^{\mathrm{inhom}}\,\xi_{iR}\xi_{jR}\Big]_{z=0}\Bigg\} \qquad (5.109)
$$

For the last expression we explicitly used the kinematic boundary condition for the second perturbative order, eq. (5.64). In appendix D these solutions for the flow potentials are specified for hexagons, eqs. (D.12) and (D.17), and squares, eqs. (D.13) and (D.18). The amplitudes with a tilde are obtained from those without one by replacing k_{1ij} or q_{1ij} by k_{2ij} or q_{2ij}, respectively. For $\tilde{\hat{\varphi}}_{RRij}\xi_{iR}\xi_{jR}$ this leads to a denominator $\sim k_{2ij}$, which vanishes for $i = j$ according to eq. (5.106). Nevertheless, all physical quantities derived from that potential, like velocities and strain components, stay finite. The amplitudes in eqs. (5.108) and (5.109) for the RL and LL (instead of RR) components are obtained by choosing the appropriate expressions for q_{1ij} and $D_t^{(0)}$, according to the rules given above. The only remaining condition not yet satisfied is the normal stress boundary condition, which we will discuss in the next section.

5.3.4 The normal stress boundary condition

To find the solutions to the hydrodynamic bulk equations (5.57-5.59), it was not necessary to use the normal stress boundary condition. The same situation appears in the derivation of the linear eigenvectors. There, substituting the eigenvectors into the normal stress boundary condition yields the dispersion relation restricting the linear solution to those with a specific $\omega(k)$ relation. The second order normal stress boundary condition, as will be shown below, leads to the determination of $M^{(1)}$, the first correction to the control parameter entering the final amplitude equation in linear order.

The second order normal stress boundary condition has been derived in appendix C.3 and is given as eq. (C.12). It consists of two parts, one is proportional to $\xi^{(1)}$, eq. (5.110) and the other to $\xi^{(2)}$. The latter equation can easily be fulfilled by splitting the pressure $p^{(2,2)} = p^{(2,2)B} + p^{(2,2)S}$ into one part, $p^{(2,2)B}$, that is determined by the bulk equation eq. (5.95) and the other, $p^{(2,2)S}$, by the $\xi^{(2)}$-boundary condition. This ansatz works, if $\Delta p^{(2,2)S} = 0$ in the bulk. Indeed, $p^{(2,2)S} \sim \xi_i\xi_j e^{k_{1ij}z}$ or $\sim \xi_i\xi_j^* e^{k_{2ij}z}$ leads to the required result. This additional pressure contribution is due to the inhomogeneities arising in the normal stress boundary condition, in particular the one due to surface tension. Since the surface tension always acts normal to the surface, this is the only point, where it can enter the nonlinear dynamics. It just contributes to the Laplace pressure, which is proportional to the curvature of the surface, a quite intuitive result.

However, this additional pressure contribution is of no importance because of two reasons. First the pressure always enters linearly the hydrodynamic bulk equations and therefore it will never give rise to inhomogeneous contributions, which have to be accounted for by Fredholm's theorem. Second the pressure enters only the normal stress boundary condition, which is actually the governing equation for the appropriate pressure contribution in the next order. In addition, also $p^{(2,2)B}$ is not needed in the following and is therefore not shown here.

The situation is different for the first part of the normal boundary condition

$$2\mu_2\epsilon_{zz}^{(2,1)}+2\nu_2\partial_z v_z^{(2,1)}-p^{(2,1)}-\mu H_c\partial_z\Phi^{(2,1)}+H_c^{\text{vac}}\partial_z\Phi^{(2,1)\text{vac}} \;=\; \frac{k_c\mu}{1+\mu}M^{(1)}M_c\xi^{(1)} \quad (5.110)$$

It serves to determine the yet unknown control parameter $M^{(1)}$, which defines the expansion parameter ϵ, on which the amplitude equation concept is based on. In contrast to bulk instabilities, where $M^{(1)}$ follows directly from Fredholm's alternative, here we have to employ the normal boundary condition, since the Rosensweig instability basically is a surface instability. The same is true for the Marangoni instability, where again the driving force of the instability is not contained in the bulk equations, but acts purely at the surface. In some previous discussions [54, 56] this problem was circumvented by using a scalar product artificially implementing the driving force into Fredholm's theorem. This special scalar product made use of the fact, that the free boundary was treated as undeformable. In the presence of a deformable surface, however, this specific scalar product seems to fail.

Satisfying the normal stress boundary condition (5.110) provides us with the necessary relation between the control parameter $M^{(1)}$ and the scaled growth rate $\sigma^{(1)}$. Starting from the general second order normal stress boundary condition eq. (C.16), its $\xi^{(1)}$ part, corresponding to (5.110), is given by

$$-(2\tilde{\mu}_2\partial_y\partial_z+\rho G\partial_y)\Psi_x^{(2,1)}+(2\tilde{\mu}_2\partial_z\partial_x+\rho G\partial_x)\Psi_y^{(2,1)}+(2\tilde{\mu}_2\partial_z^2+\rho G\partial_z)\varphi^{(2,1)}-\partial_t^{(0)}p^{(2,1)}$$
$$= \partial_t^{(0)}\big(H_c\mu\partial_z\Phi^{(2,1)}-H_c^{\text{vac}}\partial_z\Phi^{(2,1)\text{vac}}\big)+M^{(1)}M_ck_c\frac{\mu}{1+\mu}\partial_t^{(0)}\xi^{(1)}$$
$$+\rho G\partial_t^{(1)}\xi^{(1)}+2\mu_2\partial_t^{(1)}\epsilon_{zz}^{(1)} \tag{5.111}$$

Using the expression for the linear eigenvector $\epsilon_{zz}^{(1)}$ (eq. (3.30)) and the expressions for the solutions of the second perturbative order (eqs. (5.81,5.84-5.87)) we can rewrite this equation as

$$2\nu_2 k_c^2(q-k_c)^2\tilde{\mu}_2\frac{\partial_t^{(1)}}{[\partial_t^{(0)}]^2}\hat{\xi}^{(1)}+2\rho(q^2+k_c^2)\tilde{\mu}_2\frac{\partial_t^{(1)}}{\partial_t^{(0)}}\hat{\xi}^{(1)}-2\rho k_c^2(\mu_2+\tilde{\mu}_2)\frac{\partial_t^{(1)}}{\partial_t^{(0)}}\hat{\xi}^{(1)}$$
$$+2k_c^3\frac{(q-k_c)^2}{q}\tilde{\mu}_2(\mu_2+\tilde{\mu}_2)\frac{\partial_t^{(1)}}{[\partial_t^{(0)}]^3}\hat{\xi}^{(1)}$$
$$=2\rho k_c^2\frac{\mu}{1+\mu}M^{(1)}M_c\hat{\xi}^{(1)} \tag{5.112}$$

If we expand the last expression in terms of $\partial_t^{(0)}$ and keep the lowest order, we find

$$(\sigma^{(1)}\pm i\omega^{(1)})\hat{\xi}^{(1)} \;=\; \frac{\mu M^{(1)}M_c}{\nu_2(1+\mu)}\hat{\xi}^{(1)} \tag{5.113}$$

The real and the imaginary part have to be satisfied separately and provide the scaled growth rate $\sigma^{(1)}$ and the scaled frequency $\omega^{(1)}$ as a function of the control parameter

$$\sigma^{(1)}=\frac{\mu M^{(1)}M_c}{\nu_2(1+\mu)} \quad\text{and}\quad \omega^{(1)}=0 \tag{5.114}$$

The fact that $\omega^{(1)}$ vanishes states, that the instability remains stationary and excludes possible soft mode oscillatory branches beyond the linear threshold. For the slow growth rate $\sigma^{(1)}$ we obtain the physical result that the growth is the faster the farther one is beyond the linear threshold and it is the slower the more viscous the medium under consideration is. We also observe that the elastic contributions in eq. (5.110) cancel upon substituting the solutions of the eigenvectors. This, on the one hand, states that eq. (5.114) applies to ferrofluids and ferrogels, alike, and on the other hand it states that the growth process is solely given by the dissipative mechanisms in the system under consideration. Eq. (5.114) additionally tells us, that the boundary behaves qualitatively different with respect to the temporal properties if compared to the bulk (cf. eq. (5.73)), since it does not scale with $\sigma^{(0)}$. This qualitative difference is manifest in the kinematic boundary condition which always connects the velocity field to the temporal change of the amplitude, as we discussed already. It is therefore reasonable to compare the scaled time derivative from the bulk with the time derivative in eq. (5.114).

In order to combine the results from the surface with the solvability condition of the bulk equations (5.73), we need to rewrite the growth rate $\sigma^{(1)}$ in dimensionless form. By multiplying eq. (5.114) with the typical time scale[3] $\tau_0 = \nu_2 k_c (\rho G + \mu_2 k_c)^{-1}$ and by defining $\tau_0 \sigma^{(1)}$ as $\tilde{\partial}_T^{(1)}$ we obtain

$$\tilde{\partial}_T^{(1)} \hat{\xi}_i \;\; = \;\; \frac{k_c \mu M^{(1)} M_c}{2(1+\mu)(\rho G + \mu_2 k_c)} \hat{\xi}_i \tag{5.115}$$

and by adding the solvability condition from the bulk equations (5.73) with the one from the surface (5.115), we finally end up with a rudimentary form of an amplitude equation for the second order

$$\tilde{\partial}_T^{(1)} \hat{\xi}_i \;\; = \;\; \frac{k_c \mu M^{(1)} M_c}{2(1+\mu)(\rho G + \mu_2 k_c)} \hat{\xi}_i - \frac{k_c}{4} \sum_{j,k}^{i \neq j \neq k} \hat{\xi}_j^* \hat{\xi}_k^* \tag{5.116}$$

In the last step we explicitly assumed that the dimensionless time derivatives at the surface and in the bulk are the same even though we scaled them differently. By adding the two subsystems we therefore accounted for the singular behavior of the kinematic boundary condition. Or to phrase it differently, we scaled out the singular property of the kinematic boundary condition at the crucial places.

We obtain a corresponding equation for usual ferrofluids. The linear contributions can be obtained, as we have seen already, upon taking the limit $\mu_2 \to 0$. The nonlinear contributions, however, have to be calculated separately which is done in appendix E.

By now we have solved the second order problem completely, with the amplitudes of the critical modes satisfying eq. (5.116).

5.4 The third perturbative order

With the complete solution of the second order problem at hand we can now discuss the third order, in order to obtain the desired amplitude equation. As in the second order,

---

[3]The choice of τ_0 seems to be arbitrary at this stage. In section 5.5, however, we can a posteriori derive that this particular choice is correct.

the solvability condition consists of two parts. One due to Fredholm's theorem and one that guarantees the normal stress to be compensated at the boundary. However, we will have to find solutions of the third order problem proportional to the main characteristic modes, only.

The complete set of hydrodynamic bulk equations for the hydrodynamic variables reads in third perturbative order

$$\rho\partial_t^{(0)}v_i^{(3)} + \partial_i p^{(3)} - 2\mu_2\partial_j\epsilon_{ij}^{(3)} - \nu_2\big(\partial_j\partial_i v_j^{(3)} + \partial_j\partial_j v_i^{(3)}\big) = -\rho\,\partial_t^{(2)}v_i^{(1)} - \rho\,\partial_t^{(1)}v_i^{(2)}$$
$$-\partial_j\big(\rho\,v_i^{(1)}v_j^{(2)} + \rho\,v_i^{(2)}v_j^{(1)} - 2\mu_2\epsilon_{jk}^{(1)}\epsilon_{ki}^{(2)} - 2\mu_2\epsilon_{jk}^{(2)}\epsilon_{ki}^{(1)}\big) \quad (5.117)$$

$$\partial_t^{(0)}\epsilon_{ij}^{(3)} - \frac{1}{2}\big(\partial_i v_j^{(3)} + \partial_j v_i^{(3)}\big) = -\partial_t^{(2)}\epsilon_{ij}^{(1)} - \partial_t^{(1)}\epsilon_{ij}^{(2)} - v_k^{(1)}\partial_k\epsilon_{ij}^{(2)} - v_k^{(2)}\partial_k\epsilon_{ij}^{(1)} \quad (5.118)$$

$$\partial_i^{(0)}v_i^{(3)} = 0 \quad (5.119)$$

We restrict our attention now to the contributions proportional to $\xi^{(1)}$. The hydrodynamic equations, written in terms of the flow potentials, then reduce to

$$\Delta\varphi^{(3)} = 0 \quad (5.120)$$

$$\rho\,\Delta\partial_t^{(0)}\varphi^{(3)} + \Delta p^{(3)} = -\partial_t^{(1)}\rho\,\Delta\varphi^{(2,1)} - \partial_t^{(2)}\rho\,\Delta\varphi^{(1)} \quad (5.121)$$

$$\rho\,[\partial_t^{(0)}]^3\Psi_m^{(3)} - \tilde{\mu}_2\Delta\partial_t^{(0)}\Psi_m^{(3)} = -\mu_2\Delta\partial_t^{(1)}\Psi_m^{(2,1)} - \rho\,[\partial_t^{(0)}]^2\partial_t^{(1)}\Psi_m^{(2,1)}$$
$$-\mu_2\Delta\partial_t^{(2)}\Psi_m^{(1)} - \rho\,[\partial_t^{(0)}]^2\partial_t^{(2)}\Psi_m^{(1)} \quad (5.122)$$

To find the solutions, we follow the same lines as in the previous order. The particular inhomogeneous solutions for the vector potential read

$$\Psi_a^{(3,1)\text{inhom}} = \epsilon_{zba}\frac{\mu_2 + \tilde{\mu}_2}{q\tilde{\mu}_2}\left[\partial_t^{(2)} - \frac{[\partial_t^{(1)}]^2}{\partial_t^{(0)}} - (1 - qz)\rho\frac{\mu_2 + \tilde{\mu}_2}{4q^2\tilde{\mu}_2^2}\partial_t^{(0)}[\partial_t^{(1)}]^2\right]ze^{qz}\partial_b\xi^{(1)} \quad (5.123)$$

for $\{a, b\} \in \{x, y\}$ while the inhomogeneities in (5.121) are compensated by

$$p^{(3,1)\text{inhom}} = -\rho\partial_t^{(1)}\varphi^{(2,1)} - \rho\partial_t^{(2)}\varphi^{(1)} \quad (5.124)$$

The general homogeneous solutions take the form

$$\Psi_x^{(3,1)\text{hom}} = -\partial_y\hat{\Psi}^{(3,1)}e^{qz}\xi^{(1)}, \quad \Psi_y^{(3,1)\text{hom}} = \partial_x\hat{\Psi}^{(3,1)}e^{qz}\xi^{(1)} \quad \text{and} \quad \varphi^{(3,1)} = \hat{\varphi}^{(3,1)}e^{k_c z}\xi^{(1)} \quad (5.125)$$

where the amplitude for the vector potential is given by

$$\hat{\Psi}^{(3,1)} = \frac{2k_c}{q^2 + k_c^2}\hat{\varphi}^{(3,1)} - 2\frac{\mu_2 + \tilde{\mu}_2}{\tilde{\mu}_2(q^2 + k_c^2)}\left(\partial_t^{(2)} - \frac{[\partial_t^{(1)}]^2}{\partial_t^{(0)}}\right) \quad (5.126)$$

The homogeneous solution for the pressure reads

$$p^{(3,1)\text{hom}} = -\rho\partial_t^{(0)}\varphi^{(3,1)} \quad (5.127)$$

and upon exploiting the kinematic boundary condition we obtain the amplitude for the scalar potential

$$\hat{\varphi}^{(3,1)} = \frac{q^2 + k_c^2}{k_c(q^2 - k_c^2)}\left(\partial_t^{(2)} - 2k_c^2\frac{\mu_2 + \tilde{\mu}_2}{\tilde{\mu}_2(q^2 + k_c^2)}\left(\partial_t^{(2)} + \frac{[\partial_t^{(1)}]^2}{\partial_t^{(0)}}\right)\right) \quad (5.128)$$

As in the second order, the normal stress boundary condition is not used when deriving the solutions. Again, it allows to calculate the linear contributions to the amplitude equations.

Taking into account only contributions proportional to $\xi^{(1)}$, eq. (C.22) reduces to

$$2\mu_2\epsilon_{zz}^{(3,1)} + 2\nu_2\partial_z v_z^{(3,1)} - p^{(3,1)} - \mu H_c\partial_z\Phi^{(3,1)} + H_c^{\text{vac}}\partial_z\Phi^{(3,1)\text{vac}}$$
$$= \mu H^{(2)}\partial_z\Phi^{(1)} - H^{(2)\text{vac}}\partial_z\Phi^{(1)\text{vac}} + \mu H^{(1)}\partial_z\Phi^{(2,1)} - H^{(1)\text{vac}}\partial_z\Phi^{(2,1)\text{vac}} \quad (5.129)$$

With the help of the explicit expressions of the eigenfunctions, eq. (5.129) can be written as

$$2k_c^2\nu_2(q-k_c)^2\tilde{\mu}_2\frac{\partial_t^{(2)}}{[\partial_t^{(0)}]^2}\hat{\xi}^{(1)} + \rho(q^2+k_c^2)\tilde{\mu}_2\left(2\frac{\partial_t^{(2)}}{\partial_t^{(0)}} + \frac{[\partial_t^{(1)}]^2}{[\partial_t^{(0)}]^2}\right)\hat{\xi}^{(1)}$$

$$-4k_c^4\frac{(q-k_c)^2}{(q^2+k_c^2)}\tilde{\mu}_2(\mu_2+\tilde{\mu}_2)\left(\frac{\partial_t^{(2)}}{[\partial_t^{(0)}]^3} - \frac{[\partial_t^{(1)}]^2}{[\partial_t^{(0)}]^4}\right)\hat{\xi}^{(1)} + 4k_c^3q\frac{\mu_2+\tilde{\mu}_2}{q^2+k_c^2}\rho\left(\frac{\partial_t^{(2)}}{\partial_t^{(0)}} - \frac{[\partial_t^{(1)}]^2}{[\partial_t^{(0)}]^2}\right)\hat{\xi}^{(1)}$$

$$-2k_c^3\rho\frac{\mu_2+\tilde{\mu}_2}{q}\frac{\partial_t^{(2)}}{\partial_t^{(0)}}\hat{\xi}^{(1)} + 2k_c^3\rho\left(\frac{\mu_2+\tilde{\mu}_2}{q} + \rho[\partial_t^{(0)}]^2\frac{(\mu_2+\tilde{\mu}_2)^2}{4q^3\tilde{\mu}_2^2}\right)\frac{[\partial_t^{(1)}]^2}{[\partial_t^{(0)}]^2}\hat{\xi}^{(1)}$$

$$-2k_c^2\rho(\mu_2+\tilde{\mu}_2)\frac{\partial_t^{(2)}}{\partial_t^{(0)}}\hat{\xi}^{(1)} + 2\mu_2 k_c\frac{\mu_2+\tilde{\mu}_2}{\tilde{\mu}_2}\left(2k_c^2(k_c-q)\tilde{\mu}_2 + \frac{k_c^2}{q}\rho[\partial_t^{(0)}]^2\right)\frac{[\partial_t^{(1)}]^2}{[\partial_t^{(0)}]^3}\hat{\xi}^{(1)}$$

$$= \rho k_c^2\frac{\mu}{1+\mu}\left(2M^{(2)}M_c + [M^{(1)}]^2\right)\hat{\xi}^{(1)}$$

$$(5.130)$$

If expanded in terms of $\partial_t^{(0)}$ we find

$$(\sigma^{(2)} \pm i\omega^{(2)})\hat{\xi}^{(1)} + \frac{\mu_2}{\nu_2}\frac{[\sigma^{(1)}]^2}{[\sigma^{(0)}]^2}\hat{\xi}^{(1)} = \frac{\mu(2M^{(2)}M_c + [M^{(1)}]^2)}{2\nu_2(1+\mu)}\hat{\xi}^{(1)} \quad (5.131)$$

from which $\omega^{(2)} = 0$ follows. In the last expression we made use of the results of the previous order, namely that $\omega^{(1)} = 0$ in the static limit. For the second contribution on the left hand side we can substitute the scaled time derivative $\tilde{\partial}_T^{(1)}$ of the second perturbative order and we obtain

$$\nu_2\sigma^{(2)}\hat{\xi}^{(1)} + \mu_2[\tilde{\partial}_T^{(1)}]^2\hat{\xi}^{(1)} = \frac{\mu(2M^{(2)}M_c + [M^{(1)}]^2)}{2(1+\mu)}\hat{\xi}^{(1)} \quad (5.132)$$

which results in a second order time derivative of the pattern amplitudes due to the bulk elastic properties of the medium. This contribution is proportional to the elastic shear modulus μ_2 and therefore accounts for the reversible bulk processes in the medium whereas the first order time derivative remains a purely dissipative process. Eq. (5.132) additionally suggests the time scale ν_2/μ_2 as the typical time scale to compare oscillatory processes with dissipative ones.

To combine the surface condition with the solvability condition from the bulk equations, we multiply by the typical time scale τ_0 and finally obtain

$$\tilde{\partial}_T^{(2)}\xi^{(1)} + \frac{\mu_2 k_c}{\rho G + \mu_2 k_c}[\tilde{\partial}_T^{(1)}]^2\xi^{(1)} = \frac{k_c\mu(2M^{(2)}M_c + [M^{(1)}]^2)}{2(1+\mu)(\rho G + \mu_2 k_c)}\xi^{(1)} \quad (5.133)$$

Note, the second term is absent in a ferrofluid without elasticity.

5.5   Amplitude equation

We are finally left with satisfying Fredholm's theorem for the third order bulk hydrodynamic equations. The general solvability condition for the equations (5.117-5.119) reads

$$
\langle \bar{v}_i \,|\, \rho \partial_t^{(2)} v_i^{(1)} \rangle + \langle \bar{\epsilon}_{ij} \,|\, \partial_t^{(2)} \epsilon_{ij}^{(1)} \rangle + \langle \bar{v}_i \,|\, \rho \partial_t^{(1)} v_i^{(2,1)} \rangle + \langle \bar{\epsilon}_{ij} \,|\, \partial_t^{(1)} \epsilon_{ij}^{(2,1)} \rangle
$$
$$
= -\langle \bar{v}_i \,|\, \rho \partial_t^{(1)} v^{(2,2)} \rangle - \langle \bar{\epsilon}_{ij} \,|\, \partial_t^{(1)} \epsilon_{ij}^{(2,2)} \rangle + 2\mu_2 \langle \bar{v}_i \,|\, \partial_j (\epsilon_{jk}^{(1)} \epsilon_{ki}^{(2,1)} + \epsilon_{jk}^{(2,1)} \epsilon_{ki}^{(1)}) \rangle
$$
$$
- \rho \langle \bar{v}_i \,|\, \partial_j (v_i^{(1)} v_j^{(2,1)} + v_i^{(2,1)} v_j^{(1)}) \rangle - \langle \bar{\epsilon}_{ij} \,|\, (v_k^{(1)} \partial_k) \epsilon_{ij}^{(2,1)} + (v_k^{(2,1)} \partial_k) \epsilon_{ij}^{(1)} \rangle
$$
$$
- \rho \langle \bar{v}_i \,|\, \partial_j (v_i^{(1)} v_j^{(2,2)} + v_i^{(2,2)} v_j^{(1)}) \rangle + 2\mu_2 \langle \bar{v}_i \,|\, \partial_j (\epsilon_{jk}^{(1)} \epsilon_{ki}^{(2,2)} + \epsilon_{jk}^{(2,2)} \epsilon_{ki}^{(1)}) \rangle
$$
$$
- \langle \bar{\epsilon}_{ij} \,|\, (v_k^{(1)} \partial_k) \epsilon_{ij}^{(2,2)} + (v_k^{(2,2)} \partial_k) \epsilon_{ij}^{(1)} \rangle \tag{5.134}
$$

where we already separated the contributions from the second order eigenvectors that are proportional to $\xi^{(1)}$ from those proportional to $\xi^{(2)}$. The first two contributions on the left hand side of eq. (5.134) can be discussed in the same way as the equivalent terms in the second perturbative order by replacing in eq. (5.68) $\sigma^{(1)}$ and $\omega^{(1)}$ with $\sigma^{(2)}$ and $\omega^{(2)}$, respectively. Thus these contributions yield the scaled dimensionless time derivative $\tilde{\partial}_T^{(2)} = \sigma^{(2)}/\sigma^{(0)}$ for the bulk part. The third and the fourth contribution on the left hand side of eq. (5.134) can in principle contribute to the second time derivative, since the second order eigenvectors $v_i^{(2,1)}$ and $\epsilon_{ij}^{(2,1)}$ are proportional to $\partial_t^{(1)}$ (cf. eqs. (5.88-5.94)). Discussing the last contribution first, we obtain upon exploiting the result of the second order, $\omega^{(1)} = 0$,

$$
\langle \bar{\epsilon}_{ij} \,|\, \partial_t^{(1)} \epsilon_{ij}^{(2,1)} \rangle = 4 \frac{\rho \mu_2}{\nu_2 k_c} [\sigma^{(1)}]^2 \sum_{i=1}^{N} \hat{\xi}_i \hat{\xi}_i^* + \mathcal{O}([\omega^{(0)}]^5) \tag{5.135}
$$

This contribution is at least of the order $[\sigma^{(0)}]^2$ and therefore vanishes in the limit of a static instability. Similarly, the contribution due to $\langle \bar{v}_i \,|\, \partial_t^{(1)} v_i^{(2,1)} \rangle$ is at least of the order $[\sigma^{(0)}]^3$ and can also be neglected. Let us now focus on the right hand side of eq. (5.134) and discuss those contributions first that are due to the eigenvectors $\epsilon_{ij}^{(2,1)}$ and $v_i^{(2,1)}$ of the second perturbative order, which are proportional to the main characteristic modes $\xi^{(1)}$. These contributions involve the combinations of three amplitudes $\xi^{(1)}$ and due to the lateral integration they therefore remain finite only in the case of hexagons. If we use eq. (5.73) to substitute e.g. $\hat{\xi}_1 \hat{\xi}_2 \sigma^{(1)} \hat{\xi}_3$ by $-k_c \sigma^{(0)} |\hat{\xi}_1|^2 |\hat{\xi}_2|^2$, we finally obtain

$$
\langle \bar{\epsilon}_{ij} \,|\, (v_k^{(1)} \partial_k) \epsilon_{ij}^{(2,1)} \rangle = \frac{64}{9} \mu_2 k_c^3 \sigma^{(0)} \left(|\hat{\xi}_1|^2 |\hat{\xi}_2|^2 + |\hat{\xi}_1|^2 |\hat{\xi}_3|^2 + |\hat{\xi}_2|^2 |\hat{\xi}_3|^2 \right) + \mathcal{O}([\omega^{(0)}]^3) \tag{5.136}
$$

Note, that this term only contributes to the cubic coefficient for the hexagonal pattern and vanishes for any other pattern. All other contributions in (5.134) involving the eigenvectors $v_i^{(2,1)}$ or $\epsilon_{ij}^{(2,1)}$ are at least of the order $[\sigma^{(0)}]^2$ and vanish in the static limit. The remaining contributions involve the eigenvectors of the second perturbative order that are proportional to the higher harmonics $\xi^{(2)}$. Since their analytical expressions are bulky, the corresponding contributions to the cubic coefficients have been calculated with *Mathematica*. For the term $\langle \bar{\epsilon}_{ij} \,|\, \partial_t^{(1)} \epsilon_{ij}^{(2,2)} \rangle$ one has to exploit eq. (5.73) in the same manner

as done for eq. (5.136). The final results for the cubic coefficients A' and $B'(\theta_{ij})$ are given, for the different regular surface patterns under consideration, by

$$A' = 184\mu_2 k_c^3 \tag{5.137}$$

$$B'(\theta_{ij}=2\pi/3) = (1256315969/10368 - 69828\sqrt{3})\mu_2 k_c^3 \tag{5.138}$$

$$B'(\theta_{ij}=\pi/2) = (31831/2 - 11072\sqrt{2})\mu_2 k_c^3 \tag{5.139}$$

and the solvability condition in the third perturbative order which is due to the bulk equations can be written for the hexagonal pattern as

$$\tilde{\partial}_T^{(2)}\hat{\xi}_1 = -\frac{A'}{16\mu_2 k_c}\,|\hat{\xi}_1|^2\,\hat{\xi}_1 - \frac{B'(\theta_{ij}=2\pi/3)}{32\mu_2 k_c}(|\hat{\xi}_2|^2 + |\hat{\xi}_3|^2)\hat{\xi}_1 \tag{5.140}$$

with all its cyclic permutations $1 \to 2 \to 3 \to 1$ and their complex conjugates. Correspondingly one finds in the case of the square pattern

$$\tilde{\partial}_T^{(2)}\hat{\xi}_1 = -\frac{A'}{16\mu_2 k_c}\,|\hat{\xi}_1|^2\,\hat{\xi}_1 - \frac{B'(\theta_{ij}=\pi/2)}{32\mu_2 k_c}\,|\hat{\xi}_5|^2\,\hat{\xi}_1 \tag{5.141}$$

From those equations (5.137-5.141) it becomes clear that the dependence of the cubic coefficients on the material parameters is solely given by the characteristic wave vector k_c. Thus they are independent of the elastic shear modulus and the magnetic susceptibility. The same is true for the quadratic coefficient as observed in eq. (5.74). This behavior could have been anticipated by inspecting the general expressions for Fredholm's theorem (eqs. (5.65) and (5.134)). The lowest order in the expansion with respect to $\partial_t^{(0)}$ is always proportional to the shear modulus μ_2 (since the adjoint strain field, eqs. (5.51-5.56), is proportional to the shear modulus) which therefore cancels in eqs. (5.68) and (5.69). This behavior is due to the assumption of linear elasticity (section 2.2.1). Similarly the assumption of a linearly magnetizable medium and the negligence of magnetostrictive effects results in cubic coefficients that are independent of the magnetic susceptibility.

Adding Fredholm's theorem in the third order expansion (5.140) to the corresponding solvability condition from the normal stress at the boundary (5.133), we obtain for the hexagonal pattern

$$\tilde{\partial}_T^{(2)}\hat{\xi}_1 + \frac{\mu_2 k_c}{2(\rho G + \mu_2 k_c)}[\tilde{\partial}_T^{(1)}]^2\hat{\xi}_1 = \frac{k_c\mu\left(2M^{(2)}M_c + [M^{(1)}]^2\right)}{4(1+\mu)(\rho G + \mu_2 k_c)}\hat{\xi}_1 \tag{5.142}$$

$$-\frac{A'}{32\mu_2 k_c}\,|\hat{\xi}_1|^2\,\hat{\xi}_1 - \frac{B'(\theta_{ij}=2\pi/3)}{64\mu_2 k_c}(|\hat{\xi}_2|^2 + |\hat{\xi}_3|^2)\hat{\xi}_1$$

where we assume, as done in the second order, that the scaled time derivatives at the surface and in the bulk are the same, because of the kinematic boundary condition.

Recall now the results for the hexagonal pattern that we obtained from the solvability condition in the second order, eq. (5.116)

$$\tilde{\partial}_T^{(1)}\hat{\xi}_1 = \frac{k_c\mu M_c M^{(1)}}{2(1+\mu)(\rho G + \mu_2 k_c)}\hat{\xi}_1 - \frac{k_c}{2}\hat{\xi}_2^*\hat{\xi}_3^* \tag{5.143}$$

If we follow the standard methods and multiply the third order equation (5.142) by ϵ^3

and the second order equation (5.143) by ϵ^2, we obtain

$$
\begin{aligned}
(\epsilon^2\tilde{\partial}_T^{(2)}+\epsilon\tilde{\partial}_T^{(1)})\epsilon\hat{\xi}_1+\frac{\mu_2 k_c}{2(\rho G+\mu_2 k_c)}\epsilon^2[\tilde{\partial}_T^{(1)}]^2\epsilon\hat{\xi}_1 =& \frac{k_c\mu(2\epsilon^2 M_c M^{(2)}+\epsilon^2[M^{(1)}]^2+2\epsilon M_c M^{(1)})}{4(1+\mu)(\rho G+\mu_2 k_c)}\epsilon\hat{\xi}_1 \\
&-\frac{k_c}{2}\epsilon^2\hat{\xi}_2^*\hat{\xi}_3^*-\frac{A'}{32\mu_2 k_c}\epsilon^3\,|\hat{\xi}_1|^2\,\hat{\xi}_1 \\
&-\frac{B'(\theta_{ij}=2\pi/3)}{64\mu_2 k_c}\epsilon^3(|\hat{\xi}_2|^2+|\hat{\xi}_3|^2)\hat{\xi}_1 \quad (5.144)
\end{aligned}
$$

By the definition of ϵ and the series expansion of the magnetization

$$
\begin{aligned}
M^2 - M_c^2 &= \left(M_c+\epsilon M^{(1)}+\epsilon^2 M^{(2)}+\dots\right)^2 - M_c^2 \\
&= 2\epsilon M_c M^{(1)}+2\epsilon^2 M_c M^{(2)}+\epsilon^2[M^{(1)}]^2+\dots \quad (5.145)
\end{aligned}
$$

we define the control parameter $\tilde{\epsilon}$ in the usual way

$$
(M^2 - M_c^2) = M_c^2\tilde{\epsilon} \quad (5.146)
$$

Substituting the series expansion of the time derivative in terms of ϵ (cf. eq. 5.5)

$$
\begin{aligned}
\epsilon\tilde{\partial}_T^{(1)}+\epsilon^2\tilde{\partial}_T^{(2)} &\longrightarrow \partial_T \quad (5.147) \\
[\epsilon^1\tilde{\partial}_T^{(1)}]^2 &\longrightarrow \partial_T^2 \quad (5.148)
\end{aligned}
$$

and using the standard scaling

$$
\epsilon k_c\sqrt{A}\hat{\xi}_i \longrightarrow \xi_i \quad (5.149)
$$

the amplitude equation can be written as[4]

$$
\partial_T\xi_1+\frac{\delta}{2}\partial_T^2\xi_1 = \frac{1}{2}\tilde{\epsilon}\xi_1-\frac{1}{2\sqrt{A}}\xi_2^*\xi_3^*-|\xi_1|^2\,\xi_1-\frac{B_{120}}{A}(|\xi_2|^2+|\xi_3|^2)\xi_1 \quad (5.150)
$$

where we introduce the dimensionless parameter $\delta = \mu_2 k_c(\rho G+\mu_2 k_c)^{-1}$ and where the abbreviations A and B_{120} are given by

$$
A = \frac{A'}{32\mu_2 k_c^3} \approx 5.750 \quad\text{and}\quad B_{120} = \frac{B'(\theta_{ij}=2\pi/3)}{64\mu_2 k_c^3} \approx 3.544 \quad (5.151)
$$

Starting from eq. (5.141) instead of eq. (5.140) we obtain the corresponding amplitude equation for the square pattern

$$
\partial_T\xi_1+\frac{\delta}{2}\partial_T^2\xi_1 = \frac{1}{2}\tilde{\epsilon}\xi_1-|\xi_1|^2\,\xi_1-\frac{B_{90}}{A}\,|\xi_5|^2\,\xi_1 \quad (5.152)
$$

where the cubic coefficient B_{90} is analogously given as

$$
B_{90} = \frac{B'(\theta_{ij}=\pi/2)}{64\mu_2 k_c^3} \approx 4.021 \quad (5.153)
$$

---

[4]Recall that $\rho G k_c^{-1} = \sqrt{\rho G\sigma_T}$

The fact that the linear contribution on the right hand side of eqs. (5.150) and (5.152) is only proportional to the control parameter $\tilde{\epsilon}$ justifies a posteriori our choice of the typical time scale τ_0.

Let us first consider the static solutions of eq. (5.150). The quadratic contribution gives rise to a transcritical bifurcation from the flat surface to a hexagonal pattern at the linear threshold. As discussed for the phenomenological amplitude equation (5.9), a bistable regime exists for negative control parameter values $\tilde{\epsilon}$ with its lower boundary given by

$$\tilde{\epsilon}_A \;\; = \;\; -\frac{1}{8(A + 2B_{120})} \tag{5.154}$$

The solution for the hexagonal pattern takes the form $\xi_i = -\mid \xi_i \mid e^{i\Phi_i}$ for $i \in \{1, 2, 3\}$, where the magnitude of the amplitudes reads

$$\mid \xi_i \mid \;=\; \frac{1 + \sqrt{1 + 8(A + 2B_{120})\tilde{\epsilon}}}{4\sqrt{A}(1 + 2B_{120}/A)} \tag{5.155}$$

and where the phases have to fulfill the condition $\sum_i \Phi_i = 0$.

Investigating the values of the cubic coefficients we realize, that $B_{120}/A < 1$ indicating that the hexagon solution is always stable with respect to stripe solutions at the linear threshold. Stripes and squares are mutually exclusive pattern and since $B_{90} + 2B_{30} < A + 2B_{120}$ and $B_{90}/A < 1$, the hexagons are loosing stability with respect to squares at the critical control parameter $\tilde{\epsilon}_B$ given by (cf. section 5.1.2)

$$\tilde{\epsilon}_B \;\; = \;\; \frac{B_{90} + 2B_{30}}{2(A + 2B_{120} - B_{90} - 2B_{30})^2} \tag{5.156}$$

where the cubic coefficient $B_{30} \approx 4.188$ describes the nonlinear interaction between the hexagonal and the square pattern.

The square pattern is stable for control parameters larger than

$$\tilde{\epsilon}_S \;\; = \;\; \frac{A + B_{90}}{2(A + B_{90} - B_{120} - B_{30})^2} \tag{5.157}$$

Since $\tilde{\epsilon}_S < \tilde{\epsilon}_B$, also a bistable regime between the hexagons and squares exists.

Let us now focus on the dynamical behavior of the patterns beyond the linear threshold. We assume that the hexagonal pattern with the amplitude $\mid \xi_i \mid$, eq. (5.155), has developed and disturb it homogeneously in space by a small excess amplitude r, $\mid \xi_i \mid \rightarrow \mid \xi_i \mid + r$. The linearized amplitude equation (5.150) for the disturbances r then reads

$$\partial_T r + \frac{\delta}{2}\partial_T^2 r \;\; = \;\; \left[\frac{1}{2}\tilde{\epsilon} - \frac{1}{\sqrt{A}}\mid \xi_i \mid - 3\left(1 + 2\frac{B_{120}}{A}\right)\mid \xi_i \mid^2\right] r \tag{5.158}$$

Substituting the solution (5.155) in the right hand side of eq. (5.158) it can be simplified to $-(\tilde{\epsilon}/2 + \mid \xi_i \mid /(2\sqrt{A}))r$, which is always negative above the linear threshold. This reflects the fact that the exponential growth of the infinitesimal disturbances of the flat surface above the linear threshold gets nonlinearly saturated by the cubic coefficients and
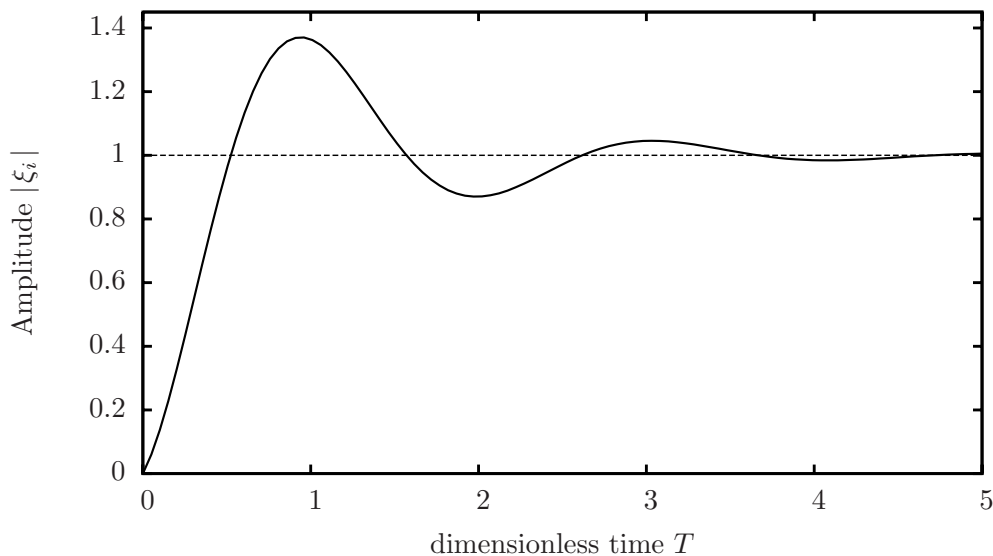
Figure 5.3: Qualitative time dependent behavior (not to scale) of the surface spikes according to eq. (5.158). The time T as well as the amplitudes $|\xi_i|$ are dimensionless variables. If the control parameter $\tilde\epsilon$ is slightly beyond the critical threshold the plot may be considered as the qualitative dynamics from the flat surface $|\xi_i| = 0$ to the spike surface $|\xi_i| = 1$.

a stable pattern develops. Eq. (5.158) therefore takes the form of a damped harmonic oscillator which can be solved by using the ansatz $r = |r| e^{\lambda T}$ with the eigenvalues

$$\lambda_{1/2} = -\frac{1}{\delta} \pm \sqrt{\frac{1}{\delta^2} - \frac{\tilde\epsilon\sqrt{A} + |\xi_i|}{\sqrt{A}\delta}} \tag{5.159}$$

where the eigenfrequency Ω of the oscillator is given by $\Omega^2 = \frac{\tilde\epsilon\sqrt{A} + |\xi_i|}{\sqrt{A}\delta}$.

These last results are still in dimensionless units. If we choose the time scale ν_2/μ_2 to compare dissipative and oscillatory processes as suggested by eq. (5.132), the eigenvalues read

$$\lambda_{1/2} = -\frac{(\sqrt{\rho G \sigma_T} + \mu_2)}{\nu_2} \pm \sqrt{\frac{(\sqrt{\rho G \sigma_T} + \mu_2)^2}{\nu_2^2} - \frac{\mu_2(\tilde\epsilon\sqrt{A} + |\xi_i|)\sqrt{\rho G \sigma_T} + \mu_2}{\sqrt{A}\nu_2^2}} \tag{5.160}$$

This result is intuitive, since the damping rate is inversely proportional to the dissipative processes, given by ν_2, whereas the eigenfrequency increases with increasing shear modulus. We also realize that the relaxation towards the equilibrium pattern becomes faster in a stronger gravitational field as well as for larger surface tensions and elastic higher shear moduli of the medium.

The bifurcation from the flat surface towards hexagons is transcritical and therefore involves a non continuous transition. If the control parameter is slightly above its critical value, the still flat surface (at $T = 0$) can be interpreted as a disturbance to the stable stationary solution (5.155). The dynamics towards hexagons from the flat surface is then described by equation (5.158) giving rise to an overshoot and a damped oscillation towards the equilibrium value (cf. fig. 5.3).
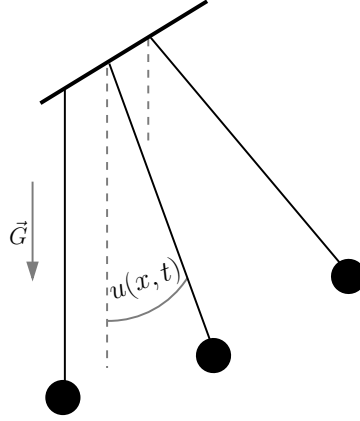
Figure 5.4: Sketch of a physical situation which is described by the sine-Gordon equation (5.161). The line of pendulums connected by a torsion wire is exposed to the gravitational field, which is directed downwards. The angle from the normal is denoted by $u(x,t)$.

5.6   On the Newell-Operator

In the previous discussion on the nonlinear properties of the Rosensweig instability we assumed spatially homogeneous patterns with no long wavelength variations. By additionally rescaling the spatial coordinates in the same way as the time coordinate (5.4), one could also implement these possible variations in space as we mentioned already in section 5.1.1. As a consequence, the amplitude equation additionally contains derivatives of the amplitudes with respect to the scaled spatial coordinates. For typical nonlinear differential equations these linear contributions to the amplitude equation can be obtained systematically by a standard method exploiting the linear properties of the system [81, 82]. This method is described in [83] and we summarize some of the ideas before we discuss a possible application to the Rosensweig instability.

We illustrate this standard method by assuming the following nonlinear model equation [83], the so-called sine-Gordon equation

$$\partial_t^2 u - c^2 \partial_x^2 u + \omega_p^2 \sin u \;\; = \;\; 0 \tag{5.161}$$

A physical system that is described by this equation is e.g. a line of pendulums that are connected by a horizontal torsion wire, where the twist angle is denoted by $u(x,t)$ (cf. fig. 5.4). The second contribution in eq. (5.161) is then given by the twist of the wire while, the third contribution is due to gravity. Expanded in terms of u, the sine-Gordon equation reads

$$\partial_t^2 u - c^2 \partial_x^2 u + \omega_p^2 u \;\; = \;\; \frac{1}{6}\omega_p^2 u^3 + \mathcal{O}(u^5) \tag{5.162}$$

The linear parts can be solved by a sinusoidal ansatz $u = a e^{-i\omega t + ikx} + c.c.$, where the frequency ω and the wave vector k are not independent from each other, but related by the dispersion relation

$$\omega^2 \;\; = \;\; \omega_p^2 + c^2 k^2 \tag{5.163}$$

Note, that the dispersion relation is the Fourier transform of the linearized equation (5.161) and therefore contains only the linear properties of the basic equation.

To account for the nonlinear contributions of the model equation (5.161) we can apply the same ideas as in the case of the Rosensweig instability and expand the torsion angle u in terms of a small parameter ϵ

$$u = \epsilon(u_0 + \epsilon u_1 + \epsilon^2 u_2 + \dots) \tag{5.164}$$

where, however, ϵ has a different meaning as in the previous sections. In particular it is not connected to a control parameter, but merely models an expansion for small amplitudes of the pendulums. In addition we can also rescale time according to $T_1 = \epsilon t$ and $T_2 = \epsilon^2 t$ and obtain by solving the different orders in ϵ successively the following nonlinear solution[5]

$$u = \epsilon a e^{ikx - it\left(\omega - \frac{\omega_p^2}{4\omega}\epsilon^2 a a^*\right)} - \epsilon^2 \frac{a^3}{48} e^{3(kx - \omega t)} + c.c. \tag{5.165}$$

where the solvability conditions in the second and third order in ϵ read, respectively

$$\partial_{T_1} a = 0 \tag{5.166}$$

$$\partial_{T_2} a = \frac{i\omega_p^2}{4\omega} |a|^2 a \tag{5.167}$$

Until now we followed the same approach as previously in our discussion of the Rosensweig instability. Additionally we will now rescale space according to $X_1 = \epsilon x$. To avoid resonant growth in the second order in ϵ, the amplitudes have to fulfill

$$\partial_{T_1} a + \frac{c^2 k}{\omega} \partial_X a = 0 \tag{5.168}$$

which states that the amplitude a has to travel with the group velocity

$$\omega' = \partial_k \omega(k) = \frac{c^2 k}{\omega} \tag{5.169}$$

where one uses the dispersion relation $\omega(k)$, eq. (5.163). In the third order the solvability condition reads

$$\frac{\partial a}{\partial T_2} = \frac{i\omega''}{2}\frac{\partial^2 a}{\partial \zeta^2} + \frac{i\omega_p^2}{\omega} |a|^2 a \tag{5.170}$$

with $\zeta = (X - \omega' T_1)$, which is also known as the nonlinear Schrödinger equation. The linear contributions arising in eq. (5.170) have been calculated by using the linear properties of the basic equation (5.161), in particular the dispersion relation (5.163). The structure of these linear contributions is universal and can be collected into an operator

$$\mathcal{L}_N = \frac{\partial}{\partial T_2} - \frac{i\omega''}{2}\frac{\partial^2}{\partial \zeta^2} \tag{5.171}$$

The question that arises is, whether we can similarly calculate the corresponding coefficients for the scaled spatial derivatives in the case of the Rosensweig instability by

---

[5]Note, that eq. (5.165) is already the nonlinear solution where the second order correction to the frequency (given by eq. (5.167)) has already been substituted.

simply taking the derivative of the known dispersion relation (3.20) with respect to the wave vector k. But there is a fundamental difference between the system of equations we used to describe the Rosensweig instability (cf. section 2.2.1) and the sine-Gorden equation (5.161). We realize, that for the latter case the dispersion relation is solely determined by the sine-Gordon equation itself, in particular it is nothing but the Fourier transform of the linearized sine-Gordon equation. In the case of the Rosensweig instability we additionally have to satisfy boundary conditions. If these were only determined by the stress balance at a fixed surface, the determination of corresponding contributions to the amplitude equation could be done by just using the operator $\mathcal{L}_N$.

In the case of the Rosensweig instability, however, we additionally have to take into account the deformability of the surface and along with it the kinematic boundary condition. If the surface deforms, also its normal vector $\mathbf{n}$ changes in the course of time, which we took into account in our previous discussions by explicitly expanding the latter in terms of the surface deflection ξ. All the different orders of $\mathbf{n}$ involve gradients of the surface deflection ξ as can be seen in eqs. (B.17-B.19). Upon rescaling the spatial coordinates we also must expand the gradients appearing in $\mathbf{n}$ in terms of ϵ, which leads to additional contributions to the higher order boundary conditions solely due to the large scale variations of the normal vector. These contributions are not contained in the linear dispersion relation and, of course, cannot be implemented into it by any means, since the dispersion relation only considers the linear properties of the system of equations and therefore assumes a still flat surface. One rather has to expand the set of boundary conditions with the scaled spatial coordinates from the beginning. The contributions to the second spatial derivative in the amplitude equation may then be separated into those due to gradients in the stress tensor (for example $\partial_j v_i$), which are the ones that follow directly from the dispersion relation, and those solely due to the deformability of the surface. Furthermore we have to evaluate the boundary conditions at the physical boundary, $z = \xi$. In our calculations we accounted for this fact by expanding the eigenvectors in term of ξ around $z = 0$. This again involves gradients with respect to z, which have to be rescaled as well and which are not contained in the dispersion relation. Additionally, one has to expect contributions to the second order spatial derivatives in the amplitude equation that are due to the bulk equations. In the case of the scaled time derivative we showed that possible contributions due to the bulk scale out in the static limit, but it is far from obvious that this is also the case for the spatial derivatives.

The previous discussion suggests that also in the case of a deformable surface the linear contributions to the amplitude equation are of a common structure and can be collected into an extended operator similar to $\mathcal{L}_N$. The determination of the latter is, however, beyond the scope of this thesis and will be left for future work.

5.7   Discussion and comparison

In this chapter we succeeded in deriving an amplitude equation for the Rosensweig instability in isotropic magnetic gels based on the fundamental hydrodynamic equations. An important step was to find the adjoint linear system of equations together with its corresponding boundary conditions in the presence of a deformable surface. Two assumptions turned out to be very important in order to find the adjoint system. Besides the dynamic treatment of the Rosensweig instability, the medium has to be considered compressible for

the adjoining process. The reason for the latter assumption is to maintain the symmetry of the stress tensor during the adjoining process. While we can assume an incompressible medium after the adjoining process, the dynamic treatment of the system of equations turns out to be also important in the discussion of the higher perturbative orders.

With the help of the adjoint system we were able to satisfy Fredholm's theorem and to perform a weakly nonlinear analysis. It turned out that due to the decoupling of the magnetic bulk equations from the hydrodynamic ones, Fredholm's theorem does not contain a control parameter. We solved this problem by observing that the normal stress boundary condition consists of two parts. One is proportional to the higher harmonics of the characteristic wavelength and merely increases the hydrostatic pressure in the medium. The other one is proportional to the main characteristic wave vector and serves as an additional solvability condition providing the dependence between the scaled growth rate and the control parameter. Both solvability conditions show qualitative different behavior in the static limit. While the solvability condition obtained from the normal stress boundary remains finite, the bulk contributions scale with the linear growth rate. The latter behavior is mediated by the kinematic boundary condition and has been taken into account while combining both solvability conditions into one. Furthermore it reveals the fact that both states, the initial flat surface and the final spiked one, are motionless states where the velocity field vanishes identically. While combining the bulk solvability condition with the normal stress boundary one has some freedom to choose the relative weight of the boundary with respect to the bulk via the two differently scaled time derivatives. It seems reasonable to weigh these single contributions equally with respect to each other, which is implicitly also done, for example, in the nonlinear discussions using an extended scalar product [54, 56].

Upon combining the second and the third order solvability condition following the standard procedure, we obtained a set of amplitude equations for the special cases of stripes, squares and hexagons. The latter contains a quadratic coefficient that renders the bifurcation from the flat surface to the hexagonal pattern transcritical. The calculated cubic coefficients additionally reveal that at the linear onset hexagons are the stable surface pattern. For high magnetic field strengths instead, hexagons become unstable and a square pattern develops. Both transitions, from the flat surface to hexagons and from hexagons to squares, involve bistable regions. We obtained qualitatively the same results in the case of ferrofluids, where the derivation of the corresponding amplitude equation and the determination of the nonlinear coefficients has been discussed in appendix E.

The results for the static patterns in this chapter are in qualitative accordance with the bifurcation scenario obtained with the energy method (chapter 4). The cubic coefficients in this chapter, however, are independent from the elastic shear modulus and the magnetic susceptibility. This is due to the assumptions of chapter 2, where we modeled the magnetic gel as a linear elastic and a linearly magnetizable medium and where we neglected magnetostrictive effects. The results in this chapter are therefore valid for a finite magnetic susceptibility and for finite shear moduli. As we realized in chapter 4, this was different for the energy method even though the same approximations were used. However, we minimized the energy density with respect to the higher harmonics and the main characteristic modes independently. As a consequence, the forth order coefficients of the energy method (these coefficients qualitatively correspond to the cubic coefficients in an $\epsilon-$expansion) showed an inverse proportionality on the control parameter $\tilde{\epsilon}$. This dependence is omitted in the subsequent discussions of the energy method for simplicity,

which renders this approach valid in the asymptotic limit of a vanishing magnetic susceptibility only. In retrospect this minimization procedure and the simplification afterwards seems to be unsystematic.

In addition to the static properties of the surface patterns, the analysis in this chapter provides us with nonlinear dynamical processes. We obtain the typical first order time derivative that describes the growth of the surface spikes beyond the linear threshold but that also accounts for the dissipative processes in the medium. The typical time scale of the growth (or relaxation) processes increases for increasing viscosities and becomes smaller for increasing surface tension and shear moduli. Additionally, however, we find a second order time derivative in the case of magnetic gels.

The analysis in this chapter elucidated the main aspects of the underlying mechanism that lead to the Rosensweig instability. But it also unraveled that for a better quantitative understanding additional phenomena have to be taken into account. Two nonlinear properties have been neglected. The nonlinear magnetization behavior, that already effects the linear threshold, and nonlinear elastic properties. Additionally, the magnetostrictive effect might influence the bifurcation behavior in magnetic gels.

Chapter 6

Rosensweig instability in films and membranes

6.1 Motivation

In the previous chapters we have emphasized, that in the scope of our assumptions the driving force of the Rosensweig instability is manifest in the boundary only, i.e. the bulk equations for the hydrodynamic variables and for the magnetic field are decoupled. On the one hand this enabled us to find the eigenvectors for the magnetic field and the hydrodynamic variables separately, but on the other hand we had to find a solution on how to implement the driving force into the amplitude equation. With the previous discussions on the Rosensweig instability in mind the question arises, how the characteristics of the Rosensweig instability will change if we reduce the elastic medium to be a boundary layer only, namely if we deal with thin films or membranes made of a magnetic gel. Rannacher and Engel focused in [84] on a thin but still finite film thickness allowing for peristaltic perturbations of the initial state where both surfaces were parallel. Here, however, we want to discuss the linear stability of the membrane in the limit of a macroscopically vanishing film thickness treating a quasi-two dimensional elastic magnetic medium. This restricts us to modes where both surfaces are distorted in phase keeping the film thickness constant[1].

Before we start with the Rosensweig instability in magnetic membranes, we elaborate on the thin film limit in order to obtain the viscoelastic properties of the membrane. This part briefly summarizes the work of Harden and Pleiner [86].

6.2 Film properties in viscoelastic media

If we discuss thin films or membranes sandwiched between two fluids, it is reasonable to start with three media, the membrane m of thickness d, whose mid-plane is placed at $z = 0$, the fluid a above the membrane ($z > d/2$) and the fluid b below the membrane ($z < -d/2$) as depicted schematically in fig. 6.1. In our discussion of the Rosensweig instability, we will allow the fluids a and b to be ferrofluids with the magnetic permeabilities μ_a and μ_b, respectively. Besides their superparamagnetic property, we assume that they behave as usual Newtonian liquids. We will first concentrate on the hydrodynamic degrees of

---

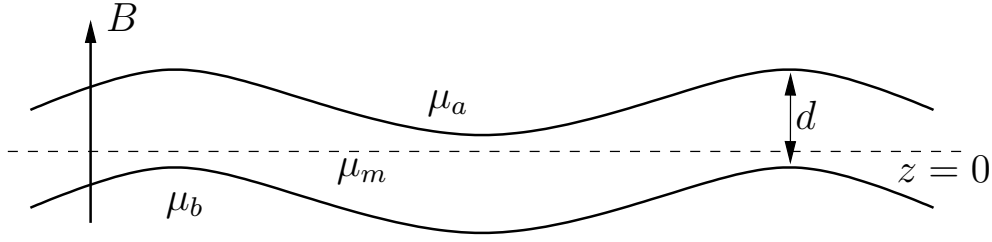[1]The discussions in this chapter have been published in [85].

Figure 6.1: Periodic lateral perturbations $\xi(x, y, t)$ with wave vector k of a flat ferrogel film around $z = 0$ between media of different magnetic permeabilities $\mu_b = 1 + \chi_b$ (below) and $\mu_a = 1 + \chi_a$ (above) in the thin film limit $kd \ll 1$. The magnetic field $\mathbf{B}$ and gravity $\mathbf{G} = -G\mathbf{e}_z$ are along the z-axis.

freedom and discuss the necessary extensions for the magnetic properties in section 6.3. In the framework of the generalized hydrodynamic theory as described in chapter 2, the fluids a and b can be modeled by the following linearized set of equations

$$\rho^{(\alpha)}\partial_t v_i^{(\alpha)} + \partial_j T_{ij}^{(\alpha)} = \rho^{(\alpha)} G_i \tag{6.1}$$

$$\partial_i v_i^{(\alpha)} = 0 \tag{6.2}$$

for $\alpha \in \{a, b\}$ and where the stress tensor T_{ij}^{α} is given for a Newtonian liquid by

$$T_{ij}^{\alpha} = p^{(\alpha)}\delta_{ij} - \nu_2^{(\alpha)}(\partial_i v_j^{(\alpha)} + \partial_j v_i^{(\alpha)}) \tag{6.3}$$

with $\nu_2^{(\alpha)}$ denoting the viscosity of liquid α.

For the membrane we assume a ferrogel that can be either isotropic with a magnetic susceptibility μ_m or anisotropic. Within the scope of our assumptions, the elastic medium can be modeled by

$$\partial_t \rho^{(m)} + \partial_i g_i^{(m)} = 0 \tag{6.4}$$

$$\rho^{(m)}\partial_t v_i^{(m)} + \partial_j T_{ij}^{(m)} = \rho^{(m)} G_i \tag{6.5}$$

$$\partial_t \epsilon_{ij}^{(m)} + Y_{ij}^{(m)} = 0 \tag{6.6}$$

where $T_{ij}^{(m)}$ denotes the linearized stress tensor of the magnetic membrane and where $Y_{ij}^{(m)}$ is the quasi current associated with the strain field. Until now we discussed a macroscopically thick elastic medium where all densities are taken with respect to the volume and where the macroscopic properties like the shear modulus $\mu_2^{(m)}$ or the shear viscosity $\nu_2^{(m)}$ are the usual bulk elastic and viscous properties as discussed in chapter 2. If we take the limit $kd \to 0$, the membrane becomes quasi-two dimensional rendering all densities areal ones rather than densities with respect to the volume. In turn also the stress tensor $T_{ij}^{(m)}$ and the quasi current $Y_{ij}^{(m)}$ have to be taken with respect to the area rather than with respect to the volume. This amounts to introduce effective in-plane elastic and viscous properties of the medium. In this case the stress tensor $T_{ij}^{(m)}$ is given by [86]

$$\begin{aligned} T_{ij}^{(m)} = {} & p\delta_{ij} - \nu_\parallel \delta_{ij}\partial_k v_k^{(m)} - \frac{\nu_s}{2}(\partial_i v_j^{(m)} + \partial_j v_i^{(m)}) - (\nu_\perp - \nu_b\Delta_\perp)\delta_{iz}\partial_j v_z^{(m)} \\ & - c_\parallel \epsilon_{kk}^{(m)}\delta_{ij} - 2c_s \epsilon_{ij}^{(m)} - (c_\perp - c_b\Delta_\perp)\epsilon_{iz}^{(m)}\delta_{jz} \end{aligned} \tag{6.7}$$

with $\Delta_\perp = \partial_x^2 + \partial_y^2$, the longitudinal elastic modulus $c_\parallel = (\mu_1 + \mu_2)d$, the shear elastic modulus $c_s = \mu_2 d$, the transverse elastic modulus $c_\perp \sim c_s$ and the bending elastic coefficient $c_b = \mu_2 d^3(3\mu_1 + \mu_2)/24(\mu_1 + \mu_2)$ and where the corresponding in-plane viscosities $\nu_\parallel$, ν_s, $\nu_\perp$ and ν_b acquire the same structure. These explicit expressions for the in-plane material properties in terms of the bulk material properties can be derived by integrating the energy density per unit volume across the film thickness [86, 87]. If one assumes only homogeneous deformations, no bending contributions are obtained in eq. (6.7) and one only retains $c_\parallel$, c_s, $c_\perp$ and the corresponding viscosities. The bending moduli c_b and ν_b are obtained by assuming a deformation profile depending on z ($u_i(x, y, z) = u_i(x, y) + f[\partial_j u_i]z)^2$. The energy density is then expanded around the film midpoint $z = 0$ to second order in z and the integration across the film thickness results in contributions proportional to d^3. It should be mentioned that in the latter case the order d^3 is not accurate since one misses contributions to $c_\parallel$, c_s and $c_\perp$ due to stretching that are proportional to d^3 [87]. For very thin films and in the long wavelength limit, however, these contributions are assumed to be negligible.

The same arguments apply to the quasi current associated with the strain field $Y_{ij}^{(m)}$ and one obtains

$$Y_{ij}^{(m)} = -\frac{1}{2}(\partial_i v_j^{(m)} + \partial_j v_i^{(m)}) + \frac{1}{2}\mathcal{T}_{ijkl}^{-1}(c_\parallel \epsilon_{nn}^{(m)}\delta_{kl} + 2c_s\epsilon_{kl}^{(m)} + [c_\perp - c_b\Delta_\perp]\epsilon_{kz}^{(m)}\delta_{lz}) \tag{6.8}$$

where the tensor $\mathcal{T}_{ijkl}^{-1}$ contains the relaxation coefficients if we consider a viscoelastic material with a transient elastic network [86]. In the following discussion, however, we will focus on gels with time independent elastic moduli for which $\mathcal{T}_{ijkl}^{-1}$ vanishes.

Besides the bulk equations, the observables are subject to certain boundary conditions. Since we restrict our discussion to very thin films only, where the thickness d of the film is kept constant, we obtain for the kinematic boundary condition

$$v^{(a)} = v^{(b)} = v^{(m)} = \partial_t \xi \tag{6.9}$$

which implies that the upper boundary between the membrane and fluid a and the lower boundary between the membrane and the fluid b are deflected in phase (cf. fig. 6.1). In the limit $kd \ll 1$, the set of boundary conditions that guarantees stress free boundaries between fluid b and m at $z = -d/2$ and between the membrane m and fluid a at $z = d/2$, can be substituted by effective boundary conditions between fluids a and b, evaluated at $z = 0$. These effective boundary conditions involve an additional stress source $P_i^{(m)}$ which is due to the presence of the membrane

$$T_{iz}^{(a)} - T_{iz}^{(b)} = P_i^{(m)} \tag{6.10}$$

The additional stress source $P_i^{(m)}$ can either be postulated introducing phenomenological in-plane elastic moduli of shear, compression and of transverse displacement as done in [88] or it can be derived from the effective in-plane elastic and viscous properties that we obtained in the derivation of $T_{ij}^{(m)}$. In doing so, we consider a cylindrical volume V that contains a small area ΔA of membrane as depicted in fig. 6.2 and whose axis is parallel to the surface normal of the membrane. This is pretty much the same situation

---

[2]Recall that **u** has been introduced in chapter 2 and denotes the displacement field.
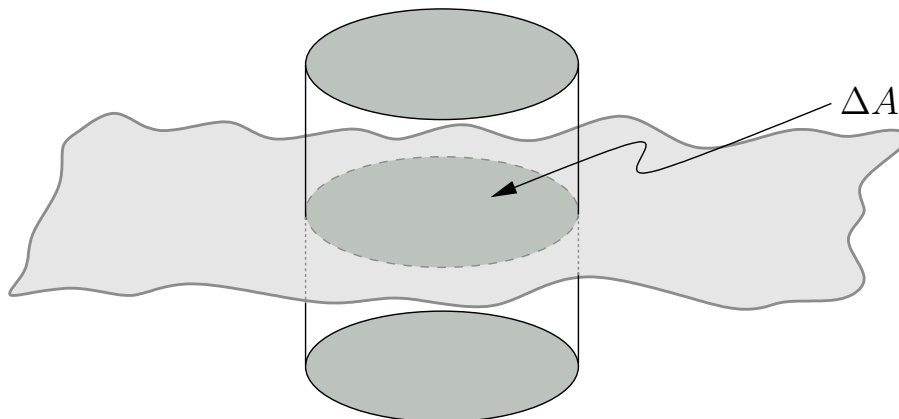
Figure 6.2: This sketch qualitatively depicts the path to the surface properties of the medium. The way we calculate the moduli does not differ from the way the usual magnetic boundary conditions are obtained [69].

as in the derivation of the boundary conditions for the electric and magnetic field in Maxwell's theory [69]. Any temporal change of momentum within the volume V has to be compensated by a momentum flux through the volume's surface ∂V. After using the divergence theorem of vector calculus, we obtain

$$\int_V \partial_t g_i^{(\alpha)} dV \;=\; \int_{\partial V} T_{ij}^{(\alpha)} \, df_j \tag{6.11}$$

where df_j denotes the j-th component of the surface element and where $\alpha \in \{a, b, m\}$. The contribution to the right hand side of eq. (6.11) that is due to the integration of the cylindrical mantle vanishes by symmetry for infinitesimally small volumes V, giving

$$\int_{\partial V} T_{ij}^{(\alpha)} \, df_j \;=\; (T_{iz}^{(a)} - T_{iz}^{(b)})\Delta A \tag{6.12}$$

On the other hand, since V is infinitesimally small, the left hand side of eq. (6.11) is solely governed by the magnetic membrane and we obtain, if we use the momentum conservation equation for the membrane (6.5),

$$\int_V \partial_t g_i^{(\alpha)} dV \;=\; \partial_j T_{ij}^{(m)} \Delta A \tag{6.13}$$

Altogether we find as an effective boundary condition between the media a and b

$$T_{iz}^{(a)} - T_{iz}^{(b)} \;=\; \partial_j T_{ij}^{(m)} \tag{6.14}$$

which has to be evaluated at $z = 0$ and which states, that the discontinuity of stress between the fluids a and b is given by the gradient of the membrane stress tensor which we have derived previously in eq. (6.7). We should state here, that in eq. (6.14) the equality of units is satisfied, since in $T_{ij}^{(m)}$ all material parameters are taken with respect to the area rather than with respect to the volume.

6.3 Magnetic surface properties

For the discussion of the Rosensweig instability in thin films or membranes we have to extend the approach of the previous section to account additionally for the superparamagnetic properties of the media. In the scope of our assumptions, as described in chapter 2, this can be done by adding the corresponding Maxwell stress tensor to (6.7) and (6.3). What we are left with is the determination of the membrane magnetic properties and in particular with the determination of the in-plane magnetic permeability.

In taking the limit towards infinitely thin membranes, we follow the lines of [86, 87] and consider the magnetic energy density within the membrane. It is given by

$$w^{(m)} = \frac{1}{2}B^{(m)}H^{(m)} = \frac{1}{2\mu_m}B^{(m)}B^{(m)} \tag{6.15}$$

where we express the energy density in terms of the flux density $B^{(m)}$ because of the following reason: In the ground state when the membrane is not deformed and the applied magnetic field is normal to the membrane, the magnetic boundary conditions demand the flux density B to be the same in any of the three regions a, b or m. This remains true even in the limit of infinitely thin membranes.

In that case we can integrate the energy density (6.15) across the membrane thickness and obtain the magnetic energy density per area

$$w^{(m)\text{area}} = \int\limits_{-d/2}^{d/2} \frac{1}{2\mu_m}B^{(m)}B^{(m)}\,dz = \frac{d}{2\mu_m}B^{(m)}B^{(m)} \tag{6.16}$$

defining an effective in-plane magnetic permeability by

$$\mu' = \frac{\mu_m}{d} \tag{6.17}$$

It is then useful to take

$$H' = \frac{1}{\mu'}B^{(m)} \tag{6.18}$$

with $H' = H^{(m)}d$ as the in-plane magnetic field. Thereby the in-plane magnetization $M' \equiv \chi H'$ becomes a density per area rather than per volume. It can intuitively be interpreted as the number of magnetic dipoles per unit area.

6.4 Non-magnetic film modes

With the set of hydrodynamic equations on hand, the dispersion relation of surface waves $\xi = \xi_0 \exp i(\omega t - kx)$ can be derived. For a non-magnetic, viscoelastic thin film on top of a simple fluid, this has been done some time ago in [86]. The fluid above the film is assumed to be vapor or air and is approximated as vacuum. In that case the dispersion relation between the frequency of the surface wave and its wave vector k reads implicitly $D(k,\omega) = 0$ with

$$
\begin{aligned}
D(k,\omega) &= \left[\tilde{\mathcal{C}}^{(z)}(k,\omega)k^3 + i\nu_2^{(b)}k(q+k)\omega - \rho^{(b)}\omega^2\right]\left[\mathcal{C}^{(x)}(k,\omega)k^3 + i\nu_2^{(b)}k(q+k)\omega\right] \\
&\quad + \nu_2^{(b)2}k^2(q-k)^2\omega^2
\end{aligned} \tag{6.19}
$$

where $\rho^{(b)}$ and $\nu_2^{(b)}$ are the density and viscosity of the underlying simple fluid. The surface disturbances decay exponentially inside the lower bulk fluid. For most of the variables or excitations involved the wavelength $1/k$ also acts as the decay length, except for the rotational part of the velocity field, whose decay length is $1/q$ with $q^2 = k^2 + i\rho^{(b)}\omega/\nu_2^{(b)}$. Equation (6.19) describes the well-known Lucassen mode spectrum [89, 88, 90]. In the case of a viscoelastic bulk fluid (or elastic gel), eq. (6.19) remains valid [71], if $\nu_2^{(b)}$ is replaced by $\nu_2^{(b)} + E_0\tau/(1 + i\omega\tau)$ with τ the elastic relaxation time and E_0 the elastic plateau modulus ($\tau \to \infty$ in the gel case).

This dispersion relation reflects the coupling of transverse elastic and longitudinal sound bulk modes at the surface. It contains in-layer compressional and transverse (normal to the interface) deformations and flow of the gel layer. The in-layer shear mode is decoupled and does not take part in the surface waves. The material properties of the gel film are contained in the functions

$$
\begin{align}
\mathcal{C}^{(x)}(k,\omega) &= \varepsilon + i\omega\nu_\parallel + c_\parallel \tag{6.20} \\
\mathcal{C}^{(z)}(k,\omega) &= \sigma_T + i\omega(\nu_\perp + \nu_b k^2) + c_\perp + c_b k^2 \tag{6.21}
\end{align}
$$

which appear on the r.h.s. of the transverse and normal stress boundary conditions [86]

$$
T_{iz}^{(a)} - T_{iz}^{(b)} = \partial_j T_{ij}^{(m)} \tag{6.22}
$$

with $\{i,j\} = \{x,y,z\}$ and the superscripts a, b referring to the media above and below the film m, respectively. Here ε and σ_T are the film compressional (or Gibbs) modulus and the surface tension, respectively. In contrast to ordinary 3D elastic moduli, the film elastic moduli have the same dimension as the surface tension. Therefore, to simplify notation, the combinations $\tilde{\varepsilon} = \varepsilon + c_\parallel$ and $\tilde{\gamma} = \sigma_T + c_\perp$ can be defined. Similarly, the abbreviation $\tilde{\mathcal{C}}^{(z)}(k,\omega) = \mathcal{C}^{(z)}(k,\omega) + \rho^{(b)}G/k^2$ in eq. (6.19) already contains the gravity effect on the film.

In the case of a viscoelastic (rather than elastic) gel, $c_\parallel$ and $c_\perp + c_b k^2$ have to be replaced by $i\omega\tau_\parallel c_\parallel/(1 + i\omega\tau_\parallel)$ and $i\omega\tau_\perp (c_\perp + c_b k^2)/(1 + i\omega\tau_\perp)$, respectively, with $\tau_\parallel$ and $\tau_\perp$ being the longitudinal and transverse elastic relaxation times. For a liquid film, $c_\parallel$, $c_\perp$, and c_b are simply zero.

In the (hydrodynamically) symmetric case with fluids of the same density $\rho^{(a)} = \rho^{(b)} = \rho$ and viscosity below and above the elastic layer, the relevant dispersion relation [86] is much simpler than eq. (6.19)

$$
D^{sym}(k,\omega) = k^3(q - k)\mathcal{C}^{(z)}(k,\omega) - 2\rho q\omega^2 \tag{6.23}
$$

In particular, there is no gravity force, as long as the inertia of the film itself can be neglected.

6.5 Ferrogel film surface modes

As discussed in chapters 2 and 3 and shown in appendix A, the influence of an external magnetic field on a ferrogel (and ferrofluid) surface deformation is manifest only in the boundary conditions (magnetostriction neglected), in particular in the normal stress boundary condition. Here, the stabilizing contributions of surface tension σ_T, gravity G,

and elasticity μ_2 are amended by a destabilizing addition due to the external magnetic field $\mathbf{B}$ by the replacement

$$\sigma_T k^2 + \rho G + \mu_2 k \quad \longrightarrow \quad \sigma_T k^2 + \rho G + \mu_2 k - \kappa B^2 k \tag{6.24}$$

as can be seen from eq. (3.19) in chapter 3. Here $\kappa = \chi^2 (1+\chi)^{-1} (2+\chi)^{-1}$ with χ the magnetic susceptibility of the ferrogel. The external magnetic field induces a magnetization $\mathbf{M} = \chi \mathbf{B}/(1+\chi)$ in the ferrogel. The magnetic field effect is quadratic meaning that the orientation of the field (parallel or antiparallel) with respect to gravity or to the surface normal does not matter.

For a (magnetic) film the magnetic influence on surface deformations comes from two surfaces, an upper and lower one to fluid a and b with magnetic susceptibilities χ_a and χ_b, respectively. For a very thin film or a film with equal deformations at both surfaces (disregarding peristaltic motions) the magnetic properties of the bulk fluids enter only via the l.h.s. of the normal stress boundary condition (6.22). Therefore, the magnetic destabilizing influence from the two surfaces leads to a contribution with $\kappa \to \kappa_1 \sim (\chi_a - \chi_b)^2$ in eq. (6.24) independent of the magnetic properties of the film. If the two bulk fluids are magnetically equivalent (magnetically symmetric case), there is no destabilizing effect of a normal magnetic field coming from the boundaries. A rigorous and complete derivation of κ_1 is given in the appendix B.5 with the result

$$\kappa_1 = \frac{(\chi_a - \chi_b)^2}{(\mu_a + \mu_b)\mu_a \mu_b} \tag{6.25}$$

with permeabilities $\mu = 1 + \chi$. In the case $\chi_a = 0$ (vacuum) the expression for χ_1 used in eq. (3.19) of chapter 3 is reobtained.

However, as is the case for viscous and elastic film properties, the magnetic properties of the film itself enter the $\mathcal{C}^{(z)}$ function (6.21) via the right hand side of eq. (6.22). A uniaxial ferrogel film does have a permanent (surface) magnetization [14, 15, 91], while in an isotropic one a considerably large surface magnetization can be induced by an external field. This induced magnetization is always parallel to the external field and has a stabilizing effect on surface waves (cf. appendix B.5). The frozen-in surface magnetization M_0', however, deforms with the membrane or film and produces a stabilizing (destabilizing) effect, if it is parallel (antiparallel) to an external field (cf. appendix B.5). This influence of a permanent surface magnetization on surface deformations is of the same k-order as the film elasticity and the surface tension and can be described by the replacement

$$\tilde{\gamma} \to \tilde{\gamma} \pm M_0' B \tag{6.26}$$

where we are interested in the destabilizing case, only. Taking together both magnetic contributions to the normal stress boundary condition (6.22) the $\mathcal{C}^{(z)}$ function

$$\mathcal{C}^{(z)}(k,\omega) = \tilde{\gamma} - M_0' B + i\omega(\nu_\perp + \nu_b k^2) + c_b k^2 - \kappa_1 B^2 k^{-1} \tag{6.27}$$

replaces eq. (6.21), while eq. (6.20) remains the same. Using these two functions in the dispersion relation (6.19) for a half-space surface, or in eq. (6.23) for the hydrodynamically symmetric interface (or in eq. (B24) of Ref. [86] for the general case) describes propagating, weakly damped surface waves at magnetic films that can be excited and maintained by thermal fluctuations, external mechanical (acoustic) forces, or other means. The wave propagation speed is clearly reduced due to the action of the magnetic field, which "softens" the stiffness of the film or membrane. Non-propagating modes are also possible.

6.6   Rosensweig instability

As done in section 3.4, eqs. (6.19-6.20), and (6.27) can be slightly reinterpreted: These are conditions for an external field strength B, at which a surface perturbation ξ with wave vector k and (real) frequency ω_0 relaxes to zero or grows exponentially for σ negative or positive, respectively ($\omega = \omega_0 - i\sigma$). For $\sigma = 0$ such a surface perturbation is marginally stable (or unstable) against infinitesimal disturbances, since eq. (6.19) has been obtained by linearizing the dynamic equations and the boundary conditions about the ground state. The functions ω_0 and B still depend on k and the latter has to be minimized with respect to k in order to get the true linear instability threshold. There is no guarantee that a threshold exists for a finite frequency due to the additional requirement $\omega_0^2 > 0$. We therefore discuss first the stationary case. Assuming $\omega_0 = 0$ the threshold condition $\sigma = 0$ leads to $\tilde{\mathcal{C}}^{(z)}(k, \omega{=}0) = 0$. We will further analyze this condition for the special cases, where the surface magnetism can be either neglected or has only a small influence in section 6.6.1, a permanently magnetized film with no magnetic contrast of the surrounding fluids in section 6.6.2, while the general case, when both destabilizing magnetic field effects are present, is discussed in section 6.6.3. The possibility of an oscillatory instability and the case of hydrodynamically symmetric configurations is discussed in the final subsection 6.6.4.

6.6.1   Stationary, asymmetric case without surface magnetism

Dealing with the case of a strong magnetic contrast between the upper and lower bulk fluid (e.g. vacuum and a ferrofluid, respectively), we neglect the surface magnetic effect. Experimentally, this case can be realized by a ferrogel (or a non-magnetic gel) on top of a ferrofluid and vapor or vacuum above the film. In that case the threshold magnetic field is

$$\kappa_1 B^2(k) = \tilde{\gamma} k + \frac{\rho^{(b)} G}{k} + c_b k^3 \tag{6.28}$$

and is finite for a non-zero magnetic contrast, $\chi_a \neq \chi_b$, of the bulk fluids, only. Minimizing with respect to k leads to the critical wave vector

$$k_c^2 = \frac{1}{6c_b} \left(\sqrt{\tilde{\gamma}^2 + 12\rho^{(b)} G c_b} - \tilde{\gamma} \right) \tag{6.29}$$

and the critical magnetic field $B_c = B(k = k_c)$. Slightly above the minimum, the curvature of the marginal stability curve is given by

$$\kappa_1 (B(k)^2 - B_c^2) = (1/k_c) \sqrt{\tilde{\gamma}^2 + 12\rho^{(b)} G c_b} (k - k_c)^2 \tag{6.30}$$

The linear threshold conditions for this stationary instability are completely independent of the viscosities of both, the underlying fluid as well as the film itself, resembling the case of bulk free surface Rosensweig instabilities in ferrofluids and ferrogels (cf. chapter 3). In contrast to the latter case, here the critical wave vector does depend on the transverse elastic properties ($c_\perp$) of the ferrogel (through $\tilde{\gamma}$) as well as on the bending elastic modulus c_b. The reason is that both effects enter the normal stress boundary condition with a k-dependence different from that of the magnetic field (cf. eq. (6.27)), or to

phrase it differently, the magnetic field deformations do not introduce a specific internal length scale compared to ordinary 3 D elasticity, but they do in relation with surface elasticity.

On the other hand, the linear growth rate σ of the most unstable mode is completely determined by the (transverse) viscous properties of the film and the bulk fluid

$$\sigma = \frac{\kappa_1(B^2 - B_c^2)}{\nu_\perp k_c + \nu_b k_c^3 + 2\nu_2^{(b)}} \tag{6.31}$$

where the wave vector of the most unstable mode $k_u = k_c(1 - \tilde{\delta})$ with

$$\tilde{\delta} = \frac{\kappa_1(B^2 - B_c^2)}{2\tilde{\gamma} + 12c_b k_c^2} \frac{\nu_\perp + 3\nu_b k_c^2}{\nu_\perp k_c + \nu_b k_c^3 + 2\nu_2^{(b)}} \tag{6.32}$$

is slightly smaller than the critical one. If the dissipation in the film or membrane can be neglected, the growth rate, $\sigma = \kappa_1(B^2 - B_c^2)/(2\nu_2^{(b)})$, is given by the bulk fluid viscosity as in the case of a bulk ferrofluid or ferrogel (cf. section 5.3.4), and the most unstable mode is the critical one, $k_u = k_c$ in linear order [27].

The linear threshold conditions for the stationary instability are also independent of the longitudinal material properties (ϵ, $c_\parallel$) of the film and therefore indistinguishable from those of an incompressible film.

Since we are operating in the long wavelength limit, usually the bending elasticity is less important than ordinary elasticity, except for very thin films, where $c_\perp$ and γ are zero or can be neglected. In the former case, in particular for $\rho^{(b)}Gc_b \ll \tilde{\gamma}^2$ the critical quantities can be simplified to

$$k_c^2 = \frac{\rho^{(b)}G}{\tilde{\gamma}}\left(1 - 3\frac{\rho^{(b)}Gc_b}{\tilde{\gamma}^2}\right) \tag{6.33}$$

$$\kappa_1 B_c^2 = 2\sqrt{\rho^{(b)}G\tilde{\gamma}}\left(1 + \frac{1}{2}\frac{\rho^{(b)}Gc_b}{\tilde{\gamma}^2}\right) \tag{6.34}$$

Of course, the critical wavelength and field increase with increasing elasticity and scale at onset with the relevant elastic modulus of the ferrogel $c_\perp$ with exponents $1/2$ and $1/4$, respectively. In the pure ferrofluid case, $c_\perp = 0 = c_b$, the critical values are identical to those of the usual Rosensweig instability, i.e. there is no difference between a bulk free surface and a film, except for a possible difference in the surface tension σ_T in the two cases.

In the opposite, bending dominated regime, $\rho^{(b)}Gc_b \gg \tilde{\gamma}^2$ the critical values are

$$k_c^4 = \frac{\rho^{(b)}G}{3c_b}\left(1 - \frac{\tilde{\gamma}}{\sqrt{3\rho^{(b)}Gc_b}}\right) \tag{6.35}$$

$$\kappa_1^2 B_c^4 = \frac{16}{9}\rho^{(b)}G\sqrt{3\rho^{(b)}Gc_b}\left(1 + \frac{3}{2}\frac{\tilde{\gamma}}{\sqrt{3\rho^{(b)}Gc_b}}\right) \tag{6.36}$$

Here, the critical wavelength and field scale at onset with the bending elastic modulus of the ferrogel film c_b with exponents $1/4$ and $1/8$, respectively.

6.6.2   Permanent-magnetic, symmetric case

We now consider a film consisting of a permanent-magnetic gel with the intrinsic (surface) magnetization M_0' to be rigidly anchored to the elastic degrees of freedom. In particular we choose it to be always antiparallel to the external field B. In this section we just discuss the case of a magnetic symmetry between the bulk fluids a and b, being either both non-magnetic or having the same magnetic susceptibility. For this case the magnetic contribution stemming from the left hand side of eq. (6.22) cancels (κ_1 in eq. (6.25) is zero) and only the divergence of the magnetic membrane stress tensor gives a field dependent contribution to the threshold condition for a stationary instability

$$\tilde{\mathcal{C}}^{(z)}(k) \;\; = \;\; \Delta\rho\, G k^{-2} + \tilde{\gamma} - M_0' B + c_b k^2 = 0 \qquad (6.37)$$

Here, $\Delta\rho$ is the density difference between the medium above and below the film or membrane. Eq. (6.37) leads to an instability with a characteristic mode

$$k_c^4 \;\; = \;\; \frac{\Delta\rho\, G}{c_b} \qquad (6.38)$$

when the applied critical field reaches the threshold value

$$B_c \;\; = \;\; \frac{1}{M_0'}\Big(\tilde{\gamma} + 2\sqrt{c_b \Delta\rho\, G}\Big). \qquad (6.39)$$

Note that the critical wave vector is independent of M_0', dominated by the bending elastic coefficient, and rather similar to eq. (6.35). The threshold field is inversely proportional to the magnitude of the intrinsic permanent magnetization.

6.6.3   The general case

We now discuss the general case, where both destabilizing magnetic field effects are present, i.e. a uniaxial film with the permanent magnetization opposite to the field and a magnetic contrast between the two surrounding fluids. The condition for marginal stability against stationary convection, eq. (6.27),

$$\tilde{\mathcal{C}}^{(z)}(k) = \Delta\rho\, G k^{-2} + \tilde{\gamma} + c_b k^2 - M_0' B - \kappa_1 B^2 k^{-1} = 0 \qquad (6.40)$$

leads to the neutral curve $B = B(k)$. In principle, one could expect a competition between the two different instabilities described in the two preceding subchapters, i.e. a transition from a stationary instability with a wave vector like that of eq. (6.29) to one like that of eq. (6.38).

    The minimum threshold condition $dB/dk = 0$ allows us the calculate the critical wave vector k_c as a real root of

$$\kappa_1(3c_b k_c^4 + \tilde{\gamma} k_c^2 - \Delta\rho\, G)^2 + 2M_0'^2(c_b k_c^4 - \Delta\rho\, G)k_c^3 = 0 \qquad (6.41)$$

In dimensionless form eq. (6.41) contains three relevant numbers $R_B = c_b/(\Delta\rho\, G d^4)$, $R_E = \tilde{\gamma}/(\Delta\rho\, G d^2)$, and $R_M = M_0'^2/(\Delta\rho\, G \kappa_1 d^3)$, if the wave vector is scaled by the film thickness d. For $R_M > R_B, R_E$ there are two different minimum solutions, k_{c1} and k_{c2}, possible. However, the critical fields associated with these wave vectors, $B_{c1} = B(k_{c1})$ and $B_{c2} =$

$B(k_{c2})$, are never equal, except in the limit $R_M \to \infty$, where $k_{c1} = -k_{c2}$ and the case of section 6.6.2 is reached. For $R_M \lesssim R_B, R_E$ there is only one minimum solution of eq. (6.41), which tends for smaller R_M to the solution of section 6.6.1. Thus, for a given set of material parameters there is always one definite instability at a minimum B_c, and never a competition between instabilities of different k_c.

6.6.4   Additional remarks

Finally we will explore the possibility of an oscillatory instability. If we assume that the film compressional modulus, $\tilde{\varepsilon}$, and the longitudinal elastic modulus $c_\parallel$ and viscosity $\nu_\parallel$ can be neglected (incompressible film), one can show that the curve of marginal stability, $B = B(k, \omega)$ has its minimum at $\omega_0 = 0$, and thus any oscillatory state would have a higher threshold than the stationary one. In the general case, the proof of the non-existence of an oscillatory instability is much more involved. One can show (under the proviso that $\nu_\perp + \nu_b k^2$ and $\nu_\parallel$ are of the same order of magnitude) that there is no finite frequency possible if $\tilde{\varepsilon} k^2 \leq \sqrt{3}(\tilde{\gamma} k^2 + \Delta \rho \, G + c_b k^4)$. In the opposite case the threshold of an oscillatory instability (if it exists) is higher than that for the stationary one.

   If the densities of the two bulk fluids above and below the film or membrane are identical, their gravitational influence on the interface undulations cancels. The thin film itself is not sensitive to gravity, since its volume is going to zero in the two-dimensional limit. Therefore, the gravity term is absent in the normal stress boundary condition and the linear instability criterion in the stationary case is $\mathcal{C}^{(z)} = 0$ (instead of $\tilde{\mathcal{C}}^{(z)} = 0$). The general marginal stability curve $B = B(k)$ then has a minimum for a vanishing $k_c^2 \sim \Delta \rho \, G \to 0$ leading to a vanishing threshold $B_c^4 \sim \Delta \rho \, G \to 0$[3]. The lowest wave vector for a finite experimental set-up of horizontal dimension L, $k_c = 2\pi/L$ gives $\kappa_1 B_c^2 \approx 2\pi\tilde{\gamma}/L$, since effects of bending and surface magnetization are negligible for large L. This means there is only one surface excitation (spike) in the whole sample, governed by the (effective) surface tension. This is a very well known scenario, theoretically and experimentally [92], for ordinary ferrofluid free surfaces under strongly reduced gravity conditions.

6.7   Discussion

The driving force of the Rosensweig instability manifests itself in the boundary conditions, only, for ferrofluids as well as ferrogels (if magnetostriction is neglected). The question arises, how will the characteristics of the onset of the instability change, if the elastic medium itself is very thin so that it can be considered as a film or a membrane. In the present chapter we have addressed this question by extending previously obtained dispersion relations of surface waves at a half-space ferrogel boundary to those of the membrane surfaces. The very thin membrane is surrounded by two Newtonian fluids that can be ferrofluids with different magnetic properties. Possible generalizations to viscoelastic surrounding fluids and to viscoelastic (rather than elastic) membranes have been sketched. The magnetic film itself can be either a superparamagnetic isotropic magnetic gel, or an anisotropic ferromagnetic one having a finite intrinsic magnetization.

---

[3]Since the limits $k \to 0$ and $\kappa_1 \to 0$ are not interchangeable, the formulas of section 6.6.2 are not applicable to the case of vanishing gravity; rather, one has to establish relations between the smallness of $\Delta \rho \, G$, the smallness of k_c, and the smallness of κ_1, in order to get a definite result for B_c in that case.

Apart from the material properties of the surrounding fluids, the derivation of dispersion relations in thin films makes use of certain effective (frequency and wave vector dependent) surface material parameters that describe the internal film properties. For surface waves an effective elastic surface modulus is introduced that contains the intra-layer elastic and viscous properties. In the same manner we introduce in our discussion an effective surface permeability for the magnetic film describing the induced or permanent magnetic film properties, which generally are different from the bulk quantities. In recent experiments [93] this kind of difference between bulk and surface behavior in the magnetic properties has been seen when spin coating a ferrofluid.

In our discussion we have restricted ourselves to modes where the upper and the lower surface of the membrane move in phase, resulting in an undulated membrane of constant thickness (in linear approximation). This is complementary to a previous discussion of films of finite thickness, where just peristaltic motions where taken into account [84]. For superparamagnetic films we get two different additional contributions to the dispersion relation. One is due to the magnetic asymmetry between the surrounding liquids. This contribution is of the same character as the magnetic part of surface waves in the half-space case and vanishes in the symmetric case (no magnetic contrast between the two surrounding fluids). The second contribution comes from the magnetizability of the thin film itself. This last contribution, however, acts always stabilizing and effectively stiffens the membrane. Thus, a (symmetric) superparamagnetic membrane in air, for instance, will never become unstable to undulations of the type described here. An intuitive reason for this is the fact that in the symmetric case the magnetic field is not distorted in the limit of an infinitely thin membrane even if the membrane itself is subject to small perturbations. As a result, no destabilizing force acts on the magnetic dipoles in the film. In the present discussion we therefore focus on the case of high magnetic contrast between the surrounding fluids discussing the influence of the surface elastic properties to the characteristics of the Rosensweig instability. Due to the elastic and bending elastic surface properties, the characteristic mode at onset is shifted to higher wavelengths and the critical magnetic field towards higher field strengths. We can distinguish the limiting cases of a bending dominated regime and the regime where surface elasticity plays the important role.

For an anisotropic magnetic thin film or membrane, its permanent magnetization can lead to the Rosensweig instability, if the applied field is strong enough and oriented antiparallel to it. In this case the magnetic asymmetry between the surrounding liquids is not needed and such a magnetic film surrounded by air can become unstable.

Finally, the general case of an anisotropic magnetic membrane separating two liquids of different magnetic properties has been discussed. In principle, there is a competition between the previously discussed instability mechanisms (either based on the magnetic contrast or on the permanent film magnetization), which generally occur at a different wavelength. However, it turns out that such a pattern competition does not occur in the system under consideration, because the critical magnetic field according to one of the mechanisms is always smaller than the other one. Only in the limiting case of infinitely high intrinsic magnetization (infinitely low magnetic contrast) both critical fields can be equal. In this case, however, the different characteristic modes at onset are of the same magnitude, but of opposite sign, and no competition of two different spatial modes arises.

Chapter 7

The adjoint system for the Marangoni convection

In this chapter we will apply the method that we introduced in chapter 5 to derive the adjoint system for the Rosensweig instability to the case of the Marangoni instability. Also in the case of the Marangoni instability the adjoint system taking into account the deformability of the surface was unknown and nonlinear discussions where therefore restricted to flat surfaces[1].

7.1 Introduction to Marangoni convection

The Marangoni instability is a prominent example of a surface tension driven instability. If a temperature gradient is applied to a layer of a fluid with a free surface, the conducting state becomes unstable beyond a certain critical temperature gradient when heating is done from below and convection starts. For thick layers the instability is driven by buoyancy (classical Rayleigh-Bénard convection), but if the layer is smaller than about $1\,\mathrm{mm}$, Pearson [94] proposed fluctuations of the surface tension, that arise due to temperature fluctuations at the free surface, being the mechanism driving the convection.

The Marangoni instability was investigated extensively theoretically. Nield [95] first compared linearly the competition between the buoyancy and the surface tension driven instability mechanism, but both, Pearson and Nield, still considered a flat, undeformable surface. Scriven and Sternling [96] and later on Smith [97] accounted for a free deformable surface. In Ref. [96] only capillary effects have been considered and an always unstable conducting regime was obtained due to missing stabilizing gravitational contributions for the long wavelength limit. Smith discussed a layer model, a light fluid above a heavier one. A comprehensive linear study was first given by Takashima [50, 51] in 1981, who also discussed the possibility of an oscillatory branch that could arise for negative Marangoni numbers. Pérez-García and Carneiro [98] generalized this approach to the combination of both, surface driven and buoyancy driven convection, which matches the results of Takashima in the limit of negligible buoyancy forces. All nonlinear theoretical discussion up to now assumed a flat, undeformable surface. Rosenblat et al., for instance, discussed the nonlinear regime in a cylindrical container [52] in terms of an extended Galerkin method. This discussion was later on extended to rectangular vessels [53, 54], but for this

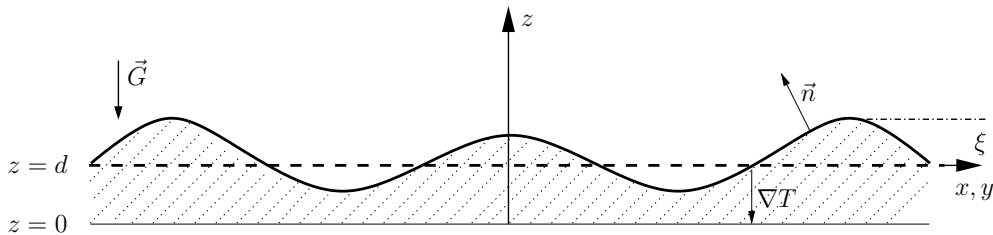---

[1]This chapter is based on [74].

Figure 7.1: Qualitative sketch of the geometry under consideration in the case of pure Marangoni convection. The fluid is confined between the rigid surface at $z = 0$ and the deformable surface initially at $z = d$. The deflection of the deformable surface with respect to the flat surface is denoted by ξ with its unit normal vector $\mathbf{n}$ pointing upwards. The applied temperature gradient is always parallel, the acceleration due to gravity G always antiparallel to the $z-$axis.

approach no adjoint system is needed. The case of a horizontally infinite layer of fluid was studied in Refs. [55] and [99]. In Ref. [56] a two layer model was considered, where the adjoint system was derived using the ansatz of [99] provided the surface is flat.

Inspired by the result of the case of the Rosensweig instability, we apply the same formalism (section 5.2) to the case of stationary Marangoni convection to find the adjoint system of equations for this case as well. However, there exists a crucial difference between these two instabilities. While in the case of magnetic fluids the external force acts normal to the free surface, in the case of Marangoni convection the external force is acting tangentially to the surface. We can therefore verify our formalism for any arbitrary direction of the driving force. This external force for the Marangoni instability is, as mentioned already, mediated by temperature fluctuations. The surface tension σ_T is therefore assumed to be temperature dependent and reads in a series expansion up to linear order in T

$$\sigma_T(T) \;=\; \sigma_T(T_R) - \gamma(T - T_R) \tag{7.1}$$

with the change in surface tension due to temperature fluctuations $\gamma = -(\partial \sigma_T(T)/\partial T)_{T=T_R}$ and where T_R represents an arbitrary reference temperature. For the following discussion we will refer to $\sigma_T(T_R)$ as σ_T.

7.2   Basic equations and the adjoint system

To find the adjoint system for the purely surface driven convection we assume a viscous Newtonian fluid. As done in the case of the Rosensweig instability, we assume it to be compressible with a barotropic equation of state at the beginning, but in the end we will again use the limit of an incompressible fluid. Additionally we have to incorporate the equation of heat transport with the temperature T and the thermal diffusivity $\tilde{\chi}$. All the other variables are denoted in the same way as in the previous discussion. As we want to discuss the purely surface driven contribution of convection, all contributions due to

buoyancy are neglected. The system of equations thus reads

$$\partial_t \rho + \partial_k(\rho v_k) = 0 \tag{7.2}$$

$$\partial_t g_i + \partial_j T_{ij} = \rho G_i \tag{7.3}$$

$$\partial_t T + v_j \partial_j T = \tilde{\chi} \partial_j \partial_j T \tag{7.4}$$

The stress tensor T_{ij} of the fluid under consideration takes the form

$$T_{ij} = v_j g_i + p\delta_{ij} - \nu_2(\partial_j v_i + \partial_i v_j) - \hat{\nu}(\partial_k v_k)\delta_{ij} \tag{7.5}$$

We require the normal as well as the tangential stress at the free surface between the Newtonian fluid and the vacuum to be balanced, leading to the normal and tangential boundary conditions, respectively

$$p - \rho_0 G\xi - 2\nu_2 \partial_z v_z - \hat{\nu}(\partial_k v_k) = -\sigma_T(\partial_x^2 + \partial_y^2)\xi \tag{7.6}$$

$$\nu_2(\partial_y v_z + \partial_z v_y) = -\gamma\partial_y T + \gamma\beta\partial_y \xi \tag{7.7}$$

$$\nu_2(\partial_x v_z + \partial_z v_x) = -\gamma\partial_x T + \gamma\beta\partial_x \xi \tag{7.8}$$

where β denotes the applied temperature gradient across the fluid.

Additionally we have to specify the phenomenological boundary conditions at the surface. Again the kinematic boundary condition (2.44) for a free deformable surface is assumed to hold. Second, we assume the heat flux Q through the surface to be proportional to the local temperature gradient, where κ denotes the coefficient of (surface) heat conduction.

$$Q(T) = -\kappa\partial_z T \tag{7.9}$$

At the bottom ($z = 0$) of the container we assume the usual rigid boundary conditions

$$v_i = \partial_z v_z = T = 0 \tag{7.10}$$

The state vector $|\phi\rangle$ now becomes six dimensional and is defined by

$$|\phi\rangle = (v_x, v_y, v_z, p, T, \rho) \tag{7.11}$$

so that the system of equations reads again in the general form

$$\mathcal{L}_0 |\phi\rangle = 0 \tag{7.12}$$

We use the usual scalar product, however, now the $z-$integration is bounded between the bottom plate ($z = 0$) and the free surface ($z = \xi$).

$$\langle\bar{\phi} \mid \phi\rangle = \lim_{L\to\infty} \frac{1}{4L} \int_{-L}^{L} dx \int_{-L}^{L} dy \int_{0}^{\xi} dz \int_{0}^{t} dt \; \bar{\phi}\phi \tag{7.13}$$

The adjoint linear operator then turns out to be

$$\mathcal{L}_0^\dagger = \begin{pmatrix} A & C \\ B & D \end{pmatrix}$$

$$A = \begin{pmatrix} -\rho\partial_t - \nu_2\partial_i^2 - (\hat\nu + \nu_2)\partial_x^2 & -\hat\nu\partial_x\partial_y - \nu_2\partial_y\partial_x & -\hat\nu\partial_x\partial_z - \nu_2\partial_z\partial_x \\ -\hat\nu\partial_y\partial_x - \nu_2\partial_x\partial_y & -\rho\partial_t - \nu_2\partial_i^2 - (\hat\nu + \nu_2)\partial_y^2 & -\hat\nu\partial_y\partial_z - \nu_2\partial_z\partial_y \\ -\hat\nu\partial_z\partial_x - \nu_2\partial_x\partial_z & -\hat\nu\partial_z\partial_y - \nu_2\partial_y\partial_z & -\rho\partial_t - \nu_2\partial_i^2 - (\hat\nu + \nu_2)\partial_z^2 \end{pmatrix}$$

$$(7.14)$$

$$B = \begin{pmatrix} -\partial_x & -\partial_y & -\partial_z \\ 0 & 0 & 0 \\ 0 & 0 & 0 \end{pmatrix} \qquad C = \begin{pmatrix} -\partial_x & 0 & 0 \\ -\partial_y & 0 & 0 \\ -\partial_z & -\beta & 0 \end{pmatrix} \tag{7.15}$$

$$D = \begin{pmatrix} 0 & 0 & -\frac{1}{\rho_0}\partial_t \\ 0 & -\partial_t - \tilde\chi\partial_i^2 & 0 \\ -\frac{1}{\rho_0}\partial_t & 0 & -\frac{c^2}{\rho_0}\partial_t \end{pmatrix} \tag{7.16}$$

The surface contributions of the integration by parts should vanish to fulfill eq. (5.22) leading to the corresponding boundary conditions in the adjoint case.

$$i\omega 2\nu_2\partial_z\bar v_z + i\omega\hat\nu(\partial_k\bar v_k) + i\omega\bar p + \rho G\bar v_z + \sigma_T k^2\bar v_z = 0 \tag{7.17}$$
$$\bar v_x(-ik_x)\hat T(z) - \bar v_x\gamma\beta(-ik_x) + \hat v_x(z)\nu_2(\partial_z\bar v_x + \partial_x\bar v_z) = 0 \tag{7.18}$$
$$\bar v_y(-ik_y)\hat T(z) - \bar v_y\gamma\beta(-ik_y) + \hat v_y(z)\nu_2(\partial_z\bar v_y + \partial_y\bar v_z) = 0 \tag{7.19}$$
$$-\tilde\chi\bar T\partial_z T + \tilde\chi T\partial_z\bar T = 0 \tag{7.20}$$

In the last set of equations we have used the fact, that every variable of the original system is modulated by ξ, in particular we used $T(z) = \hat T(z)\xi$ and $v_{x,y}(z) = \hat v_{x,y}(z)\xi$. Actually eq. (7.20) just states, that the adjoint temperature may differ from the original one by just a constant. For the phenomenological boundary conditions we take the same form as for the original case, namely

$$\bar v_z = i\bar\omega\bar\xi \tag{7.21}$$
$$\bar Q(\bar T) = -\kappa\,\partial_z\bar T \tag{7.22}$$

The boundary conditions at the rigid bottom turn out to be self-adjoint, but are repeated here

$$\bar v_i = \partial_z\bar v_z = 0 \tag{7.23}$$
$$\bar T = 0 \tag{7.24}$$

7.3 The dimensionless representation

For the further discussion we give the dimensionless version of the problem discussed in the previous section, because it is common in all the other discussion regarding convection. Following the usual steps [100], the linearized dynamical equations for the deviations from the conducting state of the temperature Θ and the vertical component of the velocity v_z read

$$(D^2 - k^2)(D^2 - k^2 - i\omega)v_z(z) = 0 \tag{7.25}$$
$$(D^2 - k^2 - i\omega\mathcal{P})\Theta(z) = -v_z(z) \tag{7.26}$$

The boundary conditions at the free surface using the stress balance then read

$$(D^2 + k^2)v_z(z) = -\mathcal{M}k^2\left(\Theta(z) - \frac{1}{\mathcal{P}}\xi\right) \tag{7.27}$$

$$\mathcal{C}\mathcal{P}(i\omega - D^2 + 3k^2)Dv_z(z) = -(\mathcal{B} - k^2)k^2\xi \tag{7.28}$$

And for the phenomenological boundary conditions we have

$$v_z(z) = i\omega\xi \tag{7.29}$$

$$\mathcal{P}(D + \mathcal{F})\Theta(z) = \mathcal{F}\xi \tag{7.30}$$

At the bottom, the equations reduce to

$$v_z = Dv_z = \Theta = 0 \tag{7.31}$$

While rescaling the variables we have introduced dimensionless numbers such as the Prandtl number $\mathcal{P} = \nu_2/\tilde{\chi}$, the Marangoni number $\mathcal{M} = \gamma\beta d^2/(\rho\tilde{\chi}\nu_2)$, the Crispation number $\mathcal{C} = \rho\nu_2\tilde{\chi}/(\sigma_T d)$, the Bond number $\mathcal{B} = \rho G d^2/\sigma_T$ and the Biot number $\mathcal{F} = (\partial Q/\partial T)d/\kappa$ as well as the dimensionless derivative with respect to z, $D = d/dz$.

Using the same arguments for the adjoint set of equations we find

$$(D^2 - k^2)(D^2 - k^2 + i\bar{\omega})\bar{v}_z(z) = -A\bar{\Theta}(z) \tag{7.32}$$

$$(D^2 - k^2 + i\bar{\omega}\mathcal{P})\bar{\Theta}(z) = 0 \tag{7.33}$$

It is worth mentioning here that in eq. (7.32) an additional number, $A = \beta^2 d^4/(\tilde{\chi}\nu_2)$, arises. This is, however, consistent with condition (7.20), which allows the temperature in the adjoint case to differ from the original temperature by a constant factor. One could rescale the dimensionless adjoint temperature by exactly this number A, resulting in a dimensionalized adjoint temperature. This, however, is not surprising since also in the discussion of the adjoint system of the Rosensweig problem, the adjoint strain field acquired a different physical unit due to the dynamic coupling between velocity field and the strain field. The adjoint boundary conditions stemming from the adjoining process turn out to be

$$-\mathcal{M}(D\bar{v}_z(z))k^2\left(\hat{\Theta} - \frac{1}{\mathcal{P}}\right) = (D\hat{v}_z)(D^2 + k^2)\bar{v}_z(z) \tag{7.34}$$

$$\mathcal{C}\mathcal{P}(\omega\bar{\omega} - i\omega D^2 + 3i\omega k^2)D\bar{v}_z(z) = -(\mathcal{B} - k^2)k^2\bar{v}_z(z) \tag{7.35}$$

While the ones describing the free surface are

$$\bar{v}_z(z) = i\bar{\omega}\bar{\xi} \tag{7.36}$$

$$\mathcal{P}(D + \mathcal{F})\bar{\Theta}(z) = \mathcal{F}\bar{\xi} \tag{7.37}$$

The self-adjoint boundary conditions at the bottom are repeated here in dimensionless form

$$\bar{v}_z = D\bar{v}_z = 0 \tag{7.38}$$

$$\bar{\Theta} = 0 \tag{7.39}$$

Also in the dimensionless representation we explicitly made use of the fact that the macroscopic variables are modulated by ξ, in particular we used $Dv_z(z) = (D\hat{v}_z(z))\xi$ and $\Theta(z) = \hat{\Theta}(z)\xi$.

At that point we should mention a crucial point. While the adjoint boundary conditions in the case of the Rosensweig instability (5.31-5.33) turned out to be independent of the eigenvectors of the original case, the tangential boundary condition (7.34) contains the eigenvectors of the original case. By inspection of the adjoining-process this is due to coupling between the temperature and the velocity field, even though this coupling does not drive the instability. A similar coupling in the bulk equations of the Rosensweig case – the magnetic field to the velocity or the strain field – was missing. As a consequence, the adjoint dispersion relation will also depend on the original eigenvectors, which is discussed in detail in section 7.6.

7.4   The dispersion relation

We start solving the system of equations in the original case. Previous analytical work accounting for a stationary instability with finite deformation of the surface always assumed stationary equations from the beginning. However, to find a connection between the adjoint and original case, we need the general dispersion relation of surface waves propagating on the free surface.

To solve the dynamical equations (7.25) and (7.26) subject to the boundary conditions (7.27-7.31) we used an ansatz with hyperbolic functions [72][2]. In particular we used, after substitution of eq. (7.26) into eq. (7.25), the following solutions

$$\Theta(z) \;=\; \sum_{i=1}^{3}\big(A_i\cosh(\lambda_i z) + B_i\sinh(\lambda_i z)\big) \tag{7.40}$$

$$v_z(z) \;=\; -\sum_{i=1}^{2}\big(\lambda_i^2 - k^2 - i\omega\mathcal{P}\big)\big(A_i\cosh(\lambda_i z) + B_i\sinh(\lambda_i z)\big) \tag{7.41}$$

together with the roots

$$\lambda_1^2 \;=\; k^2 \tag{7.42}$$
$$\lambda_2^2 \;=\; k^2 + i\omega \tag{7.43}$$
$$\lambda_3^2 \;=\; k^2 + i\omega\mathcal{P} \tag{7.44}$$

The solvability condition of the boundary conditions gives the corresponding dispersion relation of plane waves traveling on the surface of the fluid. However, the dispersion relation can only be given implicitly and is shown in section 7.6

$$\mathcal{D}(\omega, k, \mathcal{M}) \;=\; 0 \tag{7.45}$$

We will restrict ourselves in this discussion to the stationary case, although solutions of eq. (7.45) with a finite frequency ω might exist at the threshold. On the other hand one

---

[2]The article [72] was on the competition between the Bénard-Marangoni and the Rosensweig instability in ferrofluids, but we adopt the ansatz with hyperbolic functions for the eigenvectors in geometries with a finite layer depth.

can prove analytically, that a nontrivial solution of eq. (7.45) is $\omega = 0$. Using this result we can perform the limit of a stationary instability and the solvability condition in the stationary case reduces to the neutral curve

$$\mathcal{M} \;=\; \frac{8k(\mathcal{B} + k^2)(k\cosh(k) + \mathcal{F}\sinh(k))(2k - \sinh(2k))}{8\mathcal{C}k^5\cosh k + (\mathcal{B} + k^2)\big(\sinh^3(k) - k^3\cosh(k)\big)} \tag{7.46}$$

which coincides with the result obtained by Takashima [50] assuming stationarity from the beginning. In the limit of vanishing surface deformations ($\mathcal{C} \to 0$) we find the same results as Pearson [94], Nield [95] as a special case.

These calculations and also the following ones have been checked using the ansatz of Nield [95], who used Fourier modes.

7.5 The adjoint dispersion relation

As in the the case of the Rosensweig instability, to get the adjoint system, one has to start with the fully dynamic problem. Using again hyperbolic functions the solutions can be written as

$$\bar{v}_z(z) \;=\; \sum_{i=1}^{3}\Big(\bar{A}_i\cosh(\bar{\lambda}_i z) + \bar{B}_i\sinh(\bar{\lambda}_i z)\Big) \tag{7.47}$$

$$\bar{\Theta}(z) \;=\; -(i\bar{\omega} - k^2 + \bar{\lambda}_3)(\bar{\lambda}_3 - k^2)\Big(\frac{\bar{A}_3}{A}\cosh(\bar{\lambda}_3 z) + \frac{\bar{B}_3}{A}\sinh(\bar{\lambda}_3 z)\Big) \tag{7.48}$$

together with the adjoint roots

$$\bar{\lambda}_1^2 \;=\; k^2 \tag{7.49}$$
$$\bar{\lambda}_2^2 \;=\; k^2 - i\bar{\omega} \tag{7.50}$$
$$\bar{\lambda}_3^2 \;=\; k^2 - i\bar{\omega}\mathcal{P} \tag{7.51}$$

With the help of the adjoint boundary conditions, we obtain the dispersion relation of surface waves in the adjoint space that can only be given implicitly again (section 7.6)

$$\bar{\mathcal{D}}(\bar{\omega}, \omega, k, \mathcal{M}) \;=\; 0 \tag{7.52}$$

This equation also gives $\bar{\omega}$ as a function of the frequency in the original case ω, although the expression is more complicated than for the case of the Rosensweig instability and a solution of eq. (7.52) has not been obtained analytically. Nevertheless we have to guarantee that eq. (7.52) is fulfilled even when approaching the critical point for the stationary instability. When expanding eq. (7.52) in terms of ω we obtain

$$\bar{\mathcal{D}}(\bar{\omega}, \omega, k, \mathcal{M}) \;=\; \bar{\mathcal{D}}_0(\bar{\omega}, \omega{=}0, k, \mathcal{M}) + \bar{\mathcal{D}}_1(\bar{\omega}, \omega{=}0, k, \mathcal{M})\,\omega + \mathcal{O}(\omega^2) \tag{7.53}$$

When approaching the marginal point, $\bar{\mathcal{D}}_1$ and all the contributions of higher order in ω cancel with ω becoming 0. To fulfill eq. (7.53), additionally $\bar{\mathcal{D}}_0$ has to vanish. It can be shown, that if $\bar{\omega}$ as a function ω vanishes when ω vanishes, the constant contribution $\bar{\mathcal{D}}_0$ becomes zero and the adjoint dispersion relation is satisfied (see section 7.6). Therefore the instability in the adjoint case occurs at the same point with the same characteristics.

7.6   Discussion of the dispersion relation

In this section we give the dispersion relations of the original and the adjoint Marangoni problem. In particular we discuss the adjoint dispersion relation in the limit of $\omega \to 0$.

The solvability condition of the system of dynamic equations (7.2-7.5) together with the boundary conditions (7.6-7.10) at the deformable surface yields the dispersion relation. It describes the relation between the frequency and the wave vector of surface waves propagating on a free surface. In an implicit form (and using $\lambda_1 = k$) it reads

$$\mathcal{D}(\omega, k, \mathcal{M}) \equiv$$

$$i\omega^5 \mathcal{P}^3 (\mathcal{P}-1)k \Big\{ k \Big[i\omega \mathcal{P}\mathcal{C}\lambda_3 \cosh(\lambda_3) \Big(2k\lambda_2 \big(k^2 (4i\omega\mathcal{P}(\mathcal{P}-1) + \mathcal{M}) - 2\omega^2 \mathcal{P}(\mathcal{P}-1) \big)$$

$$+ \sinh(k)\sinh(\lambda_2) \big(i\omega k^2 (\mathcal{M} + 8i\omega\mathcal{P}(\mathcal{P}-1)) - i\omega^3 \mathcal{P}(\mathcal{P}-1)$$

$$+ 2k^4 (\mathcal{M} + 4i\omega\mathcal{P}(\mathcal{P}-1)) \big) \Big)$$

$$+ k^3 \lambda_3 \mathcal{M}(\mathcal{B}+k^2)(\lambda_2 \sinh(k) - k\sinh(\lambda_2))$$

$$+ \sinh(\lambda_3) \Big(\lambda_2 k \big(\mathcal{M}k^2 (2\mathcal{P}-1)(\mathcal{B}+k^2) - 8\omega^2 \mathcal{P}^2 k^2 \mathcal{C}\mathcal{F}(\mathcal{P}-1) - 4i\omega^3 \mathcal{P}^2 (\mathcal{P}-1)\mathcal{C}\mathcal{F} \big)$$

$$+ \sinh(k)\sinh(\lambda_2) \big(k^4 (\mathcal{B}+k^2)(2\mathcal{P}-1)\mathcal{M} + i\omega\mathcal{P}\mathcal{M}k^2 (\mathcal{B}+k^2)$$

$$- 8\omega^2 \mathcal{P}^2 (\mathcal{P}-1)\mathcal{F}\mathcal{C}k^4 - 8i\omega^3 \mathcal{P}^2 (\mathcal{P}-1)\mathcal{F}\mathcal{C}k^2 + \omega^2 \mathcal{P}^2 (\mathcal{P}-1)\mathcal{F}\mathcal{C} \big) \Big)$$

$$- \lambda_2 \cosh(\lambda_2) \Big((\mathcal{B}+k^2)\lambda_3 \big(\mathcal{M}k^2 - \omega^2 \mathcal{P}(\mathcal{P}-1) \big) \cosh(\lambda_3)\sinh(k)$$

$$+ i\omega\mathcal{P} \big(2\mathcal{C}\mathcal{M}\lambda_3 k^3 + \sinh(k)\sinh(\lambda_3)(i\omega(\mathcal{P}-1)(\mathcal{B}+k^2)\mathcal{F} + \mathcal{C}\mathcal{M}k^2 (2k^2 + i\omega\mathcal{P})) \big) \Big) \Big]$$

$$+ \cosh(k) \Big[\lambda_2 \cosh(\lambda_2) \Big(i\omega\mathcal{P}\mathcal{C}\lambda_3 \cosh(\lambda_3) \big(i\omega^3 \mathcal{P}(\mathcal{P}-1) - 2k^4 (\mathcal{M} + 4i\omega\mathcal{P}(\mathcal{P}-1))$$

$$- i\omega k^2 (\mathcal{M} + 4i\omega\mathcal{P}(\mathcal{P}-1)) \big) - \sinh(\lambda_3) \big(k^4 \mathcal{M}(\mathcal{B}+k^2)(2\mathcal{P}-1)$$

$$- 8\omega^2 \mathcal{P}^2 (\mathcal{P}-1)\mathcal{F}\mathcal{C}k^4 - 4i\omega^3 \mathcal{P}(\mathcal{P}-1)\mathcal{F}\mathcal{C}k^2 + \omega^4 \mathcal{P}^2 (\mathcal{P}-1)\mathcal{F}\mathcal{C} \big) \Big)$$

$$+ k^2 \Big((\mathcal{B}+k^2)\lambda_3 (\mathcal{M}k^2 - \omega^2 \mathcal{P}(\mathcal{P}-1)) \cosh(\lambda_3)\sinh(\lambda_2)$$

$$+ i\omega\mathcal{P} \big(\mathcal{C}\mathcal{M}\lambda_2 \lambda_3 (2k^2 + i\omega) + \sinh(\lambda_2)\sinh(\lambda_3)(i\omega(\mathcal{P}-1)\mathcal{F}(\mathcal{B}+k^2)$$

$$+ \mathcal{C}\mathcal{M}(i\omega + k^2)(i\omega\mathcal{P} + 2k))) \big) \Big) \Big] \Big\}$$

$$= 0 \tag{7.54}$$

Taking the stationary limit of this expression (while neglecting the five trivial roots $\omega = 0$) results in the neutral curve given in eq. (7.46).

Using the same procedure for the adjoint problem, yields the implicit dispersion rela-

tion in the adjoint space (using $\bar{\lambda}_1 = k$)

$$\bar{\mathcal{D}}\,(\bar{\omega}, \omega, k, \mathcal{M}) \equiv \mathcal{P}(\mathcal{P}-1)i\bar{\omega}^3\Big\{ - \Big[\bar{\lambda}_3\cosh(\bar{\lambda}_3)\Big(\bar{\lambda}_2\big(i\bar{\omega}^3 k^2(\mathcal{B}+k^2)(\mathcal{P}-1)\mathcal{P}$$

$$+i\omega A\mathcal{C}\mathcal{F}(2k+i\bar{\omega}(\mathcal{P}-1))\big)\cosh(\bar{\lambda}_2)\sinh(k)$$

$$+k\cosh(k)\big(i\bar{\omega}^2\omega\mathcal{C}\mathcal{P}^2(\bar{\omega}^2+4i\bar{\omega}k^2-8k^2)\cosh(\bar{\lambda}_2)$$

$$-(i\omega A\mathcal{C}\mathcal{F}(2k^2+i\bar{\omega}(\mathcal{P}-1))+i\bar{\omega}^3 k^2(\mathcal{B}+k^2)\mathcal{P}(\mathcal{P}-1))\sinh(\bar{\lambda}_2)\big)$$

$$+i\omega\bar{\omega}^2\mathcal{C}k^2\mathcal{P}^2(\mathcal{P}-1)\big(8k^3\bar{\lambda}_2-4i\bar{\omega}k\bar{\lambda}_2+(8k^4-8i\bar{\omega}k^2-\bar{\omega}^2)\sinh(k)\sinh(\bar{\lambda}_2)\big)\Big)$$

$$+k\mathcal{F}\Big(i\omega A\mathcal{C}\mathcal{F}\big((2k^2-i\bar{\omega})\sinh(\bar{\lambda}_2)-2k\bar{\lambda}_2\sinh(k)\big)$$

$$+\sinh(\bar{\lambda}_3)\big(i\omega\mathcal{C}\bar{\lambda}_2(4k^2(\mathcal{P}-1)\mathcal{P}^2(2k^2-i\bar{\omega})\bar{\omega}^2$$

$$+A(k^2(2-4\mathcal{P})+i\bar{\omega}\mathcal{P})+\cosh(k)\cosh(\bar{\lambda}_2)(2Ak^2(2\mathcal{P}-1)-i\bar{\omega}(\mathcal{P}-1)A$$

$$+\bar{\omega}^2\mathcal{P}^2(\mathcal{P}-1)(\bar{\omega}^2+4i\bar{\omega}k^2-8k^2)))+i\bar{\omega}^3\bar{\lambda}_2 k(\mathcal{B}+k^2)(\mathcal{P}-1)\mathcal{P}$$

$$-i\bar{\omega}^3 k^2\mathcal{P}(\mathcal{P}-1)(\mathcal{B}+k^2)\cosh(k)\sinh(\bar{\lambda}_2)$$

$$-i\omega k\mathcal{C}\sinh(k)\sinh(\bar{\lambda}_2)(A(i\bar{\omega}(3\mathcal{P}-1)+k^2(4\mathcal{P}-1)$$

$$+\bar{\omega}^2\mathcal{P}^2(\mathcal{P}-1)(\bar{\omega}^2+8i\bar{\omega}k-8k^4)))\big)\Big)\Big]$$

$$+\frac{\mathcal{P}\hat{\Theta}-1}{\mathcal{P}D\hat{v}_z}k^2\mathcal{M}\Big[\cosh(\bar{\lambda}_3)\bar{\lambda}_3\Big(\bar{\lambda}_2\big(i\omega A\mathcal{C}\mathcal{F}(\mathcal{P}-1)$$

$$-2\bar{\omega}^2 k^3\mathcal{P}(\mathcal{B}+k^2)+2\bar{\omega}^2\mathcal{P}^2(\mathcal{B}+k^2)\big)$$

$$+\sinh(k)\cosh(\bar{\lambda}_2)\big(i\omega A\mathcal{C}\mathcal{F}k^2(2\mathcal{P}-1)+\omega\bar{\omega}A\mathcal{C}\mathcal{F}(\mathcal{P}-1)+2\bar{\omega}^2 k^4\mathcal{P}(\mathcal{B}+k^2)$$

$$-2\bar{\omega}^2 k^4\mathcal{P}^2(\mathcal{B}+k^2)+i\bar{\omega}^3 k^4(\mathcal{B}+k^2)-i\bar{\omega}^3 k^2\mathcal{P}^2(\mathcal{B}+k^2)\big)\Big)$$

$$+\bar{\omega}^2 k^2(\mathcal{B}+k^2)\mathcal{F}\mathcal{P}(\mathcal{P}-1)\big(2k\bar{\lambda}_2+(2k^2-i\bar{\omega})\sinh(k)\sinh(\bar{\lambda}_2)\big)\sinh(\bar{\lambda}_3)$$

$$-i\omega\mathcal{C}k\bar{\lambda}_2\cosh(\bar{\lambda}_2)\big(A\mathcal{F}\bar{\lambda}_3+k\sinh(\bar{\lambda}_3)(A\mathcal{F}\sinh(\bar{\lambda}_3)$$

$$-\bar{\omega}^3\mathcal{P}^2(\mathcal{P}-1)(\bar{\lambda}_3\cosh(\bar{\lambda}_3)+\mathcal{F}\sinh(\bar{\lambda}_3))))$$

$$-k\cosh(k)\Big(\bar{\lambda}_2\cosh(\bar{\lambda}_2)\big(\bar{\lambda}_3(i\omega A\mathcal{C}\mathcal{F}(2\mathcal{P}-1)+2\bar{\omega}k^2(\mathcal{B}+k^2)(\mathcal{P}-1)\mathcal{P})\cosh(\bar{\lambda}_3)$$

$$+2\bar{\omega}^2 k^2\mathcal{F}\mathcal{P}(\mathcal{P}-1)(\mathcal{B}+k^2)\sinh(\bar{\lambda}_3)\big)$$

$$-i\omega\mathcal{C}\big(\sinh(\bar{\lambda}_2)(k^2-i\bar{\omega})(A\mathcal{F}\sinh(\bar{\lambda}_3)+i\bar{\omega}^3\mathcal{P}(\mathcal{P}-1)(\bar{\lambda}_3\cosh(\bar{\lambda}_3)+\mathcal{F}\sinh(\bar{\lambda}_3))))\Big)\Big]\Big\}$$

$$= 0 \qquad\qquad (7.55)$$

Here $\bar{\mathcal{D}}$ stills contains ω, the frequency of surface waves in the original space. To find the relation between $\bar{\omega}$ and ω is not as simple as in the case of the Rosensweig instability. However, all what we need is to guarantee that $\bar{\omega}$ vanishes at the linear threshold of the physical problem, where $\omega = 0$. The reason for this requirement is that the resonance condition for a nonlinear expansion of the basic equations cannot be satisfied in the case of a finite adjoint frequency $\bar{\omega}$ but a vanishing frequency ω. In section 7.5 the expansion

of $\bar{\mathcal{D}}$ in terms of ω is given, eq. (7.53), and will not be repeated here. As stated already above, the adjoint dispersion relation depends on the original eigenvectors due to the dynamic bulk coupling between the temperature and the velocity field. The stationary limit for the latter one is given by

$$v_z(z) = \frac{8\mathcal{M}_c k^3 \cosh(k)}{\mathcal{P}N}\Big\{ kz \sinh(k) \cosh(kz) \tag{7.56}$$
$$- \big[kz \cosh(k) + \sinh(k) - z \sinh(k) \big] \sinh(kz) \Big\} \xi$$

while the stationary eigenvector for the temperature field reads

$$\Theta(z) = \frac{1}{\mathcal{P}N}\Big\{ 2k^2 \mathcal{M}_c \cosh(k)\big(kz \cosh(k) - (z-3)\sinh(k) \big) z \cosh(kz) \tag{7.57}$$
$$- \Big[16k^2 \mathcal{F} + \mathcal{M}_c\big(k^2(1+z) - 1 + (1 + k^2(1+z))\cosh(2k)\big)$$
$$+ k\big(\mathcal{M}_c(1 - z + k^2 z^2) - 8\mathcal{F}\big)\sinh(2k) \Big]\sinh(kz) \Big\}\xi$$

with the abbreviation

$$N = 2k\big((\mathcal{M}_c - 8)k^2 - 2\mathcal{F}\big)\cosh(k) + 4k\mathcal{F}\cosh(3k) \tag{7.58}$$
$$+ \big(8(1 - 2\mathcal{F})k^2 + \mathcal{M}_c + (8k^2 - \mathcal{M}_c)\cosh(2k)\big)\sinh(k)$$

We can substitute eqs. (7.56) and (7.57) into the constant contribution $\bar{\mathcal{D}}_0$ of eq. (7.53) resulting in the explicit expression

$$\bar{\mathcal{D}}_0(\bar{\omega}, \omega = 0, k, \mathcal{M}) = \bar{\omega}(\omega = 0)k^2(B^2 + k^2)(\mathcal{P} - 1)^2 \mathcal{P}^3 \tag{7.59}$$
$$\times \Big(k \cosh(k) + \mathcal{F}\sinh(k)\Big)\frac{2k \sinh^2(k)(\sinh(2k) - 2k)}{1 + 2k^2 - \cosh(2k)}$$

When assuming $\mathcal{P} \neq 1$ and $k \neq 0$, $\bar{\mathcal{D}}_0 = 0$ can only be satisfied if $\bar{\omega}(\omega = 0) = 0$. Thus, for a stationary instability in the original case, also the adjoint case is stationary.

Chapter 8

Conclusions

In this thesis we theoretically studied the nonlinear properties of the normal field or Rosensweig instability in isotropic magnetic gels. The Rosensweig instability, discovered in 1967, describes the phenomenon of the transition between an initially flat surface of a magnetic fluid and a deformed surface of hexagonally ordered surface spikes, as soon as a homogeneous magnetic field applied perpendicular to the flat surface exceeds a certain critical value. Magnetic gels combine the superparamagnetic behavior of magnetic fluids with the elastic properties of elastomers. If exposed to a homogeneous magnetic field also the free surface of a ferrogel undergoes a transition from an initially flat state to a state of regularly ordered surface spikes beyond a certain critical field strength. The critical magnetic field, however, increases with increasing shear modulus. The characteristic wave number instead remains unchanged compared to usual ferrofluids.

The Rosensweig instability differs from other instabilities by its static nature. A motionless flat surface becomes unstable and deforms until another motionless but deformed state is fully developed. In mathematical terms, this static property manifests itself in a vanishing frequency of the characteristic surface mode at the linear onset, a result also typical for stationary instabilities but with the difference that the velocity field there usually stays finite. This static property motivated a time independent treatment of the nonlinear equations in previous discussions. In chapter 3 we focused first on the linear properties of the Rosensweig instability and showed that its static nature should be interpreted as the limiting process of surface waves whose frequency tends to zero rather than as a time independent process from the beginning. Treating the set of hydrodynamic equations dynamically, we were able to derive the corresponding linear eigenvectors. The static limits of the latter reveal the static nature of the Rosensweig instability, namely that the velocity field vanishes identically whereas the strain field acquires a finite static value. This rather singular property is due to the deformability of the surface, which is modeled by the kinematic boundary condition. This condition relates the temporal change of the surface position to the local velocity normal to the surface. If treated in a time-independent manner, this condition maps the rigid boundary condition and the surface does not deform.

A first theoretical discussion of the nonlinear regime of the Rosensweig instability in usual ferrofluids was given by Gailitis, who energetically compared the stability of different regular surface patterns. In chapter 4 we extended this energy method with additional elastic contributions in order to describe isotropic magnetic gels. By minimizing the surface energy density for the three regular patterns of stripes, squares and hexagons

we found that the stripe pattern is never stable with respect to either of the other two patterns. At the linear onset, the hexagonal configuration of surface spikes turns out to be the energetically favored pattern. Upon further increase of the control parameter the hexagonal pattern in turn becomes energetically unstable and a square pattern develops. Both transitions, from the flat surface to hexagons and from hexagons to squares, are accompanied by hysteretic regions that become smaller for increasing elastic shear moduli.

The energy method compares the energy of the possible surface patterns but does neither predict, which of these patterns can be dynamically attained, nor takes into account the dissipative processes in the medium that become important during the growth of the surface spikes. Furthermore, it is strictly valid only in the unphysical limit of a vanishing magnetic susceptibility. These drawbacks motivated us to discuss in the fifth chapter the nonlinear regime of the Rosensweig instability using an expansion of the fundamental hydrodynamic equations in terms of the normalized difference ϵ between the applied magnetic field and the critical one.

When expanding the fundamental hydrodynamic equations in terms of ϵ, the nonlinearities give rise to inhomogeneities in the second and higher order equations. To systematically guarantee the solvability of these equations using Fredholm's theorem, the adjoint linear eigenvectors are needed. For systems involving a deformable surface in general and for the Rosensweig instability in particular, the set of adjoint linear equations with their corresponding boundary conditions were not known. For the derivation of the latter two assumptions turned out to be crucial. First, one has to treat the system dynamically and the static limit should only be used at the very end, and second, one has to start with the hydrodynamic set of equations describing a compressible medium. The incompressibility assumption can then be used once the system of equations is adjoint. The first assumption rests on the findings of the linear discussion, namely that the static character of the Rosensweig instability should be interpreted as a limiting process rather than as a static process from the beginning. The second assumption guarantees the symmetry of the stress tensor that is needed to consistently define the adjoint tangential boundary conditions. With the set of adjoint equations and the corresponding boundary conditions, the adjoint linear eigenvectors were obtained. Thereby right traveling waves in the original system transform into left traveling waves in the adjoint system and vice versa. Furthermore they show the same static properties as the original eigenvectors, namely that the adjoint velocity field vanishes in the static limit whereas the strain field acquires a finite static value.

With the adjoint linear system for the Rosensweig instability at hand, we fulfilled the solvability conditions in the second and in the third perturbative order in terms of ϵ and finally obtained the amplitude equation for the Rosensweig instability. Within the scope of our assumptions, in particular because we neglected magnetostrictive effects, the hydrodynamic and the magnetic bulk equations decouple. Since we assumed a fast relaxing magnetic field which is governed by linear static Maxwell equations, the solvability condition for the magnetic equations is fulfilled trivially. As a consequence, Fredholm's theorem applied to the hydrodynamic bulk equations does not contain the magnetic field variables, which act as the control parameter. Besides the bulk equations the Rosensweig instability crucially depends on the boundary conditions and in particular on the normal stress boundary condition. We showed in our analysis that the normal stress boundary condition cannot be fulfilled trivially in the higher perturbative orders, but rather acts as a supplement to Fredholm's theorem, in order to determine the higher order corrections

to the control parameter.

In the derived amplitude equation two contributions are important. We succeeded for the first time in deriving the quadratic coefficient in the amplitude equation from the fundamental hydrodynamic equations. The quadratic coefficient implies that hexagons are the stable configuration of surface spikes at the linear threshold and in addition that the bifurcation from the flat surface to the surface spikes is transcritical involving a bistable region between hexagonally ordered spikes and the flat surface below the linear threshold. Both results are experimentally verified properties of the Rosensweig instability. Additionally we derived a second order time derivative in the case of magnetic gels. The linearized amplitude equation therefore acquires the form of a damped harmonic oscillator. If a finite amplitude surface pattern is disturbed, this disturbance will relax in the form of a damped oscillation. In the case of the Rosensweig instability in ferrofluids, whose amplitude equation has also been derived in this thesis, this second order time derivative is not present. The amplitudes of the stable static surface patterns are determined by the cubic coefficients in the amplitude equation. They show that for high magnetic field strengths the hexagons become unstable and transform into a square pattern. A result that is in accordance with the energy method. The cubic coefficients calculated in this thesis are independent of the elastic shear modulus and the magnetic susceptibility, due to the assumption of a linear elastic as well as a linear magnetic medium.

Our discussions revealed that the Rosensweig instability is a purely surface driven instability within the scope of our assumptions. A natural question is then to ask: What happens, if the superparamagnetic medium is just a surface, namely a thin film or a membrane. In chapter 6 we discussed this question assuming a membrane, either made of an isotropic or an anisotropic magnetic gel, floating on a Newtonian liquid or on a ferrofluid. In the first case we realized, that the film does not become unstable, if we assume an isotropic magnetic gel. An intuitive reason for this is given by the character of the driving force itself. Small surface fluctuations render the applied homogeneous magnetic field locally inhomogeneous, which causes a Kelvin force. In the case of membranes we showed, that in the limit of vanishing film thickness the magnetic field remains undistorted causing no force acting to the magnetic film. This changes if we assume an anisotropic magnetic gel, where the frozen-in magnetization is rigidly anchored to the elastic medium. In this case the film becomes unstable with respect to periodical disturbances if the frozen-in magnetization is oriented opposite to the applied magnetic field. A typical property of the Rosensweig instability in isotropic magnetic gels is that its characteristic wavelength is the same as for usual ferrofluids. If we assume a non-magnetic film floating on top of a usual ferrofluid, this changes and the characteristic mode depends on the elastic properties of the membrane.

We realized in this thesis that the character of the Rosensweig instability is owed to the deformability of the surface between the magnetic medium and the vacuum above. Another very prominent example of an instability which involves a deformable surface is given by the pure Marangoni instability. In this case, temperature fluctuations at the free surface of a fluid cause fluctuations of the surface tension that in turn deform the surface and drive convection. In the case of the Marangoni convection, the adjoint system of linear equations that takes into account a deformable surface also was unknown and nonlinear discussions therefore had to assume flat and undeformable surfaces. Using the same arguments as for the Rosensweig instability, we were able to derive the adjoint system and the corresponding boundary conditions for the Marangoni instability. As shown in

chapter 7, the adjoint boundary conditions involve the linear eigenvectors of the original system. The latter property is due to a bulk coupling between the temperature field and the velocity field, although this coupling does not drive the instability. As a consequence, the solution of the adjoint system for the Marangoni convection is rather involved and an easy interpretation in terms of a translation between right and left traveling waves, as it was the case for the Rosensweig instability, is not possible. The driving force in the case of the Marangoni instability acts purely tangentially, while for the Rosensweig instability the force is orthogonal. Thus the method used to derive the adjoint systems for both instabilities should also work for any arbitrary orientation of the driving force at the surface.

Appendix A

Decoupling of the dynamic system

In this appendix we show explicitly the decoupling of the Maxwell equations and the bulk equations for the magnetic medium under the assumptions of linear magnetostatics and negligence of magnetostrictive effects. Separating the actual magnetic field into the applied magnetic field $\mathbf{H}_0$ (respectively $\mathbf{B}_0$ for the flux density) and the perturbations due to the deformed surface denoted as $\mathbf{h}$ respectively $\mathbf{b}$

$$
\begin{align}
\mathbf{H} &= \mathbf{H}_0 + \mathbf{h} \tag{A.1}\\
\mathbf{B} &= \mathbf{B}_0 + \mathbf{b} \tag{A.2}
\end{align}
$$

The latter can be expressed as the gradient of a scalar potential Φ

$$
\begin{align}
\mathbf{h} &= -\nabla\Phi \tag{A.3}\\
\mathbf{b} &= -\mu\nabla\Phi \tag{A.4}
\end{align}
$$

with μ denoting the magnetic permeability of the medium.

The magnetic field enters the dynamic bulk equations of the medium only through the stress tensor T_{ij} given by (2.35). Concentrating on the magnetic contributions of the momentum conservation equation (2.33), we obtain, since the applied magnetic field is assumed be constant, the contributions

$$
\partial_j\left(B_i h_j + H_j b_i + b_i h_j - \frac{1}{2}(B_k h_k + H_k b_k + b_k h_k)\delta_{ij} \right) \tag{A.5}
$$

Substituting the perturbed magnetic fields in terms of the scalar potential one can simplify (A.5) as

$$
\partial_j\left(-B_i\partial_j\Phi - B_j\partial_i\Phi + \mu(\partial_i\Phi)(\partial_j\Phi) + B_k(\partial_k\Phi)\delta_{ij} - \frac{1}{2}\mu(\partial_k\Phi)(\partial_k\Phi)\delta_{ij} \right) \tag{A.6}
$$

Evaluating the partial derivative ∂_j leaves us with

$$
-B_i\partial_j\partial_j\Phi - B_j\partial_j\partial_i\Phi + \mu(\partial_i\Phi)(\partial_j\partial_j\Phi) + \mu(\partial_j\Phi)\partial_j\partial_i\Phi + B_j\partial_j\partial_i\Phi - \mu(\partial_j\Phi)\partial_j\partial_i\Phi
$$
$$
\tag{A.7}
$$

Obviously the second term cancels the fifth as well as the third term cancels the sixth. The remaining two contributions cancel by realizing that the magnetic scalar potential has to satisfy the Laplace equation. In total all magnetic contributions cancel in the bulk equations for the magnetic medium.

Appendix B

Magnetic fields

Within the scope of our assumptions the hydrodynamic bulk equations completely decouple from the magnetic bulk equations. This enables us to find solutions to the bulk system separately. Furthermore, since the magnetic system is entirely independent of any hydrodynamic variable (except that the distortions of the magnetic field should be proportional to the surface deformation) it is worth determining the magnetic field for a given surface deformation $\xi(x, y, t)$ first and substitute afterwards into the system of hydrodynamic equations. In this section we give a detailed derivation for all the magnetic field expressions used in the main text.

B.1 The Heaviside-Lorentz system of electromagnetic units

Throughout this thesis the Heaviside-Lorentz or the rationalized Gauss system of electromagnetic units has been used to describe the magnetic phenomena [69]. The choice of this system is set by the fundamental hydrodynamic equations in chapter 2 and in particular by the choice of the energy density (2.7). We will therefore introduce this system of units in this section based on the book of Jackson [69] and although this thesis only considers magnetic fields we will, for completeness, include the electric degrees of freedom in this introductory section as well.

The fundamental laws in the electrodynamic theory, Coulomb's law of electrostatics and the Ampère law, only give proportionalities between measured forces, F_C and F_A respectively, and the distance and the magnitude of two electric charges or electric currents. Coulomb's law reads

$$F_C = k_1 \frac{q_1 q_2}{r^2} \tag{B.1}$$

where q_1 and q_2 are electric charges, r is the distance between them and k_1 is a proportionality constant and Ampère's law is given by

$$\frac{dF_A}{dl} = 2k_2 \frac{I_1 I_2}{r} \tag{B.2}$$

relating the force per unit length to the electric currents I_1 and I_2 that are carried by two parallel, infinitely long conducting wires of negligible cross-section separated by the distance r.

Quantity	Heaviside-Lorentz	SI
Speed of light	c	$(\mu_0\epsilon_0)^{-1/2}$
Magnetic induction	$\mathbf{B}$	$\mathbf{B}/\sqrt{\mu_0}$
Magnetic field	$\mathbf{H}$	$\sqrt{\mu_0}\mathbf{H}$
Magnetic scalar potential	Φ	$\sqrt{\mu_0}\Phi$
Magnetization	$\mathbf{M}$	$\sqrt{\mu_0}\mathbf{M}$
Magnetic permeability	μ	μ/μ_0

Table B.1: This table shows the conversion rules between the Heaviside-Lorentz system of units used in this thesis and the SI units (taken from [69]) for the macroscopic variables relevant in this thesis. The magnetic permeability of vacuum is given by $\mu_0 = 4\pi \cdot 10^{-7} H/m$ and the speed of light by $c = 2.99792458 \cdot 10^8 m/s$.

The proportionality constants k_1 and k_2 are either given by the eqs. (B.1) and (B.2) if the unit charge has been chosen independently or one can choose them arbitrarily with the consequence of defining unit charge. Due to the common definition of the electric current as the time rate of change of charge, one can give the relative dimension of k_1 with respect to k_2 as $k_1 = c^2 k_2$[1], where c denotes the speed of light. In the Heaviside-Lorentz system of units these proportionality constants are arbitrarily chosen as $k_1 = 1/(4\pi)$ and $k_2 = 1/(4\pi c^2)$ and the Heaviside-Lorentz system therefore differs from the usual Gaussian system of units by a factor 4π.

Measured in the Heaviside-Lorentz units, the magnetic and the electric field variables acquire the same physical units and the constitutive equations read

$$\mathbf{D} = \mathbf{E} + \mathbf{P} \tag{B.3}$$
$$\mathbf{H} = \mathbf{B} - \mathbf{M} \tag{B.4}$$

where $\mathbf{D}$ denotes the electric displacement field, $\mathbf{E}$ the electric field and $\mathbf{P}$ the electric polarization. The last equation is exactly the relation between the magnetic field $\mathbf{H}$, the magnetic flux density $\mathbf{B}$ and the magnetization $\mathbf{M}$ as we obtain by thermodynamic means in eq. (2.9). In the Heaviside-Lorentz system of units the Maxwell equations acquire the form

$$\nabla \cdot \mathbf{D} = \rho^{\text{el}} \tag{B.5}$$
$$\nabla \times \mathbf{H} = \frac{\mathbf{J}}{c} + \frac{\partial \mathbf{D}}{c\partial t} \tag{B.6}$$
$$\nabla \times \mathbf{E} = -\frac{\partial \mathbf{B}}{c\partial t} \tag{B.7}$$
$$\nabla \cdot \mathbf{B} = 0 \tag{B.8}$$

where ρ^{el} and $\mathbf{J}$ denote the electrical charge density and its corresponding current, respectively. In the absence of the latter and for time independent magnetic fields, which is

---

[1]At this point one can only claim that the relative dimensions of k_1 and k_2 are that of velocity squared, whereas the magnitude is still arbitrary. Deriving the wave equation from this, however, fixes the still undetermined magnitude of this velocity to that of the speed of light in vacuum (cf. [69]).

one of our assumptions, these equations become the static Maxwell equations (2.36) and (2.37) as used in this thesis. To convert the equations in this thesis to the SI system, the rules given in table B.1 can be applied.

B.2 Expansion to higher perturbative orders

B.2.1 The Maxwell equations

For the nonlinear discussion of an instability involving a deformable surface, it is convenient to distinguish the externally applied magnetic field $\mathbf{H}^{\text{ext}}$ in all orders from the distortion field $\mathbf{h}$ due to the deformed surface and correspondingly for the magnetic flux densities

$$\mathbf{H} = \mathbf{H}^{\text{ext}} + \mathbf{h} \quad \text{and} \quad \mathbf{B} = \mathbf{B}^{\text{ext}} + \mathbf{b} \tag{B.9}$$

The external magnetic field is, in our geometry, always directed parallel to the $z-$axis (cf. fig. 2.1 on p. 18), however, the magnitude remains tunable. We therefore expand the applied external field as well as the flux density according to

$$\begin{aligned} \mathbf{H}^{\text{ext}} &= \mathbf{H}_c + \epsilon \mathbf{H}^{(1)} + \epsilon^2 \mathbf{H}^{(2)} + \dots \tag{B.10} \\ \mathbf{B}^{\text{ext}} &= \mathbf{B}_c + \epsilon \mathbf{B}^{(1)} + \epsilon^2 \mathbf{B}^{(2)} + \dots \tag{B.11} \end{aligned}$$

where ϵ denotes the normalized difference between the applied magnetic field and the critical one (this is the expansion we used in eq. (5.1)).

In addition, the deformed surface will cause the magnetic field to be distorted. These deviations from the applied magnetic field are taken into account by the field $\mathbf{h}$ and $\mathbf{b}$ that are also expanded similarly as

$$\begin{aligned} \mathbf{h} &= \epsilon \mathbf{h}^{(1)} + \epsilon^2 \mathbf{h}^{(2)} + \dots \tag{B.12} \\ \mathbf{b} &= \epsilon \mathbf{b}^{(1)} + \epsilon^2 \mathbf{b}^{(2)} + \dots \tag{B.13} \end{aligned}$$

The same expansion applies to the corresponding fields in the vacuum.

The deviations from the applied field still have to satisfy the linear magnetostatic equations, $\mathbf{b} = \mu \mathbf{h}$ and $\nabla \cdot \mathbf{b} = 0 = \nabla \times \mathbf{h}$, which allows for the introduction of a magnetic scalar potential [69] $\mathbf{h} = -\nabla \Phi$ that is then governed by the Laplace equation

$$\Delta \Phi = 0 \quad \text{and} \quad \Delta \Phi^{\text{vac}} = 0 \tag{B.14}$$

The scalar magnetic potentials attain the expansion in terms of ϵ from the fields and correspondingly are written as

$$\Phi = \epsilon \Phi^{(1)} + \epsilon^2 \Phi^{(2)} + \epsilon^3 \Phi^{(3)} + \dots \tag{B.15}$$

This one to one correspondence between distortion field $\mathbf{h}$ and the scalar potential Φ within the different orders is only true within the scope of our assumptions of chapter 5 where long wavelength variations of the arising pattern are discarded.

Since the Laplace equation is linear and homogeneous, its expansion to the higher orders is trivial. The bulk solutions can be found in each order independently and in particular, Fredholm's theorem will be fulfilled in each order.

B.2.2 The boundary conditions

Since the surface normal $\mathbf{n}$ is not constant but depends on the surface deflection (as do the distorted field contributions), a higher harmonic coupling to previous orders is possible (in contrast to the system of bulk equations). For the upcoming calculation it is useful to determine first the fields at the boundary $z = \xi$

$$
\mathbf{H} = \mathbf{H}_c + \epsilon \left(\mathbf{H}^{(1)} - (\nabla\Phi^{(1)})_{z=0}\right) + \epsilon^2 \left(\mathbf{H}^{(2)} - (\nabla\Phi^{(2)}) - \xi^{(1)}(\partial_z\nabla\Phi^{(1)})_{z=0}\right)
$$
$$
+ \epsilon^3 \left(\mathbf{H}^{(3)} - (\nabla\Phi^{(3)})_{z=0} - \xi^{(1)}(\partial_z\nabla\Phi^{(2)})_{z=0} - \frac{1}{2}[(\xi^{(1)2}\partial_z^2 + 2\xi^{(2)}\partial_z)\nabla\Phi^{(1)}]_{z=0}\right) \quad \text{(B.16)}
$$

and accordingly for the magnetic field $\mathbf{H}^{\text{vac}}$ and the magnetic flux densities $\mathbf{B}$ and $\mathbf{B}^{\text{vac}}$. The contributions in (B.16) that are explicitly proportional to $\xi^{(1)}$ or $\xi^{(2)}$ are due to the deformable surface.

As mentioned, the surface normal $\mathbf{n}$, initially directed parallel to the $z-$axis, changes its orientation in the course of time as the surface perturbation grows (cf. fig. 2.1 on p. 18). To give a proper expansion of the boundary conditions, we additionally have to expand the surface normal as a function of the surface deflection $\xi(x, y, t)$

$$
\mathbf{n} = \mathbf{n}_0 + \epsilon\mathbf{n}^{(1)} + \epsilon^2\mathbf{n}^{(2)} + \epsilon^3\mathbf{n}^{(3)} \quad \text{(B.17)}
$$

with the different perturbative contributions given by

$$
\mathbf{n}^{(1)} = \begin{pmatrix} -\partial_x\xi^{(1)} \\ -\partial_y\xi^{(1)} \\ 0 \end{pmatrix}, \qquad \mathbf{n}^{(2)} = \begin{pmatrix} -\partial_x\xi^{(2)} \\ -\partial_y\xi^{(2)} \\ \frac{1}{2}(\partial_x\xi^{(1)})^2 + \frac{1}{2}(\partial_y\xi^{(1)})^2 \end{pmatrix} \quad \text{(B.18)}
$$

$$
\text{and} \qquad \mathbf{n}^{(3)} = \begin{pmatrix} -\partial_x\xi^{(3)} - \frac{1}{2}(\partial_y\xi^{(1)})^2(\partial_x\xi^{(1)}) - \frac{1}{2}(\partial_x\xi^{(1)})^3 \\ -\partial_y\xi^{(3)} - \frac{1}{2}(\partial_x\xi^{(1)})^2(\partial_y\xi^{(1)}) - \frac{1}{2}(\partial_y\xi^{(1)})^3 \\ (\partial_y\xi^{(1)})(\partial_y\xi^{(2)}) + (\partial_x\xi^{(1)})(\partial_x\xi^{(2)}) \end{pmatrix} \quad \text{(B.19)}
$$

With the previous considerations on hand, we are able to expand the boundary conditions in terms of ϵ. The fact that the normal component of the magnetic flux density is continuous at the boundary gives the following condition

$$
\begin{aligned}
\mathbf{n} \cdot \left(\mathbf{H}^{\text{vac}} - \mathbf{H}\right) &= \mathbf{n} \cdot \left(\mathbf{B}^{\text{vac}} - \mathbf{B} + \mathbf{M}\right) \\
&= \mathbf{n} \cdot \mathbf{M} \quad \text{(B.20)}
\end{aligned}
$$

Consider the linear perturbative order of the last equation

$$
\mathbf{n}^{(1)} \cdot \left(\mathbf{H}_c^{\text{vac}} - \mathbf{H}_c\right) + \mathbf{n}^{(0)} \cdot \left(\mathbf{H}^{(1)\text{vac}} - \mathbf{H}^{(1)}\right) = \mathbf{n}^{(1)} \cdot \mathbf{M}^{(0)} + \mathbf{n}^{(0)} \cdot \mathbf{M}^{(1)} \quad \text{(B.21)}
$$

For the constant contributions (constant with respect to x and y), we find

$$
H_z^{(1)\text{vac}} - H_z^{(1)} = M_z^{(1)} \quad \text{(B.22)}
$$

while the contributions proportional to $\mathbf{n}^{(1)}$ cancel identically. The corresponding expression for the second order contribution to the applied field, $H_z^{(2)\text{vac}} - H_z^{(2)} = M_z^{(2)}$, can be obtained straightforwardly.

The boundary condition for the tangential components of the magnetic field (2.38) is given in linear order

$$\mathbf{n}^{(1)} \times (\mathbf{H}_c^{\text{vac}} - \mathbf{H}_c) + \mathbf{n}^{(0)} \times \left(\mathbf{H}^{(1)\text{vac}} - \mathbf{H}^{(1)}\right) \quad = \quad 0 \tag{B.23}$$

which can be simplified substituting eq. (B.22) to (with $a \in \{x, y\}$)

$$h_a^{(1)\text{vac}} - h_a^{(1)} \quad = \quad -(\partial_a \xi^{(1)}) M_0 \tag{B.24}$$

In the second perturbative order we find

$$\mathbf{n}^{(2)} \times \left(\mathbf{H}_c^{\text{vac}} - \mathbf{H}_c\right) + \mathbf{n}^{(1)} \times \left(\mathbf{H}^{(1)\text{vac}} - \mathbf{H}^{(1)} - \nabla\Phi^{(1)\text{vac}} + \nabla\Phi^{(1)}\right)$$
$$+ \mathbf{n}^{(0)} \times \left(\mathbf{H}^{(2)\text{vac}} - \nabla\Phi^{(2)\text{vac}} + k_c \xi^{(1)} \nabla\Phi^{(1)\text{vac}} - \mathbf{H}^{(2)} + \nabla\Phi^{(2)} + k_c \xi^{(1)} \nabla\Phi^{(1)}\right) = 0 \tag{B.25}$$

which is simplified in the same manner (by exploiting the results of the previous order) to

$$\left(\partial_a \Phi^{(2)\text{vac}} - \partial_a \Phi^{(2)}\right) - (\partial_a \xi^{(2)}) M_c - (\partial_a \xi^{(1)}) M^{(1)}$$
$$+ (\partial_a \xi^{(1)})\left(\partial_z \Phi^{(1)\text{vac}} - \partial_z \Phi^{(1)}\right) - k_c \xi^{(1)}\left(\partial_a \Phi^{(1)\text{vac}} + \partial_a \Phi^{(1)}\right) \quad = \quad 0 \tag{B.26}$$

with $a \in \{x, y\}$. Upon substituting the linear solutions (B.34) and (B.35) this immediately leads to expressions (B.39) and (B.40) used in section B.4 to find the magnetic eigenvectors in the second perturbative order. Finally we deduce for the tangential boundary condition in the third perturbative order

$$\mathbf{n}^{(3)} \times (\mathbf{H}_c^{\text{vac}} - \mathbf{H}_c) + \mathbf{n}^{(2)} \times \left(\mathbf{H}^{(1)\text{vac}} - \mathbf{H}^{(1)} - (\nabla\Phi^{(1)\text{vac}}) + (\nabla\Phi^{(1)})\right)$$
$$+ \mathbf{n}^{(1)} \times \left(\mathbf{H}^{(2)\text{vac}} - \mathbf{H}^{(2)} - (\nabla\Phi^{(2)\text{vac}}) + (\nabla\Phi^{(2)}) + k_c \xi^{(1)}(\nabla\Phi^{(1)\text{vac}}) + k_c \xi^{(1)}(\nabla\Phi^{(1)})\right)$$
$$+ \mathbf{n}^{(0)} \times \left(\mathbf{H}^{(3)\text{vac}} - \mathbf{H}^{(3)} - (\nabla\Phi^{(3)\text{vac}}) + (\nabla\Phi^{(3)}) - \xi^{(1)}(\partial_z \nabla\Phi^{(2)\text{vac}}) + \xi^{(1)}(\partial_z \nabla\Phi^{(2)})\right.$$
$$\left. - \frac{1}{2}(k_c^2 \xi^{(1)2} - 2k_c \xi^{(2)})(\nabla\Phi^{(1)\text{vac}}) + \frac{1}{2}(k_c^2 \xi^{(1)2} + 2k_c \xi^{(2)})(\nabla\Phi^{(1)})\right)$$
$$= \quad 0 \tag{B.27}$$

where it will be sufficient for our discussion to consider only the contributions proportional to the main characteristic modes $\xi^{(1)}$ as discussed in section 5.3.2.

Along the same lines the boundary condition that guarantees the continuity of the normal component (2.39) of the magnetic flux density is derived. In first perturbative order we get

$$\mathbf{n}^{(1)} \cdot (\mathbf{B}_c^{\text{vac}} - \mathbf{B}_c) + \mathbf{n}^{(0)} \cdot \left(\mathbf{B}^{(1)\text{vac}} - \mathbf{B}^{(1)}\right) \quad = \quad 0 \tag{B.28}$$

which is straightforwardly simplified to

$$b_z^{(1)\text{vac}} - b_z^{(1)} \quad = \quad 0 \tag{B.29}$$

For the corresponding condition in the second perturbative order we obtain

$$\mathbf{n}^{(2)} \cdot \left(\mathbf{B}_c^{\text{vac}} - \mathbf{B}_c\right) + \mathbf{n}^{(1)} \cdot \left(\mathbf{B}^{(1)\text{vac}} - \mathbf{B}^{(1)} - \nabla\Phi^{(1)\text{vac}} + \mu\nabla\Phi^{(1)}\right)$$
$$+ \mathbf{n}^{(0)} \cdot \left(\mathbf{B}^{(2)\text{vac}} - \mathbf{B}^{(2)} - \nabla\Phi^{(2)\text{vac}} + \mu\nabla\Phi^{(2)} + k_c \xi^{(1)} \nabla\Phi^{(1)\text{vac}} + \mu k_c \xi^{(1)} \nabla\Phi^{(1)}\right) = 0 \tag{B.30}$$

which is simplified by exploiting the previous order to

$$\mu\partial_z\Phi^{(2)} - \partial_z\Phi^{(2)\text{vac}} - (\partial_x\xi^{(1)})\left(\mu\partial_x\Phi^{(1)} - \partial_x\Phi^{(1)\text{vac}}\right)$$
$$-(\partial_y\xi^{(1)})\left(\mu\partial_y\Phi^{(1)} - \partial_y\Phi^{(1)\text{vac}}\right) + k_c\xi^{(1)}\left(\mu\partial_z\Phi^{(1)\text{vac}} + \partial_z\Phi^{(1)}\right) = 0 \quad \text{(B.31)}$$

Finally, the third order boundary conditions takes the form

$$\mathbf{n}^{(3)} \cdot \left(\mathbf{B}_c^{\text{vac}} - \mathbf{B}_c\right) + \mathbf{n}^{(2)} \cdot \left(\mathbf{B}^{(1)\text{vac}} - \mathbf{B}^{(1)} - (\nabla\Phi^{(1)\text{vac}}) + \mu(\nabla\Phi^{(1)})\right)$$
$$+ \mathbf{n}^{(1)} \cdot \left(\mathbf{B}^{(2)\text{vac}} - \mathbf{B}^{(2)} - (\nabla\Phi^{(2)\text{vac}}) + \mu(\nabla\Phi^{(2)}) + k_c\xi^{(1)}(\nabla\Phi^{(1)\text{vac}}) + \mu k_c\xi(\nabla\Phi^{(1)})\right)$$
$$+ \mathbf{n}^{(0)} \cdot \Big(\mathbf{B}^{(3)\text{vac}} - \mathbf{B}^{(3)} - (\nabla\Phi^{(3)\text{vac}}) + \mu(\nabla\Phi^{(3)}) - \xi^{(1)}(\partial_z\nabla\Phi^{(2)\text{vac}}) + \mu\xi^{(1)}(\partial_z\nabla\Phi^{(2)})$$
$$-\frac{1}{2}(k_c^2\xi^{(1)2} - 2k_c\xi^{(2)})(\nabla\Phi^{(1)\text{vac}}) + \frac{1}{2}(k_c^2\xi^{(1)2} + 2k_c\xi^{(2)})(\nabla\Phi^{(1)})\Big)$$
$$= 0 \quad \text{(B.32)}$$

where again it will be sufficient for our discussion to focus on the contributions proportional to the main characteristic modes $\xi^{(1)}$.

Since we expect to find the amplitude equation as the solvability condition for the third perturbative order of the basic equations, it is sufficient to truncate the expansion of the magnetic boundary conditions here.

B.3 Solutions in linear order

With the magnetic boundary conditions in the different perturbative orders at hand, we can start to solve the magnetic Laplace equation (B.14). For the linear deviations form the ground state, the Laplace equation can be solved with the ansatz [20]

$$\Phi^{(1)} = \hat{\Phi}^{(1)}\xi^{(1)}e^{kz} \quad \text{and} \quad \Phi^{(1)\text{vac}} = \hat{\Phi}^{(1)\text{vac}}\xi^{(1)}e^{-kz} \quad \text{(B.33)}$$

Substituting this bulk solutions into the boundary conditions (B.24) and (B.29) yields the governing equations for the yet undetermined amplitudes $\hat{\Phi}^{(1)}$ and $\hat{\Phi}^{(1)\text{vac}}$

$$\partial_x\Phi^{(1)\text{vac}} - \partial_x\Phi^{(1)} = (\partial_x\xi^{(1)})M_0 \quad \text{(B.34)}$$
$$\partial_z\Phi^{(1)\text{vac}} - \mu\partial_z\Phi^{(1)} = 0 \quad \text{(B.35)}$$

Finally we obtain as the solution for the scalar magnetic potential in linear order

$$\Phi^{(1)} = -\frac{M_0}{1+\mu}\xi^{(1)}e^{kz} \quad \text{(B.36)}$$

$$\Phi^{(1)\text{vac}} = \frac{\mu M_0}{1+\mu}\xi^{(1)}e^{-kz} \quad \text{(B.37)}$$

B.4 Solutions in higher orders

In second order we obtain for the Laplace equation

$$\Delta\Phi^{(2)} = 0 \quad \text{and} \quad \Delta\Phi^{(2)\text{vac}} = 0 \quad \text{(B.38)}$$

in the medium and in vacuum, respectively. In the second order of the ϵ−expansion the magnetic boundary conditions for the tangential component of the total magnetic field $\mathbf{H} + \mathbf{h}$ can be simplified to

$$\partial_x \Phi^{(2)\mathrm{vac}} - \partial_x \Phi^{(2)} = \frac{2\mu}{1+\mu} M_c \, \partial_x \xi^{(2)} + M^{(1)} \partial_x \xi^{(1)} \tag{B.39}$$

$$\partial_y \Phi^{(2)\mathrm{vac}} - \partial_y \Phi^{(2)} = \frac{2\mu}{1+\mu} M_c \, \partial_y \xi^{(2)} + M^{(1)} \partial_y \xi^{(1)} \tag{B.40}$$

while the boundary condition for the normal component of the flux density $\mathbf{B}$ reads

$$\partial_z \Phi^{(2)\mathrm{vac}} - \mu\partial_z \Phi^{(2)} = -\frac{\mu}{1+\mu} M_c \sum_{i,j} (k_{1ij}^2 \xi_i \xi_j + k_{2ij}^2 \xi_i \xi_j^* + c.c.) \tag{B.41}$$

where we introduced abbreviations that depend on the angle θ_{ij} between the i-th and the j-th main characteristic mode

$$k_{1ij} = k_c\sqrt{2 + 2\cos\theta_{ij}} \tag{B.42}$$

$$k_{2ij} = k_c\sqrt{2 - 2\cos\theta_{ij}} \tag{B.43}$$

A convenient ansatz for the magnetic scalar potentials to solve this system of equations consists of two contributions. The first contribution $\Phi^{(2,1)}$ is proportional to the linear deflection $\xi^{(1)}$ to account for the contributions proportional to $\mathbf{M}^{(1)}$ in the boundary conditions (B.39) and (B.40). This automatically satisfies the Laplace equation (B.38) for $\Phi^{(2,1)}$ (section B.3). The second contribution $\Phi^{(2,2)}$ accounts for the higher harmonic couplings of the linear characteristic modes proportional to $\xi^{(2)}$, which are modeled by the product of two characteristic modes

$$\xi^{(2)} = k_c \sum_{i,j} (\xi_i \xi_j + \xi_i \xi_j^* + c.c.) \tag{B.44}$$

The characteristic wave vector k_c in eq. (B.44) is just added to give $\xi^{(2)}$ the same unit as $\xi^{(1)}$.

The Laplace equation (B.38) for $\Phi^{(2,2)}$ is satisfied by the ansatz

$$\Phi^{(2,2)} = k_c \sum_{i,j} (\hat{\Phi}_{ij}^{(2,2)R} \xi_i \xi_j e^{k_{1ij}z} + \hat{\Phi}_{ij}^{(2,2)I} \xi_i \xi_j^* e^{k_{2ij}z} + c.c.) \tag{B.45}$$

and by a corresponding one for the magnetic potential in vacuum.

The boundary conditions for the different Fourier modes decouple and can be satisfied separately. We obtain for the contributions proportional to $\xi^{(1)}$

$$\Phi^{(2,1)} = -\frac{M^{(1)}}{1+\mu} \xi^{(1)} e^{k_c z} \tag{B.46}$$

$$\Phi^{(2,1)\mathrm{vac}} = \frac{\mu M^{(1)}}{1+\mu} \xi^{(1)} e^{-k_c z} \tag{B.47}$$

which are of the same structure as in the linear case. The presence of $M^{(1)}$ guarantees $\Phi^{(2,1)}$ to be of second order.

The contributions due to the higher harmonics of the characteristic modes read

$$\hat{\Phi}_{ij}^{(2,2)R} = \frac{\mu}{(1+\mu)^2} M_c \Big(\frac{k_{1ij}}{k_c} - 2 \Big) \tag{B.48}$$

$$\hat{\Phi}_{ij}^{(2,2)R\text{vac}} = \frac{\mu^2}{(1+\mu)^2} M_c \Big(\frac{k_{1ij}}{\mu k_c} - 2 \Big) \tag{B.49}$$

while $\hat{\Phi}_{ij}^{(2,2)L}$ and $\hat{\Phi}_{ij}^{(2,2)L\text{vac}}$ are obtained replacing k_{1ij} by k_{2ij} in eqs. (B.48) and eqs. (B.49), respectively.

Finally we seek the necessary contributions of the magnetic field in the third perturbative order. We restrict the discussion to those proportional to the main characteristic modes $\xi^{(1)}$. The differential equations for the scalar potentials of the distortions to the magnetic fields read

$$\Delta\Phi^{(3,1)} = 0 \qquad \text{and} \qquad \Delta\Phi^{(3,1)\text{vac}} = 0 \tag{B.50}$$

with the corresponding boundary conditions (at $z = 0$) given by

$$\partial_y \Phi^{(3,1)\text{vac}} - \partial_y \Phi^{(3,1)} = M^{(2)} \partial_y \xi^{(1)} \tag{B.51}$$

$$\partial_x \Phi^{(3,1)\text{vac}} - \partial_x \Phi^{(3,1)} = M^{(2)} \partial_x \xi^{(1)} \tag{B.52}$$

$$\partial_z \Phi^{(3,1)\text{vac}} - \mu \partial_z \Phi^{(3,1)} = 0 \tag{B.53}$$

The solutions of this set of equations is obtained following the lines of the second order calculations, eqs. (B.46) and (B.47), leading to

$$\Phi^{(3,1)} = -\frac{M^{(2)}}{1+\mu} \xi^{(1)} e^{k_c z} \qquad \text{and} \qquad \Phi^{(3,1)\text{vac}} = \frac{\mu M^{(2)}}{1+\mu} \xi^{(1)} e^{-k_c z} \tag{B.54}$$

The contributions due to the higher harmonic modes could in principle be calculated in the same way as in the second order. However, these contributions again contribute only to the pressure offset and are therefore of no importance for the amplitude equation.

B.5 Magnetic fields in the case of membranes

B.5.1 The superparamagnetic case

Since the driving force of the Rosensweig instability is solely manifest in the boundaries, the question arises what happens in case of an infinitely thin deformable magnetic medium. The behavior of a magnetic membrane is discussed in chapter 6 of the main text. Here we provide the magnetic field solutions for the geometry depicted in fig. 6.1 on p. 78, to get the necessary coefficient κ_1, eq. (6.25).

Having in mind that we are interested in the limit $kd \to 0$, we assume the two boundaries ξ_+ and ξ_- at $z = +d/2$ and $z = -d/2$, respectively, to be distorted in-phase from their initially flat position by $\xi_\pm = \xi \equiv \xi_0 \exp i(\omega t - kx)$. Also for the membranes we only consider the magnetostatic limit, since the surface wave frequencies involved are much smaller than the electrodynamic ones. The magnetizations are assumed to follow instantaneously (on the time scale of the surface waves) the external fields. This leads to the

Laplace equation for the magnetic potentials of the field-distortions $\mathbf{h}^{(\alpha)} = -\nabla \Phi^{(\alpha)}$ from the initially homogenous fields $\mathbf{H}_{\text{hom}}^{(\alpha)} = \mathbf{B}^{(\alpha)}/\mu_\alpha$ in the three regions $\alpha = \{a, m, b\}$

$$\Delta \Phi^{(i)} = 0 \tag{B.55}$$

The solution of these three equations can be written as

$$\Phi^{(a)} = \hat{\Phi}^{(a)} \xi e^{-kz} \tag{B.56}$$

$$\Phi^{(m)} = \hat{\Phi}_a^{(m)} \xi e^{kz} + \hat{\Phi}_b^{(m)} \xi e^{-kz} \tag{B.57}$$

$$\Phi^{(b)} = \hat{\Phi}^{(b)} \xi e^{kz} \tag{B.58}$$

defining the amplitudes $\hat{\Phi}^{(a)}$, $\hat{\Phi}_a^{(m)}$, $\hat{\Phi}_b^{(m)}$, and $\hat{\Phi}^{(b)}$ with $k^2 = k_x^2 + k_y^2$. These functions have to fulfill the usual magnetic boundary conditions [69]

$$\mathbf{n} \times \mathbf{H}^{(a)} = \mathbf{n} \times \mathbf{H}^{(m)} \tag{B.59}$$

$$\mathbf{n} \cdot \mathbf{B}^{(a)} = \mathbf{n} \cdot \mathbf{B}^{(m)} \tag{B.60}$$

at $z = -d/2$ and

$$\mathbf{n} \times \mathbf{H}^{(m)} = \mathbf{n} \times \mathbf{H}^{(b)} \tag{B.61}$$

$$\mathbf{n} \cdot \mathbf{B}^{(m)} = \mathbf{n} \cdot \mathbf{B}^{(b)} \tag{B.62}$$

at $z = -d/2$. The amplitudes are therefore related to the external magnetic field strength B by

$$\hat{\Phi}^{(a)} = \frac{\mu_b - \mu_a}{\mu_b + \mu_a} \frac{B}{\mu_a} \tag{B.63}$$

$$\hat{\Phi}^{(b)} = \frac{\mu_a - \mu_b}{\mu_b + \mu_a} \frac{B}{\mu_b} \tag{B.64}$$

where the limit $kd \to 0$ has already been taken. The magnetic contributions to the stress tensor

$$T_{ij} = \frac{1}{2} \mathbf{B} \cdot \mathbf{H} \, \delta_{ij} - \frac{1}{2}(B_i H_j + B_j H_i) \tag{B.65}$$

enter the l.h.s. of the normal stress boundary condition (6.22) as

$$T_{zz}^{(a)} - T_{zz}^{(b)} = B \, \partial_z (\Phi^{(a)} - \Phi^{(b)}) \tag{B.66}$$

$$= -B^2 k \frac{(\mu_a - \mu_b)^2}{\mu_a \mu_b (\mu_a + \mu_b)} \xi \tag{B.67}$$

which immediately leads to the magnetic contribution in eq. (6.24) with the coefficient κ_1 given in eq. (6.25).

As we take the limit towards infinitely thin films, the magnetization $\mathbf{M}'$ in the membrane becomes a density per unit area. We therefore introduce the effective surface permeability of the infinitely thin film μ' within the same framework as done for the in-plane elastic moduli in [86] and as derived in section 6.3

$$\mathbf{H}' = \frac{1}{\mu'} \mathbf{B}^{(m)} \tag{B.68}$$

with the effective permeability of the membrane μ' given by $\mu' = \mu_m/d$.

Expanding the magnetic potential in the membrane $\Phi^{(m)}$ (at $z = 0$) in terms of the film thickness d, gives

$$\Phi^{(m)} = \frac{\mu_a + \mu_b - 2\mu_m}{\mu_a + \mu_b} \frac{B}{\mu_m} \xi + \mathcal{O}(d) \tag{B.69}$$

Substituting (B.69) into the expression of the membrane stress tensor $T_{ij}^{(m)}$ yields, after integration over the film thickness and substitution of the expression for the effective membrane permeability, a distortion linear in ξ to the effective film stress tensor $T_{ij}^{(m)}$

$$T_{zj}^{(m)} = -iB^2 \mu'^{-1} k_j \xi + \mathcal{O}(d) \tag{B.70}$$

Taking the divergence of $T_{zj}^{(m)}$ results in the source of normal stress due to the presence of the magnetic membrane in the effective boundary condition (6.22)

$$\partial_j T_{zj}^{(m)} = -B^2 k^2 \mu'^{-1} \xi \tag{B.71}$$

This contribution is always stabilizing. For the case of a large magnetic contrast between the fluids a and b the contribution (B.67) dominates in the limit of vanishing kd and is therefore used in section 6.6.1.

B.5.2 The permanent-magnetic case

Things slightly change, when assuming a membrane made of an anisotropic magnetic gel [14, 15, 91]. We take the intrinsic permanent magnetization $\mathbf{M}_0$ of the initially flat film to be oriented antiparallel to the externally applied magnetic field and assume the same geometry as done for the paramagnetic case (see fig. 6.1 on p. 78). However, the magnetization in the membrane material is fixed and is assumed not to change its magnitude while applying an external magnetic field.

The ground state for the unperturbed flat case with an intrinsic membrane magnetization M_0 and an externally applied field B is given for the surrounding media a and b by ($\alpha \in \{a, b\}$)

$$B_z^{(\alpha)} = B - M_0 \tag{B.72}$$

$$H_z^{(\alpha)} = \frac{1}{\mu_\alpha} B - \frac{1}{\mu_\alpha} M_0 \tag{B.73}$$

$$M_z^{(\alpha)} = \left(1 - \frac{1}{\mu_\alpha}\right) (B - M_0) \tag{B.74}$$

while the situation in the film is defined by

$$B_z = B - M_0 \tag{B.75}$$

$$H_z = B \tag{B.76}$$

The intrinsic magnetization $\mathbf{M}_0$ is anchored rigidly to the membrane, therefore while deforming the film, the magnetization follows as

$$\mathbf{M} = -M_0 \mathbf{e}_z + M_0 \nabla \xi \tag{B.77}$$

The magnetic flux density $\mathbf{B}^{(m)}$ in the membrane is then given by

$$\mathbf{B}^{(m)} = -M_0\mathbf{e}_z + M_0\nabla\xi + \mathbf{H}^{(m)} + B\mathbf{e}_z \tag{B.78}$$

We can split the field $\mathbf{H}^{(m)}$ in the membrane again into a constant undisturbed part, given by eq. (B.76), and a part proportional to the surface deflection ξ. Due to the latter part the static Maxwell equations can be fulfilled, which correspond to the following Poisson equation for the potential $\Phi^{(m)}$ defined by $\mathbf{h}^{(m)} = -\nabla\Phi^{(m)}$

$$\Delta\Phi^{(m)} = M_0\Delta\xi \tag{B.79}$$

whose general solution is given by

$$\Phi^{(m)} = \hat{\Phi}_a^{(m)}e^{kz}\xi + \hat{\Phi}_b^{(m)}e^{-kz}\xi + M_0\xi \tag{B.80}$$

For the distortions in the bulk fluids a and b we assume the same structure as in the superparamagnetic case, fulfilling the Laplace equation. Matching the field disturbances according to the magnetic boundary conditions (B.60) and (B.60) at the two surfaces $z = -d/2$ and $z = d/2$, fixes the amplitudes of the magnetic potential in the three regions.

When performing the limit towards thin films, we have to consider a permanent magnetization with respect to the area M_0', rather than with respect to the volume. Both quantities are related by $M_0 = M_0'/d$ when assuming a homogeneously magnetized bulk material. However, for the actual calculations it is convenient to introduce an effective membrane permeability μ_0'. Due to the definition of M_0', this effective membrane permeability is given by $\mu_0' = 1/d$. Within the limit of vanishing film thickness we then obtain

$$\Phi^{(a)} = -\frac{(B_0 - \mu_0'M_0')(\mu_a - \mu_b)}{\mu_a(\mu_a + \mu_b)}e^{-kz}\xi \tag{B.81}$$

$$\Phi^{(m)} = B(\mu_0')^{-1}\xi \tag{B.82}$$

$$\Phi^{(b)} = \frac{(B_0 - \mu_0'M_0')(\mu_a - \mu_b)}{\mu_b(\mu_a + \mu_b)}e^{kz}\xi \tag{B.83}$$

Evaluation of the right hand side of the boundary condition (6.22) in case of a permanent magnetic film material leads to

$$\partial_j T_{zj}^{(m)} = -(B - \mu_0'M_0')B(\mu_0')^{-1}k^2\xi \tag{B.84}$$

In the limit $d \rightarrow 0$ this expression simplifies to $M_0'Bk^2\xi$, which has been used in the main text, eqs. (6.26,6.27). We realize, that this contribution acts destabilizing if, as we assumed, the intrinsic magnetization and the applied magnetic field are oriented anti-parallel.

The usual magnetic normal stress difference arising from the left hand side of eq. (6.22) turns out to be

$$T_{zz}^{(a)} - T_{zz}^{(b)} = -(B_0 - \mu_0'M_0')^2k\frac{(\mu_a - \mu_b)^2}{\mu_a\mu_b(\mu_a + \mu_b)}\xi \tag{B.85}$$

which again is only non-zero in case of a magnetic contrast between the media a and b. Furthermore it is essentially the same contribution as in eq. (B.67) with the effective field $B_0 - \mu_0'M_0'$.

Appendix C

The hydrodynamic boundary conditions

C.1   Expansion of the boundary conditions

In this section we discuss the expansion of the hydrodynamic boundary conditions in terms of ϵ. Recall first, that we require the tangential stress at the free surface to vanish whereas the normal stress is balanced by surface tension and gravity

$$\mathbf{n} \times \mathrm{T} \cdot \mathbf{n} = \mathbf{n} \times \mathrm{T}^{\mathrm{vac}} \cdot \mathbf{n} \tag{C.1}$$

$$\mathbf{n} \cdot \mathrm{T} \cdot \mathbf{n} - \mathbf{n} \cdot \mathrm{T}^{\mathrm{vac}} \cdot \mathbf{n} = \sigma_T \nabla \cdot \mathbf{n} - \rho G \xi \tag{C.2}$$

The contributions of the stress tensor to the different perturbative orders are defined by the expansions of the macroscopic variables, eqs. (5.1,5.2), and by the expansion of the surface normal $\mathbf{n}$, eq. (B.17). The linear eigenvectors of the hydrodynamic set of equations are either proportional to e^{kz} or e^{qz} (cf. section 3.5). For the boundary conditions one has to evaluate them at $z = \xi$ and therefore an expansion similar to (B.16) is needed that explicitly accounts for the deformability of the surface.

C.2   The linear perturbative order

The boundary conditions in linear order are straightforwardly calculated, but are repeated here for completeness. For the tangential stress boundary condition we obtain

$$2\mu_2 \epsilon_{yz}^{(1)} + \nu_2 \big(\partial_z v_y^{(1)} + \partial_y v_z^{(1)} \big) = 0 \tag{C.3}$$

$$2\mu_2 \epsilon_{xz}^{(1)} + \nu_2 \big(\partial_z v_x^{(1)} + \partial_x v_z^{(1)} \big) = 0 \tag{C.4}$$

whereas the normal stress boundary condition reads

$$2\mu_2 \epsilon_{zz}^{(1)} + 2\nu_2 \partial_z v_z^{(1)} - p^{(1)} + G\rho \xi^{(1)} - \big(\mu H_0 \partial_z \Phi^{(1)} - H_0^{\mathrm{vac}} \partial_z \Phi^{(1)\mathrm{vac}} \big) = \sigma_T \nabla \cdot \mathbf{n}^{(1)} \tag{C.5}$$

In section 3.2 we introduced potentials for the irrotational and the rotational flow contributions. To solve the system of equations for the potentials we have to translate the boundary conditions above to the corresponding ones valid for the potentials. We

start with the tangential boundary conditions. To be able to express the strain field in terms of the gradient of the velocity field (3.9), we first have to take the derivative of eqs. (C.3,C.4) with respect to time. Upon substitution of eqs. (3.11) we end up with

$$\tilde{\mu}_2(\partial_z^2 - \partial_y^2)\Psi_x^{(1)} + \tilde{\mu}_2(\partial_y\partial_x)\Psi_y^{(1)} + 2\tilde{\mu}_2\partial_y\partial_z\varphi^{(1)} = 0 \tag{C.6}$$

$$\tilde{\mu}_2(\partial_x\partial_y)\Psi_x^{(1)} + \tilde{\mu}_2(\partial_z^2 - \partial_x^2)\Psi_y^{(1)} - 2\tilde{\mu}_2\partial_x\partial_z\varphi^{(1)} = 0 \tag{C.7}$$

where the coefficient $(\mu_2 + \nu_2\partial_t^{(0)})$ has been abbreviated by $\tilde{\mu}_2$.

For the normal stress boundary condition we additionally have to discuss the contributions that explicitly contain the surface deflection $\xi^{(1)}$. At a first glance these contributions may be considered as inhomogeneities. However, the deflection $\xi^{(1)}$ is related to the local velocity. Upon taking the time derivative of eq. (C.5) we can substitute the linearized kinematic boundary condition $\partial_t\xi^{(1)} = v_z^{(1)}$. Following the same lines as in the case of the tangential boundary conditions, we find

$$-(2\tilde{\mu}_2\partial_z\partial_y + G\rho\partial_y + \sigma_T k^2\partial_y)\Psi_x^{(1)} + (2\tilde{\mu}_2\partial_z\partial_x + G\rho\partial_x + \sigma_T k^2\partial_x)\Psi_y^{(1)}$$
$$+(2\tilde{\mu}_2\partial_z^2 + G\rho\partial_z + \sigma_T k^2\partial_z)\varphi^{(1)} - \partial_t p^{(1)} - \partial_t\big(H_0\mu\partial_z\Phi^{(1)} - H_0^{\text{vac}}\partial_z\Phi^{(1)\text{vac}}\big) = 0 \tag{C.8}$$

Additionally, we can substitute the solution for the pressure $p^{(1)}$, obtained in section 3.2, and the solutions for the magnetic fields, obtained in appendix B, to finally arrive at

$$-(2\tilde{\mu}_2\partial_z\partial_y + G\rho\partial_y + \sigma_T k^2\partial_y - \frac{\mu}{1+\mu}M_0^2\partial_z\partial_y)\Psi_x^{(1)}$$
$$+(2\tilde{\mu}_2\partial_z\partial_x + G\rho\partial_x + \sigma_T k^2\partial_x - \frac{\mu}{1+\mu}M_0^2\partial_z\partial_x)\Psi_y^{(1)}$$
$$+(2\tilde{\mu}_2\partial_z^2 + G\rho\partial_z + \sigma_T k^2\partial_z - \rho\omega^2 - \frac{\mu}{1+\mu}M_0^2\partial_z^2)\varphi^{(1)} = 0 \tag{C.9}$$

where again the explicit surface deflection $\xi^{(1)}$, arising from the magnetic solutions, has been replaced by the local velocity.

The steps leading to eq. (C.8), where we first took the time derivative of eq. (C.5) to implement afterwards the kinematic boundary condition, are very crucial. By inspection of eq. (C.5) we realize that it is finite in the stationary limit revealing the force balance between elastic, gravitation, magnetic and surface tension forces. Eq. (C.8), however, is at least linear in the time derivative and so are the eigenvectors derived from it. The latter property is in accordance with the understanding that there is no motion in the medium, if the surface pattern is fully developed. These considerations show that, due to the kinematic boundary condition, the bulk equations inherently scale one order higher with respect to the time derivative, when compared with the normal stress boundary condition. This different scaling behavior has to be taken into account, if we combine the solvability conditions from the bulk with those from the normal stress boundary condition (chapter 5).

C.3 The second perturbative order

In the second order we find the tangential boundary conditions involving the hydrodynamic fields as

$$
2\mu_2\epsilon_{xz}^{(2)}+\nu_2\big(\partial_z v_x^{(2)}+\partial_x v_z^{(2)}\big)
$$
$$
= -\xi^{(1)}\partial_z\big[2\mu_2\epsilon_{xz}^{(1)} + \nu_2(\partial_x v_z^{(1)}+\partial_z v_x^{(1)})\big] + (\partial_y\xi^{(1)})\big[2\mu_2\epsilon_{yz}^{(1)} + \nu_2(\partial_y v_x^{(1)}+\partial_x v_y^{(1)})\big]
$$
$$
-2(\partial_x\xi^{(1)})\big[\mu_2(\epsilon_{zz}^{(1)} + \epsilon_{xx}^{(1)}) + \nu_2(\partial_z v_z^{(1)} + \partial_x v_x^{(1)})\big] + \rho v_x^{(1)}v_z^{(1)} \equiv \Omega_{xz}^{(2)} \qquad (C.10)
$$

$$
2\mu_2\epsilon_{yz}^{(2)}+\nu_2\big(\partial_z v_y^{(2)}+\partial_y v_z^{(2)}\big)
$$
$$
= -\xi^{(1)}\partial_z\big[2\mu_2\epsilon_{yz}^{(1)} + \nu_2(\partial_y v_z^{(1)}+\partial_z v_y^{(1)})\big] + (\partial_x\xi^{(1)})\big[2\mu_2\epsilon_{xy}^{(1)} + \nu_2(\partial_x v_y^{(1)}+\partial_y v_x^{(1)})\big]
$$
$$
-2(\partial_y\xi^{(1)})\big[\mu_2(\epsilon_{zz}^{(1)} + \epsilon_{yy}^{(1)}) + \nu_2(\partial_z v_z^{(1)} + \partial_y v_y^{(1)})\big] + \rho v_y^{(1)}v_z^{(1)} \equiv \Omega_{yz}^{(2)} \qquad (C.11)
$$

In eqs. (C.11) and (C.10) the inhomogeneities on the right hand side have been abbreviated by $\Omega_{xz}^{(2)}$ and $\Omega_{yz}^{(2)}$, respectively. In particular these inhomogeneities are proportional to $[\xi^{(1)}]^2$.

The normal stress boundary condition (C.2) reads in second order

$$
2\mu_2\epsilon_{zz}^{(2)} + 2\nu_2\partial_z v_z^{(2)} - p^{(2)} + G\rho\xi^{(2)} - \mu H_c\partial_z\Phi^{(2)} + H_c^{\mathrm{vac}}\partial_z\Phi^{(2)\mathrm{vac}}
$$
$$
= -2\mu_2[\epsilon_{zz}^{(1)}]^2 + \rho[v_z^{(1)}]^2 - M_c B_c\big[(\partial_y\xi^{(1)})^2 + (\partial_x\xi^{(1)})^2\big] - \frac{1}{2}\mu\big(\partial_z\Phi^{(1)}\big)^2
$$
$$
+ \frac{1}{2}\big(\partial_z\Phi^{(1)\mathrm{vac}}\big)^2 - 2\mu H_c(\partial_y\xi^{(1)})(\partial_y\Phi^{(1)}) + 2H_c^{\mathrm{vac}}(\partial_y\xi^{(1)})(\partial_y\Phi^{(1)\mathrm{vac}})
$$
$$
+ \frac{1}{2}\mu(\partial_y\Phi^{(1)})^2 - \frac{1}{2}(\partial_y\Phi^{(1)\mathrm{vac}})^2 + \frac{1}{2}\mu(\partial_x\Phi^{(1)})^2 - \frac{1}{2}(\partial_x\Phi^{(1)\mathrm{vac}})^2
$$
$$
- 2\mu H_c(\partial_x\xi^{(1)})(\partial_x\Phi^{(1)}) + 2H_c^{\mathrm{vac}}(\partial_x\xi^{(1)})(\partial_x\Phi^{(1)\mathrm{vac}})
$$
$$
+ \xi^{(1)}\partial_z\Big(2\mu_2\epsilon_{zz}^{(1)} + 2\nu_2\partial_z v_z^{(1)} - p^{(1)} - \frac{\mu}{1+\mu}M_c^2 k\xi^{(1)}\Big) + \frac{\mu}{1+\mu}M^{(1)}M_c k_c\xi^{(1)}
$$
$$
- \sigma_T\Delta\xi^{(2)} \qquad (C.12)
$$

Furthermore, we obtain for the kinematic boundary condition in second order

$$
\partial_t^{(0)}\xi^{(2)} + \partial_t^{(1)}\xi^{(1)} + (\mathbf{v}^{(1)}\cdot\nabla)\xi^{(1)} = v_z^{(2)} + \xi^{(1)}\partial_z v_z^{(1)} \qquad (C.13)
$$

The physical boundary is at $z = \xi$, giving rise to an additional dependence on ξ. In eqs. (C.11-C.13) such terms have already been made explicit (e.g. the last one of (C.13)). Thus these boundary conditions are effective ones that have to be taken at $z = 0$.

Inspecting the expressions (C.12) and (C.13) one immediately realizes that two qualitatively different contributions are present. On the one hand we obtain contributions proportional to the higher harmonic coupling $[\xi^{(1)}]^2$ of the main characteristic mode. On the other hand, there are still contributions proportional to the main characteristic mode $\xi^{(1)}$ itself. The latter will allow us to find the linear contributions in an amplitude equation even though the control parameter is not present in the bulk equations.

To solve the corresponding hydrodynamic bulk equations, we introduced a scalar, $\varphi^{(2)}$, and a vector potential, $\mathbf{\Psi}^{(2)}$, in section 5.3, to discuss potential and rotational flow contributions separately. Following the same lines as done in the linear order (section C.2), we can translate the boundary conditions into a corresponding set of equations for

the amplitudes of the second order potentials $\varphi^{(2)}$ and $\mathbf{\Psi}^{(2)}$. We obtain for the tangential contributions (C.11) and (C.10)

$$\tilde{\mu}_2(\partial_z^2 - \partial_y^2)\Psi_x^{(2)} + \tilde{\mu}_2(\partial_y\partial_x)\Psi_y^{(2)} + 2\tilde{\mu}_2\partial_y\partial_z\varphi^{(2)} = 2\mu_2 v_k^{(1)}\partial_k\epsilon_{yz}^{(1)} + \partial_t^{(0)}\Omega_{yz}^{(2)} \quad \text{(C.14)}$$

$$-\tilde{\mu}_2(\partial_x\partial_y)\Psi_x^{(2)} - \tilde{\mu}_2(\partial_z^2 - \partial_x^2)\Psi_y^{(2)} + 2\tilde{\mu}_2\partial_x\partial_z\varphi^{(2)} = 2\mu_2 v_k^{(1)}\partial_k\epsilon_{xz}^{(1)} + \partial_t^{(0)}\Omega_{xz}^{(2)} \quad \text{(C.15)}$$

using $\epsilon_{xz}^{(1)} = \epsilon_{yz}^{(1)} \equiv 0$ at the boundary (cf. eqs. (C.3,C.4)). The normal stress boundary condition (C.12) translates into

$$-(2\tilde{\mu}_2\partial_y\partial_z + \rho G\partial_y)\Psi_x^{(2)} + (2\tilde{\mu}_2\partial_z\partial_x + \rho G\partial_x)\Psi_y^{(2)} + (2\tilde{\mu}_2\partial_z^2 + \rho G\partial_z)\varphi^{(2)} - \partial_t^{(0)}p^{(2)}$$

$$= \partial_t^{(0)}\left(H_c\mu\partial_z\Phi^{(2)} - H_c^{\text{vac}}\partial_z\Phi^{(2)\text{vac}}\right) + M^{(1)}M_ck_c\frac{\mu}{1+\mu}\partial_t^{(0)}\xi^{(1)} + \partial_t^{(0)}\Omega_{zz}^{(2)}$$

$$+2\mu_2 v_k^{(1)}\partial_k\epsilon_{zz}^{(1)} - 2\rho G\xi^{(1)}\partial_z v_z^{(1)} + \rho G\partial_t^{(1)}\xi^{(1)} + 2\mu_2\partial_t^{(1)}\epsilon_{zz}^{(1)} - \sigma_T\partial_t^{(0)}\Delta\xi^{(2)} \quad \text{(C.16)}$$

Eqs. (C.14-C.16) follow from (C.11-C.12) by taking the time derivative with respect to $t^{(0)}$ without loss of generality. This is why in eq. (C.16) only the contribution $\partial_t^{(0)}p^{(2)}$ and no contribution $\partial_t^{(1)}p^{(1)}$ arises, while $\partial_t^{(0)}\epsilon_{ij}^{(2)}$ gives rise to contributions $\sim v_i^{(2)}$ and $\sim \partial_t^{(1)}\epsilon_{ij}^{(1)}$ (cf. eq. (5.58)).

C.4 The third perturbative order

We take over the procedure of the previous section to the third order. If we use the solutions (5.81,5.85,5.87) of the hydrodynamic bulk equations in second order, the kinematic boundary condition reads

$$\partial_t^{(0)}\xi^{(3)} + \partial_t^{(1)}\xi^{(2)} + \partial_t^{(2)}\xi^{(1)} + (\mathbf{v}^{(1)}\cdot\nabla)\xi^{(2)} + (\mathbf{v}^{(2)}\cdot\nabla)\xi^{(1)} \quad \text{(C.17)}$$

$$= v_z^{(3)} + \xi^{(1)}\partial_z v_z^{(2,2)} + \xi^{(1)}\partial_z v_z^{(2,1)\text{hom}} - \frac{\mu_2+\tilde{\mu}_2}{q\tilde{\mu}_2}k_c^2\xi^{(1)}\partial_t^{(1)}\xi^{(1)} + \xi^{(2)}\partial_z v_z^{(1)} + \frac{1}{2}\xi^{(1)2}\partial_z^2 v_z^{(1)}$$

The tangential boundary conditions are of the usual structure and given as

$$2\mu_2\epsilon_{yz}^{(3)} + \nu_2\left(\partial_z v_y^{(3)} + \partial_y v_z^{(3)}\right) = \Omega_{yx}^{(3)} \quad \text{(C.18)}$$

$$2\mu_2\epsilon_{yz}^{(3)} + \nu_2\left(\partial_z v_y^{(3)} + \partial_y v_z^{(3)}\right) = \Omega_{xz}^{(3)} \quad \text{(C.19)}$$

where inhomogeneous contributions, which are at least proportional to the higher harmonic couplings, are collected in the abbreviation $\Omega_{ij}^{(3)}$, as done similarly in second order. The only reason why we have to consider the third order boundary conditions is to obtain the linear contributions to the amplitude equation. The general solution involving the higher harmonic couplings is not needed. Since $\Omega_{ij}^{(3)}$ is at least proportional to the higher harmonic couplings it is therefore unimportant in this discussion and is not shown here. Taking the time derivative of eqs. (C.18,C.19) together with (5.118) we find

$$\tilde{\mu}_2(\partial_z^2 - \partial_y^2)\Psi_x^{(3)} + \tilde{\mu}_2(\partial_y\partial_x)\Psi_y^{(3)} + 2\tilde{\mu}_2\partial_y\partial_z\varphi^{(3)} = \partial_t^{(0)}\Omega_{yx}^{(3)} + 2\mu_2(\partial_t^{(1)}\epsilon_{yz}^{(2)} + \partial_t^{(2)}\epsilon_{yz}^{(1)})$$

$$+2\mu_2(v_k^{(1)}\partial_k\epsilon_{yz}^{(2)} + v_k^{(2)}\partial_k\epsilon_{yz}^{(1)}) \quad \text{(C.20)}$$

$$-\tilde{\mu}_2(\partial_x\partial_y)\Psi_x^{(3)} - \tilde{\mu}_2(\partial_z^2 - \partial_x^2)\Psi_y^{(3)} + 2\tilde{\mu}_2\partial_x\partial_z\varphi^{(3)} = \partial_t^{(0)}\Omega_{xz}^{(3)} + 2\mu_2(\partial_t^{(1)}\epsilon_{xz}^{(2)} + \partial_t^{(2)}\epsilon_{xz}^{(1)})$$

$$+2\mu_2(v_k^{(1)}\partial_k\epsilon_{xz}^{(2)} + v_k^{(2)}\partial_k\epsilon_{xz}^{(1)}) \quad \text{(C.21)}$$

For the normal stress boundary condition we obtain from eq. (C.2)

$$
\begin{aligned}
2\mu_2\epsilon_{zz}^{(3)} + 2\nu_2(\partial_z v_z^{(3)}) &- p^{(3)} + \rho G\xi^{(3)} - (\mu H_c\partial_z\Phi^{(3)} - H_c^{\text{vac}}\partial\Phi^{(3)\text{vac}}) \\
&= (\mu H^{(2)}\partial_z\Phi^{(1)} - H^{(2)\text{vac}}\partial_z\Phi^{(1)\text{vac}}) + (\mu H^{(1)}\partial_z\Phi^{(2)} - H^{(1)\text{vac}}\partial_z\Phi^{(2)\text{vac}}) \\
&\quad + \Omega_{zz}^{(3)} + \sigma_T\nabla\cdot\mathbf{n}^{(3)}
\end{aligned}
\tag{C.22}
$$

which by a similar procedure can be written as

$$
\begin{aligned}
-(2\tilde{\mu}_2\partial_z\partial_y + \rho G\partial_y)\Psi_x^{(3)} &+ (2\tilde{\mu}_2\partial_z\partial_x + \rho G\partial_x)\Psi_y^{(3)} + (2\tilde{\mu}_2\partial_z^2 + \rho G\partial_z)\varphi^{(3)} - \partial_t^{(0)}p^{(3)} \\
&= (\mu H_c\partial_z\Phi^{(3)} - H_c^{\text{vac}}\partial_z\Phi^{(3)\text{vac}}) + \frac{\mu}{1+\mu}(M_cM^{(2)} + M^{(1)2})k_c\partial_t^{(0)}\xi^{(1)} + \partial_t^{(0)}\Omega_{zz}^{(3)} \\
&\quad + \rho G(\partial_t^{(2)}\xi^{(1)} + \partial_t^{(1)}\xi^{(2)} + v_k^{(2)}\partial_k\xi^{(1)} - \xi^{(1)}\partial_z v_z^{(2)} - \xi^{(2)}\partial_z v_z^{(1)} - \frac{1}{2}\xi^{(1)2}\partial_z^2 v_z^{(1)}) \\
&\quad + 2\mu_2(\partial_t^{(2)}\epsilon_{zz}^{(1)} + \partial_t^{(1)}\epsilon_{zz}^{(2)} + (v_k^{(1)}\partial_k)\epsilon_{zz}^{(2)} + (v_k^{(2)}\partial_k)\epsilon_{zz}^{(1)}) + \sigma_T\partial_t^{(0)}\nabla\cdot\mathbf{n}^{(3)}
\end{aligned}
\tag{C.23}
$$

Appendix D

Eigenvectors in the second order

In this appendix we give the contributions to the eigenvectors in the second perturbative order that are proportional to the higher harmonic couplings $\xi^{(2)}$. Due to the fact that we have to treat the system dynamically throughout all orders, the expressions become tedious and have therefore been calculated with *Mathematica*. In the following the solutions for the hydrodynamic potentials are represented for the patterns under consideration, hexagons ($\theta_{ij} = 2\pi/3$), squares ($\theta_{ij} = \pi/2$) and stripes ($\theta_{ij} = 0$) as well as for the interaction between hexagons and squares ($\theta_{ij} = \pi/6$) (cf. fig. 5.2 on p. 59).

The inhomogeneous contributions to the vector potential, cf. eq. (5.98), separate into a contribution $\sim e^{(k_c+q)z}$ and $\sim e^{2qz}$. For the hexagonal case ($ij = ji = 12 = 23 = 31$) we obtain

$$\Psi_{NMij}^{\text{inhom}}(z) = \frac{(k_c^2 + q^2)(2\mu_2 q^2 - 5\mu_2 qk_c + \rho[D_t^{(0)}]^2)}{2q(k_c^2 - q^2)(2k_c q\tilde{\mu}_2 + q^2\tilde{\mu}_2 - \rho[D_t^{(0)}]^2)} e^{(k_c+q)z} D_t^{(0)}$$
$$+ \frac{3k_c^2 q(\mu_2 k_c^2 + 2\mu_2 q^2 - \rho[D_t^{(0)}]^2)}{(k_c^4 - 5k_c^2 q^2 + 4q^4)(\tilde{\mu}_2 k_c^2 - 4\tilde{\mu}_2 q^2 + \rho[D_t^{(0)}]^2)} e^{2qz} D_t^{(0)} \qquad \text{(D.1)}$$

with $\{N, M\} \in \{R, L\}$. The abbreviation $D_t^{(0)}$ stands for $2i\omega^{(0)} + 2\sigma^{(0)}$, $2\sigma^{(0)}$, and $-2i\omega^{(0)} + 2\sigma^{(0)}$ for $N = M = R$, $N \neq M$, and $N = M = L$, respectively. The second coefficient $\tilde{\Psi}_{NMij}^{\text{inhom}}$ reads

$$\tilde{\Psi}_{NMij}^{\text{inhom}}(z) = \frac{(k_c^2+q^2)(6k_c^3\mu_2 - 10k_c^2 q\mu_2 + k_c q^2\mu_2 + 2q^3\mu_2 + q\rho[D_t^{(0)}]^2)}{2(2k_c^4 - 2k_c^3 q - 3k_c^2 q^2 + 2k_c q^3 + q^4)(2k_c^2\tilde{\mu}_2 - 2k_c q\tilde{\mu}_2 - q^2\tilde{\mu}_2 + \rho[D_t^{(0)}]^2)} e^{(k_c+q)z} D_t^{(0)}$$
$$- \frac{k_c^2 q(k_c^2\mu_2 - 2q^2\mu_2 + \rho[D_t^{(0)}]^2)}{(3k_c^4 - 7k_c^2 q^2 + 4q^4)(3k_c^2\tilde{\mu}_2 - 4q^2\tilde{\mu}_2 + 2\rho[D_t^{(0)}]^2)} e^{2qz} D_t^{(0)} \qquad \text{(D.2)}$$

For the square pattern we get ($ij = ji = 15$)

$$\Psi_{NMij}^{\text{inhom}}(z) = \frac{(k_c^2+q^2)(4\mu_2 k_c^3 - 10\mu_2 qk_c^2 + 2\mu_2 q^3 + (k_c+q)\rho[D_t^{(0)}]^2)}{2(k_c^4 - 2qk_c^3 - 2k_c^2 q^2 + 2k_c q^3 + q^4)(\tilde{\mu}_2 k_c^2 - 2\tilde{\mu}_2 qk_c - \tilde{\mu}_2 q^2 + \rho[D_t^{(0)}]^2)} e^{(q+k_c)z} D_t^{(0)}$$
$$+ \frac{qk_c^2(2\mu_2 q^2 - \rho[D_t^{(0)}]^2)}{4(k_c^4 - 3q^2 k_c^2 + 2q^4)(2\tilde{\mu}_2 k_c^2 - 4\tilde{\mu}_2 q^2 + \rho[D_t^{(0)}]^2)} e^{2qz} D_t^{(0)} \qquad \text{(D.3)}$$
$$= \tilde{\Psi}_{NMij}^{\text{inhom}}(z) \qquad \text{(D.4)}$$

For the stripe geometry, $i = j$, we obtain

$$\Psi_{NMij}^{\text{inhom}}(z) = \frac{(k_c^2+q^2)\big(6k_c^2\mu_2-4k_cq\mu_2-2q^2\mu_2-\rho[D_t^{(0)}]^2\big)}{2(k_c-q)(3k_c^2+4k_cq+q^2)\big(3k_c^2\tilde{\mu}_2-2k_cq\tilde{\mu}_2-q^2\tilde{\mu}_2+2\rho[D_t^{(0)}]^2\big)}e^{(k_c+q)z}D_t^{(0)} \quad \text{(D.5)}$$

and

$$
\begin{aligned}
\tilde{\Psi}_{NMij}^{\text{inhom}}(z) &= \frac{k_c^2\big[4k_c^4\mu_2 - 4q^2(2q^2\mu_2 - \rho[D_t^{(0)}]^2) - k_c^2(20q^2\mu_2 + 3\rho[D_t^{(0)}]^2)\big]}{4(k_c^2-q^2)^2(4q^3\tilde{\mu}_2 + q\rho[D_t^{(0)}]^2)}e^{2qz}D_t^{(0)} \\
&\quad + Z_1\Big[4(k_c-q)^2(k_c+q)^3\big(k_c^2\tilde{\mu}_2+2k_cq\tilde{\mu}_2+q^2\tilde{\mu}_2-2\rho[D_t^{(0)}]^2\big)\Big]^{-1}e^{(k_c+q)z}D_t^{(0)} \quad \text{(D.6)}
\end{aligned}
$$

with the numerator Z_1 being given by

$$
\begin{aligned}
Z_1 &= (k_c^2+q^2)\Big(24k_c^3q\mu_2-4q^4\mu_2-2q^2\rho[D_t^{(0)}]^2+20k_c^2q^2\mu_2+3k_c^2\rho[D_t^{(0)}]^2\Big) \\
&\quad +8k_cq^3\mu_2-4k_cq\rho[D_t^{(0)}]^2 \quad \text{(D.7)}
\end{aligned}
$$

In addition, to describe the interaction between the square and the hexagonal pattern, we need to consider also the case $\theta_{ij} = \pi/6$, $(ij = ji = 14 = 36 = 25)$

$$
\begin{aligned}
\Psi_{NMij}^{\text{inhom}}(z) = N_1^{-1}\Big\{ &(k_c^2+q^2)(2q^3\mu_2-10k_c^2q\mu_2+k_c^2\mu_2(1+3\sqrt{3})+q\rho[D_t^{(0)}]^2 \quad \text{(D.8)} \\
&+\sqrt{3}k_cq^2\mu_2+k_c(1-\sqrt{3})\rho[D_t^{(0)}]^2)\Big\}\,e^{(k_c+q)z}D_t^{(0)} \\
&-\frac{k_c^2q(k_c^2\mu_2(2\sqrt{3}-3)-2(2-\sqrt{3})(q^2\mu_2-\rho[D_t^{(0)}]^2))}{((2+\sqrt{3})k_c^2-4q^2)(k_c^2-q^2)((2+\sqrt{3})k_c^2\tilde{\mu}_2-(4q^2\tilde{\mu}_2-2\rho[D_t^{(0)}]^2))}e^{2qz}D_t^{(0)}
\end{aligned}
$$

where the denominator N_1 is given by

$$
\begin{aligned}
N_1 &= 2(k_c^2-q^2)\Big\{2(2+\sqrt{3})k_c^4\tilde{\mu}_2-4(1+\sqrt{3})k_c^3q\tilde{\mu}_2+q^4\tilde{\mu}_2-q^2\rho(D_t^{(0)})^2 \\
&\quad +k_c^2\big[(1+\sqrt{3})\rho[D_t^{(0)}]^2+2(1-\sqrt{3})q^2\tilde{\mu}_2\big]+4k_cq^3\tilde{\mu}_2-2k_cq\rho[D_t^{(0)}]^2\Big\} \quad \text{(D.9)}
\end{aligned}
$$

and

$$
\begin{aligned}
\tilde{\Psi}_{NMij}^{\text{inhom}}(z) &= \frac{(3+2\sqrt{3})k_c^2\mu_2+(2+\sqrt{3})(2q^2\mu_2-\rho[D_t^{(0)}]^2)}{(k_c^2-q^2)\big[(\sqrt{3}-2)k_c^2+4q^2\big]\big[(\sqrt{3}-2)k_c^2\tilde{\mu}_2+4q^2\tilde{\mu}_2-\rho[D_t^{(0)}]^2\big]}qk_c^2e^{2qz}D_t^{(0)} \\
&\quad -N_2^{-1}\Big\{(k_c^2+q^2)\big[(3\sqrt{3}-1)k_c^3\mu_2+10k_c^2q\mu_2-2q^3\mu_2 \\
&\qquad -2q\rho[D_t^{(0)}]^2+k_c\sqrt{3}q^2\mu_2-k_c[1+\sqrt{3}]\rho[D_t^{(0)}]^2\big]\Big\}\,e^{(k_c+q)z}D_t^{(0)} \quad \text{(D.10)}
\end{aligned}
$$

with

$$
\begin{aligned}
N_2 &= 2(k_c^2-q^2)\Big[2(2-\sqrt{3})k_c^4\tilde{\mu}_2+4(\sqrt{3}-1)k_c^3q\tilde{\mu}_2+q^4\tilde{\mu}_2-q^2\rho[D_t^{(0)}]^2 \\
&\quad +2k_c^2[1+\sqrt{3}]q^2\tilde{\mu}_2+k_c^2[1-\sqrt{3}]\rho[D_t^{(0)}]^2+4k_cq^3\tilde{\mu}_2-qk_c\rho[D_t^{(0)}]^2\Big] \quad \text{(D.11)}
\end{aligned}
$$

For the scalar potential we obtain from eq. (5.109) in the geometry of hexagons ($ij = ji = 12 = 23 = 31$)

$$\hat{\varphi}_{NMij} = \left[8\rho[D_t^{(0)}]^2 k_c q(q+k_c)(k_c^2-4q^2)\right]^{-1}\left\{2k_c^5 q(12\tilde{\mu}_2-14\mu_2-3\nu_2 D_t^{(0)})-12q^4\rho[D_t^{(0)}]^2\right.$$
$$+2k_c^4\left(4\tilde{\mu}_2 q^2-16\mu_2 q^2+\nu_2 q^2 D_t^{(0)}+2\rho[D_t^{(0)}]^2\right)$$
$$+k_c^2\left(19q^2\rho[D_t^{(0)}]^2+8q^4[4\tilde{\mu}_2+4\mu_2+\nu_2]D_t^{(0)}\right)$$
$$-4k_c\left(9q^3\rho[D_t^{(0)}]^2-4q^5[3\mu_2+\nu_2 D_t^{(0)}]\right)$$
$$\left.+k_c^3\left(17q\rho[D_t^{(0)}]^2-96\tilde{\mu}_2 q^3+52\mu_2 q^3+20q^3\nu_2 D_t^{(0)}\right)\right\} D_t^{(0)} \tag{D.12}$$

and for the case of squares ($ij = ji = 15$)

$$\hat{\varphi}_{NMij} = \left[4\sqrt{2}\rho[D_t^{(0)}]^2 k_c(k_c+q)(k_c^2-2q^2)(k_c^2-2k_c q-q^2)\right]^{-1}\left\{4k_c^7(6\tilde{\mu}_2-7\mu_2-2\nu_2 D_t^{(0)})\right.$$
$$+2q^5\rho[D_t^{(0)}]^2-4k_c^6 q(10\tilde{\mu}_2-14\mu_2-5\nu_2 D_t^{(0)})$$
$$+k_c^2\left(16q^5\tilde{\mu}_2-16q^5\mu_2-8q^5\nu_2 D_t^{(0)}+9q^3\rho[D_t^{(0)}]^2\right)$$
$$+2k_c\left(5q^4\rho[D_t^{(0)}]^2-4q^6(3\mu_2+\nu_2 D_t^{(0)})\right)+k_c^5\left(3\rho[D_t^{(0)}]^2-4q^2[22\tilde{\mu}_2-14\mu_2-3\nu_2 D_t^{(0)}]\right)$$
$$-k_c^3\left(35q^2\rho[D_t^{(0)}]^2-4q^4[20\tilde{\mu}_2+15\mu_2+3\nu_2 D_t^{(0)}]\right)$$
$$\left.-k_c^4\left(13q\rho[D_t^{(0)}]^2-4q^3[18\tilde{\mu}_2-22\mu_2-9\nu_2 D_t^{(0)}]\right)\right\} D_t^{(0)} \tag{D.13}$$

For stripes ($i = j$) we obtain

$$\hat{\varphi}_{NMij} = \left[(k_c-q)(k_c+q)(3k_c+q)\rho[D_t^{(0)}]^2\right]^{-1}\left\{2k_c(2k_c-q)\rho[D_t^{(0)}]^2\right.$$
$$+(k_c-q)(3k_c+q)\left[k_c^2(6\tilde{\mu}_2-7\mu_2)-3q^2\mu_2+2k_c q(\tilde{\mu}_2+2\mu_2)\right]$$
$$\left.-\nu_2(k_c-q)(3k_c+q)(3k_c^2-2k_c q+q^2)D_t^{(0)}\right\} D_t^{(0)} \tag{D.14}$$

For $\theta_{ij} = \pi/6$, ($ij = ji = 14 = 36 = 25$) we obtain

$$\hat{\varphi}_{NMij} = -D_t^{(0)} N_3^{-1} \Big\{ 4k_c^{10} q\tilde{\mu}_2 \Big[4(329+190\sqrt{3})\tilde{\mu}_2 - 4(677+391\sqrt{3})\mu_2 + 7\nu_2(168+97\sqrt{3})D_t^{(0)} \Big]$$

$$- 4k_c^{11}\tilde{\mu}_2^2 \Big[12(97+56\sqrt{3})\tilde{\mu}_2 - 14(97+56\sqrt{3})\mu_2 - \nu_2(556+321\sqrt{3})D_t^{(0)} \Big]$$

$$+ 4(\sqrt{3}-2)q^5\rho[D_t^{(0)}]^2(4q^2\tilde{\mu}_2 - \rho[D_t^{(0)}]^2)(q^2\tilde{\mu}_2 - \rho[D_t^{(0)}]^2)$$

$$- k_c^2 q^3 \Big[(99+4\sqrt{3})\rho^3[D_t^{(0)}]^6 - q^2\rho^2[D_t^{(0)}]^4(7(73-8\sqrt{3})\tilde{\mu}_2 + 32(2+\sqrt{3})\mu_2 + 8\nu_2 D_t^{(0)})$$

$$- 16q^6\tilde{\mu}_2(16(2+\sqrt{3})\mu_2 - 4(2+\sqrt{3})\tilde{\mu}_2 + \nu_2(9+4\sqrt{3})D_t^{(0)})$$

$$+ 8q^4\rho[D_t^{(0)}]^2\tilde{\mu}_2((51-40\sqrt{3})\tilde{\mu}_2 + 32(2+\sqrt{3})\mu_2 + \nu_2(13+4\sqrt{3})D_t^{(0)}) \Big]$$

$$+ k_c^3 q^2 \Big[(113+76\sqrt{3})\rho^3[D_t^{(0)}]^6$$

$$- 32q^6\tilde{\mu}_2^2(28(2+\sqrt{3})\tilde{\mu}_2 + (71+42\sqrt{3})\mu_2 + 2\nu_2(14+9\sqrt{3})D_t^{(0)})$$

$$- q^2\rho^2[D_t^{(0)}]^4((687+552\sqrt{3})\tilde{\mu}_2 + 4(93+52\sqrt{3})\mu_2 + 4\nu_2(33+20\sqrt{3})D_t^{(0)})$$

$$+ 2q^4\rho[D_t^{(0)}]^2\tilde{\mu}_2(2(334+304\sqrt{3})\tilde{\mu}_2 + 2(577+328\sqrt{3})\mu_2 + \nu_2(418+256\sqrt{3})D_t^{(0)}) \Big]$$

$$+ k_c^4 q \Big[(61+27\sqrt{3})\rho^3[D_t^{(0)}]^6$$

$$- 16q^6\tilde{\mu}_2(4(37+16\sqrt{3})\tilde{\mu}_2 + 4(29+16\sqrt{3})\mu_2 + \nu_2(2+5\sqrt{3})D_t^{(0)})$$

$$- q^2\rho^2[D_t^{(0)}]^4(51(20+11\sqrt{3})\tilde{\mu}_2 - 8(83+48\sqrt{3})\mu_2 - 2\nu_2(162+91\sqrt{3})D_t^{(0)})$$

$$+ q^4\rho D_t^{(0)}\tilde{\mu}_2(9(326+183\sqrt{3})\tilde{\mu}_2 - 16(137+80\sqrt{3})\mu_2 - 2\nu_2(666+367\sqrt{3})D_t^{(0)}) \Big]$$

$$+ 2k_c^3\tilde{\mu}_2 \Big[2q^2\tilde{\mu}_2(4(823+475\sqrt{3})\tilde{\mu}_2 - 2(742+429\sqrt{3})\mu_2 - \nu_2(577+333\sqrt{3})D_t^{(0)})$$

$$- \rho[D_t^{(0)}]^4((1989+1148\sqrt{3})\tilde{\mu}_2 - 14(123+71\sqrt{3})\mu_2 - \nu_2(705+407\sqrt{3})D_t^{(0)}) \Big]$$

$$- k_c^5 \Big[(99+59\sqrt{3})\rho^3[D_t^{(0)}]^6$$

$$- q^2\rho^2[D_t^{(0)}]^4((1128+1143\sqrt{3})\tilde{\mu}_2 - 4(80+43\sqrt{3})\mu_2 - 6\nu_2(22+13\sqrt{3})D_t^{(0)})$$

$$+ q^4\rho[D_t^{(0)}]^2\tilde{\mu}_2((6710+4079\sqrt{3})\tilde{\mu}_2 + 4(523+319\sqrt{3})\mu_2 + 2\nu_2(432+239\sqrt{3})D_t^{(0)})$$

$$- 4q^6\tilde{\mu}_2(16(101+64\sqrt{3})\tilde{\mu}_2 + (2462+1441\sqrt{3})\mu_2 + \nu_2(1082+611\sqrt{3})D_t^{(0)}) \Big]$$

$$+ 2k_c^8 q\tilde{\mu}_2 \Big[2q^2\tilde{\mu}_2(4(841+487\sqrt{3})\tilde{\mu}_2 - 4(1449+838\sqrt{3})\mu_2 - 5\nu_2(521+301\sqrt{3})D_t^{(0)})$$

$$- \rho[D_t^{(0)}]^2((1693+980\sqrt{3})\tilde{\mu}_2 - 4(676+391\sqrt{3})\mu_2 - \nu_2(1193+689\sqrt{3})D_t^{(0)}) \Big]$$

$$+ k_c^7 \Big[2q^2\rho[D_t^{(0)}]^2\tilde{\mu}_2((4601+2657\sqrt{3})\tilde{\mu}_2 - 2(823+482\sqrt{3})\mu_2 - 15\nu_2(45+26\sqrt{3})D_t^{(0)})$$

$$- \rho^2[D_t^{(0)}]^4(9(123+71\sqrt{3})\tilde{\mu}_2 - 28(19+11\sqrt{3})\mu_2 - 2\nu_2(109+63\sqrt{3})D_t^{(0)})$$

$$- 2q^4\tilde{\mu}_2(4(1702+985\sqrt{3})\tilde{\mu}_2 + 14(268+151\sqrt{3})\mu_2 + \nu_2(1675+966\sqrt{3})D_t^{(0)}) \Big]$$

$$+ k_c^6 q \Big[\rho^2[D_t^{(0)}]^4((727+425\sqrt{3})\tilde{\mu}_2 - 8(85+48\sqrt{3})\mu_2 - 2\nu_2(151+87\sqrt{3})D_t^{(0)})$$

$$+ 2q^4\tilde{\mu}_2(4(1302+769\sqrt{3})\tilde{\mu}_2 - 8(730+413\sqrt{3})\mu_2 - \nu_2(2945+1712\sqrt{3})D_t^{(0)})$$

$$- q^2\rho[D_t^{(0)}]^2\tilde{\mu}_2(10(633+373\sqrt{3})\tilde{\mu}_2 - 8(1042+593\sqrt{3})\mu_2 - \nu_2(3838+2220\sqrt{3})D_t^{(0)}) \Big]$$

$$+ 4k_c q^4(4q^2\tilde{\mu}_2 - \rho D_t^{(0)}) \Big[12(2+\sqrt{3})q^2\tilde{\mu}_2(q^2\tilde{\mu}_2 - \rho D_t^{(0)})$$

$$+ 4\nu_2 D_t^{(0)}(2+\sqrt{3})q^2(q^2\tilde{\mu}_2 - \rho D_t^{(0)}) - (\sqrt{3}-2)\rho[D_t^{(0)}]^2(7q^2\tilde{\mu}_2 - 5\rho[D_t^{(0)}]^2) \Big] \Big\} \quad \text{(D.15)}$$

with the denominator N_3 given by

$$
\begin{aligned}
N_3 = {}& 8\sqrt{2+\sqrt{3}}\,k_c(k_c+q)\big((2+\sqrt{3})k_c^2-4q^2\big) \\
& \times\Big[\Big(2(2+\sqrt{3})k_c^4-4(1+\sqrt{3})k_c^3q-2(\sqrt{3}-1)k_c^2q^2+4k_cq^3+q^4\Big)\tilde{\mu}_2 \\
& \quad +\Big((1+\sqrt{3})k_c^2-2k_cq-q^2\Big)\rho[D_t^{(0)}]^2\Big]\Big[(2+\sqrt{3})k_c^2\tilde{\mu}_2-(4q^2\tilde{\mu}_2-\rho D_t^{(0)})\Big]\rho[D_t^{(0)}]^2
\end{aligned}
\tag{D.16}
$$

The homogeneous contributions to the vector potential follow from eq. (5.108). The solutions for hexagons ($ij = ji = 12 = 23 = 31$) read

$$
\begin{aligned}
\hat{\Psi}^{\text{hom}}_{NMij} = {}& \Big[8k_c^2(k_c+q)\rho[D_t^{(0)}]^2\big(\rho[D_t^{(0)}]^2-q(2k_c+q)\big)\big(\tilde{\mu}_2 k_c^2-4\tilde{\mu}_2 q^2+\rho[D_t^{(0)}]^2\big)\Big]^{-1} \\
& \times\Big\{4k_cq(2k_c+q)\tilde{\mu}_2^2\big[k_c^4(6\tilde{\mu}_2-7\mu_2)+2k_c^3q(\tilde{\mu}_2-4\mu_2)-8k_cq^3(\tilde{\mu}_2+2\mu_2) \\
& \quad +k_c^2q^2(13\mu_2-24\tilde{\mu}_2)\big]-2\nu_2\tilde{\mu}_2 k_c(k_c-2q)q(2k_c+q)(k_c+2q)(3k_c^2-k_cq+2q^2)D_t^{(0)} \\
& \quad +\tilde{\mu}_2\rho[D_t^{(0)}]^2\big[4q^5\tilde{\mu}_2+3k_c^3q^2(\mu_2-2\tilde{\mu}_2)+k_c^2q^3(79\tilde{\mu}_2+8\mu_2)\big]-\rho^3[D_t^{(0)}]^6(k_c-q) \\
& \quad +2k_c\rho[D_t^{(0)}]^3\tilde{\mu}_2\nu_2(k_c^2-2k_cq-5q^2)(3k_c^2-k_cq+2q^2)+2k_c\rho^2\nu_2[D_t^{(0)}]^5(3k_c^2-k_cq+2q^2) \\
& \quad -\rho^2[D_t^{(0)}]^4\big[5\tilde{\mu}_2q^3+k_c^3(17\tilde{\mu}_2-8\mu_2)+k_cq^2(\tilde{\mu}_2-4\mu_2)+k_c^2q(17\tilde{\mu}_2+4\mu_2)\big]\Big\}D_t^{(0)}
\end{aligned}
\tag{D.17}
$$

and for squares ($ij = ji = 15$) we obtain

$$
\begin{aligned}
\hat{\Psi}^{\text{hom}}_{NMij} = {}& \Big[8\rho[D_t^{(0)}]^2k_c^2(k_c+q)\big((k_c^2-2k_cq-q^2)\tilde{\mu}_2-\rho[D_t^{(0)}]^2\big)\big(4\tilde{\mu}_2 q^2-\rho[D_t^{(0)}]^2-2\tilde{\mu}_2 k_c^2\big)\Big]^{-1} \\
& \times\Big\{8k_c\tilde{\mu}_2^2(k_c^2-2k_cq-q^2)\big[2k_c\tilde{\mu}_2(3k_c+q)(k_c^2-2q^2)-\mu_2(7k_c^4-7k_c^2q^2+8k_cq^3-6q^4)\big] \\
& \quad -8\nu_2\tilde{\mu}_2 k_c(k_c^2-2q^2)(k_c^2-2k_cq-q^2)(2k_c^2-k_cq+q^2)D_t^{(0)} \\
& \quad +2\tilde{\mu}_2\rho[D_t^{(0)}]^2\big[k_c^5(33\tilde{\mu}_2-26\mu_2)-2q^5\tilde{\mu}_2-2k_cq^4(5\tilde{\mu}_2-7\mu_2)-k_c^2q^3(29\tilde{\mu}_2+12\mu_2) \\
& \qquad +k_c^3q^2(20\mu_2-81\tilde{\mu}_2)+k_c^4q(36\mu_2-15\tilde{\mu}_2)\big] \\
& \quad +4\tilde{\mu}_2 k_c\rho\nu_2(3k_c-5q)(k_c+q)(2k_c^2-k_cq+q^2)[D_t^{(0)}]^3 \\
& \quad +\rho^2[D_t^{(0)}]^4\big[5q^3\tilde{\mu}_2+k_c^3(23\tilde{\mu}_2-12\mu_2)+k_cq^2(\tilde{\mu}_2-4\mu_2)+k_c^2q(11\tilde{\mu}_2+8\mu_2)\big] \\
& \quad -4k_c\rho^2\nu_2[D_t^{(0)}]^5(2k_c^2-k_cq+q^2)+(k_c-q)\rho^3[D_t^{(0)}]^6\Big\}D_t^{(0)}
\end{aligned}
\tag{D.18}
$$

And for stripes

$$
\begin{aligned}
\hat{\Psi}^{\text{hom}}_{NMij} = {}& -\Big[8k_c^2\rho[D_t^{(0)}]^2(k_c+q)\big((k_c-q)(3k_c+q)\tilde{\mu}_2+\rho[D_t^{(0)}]^2\big)\Big]^{-1} \\
& \times\Big\{4\tilde{\mu}_2 k_c(k_c-q)(3k_c+q)\big[k_c^2(6\tilde{\mu}_2-7\mu_2)-3q^2\mu_2+2k_cq(\tilde{\mu}_2+2\mu_2)\big] \\
& \quad -4\tilde{\mu}_2 k_c\nu_2 D_t^{(0)}(k_c-q)(3k_c+q)(3k_c^2-2k_cq+q^2) \\
& \quad +\rho[D_t^{(0)}]^2\big[\tilde{\mu}_2(31k_c^3+3k_c^2q+5k_cq^2+q^3)-4k_c(5k_c^2-4k_cq+q^2)\big] \\
& \quad -4k_c\rho\nu_2[D_t^{(0)}]^3(3k_c^2-2k_cq+q^2)+\rho^2[D_t^{(0)}]^4(k_c-q)\Big\}D_t^{(0)}
\end{aligned}
\tag{D.19}
$$

For $\theta_{ij} = \pi/6$, $(ij = ji = 14 = 36 = 25)$ one obtains

$$
\begin{aligned}
\hat{\Psi}^{\text{hom}}_{NMij} = -N_4^{-1} D_t^{(0)} \Big\{ & 4k_c^9 q\tilde{\mu}_2^2 \Big[2(7+4\sqrt{3})(6\tilde{\mu}_2 - 7\mu_2) - \nu_2(40+23\sqrt{3})D_t^{(0)} \Big] \\
& -4k_c^8 q\tilde{\mu}_2 \Big[4(23+14\sqrt{3})\tilde{\mu}_2 - 4(47+29\sqrt{3})\mu_2 + 7\nu_2(12+7\sqrt{3})D_t^{(0)} \Big] \\
& +q^3\rho[D_t^{(0)}]^2(4q^2\tilde{\mu}_2 - \rho[D_t^{(0)}]^2)(q^2\tilde{\mu}_2 - \rho[D_t^{(0)}]^2) \\
& +k_c q^2(q^2\mu_2 - \rho[D_t^{(0)}]^2)\Big[4q^4\tilde{\mu}_2(3\mu_2 + \nu_2 D_t^{(0)}) - \rho^2[D_t^{(0)}]^4 \\
& \quad +q^2\rho[D_t^{(0)}]^2(7\tilde{\mu}_2 - 4\mu_2 - 4\nu_2 D_t^{(0)}) \Big] \\
& -k_c^2 q\Big[(3+\sqrt{3})\rho^3[D_t^{(0)}]^6 + 8q^6\tilde{\mu}_2^2\big(4(\tilde{\mu}_2 - 4\mu_2) + \nu_2(6-\sqrt{3})D_t^{(0)}\big) \\
& \quad +q^2\rho^2[D_t^{(0)}]^4\big((8-11\sqrt{3})\tilde{\mu}_2 + 4\sqrt{3}\mu_2 - 2\nu_2(2-\sqrt{3})D_t^{(0)}\big) \\
& \quad -q^2\tilde{\mu}_2\rho[D_t^{(0)}]^2\big((94-25\sqrt{3})\tilde{\mu}_2 - 16(2-\sqrt{3})\mu_2 - 2\nu_2(14-5\sqrt{3})D_t^{(0)}\big) \Big] \\
& -k_c^5\Big[q^2\tilde{\mu}_2\rho[D_t^{(0)}]^2\big(6(21+41\sqrt{3})\tilde{\mu}_2 + 88\mu_2 + \nu_2(30-4\sqrt{3})D_t^{(0)}\big) \\
& \quad -\rho^2[D_t^{(0)}]^4\big((41+29\sqrt{3})\tilde{\mu}_2 - 8(3+2\sqrt{3})\mu_2 - 2\nu_2(7+5\sqrt{3})D_t^{(0)}\big) \\
& \quad -2q^4\tilde{\mu}_2\big(4(6+47\sqrt{3})\tilde{\mu}_2 + 6(40+29\sqrt{3})\mu_2 + 3\nu_2(47+18\sqrt{3})D_t^{(0)}\big) \Big] \\
& -k_c^4 q\Big[\rho^2[D_t^{(0)}]^4\big((53+7\sqrt{3})\tilde{\mu}_2 - 4(11+5\sqrt{3})\mu_2 - 2\nu_2(13+5\sqrt{3})D_t^{(0)}\big) \\
& \quad -2q^4\tilde{\mu}_2^2\big(36(\sqrt{3}-6)\tilde{\mu}_2 - 8(6+\sqrt{3})\mu_2 + \nu_2(31-12\sqrt{3})D_t^{(0)}\big) \\
& \quad +2q^2\tilde{\mu}_2\rho[D_t^{(0)}]^2\big((37\sqrt{3}-187)\tilde{\mu}_2 + 2(59+16\sqrt{3})\mu_2 + \nu_2(61+18\sqrt{3})D_t^{(0)}\big) \Big] \\
& -2k_c^7\tilde{\mu}_2\Big[2q^2\tilde{\mu}_2\big(4(37+21\sqrt{3})\tilde{\mu}_2 + 2(10-7\sqrt{3})\mu_2 - \nu_2(1+\sqrt{3})D_t^{(0)}\big) \\
& \quad -\rho[D_t^{(0)}]^2\big((123+68\sqrt{3})\tilde{\mu}_2 - 8(13+7\sqrt{3})\mu_2 - \nu_2(51+29\sqrt{3})D_t^{(0)}\big) \Big] \\
& +k_c^3\Big[(1+\sqrt{3})\rho^3[D_t^{(0)}]^6 - q^2\rho^2[D_t^{(0)}]^4\big((44-7\sqrt{3})\tilde{\mu}_2 + 8(1+\sqrt{3})\mu_2 + 2\nu_2(2+3\sqrt{3})D_t^{(0)}\big) \\
& \quad +q^4\tilde{\mu}_2\rho[D_t^{(0)}]^2\big((258-71\sqrt{3})\tilde{\mu}_2 + 4(9+17\sqrt{3})\mu_2 + 6\nu_2(4+7\sqrt{3})D_t^{(0)}\big) \\
& \quad -4q^6\tilde{\mu}_2\big(56\tilde{\mu}_2 + (26+23\sqrt{3})\mu_2 + \nu_2(2+15\sqrt{3})D_t^{(0)}\big) \Big] \\
& -2k_c^6 q\tilde{\mu}_2\Big[\rho[D_t^{(0)}]^2\big((75+68\sqrt{3})\tilde{\mu}_2 - 2(83+55\sqrt{3})\mu_2 - \nu_2(83+51\sqrt{3})D_t^{(0)}\big) \\
& \quad -2q^2\tilde{\mu}_2\big(4(27+25\sqrt{3})\tilde{\mu}_2 - 4(59+26\sqrt{3})\mu_2 - \nu_2(91+59\sqrt{3})D_t^{(0)}\big) \Big] \Big\} \quad \text{(D.20)}
\end{aligned}
$$

with the denominator N_4 given by

$$
\begin{aligned}
N_4 = 8\rho[D_t^{(0)}]^2 k_c^2(k_c+q)\Big\{ & \big[2(2+\sqrt{3})k_c^4 - 4(1+\sqrt{3})k_c^3 q + 2(1-\sqrt{3})k_c^2 q^2 + 4k_c q^3 + q^4 \big]\tilde{\mu}_2 \\
& +\big[(1+\sqrt{3})k_c^2 - 2k_c q - q^2\big]\rho[D_t^{(0)}]^2\Big\}\Big\{ (2+\sqrt{3})k_c^2\tilde{\mu}_2 - (4q^2\tilde{\mu}_2 - \rho[D_t^{(0)}]^2)\Big\} \quad \text{(D.21)}
\end{aligned}
$$

With these potentials the components of the velocity field can be calculated straightforwardly. To determine the components of the strain field via eq. (5.58), however, the

inhomogeneous contributions $-v_k^{(1)}\partial_k\epsilon_{ij}^{(1)}$ have to be calculated additionally

$$
v_k^{(1)}\partial_k\epsilon_{zz}^{(1)} = \frac{D_t^{(0)}}{(k_c^2-q^2)^2}\Big\{(1-\cos\theta_{ij})\big[4k_c^4q^2e^{2qz}+(k_c^2+q^2)k_c^2e^{2k_cz}\big]
$$
$$
-2k_c^2(k_c^2+q^2)(k_c^2-2qk_c\cos\theta_{ij}+q^2)e^{(k_c+q)z}\Big\}\xi_{iN}\xi_{jM} \tag{D.22}
$$

$$
v_k^{(1)}\partial_k\epsilon_{xy}^{(1)} = \frac{-D_t^{(0)}\cos\theta_{ij}}{2(k_c^2-q^2)^2}\Big\{(1-\cos\theta_{ij})\big[4k_c^4q^2e^{2qz}+k_c^2(k_c^2+q^2)e^{2k_cz}\big]
$$
$$
-2k_c^2(k_c^2+q^2)(k_c^2-2qk_c\cos\theta_{ij}+q^2)e^{(k_c+q)z}\Big\}\xi_{iN}\xi_{jM} \tag{D.23}
$$

$$
v_k^{(1)}\partial_k\epsilon_{xx}^{(1)} = \frac{-D_t^{(0)}(k_{i,x}^2+k_{j,x}^2)}{2(k_c^2-q^2)^2}\Big\{(1-\cos\theta_{ij})\big[4k_c^2q^2e^{2qz}+(k_c^2+q^2)^2e^{2k_cz}\big]
$$
$$
-2(k_c^2+q^2)(k_c^2-2qk_c\cos\theta_{ij}+q^2)e^{(q+k_c)z}\Big\}\xi_{iN}\xi_{jM} \tag{D.24}
$$

$$
v_k^{(1)}\partial_k\epsilon_{yy}^{(1)} = \frac{-D_t^{(0)}(k_{i,y}^2+k_{j,y}^2)}{2(k_c^2-q^2)^2}\Big\{(1-\cos\theta_{ij})\big[4k_c^2q^2e^{2qz}+(k_c^2+q^2)^2)e^{2k_cz}\big]
$$
$$
-2(k_c^2+q^2)(k_c^2-2qk_c\cos\theta_{ij}+q^2)e^{(q+k_c)z}\Big\}\xi_{iN}\xi_{jM} \tag{D.25}
$$

$$
v_k^{(1)}\partial_k\epsilon_{xz}^{(1)} = \frac{-iD_t^{(0)}(k_{i,x}+k_{j,x})(k_c^2+q^2)}{2(k_c^2-q^2)^2}\Big\{(1-\cos\theta_{ij})\big[2k_c^2qe^{2qz}+k_c(k_c^2+q^2)e^{2k_cz}\big]
$$
$$
-(k_c+q)\big[2k_c^2-qk_c(1+\cos\theta_{ij})+q^2-k_c^2\cos\theta_{ij}\big]e^{(k_c+q)z}\Big\}\xi_{iN}\xi_{jM} \tag{D.26}
$$

$$
v_k^{(1)}\partial_k\epsilon_{yz}^{(1)} = \frac{-iD_t^{(0)}(k_{i,y}+k_{j,y})(k_c^2+q^2)}{2(k_c^2-q^2)^2}\Big\{(1-\cos\theta_{ij})\big[2k_c^2qe^{2qz}+k_c(k_c^2+q^2)e^{2k_cz}\big]
$$
$$
-(k_c+q)\big[2k_c^2-qk_c(1+\cos\theta_{ij})+q^2-k_c^2\cos\theta_{ij}\big]e^{(k_c+q)z}\Big\}\xi_{iN}\xi_{jM} \tag{D.27}
$$

where we have displayed only the $\xi_{iN}\xi_{jM}$ contributions to $-v_k^{(1)}\partial_k\epsilon_{ij}^{(1)}$. The contributions $\sim\xi_{iN}\xi_{jM}^*$ can be derived from eqs. (D.22-D.27) by the replacements

$$
\xi_{iN}\xi_{jM}\longrightarrow\xi_{iN}\xi_{jM}^* \quad\text{and}\quad \mathbf{k}_j\longrightarrow-\mathbf{k}_j, \cos\theta_{ij}\longrightarrow-\cos\theta_{ij} \tag{D.28}
$$

Appendix E

Usual ferrofluids

In the case of ferrofluids, the dynamic equation for the strain field (2.34) is absent and we only retain the continuity equation (2.32) and the Navier-Stokes equation (2.33). Furthermore, all contributions to the stress tensor (2.35) that are proportional to the elastic shear modulus μ_2 drop out. The expansion to the nonlinear regime follows the same lines as for magnetic gels. The solvability for the bulk hydrodynamic equations for ferrofluids then reads

$$\langle \bar{v}_i \,|\, \partial_t^{(1)}(\rho v_i^{(1)}) \rangle \;=\; -\langle \bar{v}_i \,|\, \partial_j(\rho v_i^{(1)} v_j^{(1)}) \rangle \tag{E.1}$$

Following the same lines as in section 5.3.1 we obtain for the left hand side of eq. (E.1), if we retain the lowest order of the expansion in terms of $\partial_t^{(0)}$,

$$\langle \bar{v}_i \,|\, \partial_t^{(1)}(\rho v_i^{(1)}) \rangle \;=\; -\frac{12\rho}{k_c}([\omega^{(0)}]^2 - [\sigma^{(0)}]^2)\sigma^{(1)} \sum_{i=1}^{N} \hat{\xi}_i \hat{\xi}_i^* \tag{E.2}$$

Similarly the right hand side of equation (E.1) reads

$$\langle \bar{v}_i \,|\, \partial_j(\rho v_i^{(1)} v_j^{(1)}) \rangle \;=\; -24\rho\sigma^{(0)}([\omega^{(0)}]^2 - [\sigma^{(0)}]^2)(\hat{\xi}_1\hat{\xi}_2\hat{\xi}_3 + \hat{\xi}_1^*\hat{\xi}_2^*\hat{\xi}_3^*) \tag{E.3}$$

We realize, that the lowest order in the expansion of eq. (E.1) in terms of $\partial_t^{(0)}$ is at least proportional to $[\partial_t^{(0)}]^3$ due to the deformable surface: The velocity in the original and the adjoint space have to be proportional to the time derivative of the surface deflection and, consequently, the product $\langle \bar{v}_i \,|\, \partial_j(\rho v_i^{(1)} v_j^{(1)}) \rangle$ is proportional to $[\partial_t^{(0)}]^3$. This is also the reason why the contributions to the amplitude equation in the case of ferrofluids do not contribute in the case of magnetic gels. The common factor $([\omega^{(0)}]^2 - [\sigma^{(0)}]^2)$ in (E.1) cancels and, finally, we end up with

$$\frac{\sigma^{(1)}}{\sigma^{(0)}}\hat{\xi}_1 = -\frac{4}{3}k_c\hat{\xi}_2^*\hat{\xi}_3^* \qquad \text{and} \qquad |\hat{\xi}_1|^2 = |\hat{\xi}_2|^2 = |\hat{\xi}_3|^2 \tag{E.4}$$

and the corresponding conditions for all cyclic permutations $1 \to 2 \to 3 \to 1$. As for magnetic gels, eq. (E.4) only exists for the hexagonal pattern, whereas for any other surface pattern the amplitudes show no nonlinear interaction in the second order.

The solutions for the second order eigenvectors can be taken from the discussion of magnetic gels in section 5.3.2 and 5.3.3 by simply substituting $\mu_2 = 0$ and are therefore not

shown here. With the solutions of the second order, the third order Fredholm's theorem can be fulfilled. The latter reads in the case of ferrofluids

$$\langle \bar{v}_i \,|\, \rho \partial_t^{(2)} v_i^{(1)} \rangle + \langle \bar{v}_i \,|\, \rho \partial_t^{(1)} v_i^{(2,1)} \rangle \;=\; -\langle \bar{v}_i \,|\, \rho \partial_t^{(1)} v^{(2,2)} \rangle - \rho \langle \bar{v}_i \,|\, \partial_j (v_i^{(1)} v_j^{(2,1)} + v_i^{(2,1)} v_j^{(1)}) \rangle$$
$$-\rho \langle \bar{v}_i \,|\, \partial_j (v_i^{(1)} v_j^{(2,2)} + v_i^{(2,2)} v_j^{(1)}) \rangle \tag{E.5}$$

Since the analytical expressions for the eigenvectors $v_i^{(2,2)}$ are bulky, the explicit calculation of the cubic coefficients has been performed with *Mathematica* and the results are shown below. We should mention, however, that also in the third order the right hand side of eq. (E.5) is proportional to $[\partial_t^{(0)}]^3$ and the global factor $([\omega^{(0)}]^2 - [\sigma^{(0)}]^2)$ can be canceled.

The discussion of the normal stress boundary condition in the case of ferrofluids can be taken from the sections 5.3.4 and 5.4. In the second order, the additional condition to the amplitudes (5.115) is valid for ferrogels and ferrofluids, alike, and in the corresponding third order condition (5.133) we have to substitute $\mu_2 \to 0$ with the consequence that there is no second order time derivative. The typical time scale in the case of ferrofluids is then given by $\tau_0 = \nu_2 k_c/(\rho G)$ which is in accordance with previous theoretical discussions [39]. The final amplitude equation is derived in the same way as in section 5.5 for magnetic gels and finally results for the hexagonal pattern in

$$\partial_T \xi_1 = \frac{1}{2}\tilde{\epsilon}^{\text{fl}}\xi_1 - \frac{2}{3\sqrt{A}}\xi_2^*\xi_3^* - |\xi_1|^2\,\xi_1 - \frac{B_{120}^{\text{fl}}}{A^{\text{fl}}}(|\xi_2|^2 + |\xi_3|^2)\xi_1 \tag{E.6}$$

For the square pattern the quadratic coefficient is absent and we obtain

$$\partial_T \xi_1 = \tilde{\epsilon}^{\text{fl}}\xi_1 - |\xi_1|^2\,\xi_1 - \frac{B_{90}^{\text{fl}}}{A^{\text{fl}}}|\xi_5|^2\,\xi_1 \tag{E.7}$$

where the cubic coefficients are given by

$$A^{\text{fl}} \;\approx\; 8.625 \tag{E.8}$$
$$B_{120}^{\text{fl}} \;\approx\; 3.150 \tag{E.9}$$
$$B_{90}^{\text{fl}} \;\approx\; 4.266 \tag{E.10}$$

The discussion for the different stable patterns follows the same lines as in section 5.5. At the linear onset we find hexagons to be the preferred pattern, which remains subcritically stable for control parameters larger than

$$\tilde{\epsilon}_A \;=\; -\frac{4}{9(A^{\text{fl}} + 2B_{120}^{\text{fl}})} \tag{E.11}$$

Since $B_{90}^{\text{fl}} + 2B_{30}^{\text{fl}} < A^{\text{fl}} + 2B_{120}^{\text{fl}}$ and $B_{90}^{\text{fl}}/A^{\text{fl}} < 1$, where the cubic coefficient accounting for the nonlinear interaction between hexagons and squares is given by $B_{30}^{\text{fl}} \approx 4.545$, the hexagon pattern transforms into a square pattern for control parameters larger than

$$\tilde{\epsilon}_B \;=\; \frac{2(B_{90}^{\text{fl}} + 2B_{30}^{\text{fl}})}{9(A^{\text{fl}} + 2B_{120}^{\text{fl}} - B_{90}^{\text{fl}} - 2B_{30}^{\text{fl}})^2} \tag{E.12}$$

The square pattern in turn becomes unstable again for control parameters lower than

$$\tilde{\epsilon}_S \;=\; \frac{2(A^{\text{fl}} + B_{90}^{\text{fl}})}{9(A^{\text{fl}} + B_{90}^{\text{fl}} - B_{120}^{\text{fl}} - B_{30}^{\text{fl}})^2} \tag{E.13}$$

Bibliography

[1] F. Bitter, *On inhomogeneities in the magnetization of ferromagnetic materials*, Phys. Rev. **38**, 1903 (1931).

[2] W. C. Elmore, *Ferromagnetic colloid for studying magnetic structures*, Phys. Rev. **54**, 309 (1938).

[3] R. E. Rosensweig, *Ferrohydrodynamics*, Cambridge University Press, Cambridge, UK, 1985.

[4] C. Holm, A. Ivanov, S. Kantorovich, E. Pyanzina and E. Reznikov, *Equilibrium properties of a bidisperse ferrofluid with chain aggregates: theory and computer simulations*, J. Phys.: Condens. Matter **18**, S2737 (2006).

[5] A. Y. Zubarev and L. Y. Iskakova, *Rheological properties of ferrofluids with microstructures*, J. Phys.: Condens. Matter **18**, S2771 (2006).

[6] L. M. Pop and S. Odenbach, *Investigation of the microscopic reason for the magnetoviscous effect in ferrofluids studied by small angle neutron scattering*, J. Phys.: Condens. Matter **18**, S2785 (2006).

[7] I. Hilger, E. Dietmar, W. Linß, S. Streck and W. A. Kaiser, *Developments for the minimally invasive treatment of tumours by targeted magnetic heating*, J. Phys.: Condens. Matter **18**, S2951 (2006).

[8] R. Jurgons, C. Seliger, A. Hilpert, L. Trahms, S. Odenbach and C. Alexiou, *Drug loaded magnetic nanoparticles for cancer therapy*, J. Phys.: Condens. Matter **18**, S2893 (2006).

[9] K. Aurich, G. Glöckl, E. Romanus, P. Weber, S. Nagel and W. Weitschies, *Magneto-optical relaxation measurements for the characterization of biomolecular interactions*, J. Phys.: Condens. Matter **18**, S2847 (2006).

[10] T. Tanaka, *Collapse of gels and the critical endpoint*, Phys. Rev. Lett. **40**, 820 (1978).

[11] T. Tanaka, I. Nishio, S. T. Sun and S. Ueno-Nishio, *Collapse of gels in an electric field*, Science **218**, 467 (1982).

[12] M. Zrínyi, L. Barsi and A. Büki, *Deformation of ferrogels induced by nonuniform magnetic fields*, J. Chem. Phys. **104**, 8750 (1996).

[13] G. Lattermann and M. Krekhova, *Thermoreversible ferrogels*, Macromol. Rapid Commun. **27**, 1373 (2006).

[14] Z. Varga, J. Fehér, G. Filipcsei and M. Zrínyi, *Smart nanocomposite polymer gels*, Macromol. Symp. **200**, 93 (2003).

[15] D. Collin, G. K. Auernhammer, O. Gavat, P. Martinoty and H. R. Brand, *Frozen-in magnetic order in uniaxial magnetic gels: Preparation and physical properties*, Macromol. Rapid Commun. **24**, 737 (2003).

[16] T. Mitsumata, K. Juliac, K. Furukawa, K. Iwakura, T. Taniguchi and K. Koyoma, *Anisotropy in longitudinal modulus of polymer gels containing ferrite*, Macromol. Rapid Commun. **23**, 175 (2002).

[17] J. Weilepp, J.-J. Zanna, N. Aßfalg, P. Stein, L. Hilliou, M. Mauzac, H. Finkelmann, H. R. Brand and P. Martinoty, *Rheology of liquid crystalline elastomers in their isotropic and smectic A state*, Macromolecules **32**, 4566 (1999).

[18] J.-J. Zanna, P. Stein, J.-D. Marty, M. Mauzac and P. Martinoty, *Influence of molecular parameters on the elastic and viscoelastic properties of side-chain liquid crystalline elastomers*, Macromolecules **35**, 5459 (2002).

[19] M. D. Cowley and R. E. Rosensweig, *The interfacial stability of a ferromagnetic fluid*, J. Fluid Mech. **30**, 671 (1967).

[20] S. Bohlius, H. R. Brand and H. Pleiner, *Surface waves and Rosensweig instability in isotropic ferrogels*, Z. Phys. Chem **200**, 97 (2006).

[21] C. Gollwitzer, *private communication*.

[22] A. T. Skjeltorp, *One- and two-dimensional crystallization of magnetic holes*, Phys. Rev. Lett. **51**, 2306 (1983).

[23] B. J. D. Gans, N. J. Duin, D. van den Ende and J. Mellema, *The influence of particle size on the magnetorheological properties of an inverse ferrofluid*, J. Chem. Phys. **113**, 2032 (2000).

[24] R. Saldivar-Guerrero, R. Richter, I. Rehberg, N. Aksel, L. Heymann and O. S. Rodriguez-Fernández, *Viscoelasticity of mono- and polydisperse inverse ferrofluids*, J. Chem. Phys. **125**, 084907 (2006).

[25] C. Gollwitzer, *Computergestützte Radioskopie von Oberflächeninstabilitäten in Ferrofluiden*, Diplomarbeit, Universität Bayreuth, unpublished, 2005.

[26] A. Lange, B. Reimann and R. Richter, *Wave number of maximal growth in viscous magnetic fluids of arbitrary depth*, Phys. Rev. E **61**, 5528 (2000).

[27] A. Lange, *Scaling behaviour of the maximal growth rate in the Rosensweig instability*, Europhys. Lett. **55**, 327 (2001).

[28] J.-C. Bacri and D. Salin, *First-order transition in the instability of a magnetic fluid interface*, J. Physique Lett. **45**, 559 (1984).

[29] R. Richter and J. Bläsing, *Measuring surface deformations in magnetic fluid by radioscopy*, J. Sci. Instrum. **72**, 1729 (2001).

[30] C. Gollwitzer, G. Matthies, R. Richter, I. Rehberg and L. Tobiska, *The surface topography of a magnetic fluid: a quantitative comparison between experiment and numerical simulation*, J. Fluid Mech. **571**, 455 (2007).

[31] B. Abou, J.-E. Wesfreid and S. Roux, *The normal field instability in ferrofluids: hexagon-square transition mechanism and wavenumber selection*, J. Fluid Mech. **416**, 217 (2000).

[32] C. Gollwitzer, I. Rehberg and R. Richter, *Via hexagons to squares: Experiments on hysteretic surface transformations under variation of the normal magnetic field*, J. Phys.: Condens. Matter **18**, S2643 (2006).

[33] A. Gailitis, *Formation of the hexagonal pattern on the surface of a ferromagnetic fluid in an applied magnetic field*, J. Fluid Mech. **82**, 401 (1977).

[34] R. Friedrichs and A. Engel, *Pattern and wave number selection in magnetic fluids*, Phys. Rev. E **64**, 021406 (2001).

[35] E. E. Twombly and J. W. Thomas, *Mathematical theory of non-linear waves on the surface of a magnetic fluid*, IEEE Trans. Magn. **16**, 214 (1980).

[36] E. E. Twombly and J. W. Thomas, *Bifurcation instabilities of the free surface of a ferrofluid*, SIAM J. Math. Anal. **14**, 736 (1983).

[37] M. Silber and E. Knobloch, *Pattern selection in ferrofluids*, Physica D **30**, 83 (1988).

[38] A. Schlüter, D. Lortz and F. Busse, *On the stability of steady finite amplitude convection*, J. Fluid Mech. **23**, 129 (1965).

[39] R. Friedrichs and A. Engel, *Non-linear analysis of the Rosensweig instability*, Europhys. Lett. **63**, 826 (2003).

[40] R. Friedrichs, *Low symmetry patterns on magnetic fluids*, Phys. Rev. E **66**, 066215 (2002).

[41] S. K. Malik and M. Singh, *Nonlinear dispersive instabilities in magnetic fluids*, Q. Appl. Math. **42**, 359 (1984).

[42] S. K. Malik and M. Singh, *Modulational instability in magnetic fluids*, Q. Appl. Math. **43**, 57 (1985).

[43] S. K. Malik and M. Singh, *Nonlinear focusing in magnetic fluids*, Q. Appl. Math. **44**, 629 (1987).

[44] C. Kubstrup, H. Herrero and C. Pérez-García, *Fronts between hexagons and squares in a generalized Swift-Hohenberg equation*, Phys. Rev. E **54**, 1560 (1996).

[45] H. Herrero, C. Pérez-García and M. Bestehorn, *Stability of fronts separating domains with different symmetries in hydrodynamical instabilities*, Chaos **4**, 15 (1994).

[46] O. Lavrova, G. Matthies, T. Mitkova, V. Polevikov and L. Tobiska, *Numerical treatment of free surface problems in ferrohydrodynamics*, J. Phys.: Condens. Matter **18**, S2657 (2006).

[47] A. C. Newell and J. A. Whitehead, *Finite bandwidth, finite amplitude convection*, J. Fluid Mech. **38**, 279 (1969).

[48] M. C. Cross and P. C. Hohenberg, *Pattern formation outside of equilibrium*, Rev. Mod. Phys. **65**, 851 (1993).

[49] A. Lange, *The adjoint problem in the presence of a deformed surface: The example of the Rosensweig instability on magnetic fluids*, Int. J. Mod. Phys. B **16**, 1155 (2002).

[50] M. Takashima, *Surface tension driven instability in a horizontal liquid layer with a deformable free surface. I. Stationary convection*, J. Phys. Soc. Japan **50**, 2745 (1981).

[51] M. Takashima, *Surface tension driven instability in a horizontal liquid layer with a deformable free surface. II. Overstability*, J. Phys. Soc. Japan **50**, 2751 (1981).

[52] S. Rosenblat, S. H. Davis and G. M. Homsy, *Nonlinear Marangoni convection in bounded layers. Part 1. Circular cylindrical containers*, J. Fluid Mech. **120**, 91 (1982).

[53] S. Rosenblat, G. M. Homsy and S. H. Davis, *Nonlinear Marangoni convection in bounded layers. Part 2. Rectangular cylindrical containers*, J. Fluid Mech. **120**, 123 (1982).

[54] P. C. Dauby, G. Lebon, P. Colinet and J. C. Legros, *Hexagonal Marangoni convection in a rectangular box with slippery walls*, Q. J. Mech. Appl. Math. **46**, 683 (1993).

[55] G. Lebon and A. Cloot, *Buoyancy and surface-tension driven instabilities in presence of negative Rayleigh and Marangoni numbers*, Acta Mech. **43**, 141 (1982).

[56] A. Engel and J. B. Swift, *Planform selection in two-layer Bénard-Marangoni convection*, Phys. Rev. E **62**, 6540 (2000).

[57] A. C. Skeldon and G. Guidoboni, *Pattern selection for Faraday waves in an incompressible viscous fluid*, SIAM J. Appl. Math. **67**, 1064 (2007).

[58] H. Pleiner and H. R. Brand, in *Pattern Formation in Liquid Crystals*, edited by A. Buka and L. Kramer, Springer, New York, 1996, chapter 2.

[59] D. Forster, *Hydrodynamic Fluctuations, Broken Symmetry and Correlation Functions*, Benjamin, Reading, Mass., 1975.

[60] E. Jarkova, H. Pleiner, H.-W. Müller and H. R. Brand, *Hydrodynamics of isotropic ferrogels*, Phys. Rev. E **68**, 041706 (2003).

[61] L. Onsager, *Reciprocal relation in irreversible processes I*, Phys. Rev. **37**, 405 (1931).

[62] L. Onsager, *Reciprocal relation in irreversible processes II*, Phys. Rev. **38**, 2265 (1931).

[63] S. R. deGroot and P. Mazur, *Grundlagen der Thermodynamik irreversibler Prozesse*, Hochschultaschenbücher-Verlag, Mannheim, 1969.

[64] L. D. Landau and E. M. Lifschitz, *Lehrbuch der Theoretischen Physik, Band 7 – Elastizitätstheorie*, Akademie-Verlag, Berlin, 1974.

[65] P. M. Chaikin and T. C. Lubensky, *Principles of condensed matter physics*, Cambridge University Press, Cambridge, UK, 1995.

[66] H. Temmen, H. Pleiner, M. Liu and H. R. Brand, *Convective nonlinearity in non-Newtonian fluids*, Phys. Rev. Lett. **84**, 3228 (2000).

[67] H. Pleiner, M. Liu and H. R. Brand, *The structure of convective nonlinearities in polymer rheology*, Rheol. Acta **39**, 560 (2000).

[68] A. Menzel, H. Pleiner and H. R. Brand, *Nonlinear relative rotations in liquid crystalline elastomers*, J. Chem. Phys. **126**, 234901 (2007).

[69] J. D. Jackson, *Classical Electrodynamics*, John Wiley & Sons, Inc., 1999.

[70] S. Bohlius, *Makroskopische Dynamik magnetischer Gele*, Diplomarbeit, Universität Bayreuth, unpublished, 2005.

[71] J. L. Harden, H. Pleiner and P. A. Pincus, *Hydrodynamic surface modes on concentrated polymer solutions and gels*, J. Chem. Phys. **94**, 5208 (1991).

[72] J. Weilepp and H. R. Brand, *Competition between the Bénard-Marangoni and the Rosensweig instability in magnetic fluids*, J. Phys. II **6**, 419 (1996).

[73] S. Bohlius, H. Pleiner and H. R. Brand, *Pattern formation in ferrogels: Analysis of the Rosensweig instability using the energy method*, J. Phys.: Condens. Matter **18**, S2671 (2006).

[74] S. Bohlius, H. Pleiner and H. R. Brand, *Solution of the adjoint problem for instabilities with a deformable surface: Rosensweig and Marangoni instability*, Phys. Fluids **19**, 094103 (2007).

[75] S. Bohlius, H. Pleiner and H. R. Brand, *The amplitude equation for the Rosensweig instability*, submitted to Physica D .

[76] A. C. Newell, T. Passot and J. Lega, *Order parameter equations for patterns*, Annu. Rev. Fluid Mech. **25**, 399 (1993).

[77] I. S. Aranson and L. Kramer, *The world of the complex Ginzburg-Landau equation*, Rev. Mod. Phys. **74**, 99 (2002).

[78] S. Ciliberto, P. Coullet, J. Lega, E. Pampaloni and C. Pérez-García, *Defect in Roll-Hexagon Competition*, Phys. Rev. Lett. **65**, 2370 (1990).

[79] M. Diewald, *Chemisch getriebene Konvektion*, Dissertation, Universität Bayreuth, unpublished, 1997.

[80] J. Bragard and M. G. Velarde, *Bénard-Marangoni convection: planforms and related theoretical predictions*, J. Fluid Mech. **368**, 165 (1998).

[81] H. R. Brand, P. S. Lomdahl and A. C. Newell, *Evolution of the order parameter in situations with broken rotational symmetry*, Phys. Lett. A **118**, 67 (1986).

[82] H. R. Brand, P. S. Lomdahl and A. C. Newell, *Benjamin-Feir turbulence in convective binary fluid mixtures*, Physica D **23**, 345 (1986).

[83] A. C. Newell, *Solitons in Mathematics and Physics*, SIAM Series, 1985.

[84] D. Rannacher and A. Engel, *Double Rosensweig instability on a ferrofluid sandwich structure*, Phys. Rev. E **69**, 066306 (2004).

[85] S. Bohlius, H. R. Brand and H. Pleiner, *Rosensweig instability of ferrogel thin films or membranes*, Eur. Phys. J. E **26**, 275 (2008).

[86] J. L. Harden and H. Pleiner, *Hydrodynamic modes of viscoelastic polymer films*, Phys. Rev. E **49**, 1411 (1994).

[87] M. G. Hilgers and A. C. Pipkin, *Bending energy of highly elastic membranes*, Q. Appl. Math. **50**, 389 (1992).

[88] L. Kramer, *Theory of light scattering from fluctuations of membranes and monolayers*, J. Chem. Phys. **55**, 2097 (1971).

[89] E. H. Lucassen and J. Lucassen, *Properties of capillary waves*, Advan. Colloid Interface Sci. **2**, 347 (1969).

[90] D. Langevin, *Light-scattering study of monolayer viscoelasticity*, J. Colloid and Interface Sci. **80**, 412 (1981).

[91] S. Bohlius, H. R. Brand and H. Pleiner, *Macroscopic dynamics of uniaxial magnetic gels*, Phys. Rev. E **70**, 061411 (2004).

[92] D. R. Pettit and H. R. Brand, *On the influence of near zero gravity on the Rosensweig instability in magnetic fluids*, Phys. Lett. A **159**, 55 (1991).

[93] B. Graf, *private communication*.

[94] J. R. A. Pearson, *On convection cells induced by surface tension*, J. Fluid Mech. **4**, 489 (1958).

[95] D. A. Nield, *Surface tension and buoyancy effects in cellular convection*, J. Fluid Mech. **19**, 341 (1964).

[96] L. E. Scriven and C. V. Sternling, *On cellular convection driven by surface-tension gradients: Effects of mean surface tension and surface viscosity*, J. Fluid Mech. **19**, 321 (1964).

[97] K. A. Smith, *On convective instability induced by surface-tension gradients*, J. Fluid Mech. **24**, 401 (1966).

[98] C. Pérez-García and G. Carneiro, *Linear stability analysis of Bénard-Marangoni convection in fluids with a deformable surface*, Phys. Fluids A **3**, 292 (1991).

[99] P. M. Parmentier, V. C. Regnier, G. Lebon and J. C. Legros, *Nonlinear analysis of coupled gravitational and capillary thermoconvection in thin fluid layers*, Phys. Rev. E **54**, 411 (1996).

[100] S. Chandrasekhar, *Hydrodynamic and Hydromagnetic Stability*, Oxford University Press, Oxford, 1961.

List of Publications

This thesis is directly connected to the following publications in which the results of this work have been published or will be published:

S. Bohlius, H. R. Brand and H. Pleiner,
Surface waves and Rosensweig instability in isotropic magnetic gels,
Z. Phys. Chem. **200**, 97 (2006)

S. Bohlius, H. Pleiner and H. R. Brand,
Pattern formation in ferrogels:
Analysis of the Rosensweig instability using the energy method,
J. Phys.: Condens. Matter **18**, S2671 (2006)

S. Bohlius, H. Pleiner and H. R. Brand,
Solution of the adjoint problem for instabilities with a deformable surface,
Phys. Fluids **19**, 094103 (2007)

S. Bohlius, H. R. Brand and H. Pleiner,
Rosensweig instability of ferrogel thin films or membranes,
Eur. Phys. J. E. **26**, 275 (2008)

S. Bohlius, H. Pleiner and H. R. Brand,
The amplitude equation for the Rosensweig instability,
submitted to Physica D

I'd like to thank ...

First of all, I am deeply indebted to Harald Pleiner and Helmut Brand. They gave me the opportunity to work on this topic and they shared their fascination for macroscopic theory with me. The discussions with them were always very instructive and a source of new inspiration and insight. I would like to thank Harald Pleiner for giving me all the freedom needed to follow my own ideas and for his guidance and time when things didn't seem to have a solution, and I would like to thank Helmut Brand for his constant support.

I also would like to thank Kurt Kremer for hosting me at the Max Planck Institute and for giving me all possible support to pursue my research interests. The theory group at the MPIP is extraordinary and the atmosphere is exemplary. I therefore thank all the Kremers for generating such a harmonic atmosphere where everyone is integrated and where everyone feels home immediately. Among all of you are some I am especially grateful to. I would like to thank Andrea Corsi, Bernward Mann and Christian Nowak for helping me a lot in getting started at the MPIP, Ulf Schiller for sharing an office with me for more than two years and for all the kilometers we walked together from our office to the coffee machine, and I would like to thank Christine Peter for being such a nice next-door neighbor at the institute, for her time to read over my thesis, for the "Eierspätzle" and for her contagious smile and laughter in any situation. Thank you, Thomas, for all the long discussions we had about nearly everything. And thank you, of course, for your time in general and especially for cheering me up. I would like to thank Pim Schravendijk for his perspective of the web, Ben Reynwar for trying to improve my English, Torsten Stühn for valuable help with computer problems and Martin Müller for all the discussions we had about physics.

If someone has ever been to the theory group at the MPIP in Mainz, for sure he will have met someone extremely friendly and helpful. I thank you, Doris, for being just the way you are.

I would like to thank Christian Gollwitzer and Holger Knieling for supplying me with nice pictures of the Rosensweig instability. Two of them actually found their way into this thesis (fig. 1.3). Thank you, Christian, for our discussions about this topic and about the problems an experimentalist can have to fit the assumptions that the theoreticians used in their calculations.

I also would like to thank all my old friends whose friendship has always been an important support throughout the years.

I cannot conclude without thanking my parents, my brother and Simone who never stopped believing in me and for all the love and support they gave me.